U. S. DEPARTMENT OF COMMERCE

BUREAU OF STANDARDS JOURNAL OF RESEARCH

Vol. 5 DECEMBER, 1930 No. 6

CONTENTS

RP. No.	TITLE AND AUTHOR	Page
254.	Further study of paper-coating minerals and adhesives. Merle B. Shaw, George W. Bicking, and Martin J. O'Leary	1189
255.	The structure of the spectrum of singly ionized zirconium. C. C. Kiess and Harriet K. Kiess	1205
256.	A redetermination of the constant of gravitation. Paul R. Heyl	1243
257.	The properties of pure nickel. Louis Jordan and Wm. H. Swanger (with collaboration of members of bureau staff as indicated)	1291
258.	The freezing point of nickel as a fixed point on the International Temperature Scale. H. T. Wensel and Wm. F. Roeser	1309

BUREAU OF STANDARDS JOURNAL OF RESEARCH

CONTENTS OF RECENT NUMBERS

August, 1930 (Vol. 5, No. 2)

RP194. Fire clays. Some fundamental properties at several temperatures. R. A. Heindl and W. L. Pendergast. Price 10 cents.

RP195. A precise and rapid method of measuring frequencies from 5 to 200 cycles per second. N. P. Case. Price 5 cents.

RP196. Coefficient of friction of fabrics. Alfred A. Mercier. Price 5 cents.

RP197. Accelerated tests of asphalts. O. G. Strieter. Price 10 cents.

RP198. Conductivity and density of chromic acid solutions. H. R. Moore and W. Blum. Price 5 cents.

RP199. Preliminary studies of the effect of dioxization and mold conditions on the tensile properties of carbon steel castings. J. V. McCrae and R. L. Dowdell. Price 5 cents.

RP200. The precipitation and ignition of magnesium ammonium phosphate. J. I. Hoffman and G. E. F. Lundell. Price 5 cents.

RP201. A new design of precision resistance standard. James L. Thomas. Price 5 cents.

RP202. The structure of the spectra of doubly and trebly ionized zirconium. C. C. Kiess and R. J. Lang. Price 10 cents.

RP203. Phase equilibria in the system Cr_2O_3-SiO_2. E. N. Bunting. Price 5 cents.

RP204. A method of measuring frictional coefficients of walkway materials. R. B. Hunter. Price 10 cents.

RP205. Bearing bronzes with additions of zinc, phosphorus, nickel, and antimony. E. M. Staples, R. L. Dowdell, and C. E. Eggenschwiler. Price 15 cents.

RP206. Cutting tests with cemented tungsten carbide lathe tools. T. G. Digges. Price 10 cents.

RP207. Heat transfer through metal-inclosed insulation. M. S. Van Dusen. Price 5 cents.

RP208. Effects of gases on photo-ionization of cæsium by line absorption. F. L. Mohler and C. Boeckner. Price 5 cents.

RP209. A calorimetric determination of thermal properties of saturated water and steam from 0° to 270° C. N. S. Osborne, H. F. Stimson, and E. F. Fiock. Price 20 cents.

RP210. A review of calorimetric measurements on thermal properties of saturated water and steam. Ernest F. Fiock. Price 10 cents.

September, 1930 (Vol. 5, No. 3)

RP211. An improved form of standard ionization chamber. Lauriston S. Taylor and George Singer.

RP212. Absorption measurement of the X-ray general radiation. Lauriston S. Taylor.

RP213. Change of electrical properties of rubber and gutta-percha during storage under water. Harvey L. Curtis and Arnold H. Scott.

RP214. The resistance of steels to abrasion by sand. Samuel J. Rosenberg.

RP215. An improved Victor-Meyer molecular weight apparatus. Mildred M. Hicks-Bruun.

RP216. Seams for copper roofing. K. Hilding Beij.

RP217. Apparatus for the measurement of high constant or rippled voltages. Lauriston S. Taylor.

RP218. Compressive tests of bases for subway columns. James H. Edwards, H. L. Whittemore, and A. H. Stang.

RP219. Dimensional changes caused in glass by heating cycles. A. Q. Tool, D. B. Lloyd, and G. E. Merritt.

RP220. Accurate method of measuring transmitted wave frequencies at 5,000 and 20,000 kilocycles per second. E. L. Hall.

RP221. Wind pressure on circular cylinders and chimneys. H. L. Dryden and George C. Hill.

RP222. Thermometric lag of aircraft thermometers, thermographs, and barographs. H. B. Henrickson.

RP223. Apparatus for the determination abroad ship of the salinity of sea water by the electrical conductivity method. Frank Wenner.

RP224. Note on the individualities of anyhdrofructose and difructose anhydride. R. F. Jackson and Sylvia M. Georgen.

Research papers are available as separates for purchase from the Superintendent of Documents United States Government Printing Office, Washington, D. C.

U. S. DEPARTMENT OF COMMERCE
R. P. LAMONT, Secretary
BUREAU OF STANDARDS
GEORGE K. BURGESS, Director

BUREAU OF STANDARDS JOURNAL OF RESEARCH

December, 1930
Vol. 5, No. 6

UNITED STATES
GOVERNMENT PRINTING OFFICE
WASHINGTON : 1930

For sale by the Superintendent of Documents, Washington, D. C. - Price 40 cents; $2.75 Per Year on Subscription

For a partial list of previous research papers appearing in BUREAU OF STANDARDS JOURNAL OF RESEARCH, see pages 2 and 3 of the cover

FURTHER STUDY OF PAPER-COATING MINERALS AND ADHESIVES

By Merle B. Shaw, George W. Bicking, and Martin J. O'Leary

ABSTRACT

Owing to the interest manifested among manufacturers in the investigation on Use of Glue in Coated Paper, Technologic Paper No. 323, other coating materials have recently been studied to keep the public informed of new developments in raw materials and promote the use of domestic resources. Four different clays, 2 foreign and 2 domestic, and 1 commercial compound of diatomaceous earth were the minerals employed. The domestic clays were from the same mine, but had received different refining treatment. One had been washed only; the other, chemically treated and washed. Three types of high-grade commercial adhesives—casein, glue, and modified starches—were used. The tests were confined to papers suitable for high-grade printing. The coating procedure was similar to commercial practice.

Present methods of refining American clay have improved its color, fineness, and suspension quality. The American clay that had been chemically treated and washed compared favorably in the tests with the foreign clays as paper-coating mineral. The coatings showed about the same differences in color as the clays themselves. The clay coatings were well bound to the fiber sheet and were of very good printing quality. The coating with the diatomaceous earth compound did not adhere well to the base paper.

It is doubtful whether the modified starches had quite as strong adhesive quality as the casein or glue, but all coatings containing 18 parts of starch per 100 parts of clay were well bound to the body papers. Graded as to their clay suspending property the adhesives were in the following descending order—starch, casein, and glue. There appeared to be no appreciable difference in the adhesives so far as their effect on the color of the coatings was concerned. When the coated papers were printed by the half-tone process equally good results were obtained with the three different adhesives, although the starch-bound coatings may possibly have absorbed somewhat more ink.

The publication includes chemical analyses, color measurements, and settling data for the minerals used, description of the coating procedure, and various measurements on the finished coated papers.

CONTENTS

	Page
I. Introduction and résumé of previous work	1190
II. Materials used in the investigation	1190
1. Paper	1190
2. Coating materials	1191
(*a*) Minerals	1191
(*b*) Adhesives	1194
III. Equipment used	1194
IV. Coating procedure	1196
1. Preparation of coating mixture	1196
2. Coating	1196
3. Calendering	1197
V. Test results	1197
1. Coating of paper	1197
(*a*) Minerals	1197
(*b*) Adhesives	1200
2. Printing tests	1202
VI. Conclusions	1202

I. INTRODUCTION AND RÉSUMÉ OF PREVIOUS WORK

The characteristic feature of mineral-coated papers is a thin layer of mineral matter and adhesive applied to the surface of the fiber sheet. The function of the mineral matter is to fill in the irregularities of the surface of the sheet to form a smoother and more even surface than that obtained by the other paper-manufacturing processes, while the adhesive is added to bind the particles of mineral matter together and to the body of the paper. There are many grades and uses of coated papers, and the coating materials employed are chosen according to the use for which the papers are intended. The tests described in the following pages, however, have been confined to papers for high-grade printing and lithographic purposes, for which a very even, semiabsorbent surface is required.

An investigation was previously made at the bureau to obtain data on the use of glue as adhesive in such types of coated paper. The work is fully described in Bureau of Standards Technologic Paper No. 323,[1] published in 1926. Consideration was given to the factors which materially influence the quality and price of the glue, and the printing quality of glue-bound coated papers. Eight different glues were used, with clays, satin white, and blanc fixe as the coating minerals.

Owing to the interest manifested by manufacturers in the previous work, other paper-coating materials have recently been studied to keep the public informed of new developments in raw materials and promote the use of domestic resources, which would become very important in the event of any disturbance limiting the supplies of foreign origin. The present paper describes these later tests, which are a continuation of the earlier work.

II. MATERIALS USED IN THE INVESTIGATION

1. PAPER

The base paper or body stock used for the coating tests was composed chiefly of sulphite pulp with some waste paper from experimental paper runs, and was medium rosin sized. The weight of the stock was approximately 54 pounds (500 sheets 25 by 40 inches in size). The paper was made on the Fourdrinier machine of the bureau's experimental paper mill, and was similar in its properties to that generally used in commercial coating mills.

The fibrous part of coated paper is sometimes regarded as a mere carrier of the coating and for this reason is sometimes very poor material. The quality of the body paper—its formation, cleanliness, color, and surface characteristics—is, however, of considerable importance. For good results in coating it is essential that the paper be well closed and the surface smooth and even. If it is too soft sized the coating mixture permeates too deeply and a poor bond between mineral and paper results. If it is too hard sized the coating will not adhere well to the surface. Freedom from surface dirt, specks, rosin, or lime spots, and other imperfections which may cause a local thinning or thickening of the coat is necessary to

[1] Use of Glue in Coated Paper, by George K. Hamill, V. H. Gottschalk, and George W. Bicking. Copies may be obtained from the Superintendent of Documents, Government Printing Office, Washington, D. C. Price 15 cents each.

insure uniform distribution of the coating on the body stock. The color of the base paper is a factor in the appearance of the coated sheet. The more nearly it corresponds to the color of the coating, the more satisfactory will be the results obtained.

2. COATING MATERIALS

(a) MINERALS

Four different coating clays—two foreign, two domestic—and a commercial compound of domestic diatomaceous earth,[2] designated herein as mineral No. 5, were the minerals employed. The foreign clays were graded as No. 1 and medium. The two domestic clays were from the same mine, but had received different refining treatment. One, clay A, had been washed only; the other, B, had been chemically treated, bleached, and washed. The following chemical analyses, color measurements, and settling data (Tables 1 to 3) give additional information on these materials.

TABLE 1.—*Chemical analyses of coating minerals* [1]

Constituents	Foreign clay		Domestic clay		Mineral No. 5
	No. 1	Medium	A	B	
	Per cent	*Per cent*	*Per cent*	*Per cent*	*Per cent*
Silica (SiO_2)	46.7	46.2	44.4	44.3	28.4
Iron oxide (Fe_2O_3)	.7	1.0	.4	.4	.4
Alumina (Al_2O_3)[2]	37.5	37.6	39.8	41.0	.8
Calcium oxide (CaO)	Trace.	Trace.	Trace.	Trace.	47.6
Magnesium oxide (MgO)	.3	.5	.5	.1	.7
Loss at 110° C. (2 hours)	.4	.3	.6	.4	2.2
Further loss on ignition	12.4	12.5	13.7	14.0	20.0
Specific gravity at 15.6° C[3]	2.71	2.75	2.67	2.70	2.63

[1] Analyses made by chemistry division, Bureau of Standards.
[2] Includes TiO_2, P_2O_5, Mn_3O_4 if present.
[3] Specific gravity determined by A.S.T.M. method D 153-27.

Clays consist of finely divided mineral matter, chiefly silica and alumina, derived from rocks by disintegration. They may be either residual or transported. The residual (or primary) clays are those which remain overlying the rocks from which they have been formed, and they are thus distinguished from transported (sedimentary or secondary) clays, which have been carried from their place of origin by eroding influences and redeposited. Because of the largeness of the deposits and their residual character, foreign clays are in their natural state considered homogeneous. The majority of American clays are transported and, therefore, may contain more impurities. For this reason more attention in refining is needed for the American clays, but by modern improved methods of handling and purification, the extraneous substances are reduced to a satisfactory minimum, and the American clays now available are greatly improved.

As shown in the chemical analyses of Table 1, the domestic clays tested were similar to the foreign clays in composition. Mineral No. 5 had a very high lime content. The low moisture content of the

[2] Fine powder obtained from the accumulated deposits of diatoms, microscopic unicellular algæ remarkable for their silicified cell walls, which persist after the death of the organism.

clays, "loss at 110° C.," was doubtless due to the fact that they had been kept in a dry place for a considerable time before the tests. Under "further loss on ignition" is given the loss chiefly of chemically combined water and organic matter.

The color or degree of whiteness is important in the selection of minerals for use in high-grade papers. A Pfund colorimeter [3], which gives numerical values as a basis for comparison, was used to determine the color characteristics reported in Table 2 and shown graphically in Figure 1. Magnesium oxide was included with the samples in order to give a value of white for comparative purposes.

TABLE 2.—*Color measurements of coating minerals* [1]

	Brightness values		
	Blue (wave length 460 mμ)	Green (wave length 550 mμ)	Red (wave length 625 mμ)
Magnesium oxide [2]	0.871	0.928	0.937
Foreign clay No. 1	.791	.850	.870
Foreign clay medium	.750	.812	.834
Domestic clay A	.753	.838	.876
Domestic clay B	.807	.901	.922
Mineral No. 5	.763	.834	.869

[1] Measurements made by R. E. Lofton, Bureau of Standards.
[2] Magnesium oxide was included for comparison.

The color characteristics are shown in terms of the relative brightness of the three primary components—blue, green, and red. If the sample being tested were truly color neutral, "white" or gray, it would reflect nonselectively and the brightness values for the three colors would be the same. The color curve would be a straight, horizontal line, but since white has a higher brightness value than gray the curve for white would be higher on the vertical scale. As the color becomes more selective; that is, shows a tint or dominant hue, the values for the reflection coefficient diverge.

As shown in Figure 1 the domestic clays are somewhat more deficient in blue (that is, are more yellowish) than the foreign clays, but higher in brightness. The refining treatment given clay B improved its color characteristics. If a small amount of blue dye were added with the clay, it would doubtless be as good in color as the foreign clays. Its color curve would then be more nearly horizontal, but the brightness values would be somewhat lower.

The relative rates of settling from water suspensions are shown for the different clays in Table 3 and Figure 2. Using a water-clay ratio of 19.6 to 1, 200 ml of clay slip (clay content, 10 g) was placed in a graduated glass cylinder and the volume of clear supernatant liquid determined at various times. No electrolyte was added to deflocculate the clays.

The curves of Figure 2 afford a fairly accurate comparison of the fineness of the clay particles. The washing and chemical treatment of clay B apparently removed some of the coarse particles. It may

[3] Pfund, A. H., A New Colorimeter for White Pigments and Some Results Obtained by Its Use, Am. Soc. for Test. Matrls.; June, 1920.

possibly also have developed some colloidal property which increased the suspending quality of the clay. Whereas domestic clay A settled comparatively rapidly, the settling rate and final volume of wet clay were practically the same for domestic clay B as for the foreign clays. Fineness of grain and good suspension quality are essential to a free-flowing coating slip that will spread well on the paper and have good covering power. It is believed a clay of fine particle size will also take a better finish.

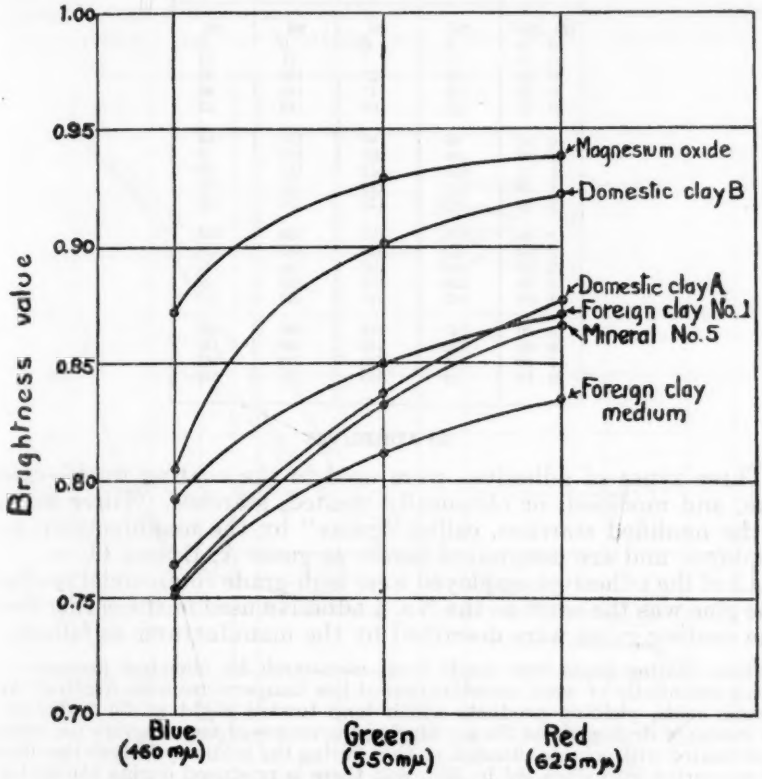

FIGURE 1.—*Color characteristics of coating minerals*

The water used for the slips had a pH value of 6.9, which is practically neutral. The pH of the clear liquid above the clay suspensions was 7.1 for foreign clay No. 1, 6.7 for foreign clay medium, 5.5 for domestic clay A, and 6.0 for domestic clay B; that is, the foreign clays were nearly neutral, whereas the domestic clays were somewhat acid in character. The corresponding value for the diatomaceous earth compound was 8.4.

TABLE 3.—*Rate of settling of clay in water*

(200 ml of clay slip; $\frac{W}{C}=\frac{19.6}{1}$)

Time interval	Clear liquid above clay suspension			
	Foreign clay		Domestic clay	
	No. 1	Medium	A	B
Hr. Min.	*ml*	*ml*	*ml*	*ml*
0 0	0	0	0	0
0 10	13	7	77	14
0 20	30	27	133	27
0 30	53	47	145	40
0 40	82	68	149	52
0 50	99	86	151	65
1 00	109	103	153	76
1 15	115	112	155	90
1 30	120	116	157	105
1 45	123	119	158	120
2 00	126	122	159	132
2 30	132	126	162	138
3 00	136	130	165	142
3 30	139	134	166	144
4 00	142	137	167	146
5 00	147	142	168	150
6 00	152	146	169	153
7 00	155	150	170	155
24 00	162	160	171	164

(b) ADHESIVES

Three types of adhesives were used in the coating work—casein, glue, and modified, or chemically treated, starches. Three samples of the modified starches, called "gums" by the manufacturer, were employed and are designated herein as gums A, B, and C.

All of the adhesives employed were high-grade commercial products. The glue was the same as the No. 4 adhesive used in the earlier work.[4] The coating gums were described by the manufacturer as follows:

> These coating gums were made from cornstarch by chemical processes consisting essentially of weak esterification at low temperature with relatively weak organic acids, yielding products which tend toward slight acidic hydrolysis in the course of drying of the films. During the course of manufacture the starches were treated with soluble silicates, so that during the acidic hydrolysis the silicates are converted into silica gel in situ, and there is produced during the drying of the adhesive in contact with the clay coat, a combination of starch and silica gel. The silica gel assists in the bonding of the starch and clay and renders the coat somewhat more resistant to the leaching effects of water than is obtainable with the ordinary types of soluble starches previously used for such purposes.

All of the adhesives possessed the qualities given in Technologic Paper No. 323 as desired in adhesives for coating purposes, namely:

> Minimum of insoluble matter, such viscosity as to permit the use of ordinary equipment at the desired dilution of the coating mixture and within the temperature range of working conditions, high adhesiveness, good clay-suspending power, minimum of foam-causing impurities and grease.

III. EQUIPMENT USED

The paper mill of the bureau is equipped for coating paper on a semicommercial scale under practical mill conditions. The equipment

[4] B. S. Tech. Paper No. 323, p. 647.

employed consists of a 14-inch Waldron flat-bed brush coater with festoon dryer and rewinder, mixing tanks with power-driven agitators of the wooden-gate type, and a 5-roll supercalender.

The coating machine is the "single" coater type, applying the coating substance to but one side of the paper. It has 6 brushes, 2 rotating and 4 having a laterally reciprocating movement, to spread and smooth the coating material. The brushes, the first of which consists of comparatively coarse bristles and the last of fine, are placed in the following order: One rotating which applies the coating substance, one working across the surface of the paper with a reciprocating motion, another rotating, and three more reciprocating, the

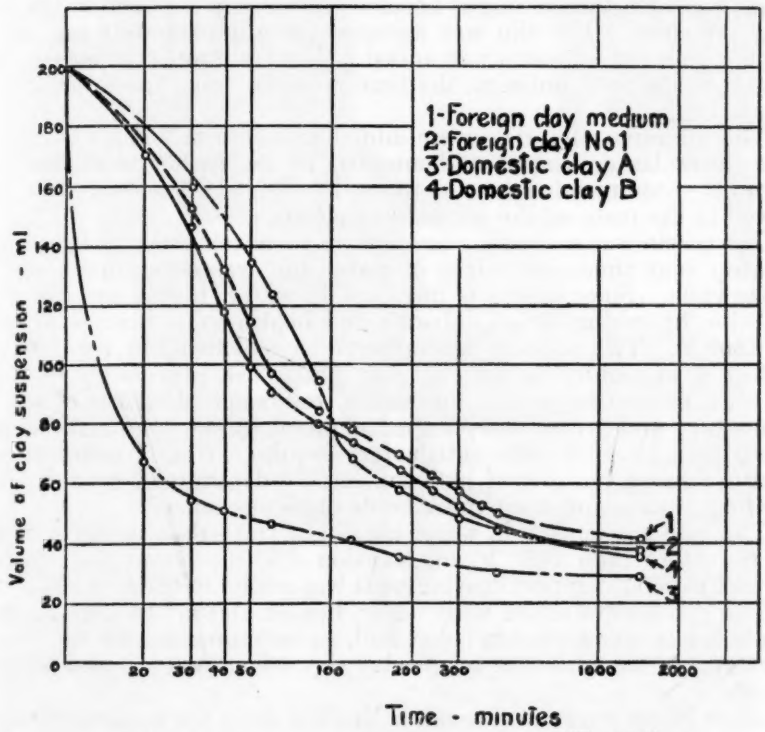

FIGURE 2.—*Rate of settling of clay in water* $\left(\frac{W}{C}=\frac{19.6}{1}\right)$

last having very fine badger bristles to eliminate any remaining marks made by the coarser ones. The pressure of the brushes on the paper can be adjusted so as to distribute the coating materials uniformly and smoothly over the paper.

The festoon rack is 15 feet long and has a capacity of 28 loops, each 6 feet in length. With the uptake rack and the rack from the festoons to the reel, the capacity of the dryer is approximately 400 lineal feet. The dryer is inclosed in a cabinet equipped for air conditioning and temperature control. The photograph of Figure 3, however, was made before the cabinet was installed.

The mixing tanks used for preparing the coating mixtures are shown in Figure 4.

The supercalender (fig. 5) is equipped to calender paper either in the web or in sheets. The drive is such that the calender can be run at almost any speed desired. The lever-weight arms are raised or lowered hydraulically. The calender is supplied with 3 steel and 3 cotton rolls, so that the rolls can be alternated or the 3 cotton rolls can be used together.

IV. COATING PROCEDURE

1. PREPARATION OF COATING MIXTURE

The clay used in the coating mixtures was soaked in water overnight in order that it might become thoroughly wet before the slip was prepared. The slip was agitated for approximately one hour, after which the adhesive was added. The resultant coating mixture was agitated until uniform, the time required being from one to two hours.

The adhesive materials were added in solution. The casein and glue formulas developed and adopted in the earlier work and the formula recommended for the gums by the manufacturer were followed in the tests on the respective materials.

The casein was soaked for one hour at room temperature in approximately four times its weight of water and was occasionally stirred meanwhile. Since casein is insoluble in water, it was brought into solution by adding alkali solvents and heating the mixture to 130° to 150° F. The solution was allowed to cool to room temperature before it was added to the clay slip. Soda ash is probably the best solvent, or cutting alkali, for casein, but small amounts of borax, ammonia, and trisodium phosphate (alone or in combination) are used by mills with very satisfactory results. Nearly every manufacturer has a formula of his own, largely determined by the mill's coating process and the requirements of its customers.

The glue was soaked in water overnight and subsequently warmed to not more than 135° F. for solution. The solution was allowed to cool to room temperature before it was added to the clay slip.

The gums were mixed with water, heated at 185° to 190° F. until the solution was amber in color, and, as recommended by the manufacturer, added while hot to the clay slip, which was at room temperature.

After being screened through a No. 200 sieve the coating mixtures were ready to be applied to the body paper. The small scale coating equipment employed did not permit using the relatively high concentration used with commercial equipment, therefore, the mixtures were of lower concentration and the coatings obtained were consequently of comparatively light weight.

2. COATING

The coating procedure was similar to the commercial practice used in applying a single coating to paper. A roll revolving in the prepared coating mixture transferred the coating substance to a revolving brush, which, in turn, applied it to the surface of the paper. By means of the series of brushes pressing against the paper as it passed over the flat bed of the machine, the mixture was immediately smoothed out and brought into good contact with the paper. After leaving the brushes the paper was hung in a series of festoons or loops and

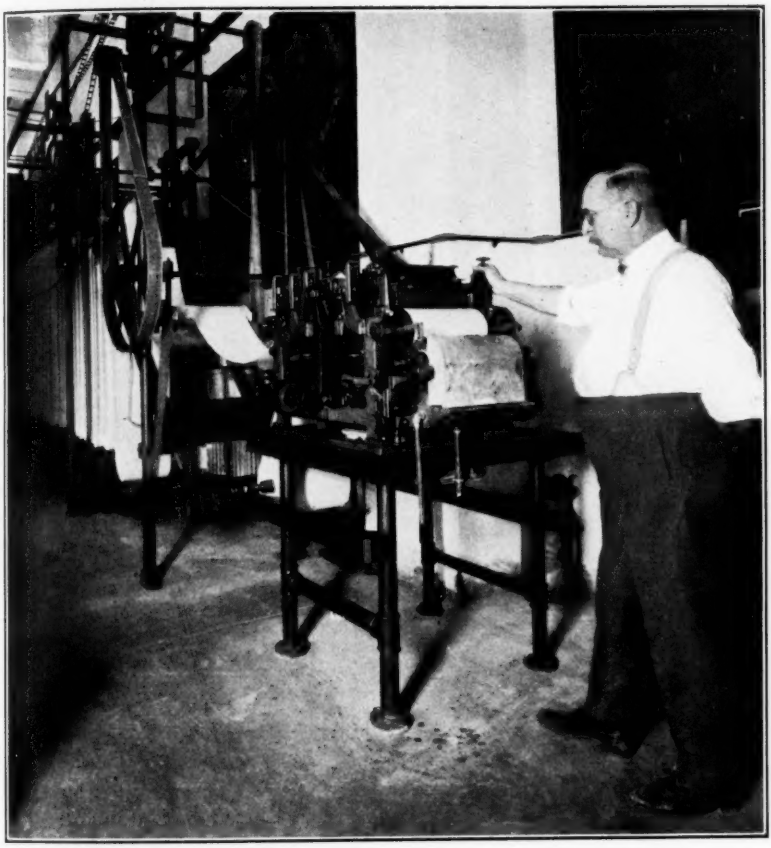

FIGURE 3.—*Paper coating machine (without drying cabinet)*

Paper shown festooned for drying.

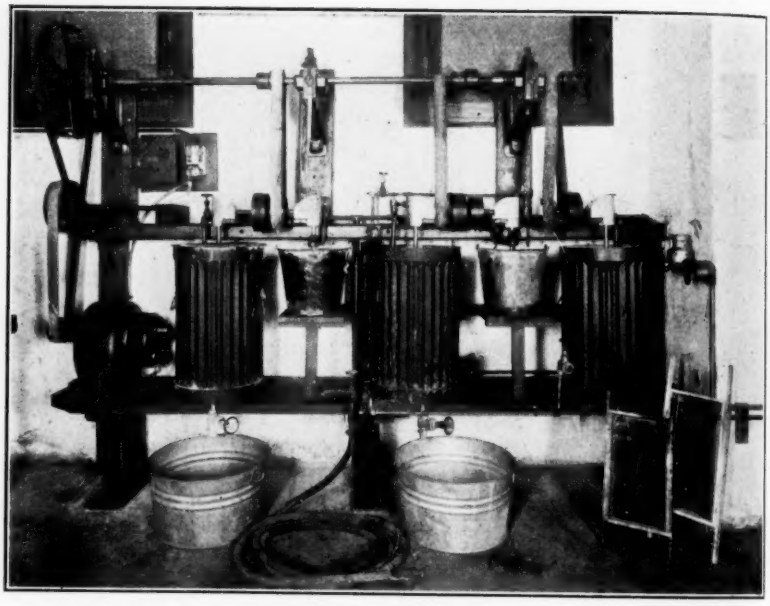

FIGURE 4.—*Mixing vessels*

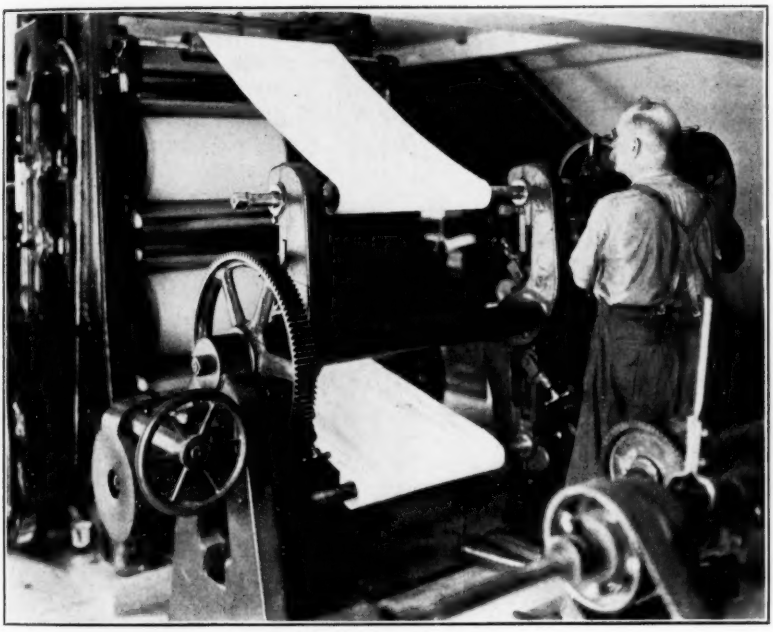

FIGURE 5.—*Supercalender*

carried along on an overhead trackway through the drying gallery, heated by hot air rising from near the floor, and then reeled up ready for calendering.

In order to sufficiently dry the coated paper in the short time required for it to pass through the cabinet, it was necessary to shut off the humidifying feature of the equipment. The moisture content of the paper entering the cabinet was approximately 35 per cent, and the interval permitted for drying was about 10 minutes (for 400 feet). If the paper admitted had been low in moisture content or could have been left longer to become dry and conditioned, the automatic humidity control would have been used. The temperature of the drying cabinet was from 110° to 120° F., but the paper was kept comparatively cool by the rapid evaporation caused by the large volume of warm air circulated from beneath.

3. CALENDERING

A combination of alternate steel and cotton rolls was used in calendering the paper, which was passed through in the web. No attempt was made to obtain a high glossy finish, the smoothness imparted by light calendering being sufficient for high-grade printing except for special cases.

V. TEST RESULTS

1. COATING OF PAPER

(a) MINERALS

The clays worked satisfactorily with the different adhesives. No attempt was made, however, to determine the minimum amount of each adhesive that could be used with them. The suspension quality of the clays was good, the coating mixtures screened satisfactorily, and the slips were spread without difficulty by the coating machine. Nearly any finish desired could have been obtained in the calendering but 70 per cent gloss [5] was the finish arbitrarily adopted.

The measurements on the coated papers are given in Table 4.

[5] The gloss of the finished papers was determined according to the Paper Testing Methods published by the Technical Association of the Pulp and Paper Industry, 18 East Forty-first Street, New York, N. Y.

TABLE 4.—*Coating mixtures and measurements on the finished coated papers* [1]

Run No.	Coating mixture: Mineral: Kind	Mineral: Amount	Water added to mineral	Adhesive: Kind	Adhesive: Amount	Water added to adhesive	Ratio of water to solids [2]	Density [3]	Coated paper: Weight (25 by 40 inches, 500 sheets): Body stock	Weight: Coated paper	Color measurements (Brightness values): Blue (wave length 460 mμ)	Green (wave length 550 mμ)	Red (wave length 625 mμ)	White [4]	Gloss
		g	*g*		*g*	*g*		*Sp. gr. °F.*	*Pounds*	*Pounds*					*Per cent*
133	Foreign clay No. 1	2,000	2,500	Casein	350	1,500	1.9–1	1.24 at 77	54.2	68.2	0.769	0.864	0.912	0.867	66.7
134	do	2,000	2,500	do	350	1,500	1.9–1	1.24 at 76	54.2	67.6	.778	.871	.923	.878	66.7
143	do	2,000	2,500	Glue	250	2,000	2.0–1	1.24 at 81	54.2	65.4	.765	.858	.907	.868	74.6
149	do	2,000	3,000	Gum A	480	1,500	2.2–1	1.20 at 80	54.2	68.4	.756	.854	.914	.872	64.8
151	do	2,000	3,000	Gum B	480	1,500	2.0–1	1.25 at 89	54.2	73.4	.755	.853	.909	.870	72.9
152A	do	2,000	3,000	do	360	1,500	2.1–1	1.23 at 89	54.2	66.2	.767	.858	.908	.873	69.7
152B	do	2,000	3,000	do	360	1,500	2.4–1	1.20 at 80	54.2	62.6	.762	.853	.913	.874	70.5
153A	do	2,000	3,000	do	240	1,000	1.8–1	1.27 at 88	54.2	70.1	.783	.861	.920	.881	76.4
153B	do	2,000	3,000	do	240	1,000	2.2–1	1.22 at 88	54.2	63.6	.786	.864	.922	.878	69.5
135	Foreign clay medium	2,000	2,500	Casein	350	1,500	1.9–1	1.25 at 76	54.2	63.5	.756	.858	.906	.863	67.7
136	do	2,000	2,500	do	350	1,500	1.9–1	1.25 at 78	54.2	70.9	.751	.857	.899	.865	72.9
137	do	2,000	2,500	do	350	1,500	1.9–1	1.24 at 82	54.2	68.9	.747	.850	.898	.858	69.7
144	do	2,000	2,500	Glue	250	2,000	2.0–1	1.24 at 83	54.2	65.5	.741	.848	.896	.853	74.8
138	Domestic clay A	2,000	2,500	Casein	350	1,500	1.9–1	1.25 at 77	54.2	72.3	.752	.867	.913	.869	72.2
139	do	2,000	2,500	do	350	1,500	1.9–1	1.24 at 80	54.2	70.3	.742	.853	.907	.862	71.7
142	do	2,000	2,500	do	350	1,500	1.9–1	1.24 at 80	54.2	67.3	.741	.858	.912	.870	71.7
156	do	2,000	3,000	do	350	2,000	2.3–1	1.20 at 87	54.2	62.3	.763	.861	.924	.878	69.0
145	do	2,000	2,500	Glue	250	2,000	2.0–1	1.24 at 82	54.2	65.2	.743	.850	.900	.865	77.7
147	do	2,000	3,000	do	250	2,500	2.4–1	1.20 at 83	54.2	63.5	.742	.850	.908	.864	75.2
148A	do	2,000	3,000	do	250	2,000	2.2–1	1.22 at 82	54.2	68.2	.752	.852	.917	.874	66.7
148B	do	2,000	3,000	do	250	2,000	2.4–1	1.20 at 82	54.2	63.8	.747	.855	.916	.868	69.2
155	do	2,000	3,000	do	250	1,000	2.4–1	1.20 at 84	54.2	62.6	.755	.863	.924	.880	74.8
150A	do	2,000	3,000	Gum A	480	1,500	2.4–1	1.23 at 85	54.2	68.7	.732	.848	.912	.870	64.3
150B	do	2,000	3,000	do	480	1,500	2.4–1	1.23 at 85	54.2	61.9	.747	.855	.918	.871	64.0
150C	do	2,000	3,000	do	480	1,500	2.6–1	1.19 at 80	54.2	61.6	.742	.850	.914	.868	61.6
154	do	2,000	3,000	do	360	1,500	2.3–1	1.21 at 84	54.2	66.2	.728	.850	.912	.875	71.0
157	do	2,000	3,000	do	360	1,500	2.3–1	1.22 at 88	[5] 52.9	65.6	.682	.773	.827	.790	68.5

159	Domestic clay B	2,000	3,000	Casein	350	1,500	2.3–1	1.21 at 80	[5] 52.9	66.0	.685	.769	.822	.787	70.0
165	do	2,000	3,000	do	300	1,500	2.3–1	1.21 at 80	[5] 52.9	66.0	.671	.756	.815	.778	71.2
158	do	2,000	3,000	Glue	250	2,000	2.4–1	1.20 at 80	[5] 52.9	63.4	.672	.755	.810	.768	71.2
160	do	2,000	3,000	do	250	2,000	2.4–1	1.22 at 80	[5] 52.9	67.4	.688	.767	.820	.777	71.5
161	do	4,000	7,000	Gum B	720	3,000	2.3–1	1.22 at 80	[5] 52.9	69.1	.671	.761	.813	.769	76.6
163	do	2,000	3,000	do	360	2,000	2.3–1	1.21 at 80	[5] 52.9	70.0	.675	.766	.812	.785	72.4
164	do	2,000	2,500	do	360	3,000	2.5–1	1.20 at 84	[5] 52.9	66.1	.665	.752	.808	.767	69.5
166	do	2,000	3,500	do	360	2,000	2.3–1	1.22 at 85	[5] 52.9	66.1	.670	758	.820	.785	69.5
162	do	4,000	7,000	Gum C	720	3,000	2.1–1	1.23 at 80	[5] 52.9	69.5	.672	.754	.808	.768	76.2
------	Mineral No. 5 [6]														

[1] Color and gloss measurements made by W. L. Holt, Bureau of Standards.
[2] Solids include coating mineral, adhesive, and chemicals used in the coating mixture.
[3] Specific gravity determined by hydrometer method.
[4] Measurements made without color filter.
[5] Body stock for these tests different from that for the preceding.
[6] Results obtained with mineral No. 5 were unsatisfactory, as shown in text, therefore, measurement on the papers coated with this mineral were not made.

As indicated in the table the coatings showed about the same differences in color as the clays themselves; that is, the coated paper for which domestic clay B was used was somewhat better in color than that coated with sample A, and compared favorably with the color of the papers coated with the foreign clays. There appears to be no appreciable difference in the adhesives so far as their effect on the color of the coatings is concerned. Since starch is comparatively a very white material it might be expected to affect the color least, with casein and glue following in order, but these differences were not shown in the measurements. The weight of the single coat applied was approximately from 10 to 15 pounds on a basis paper 25 by 40 inches, 500 sheets.

Mineral No. 5 is primarily a ceramic material, but because of its softness and fineness was thought to be a possible coating mineral. Casein and glue were used as the adhesives in the coating tests. When the casein mixture was added to the slip of mineral and water the resultant mixture was very fluid, whereas when the glue solution was added to the mineral slip the mixture was very thick and plastic. The coating did not hold well; that is, could be easily picked off. It was thought that the loss of binding quality of the adhesive was caused by the alkalinity of the mineral matter. (The chemical analysis, p. 1191, shows the lime content of the mineral to be very high.

It was thought that the addition of alum might give a product having some of the characteristics of satin white (a prepared compound of aluminum sulphate and lime used as coating material), therefore, preliminary tests were made to determine the amount of alum required to neutralize the alkalinity of the mineral. For 100 g of mineral 200 g of alum was needed to make the mixture neutral. Coating runs were made, but the binding quality of the coat was still unsatisfactory.

It is believed that mineral No. 5 is unsatisfactory for use as a coating material when casein or glue is used as adhesive and handled in accordance with the usual coating procedure. There is a possibility that with a special adhesive, one that could be employed when considerable alkali (lime) is present, it might be suitable for coating use.

The color of mineral No. 5 is not so good as most grades of coating clays. The greater cost of the material as compared with good grades of clay would also doubtless be a deciding factor in its use for paper coating.

(b) ADHESIVES

The amount of casein employed was, except in one case, 17.5 per cent, and of glue 12.5 per cent, based on the weight of the mineral being used. The results attributable to these materials were very satisfactory, and duplicated those previously obtained. (Tech. Paper No. 323.)

In the work with the starches two different proportions of gum A, 24 and 18 per cent, based on the clay content, were employed. No trouble was experienced in the tests (runs Nos. 149, 150, 154, and 157) and the adhesive quality of the gum, as judged by the sealing wax pick test,[6] which approximates the sort of surface pull received by the paper in the printing operation, was satisfactory.

[6] The end of a stick of sealing wax is softened by warming and then applied with firm pressure to the coating. With the paper held down firmly on either side of the wax, the stick is drawn away from the paper by a steady vertical pull. If fibers from the body stock adhere to the wax, it is an indication that the coating is firmly bound and should not pick off in the printing process. The test is comparative only, and requires that the area of contact between wax and paper be the same for all samples to be compared.

In the first series of runs with gum B (Nos. 151 to 153) 24, 18, and 12 per cent of gum, respectively, were used. There seemed to be a tendency for the gum solutions to jell after being added to the clay slip. Small jell particles remained in the coating mixture even after it had been screened through a No. 200 sieve. Spots of localized variations in thickness and translucency ("bird's-eyes") were noted in the coated papers and were thought probably to have been caused by the jell particles. Graded in regard to the degree of adhesion of the coating to the body stock, the papers were in the same relative order as the amounts of gum used.

A greater quantity of water was used in preparing the gum mixture for the next runs with gum B. Whereas the ratio had been 1 part of gum to 4 parts of water in the previous runs, for runs Nos. 163 and 164, 6 and 8 parts of water, respectively, were used. It was believed that the greater dilution might prevent the formation of jell particles, but the coating was no better than that obtained when 4 parts of water were used.

In the belief that the chemical preparation of the gum might be such that when the mixture is agitated a comparatively long time the jell develops in the slip rather than on the paper during the coating and drying processes, the coating mixture for the next run (No. 168) was agitated for a shorter time, and the interval between the adding of the gum to the clay slip and the application of the coat to the paper was briefer. There was no formation of jell in the coating mixture before it was applied to the paper, and none of the trouble experienced in the previous tests was encountered.[7]

[7] Since the tests were made it has been found that the tendency for the gum to jell during the agitation of the clay mixture can be eliminated also by increasing the hydroxyl ion concentration of the coating mixture. Reports to the bureau of subsequent commercial mill tests stated the following:

"In light of the experience gained at the Bureau of Standards, where the pH of the coating mixture was approximately 8, it was found desirable in commercial mill tests to cook the gum at a higher pH or basicity. In the commercial runs one-half per cent, based on the weight of gum, of 26° Bé. ammonia was added to the water in which the gum was to be cooked, and the gum was thoroughly stirred in the water before the direct steam was admitted for cooking. The heating was either continued for a longer period or at a slightly higher temperature (approximately 195° to 205° F.) than was used at the Bureau of Standards. It was found preferable to judge the completion of the cooking by the color reaction of the gum, which was a deep amber when the cooking was completed. It is believed that the gum has better binding quality when handled this way.

"Further commercial experience showed that it is preferable to add from one-fourth to one-half per cent, based on the clay, of 26° Bé. ammonia to the water in which the clay is stirred, as this makes an improvement in the final coating mixture, in addition to helping to smooth down the clay. When the hot gum solution is added the pH of the resulting coating mixture is approximately 10.

"Operating on the above basis, the formula for commercial runs would be as follows:

Clay slip	Gum
100 pounds clay. 75 pounds water. One-fourth to one-half pound 26° Bé. ammonia.	18 pounds gum. 72 pounds water. 2 to 3 ounces 26° Bé. ammonia.

"Coating gums B and C have been successfully used commercially in coating also with mixtures of clay and satin white. Due to the fine state of subdivision of satin white and to its somewhat alkaline reaction a larger percentage of gum C should probably be used, depending upon the amount of satin white admixed with the clay. Unlike the procedure with casein as the adhesive, the clay satin-white slip should be at a fairly high temperature when the coating gum is added, as this provides the lower viscosity and a better spreading mixture.

"A typical formula for work with satin-white mixtures is as follows:

Clay satin-white slip	Gum
75 to 100 pounds water. 100 pounds clay. 200 pounds satin white.	228 pounds water. One-fourth pound ammonia (26° Bé.). 57 pounds coating gum.

Stir the clay satin-white mixture for two hours or until perfectly smooth and then add the solution of coating gum. To prepare the gum solution stir cold until gum is dispersed evenly, then apply heat by direct steam until 190° to 195° F. is reached, maintaining this or a slightly higher temperature for a sufficiently long period to produce a clear amber-colored solution. Cool the gum solution to 140° to 160° F. and add to the clay satin-white slip, stirring continually meanwhile. Then adjust the coating mixture to the necessary concentration and fluidity for application on the coating machine."

Gum C was used for run No. 162. The coating was very satisfactory.

The relative effect of the adhesive on the suitability of the coated papers for writing was shown in a general way by writing on the papers with a pen and ordinary blue-black ink and noting the ease with which the operation was effected and the definition of the lines. In each case the quality of the writing was satisfactory, but the casein-bound coatings offered the least resistance to the mechanical action of the pen, the effort required in execution being greatest where starch was the adhesive employed.

2. PRINTING TESTS

Printing tests were made at the Government Printing Office on the coated papers. The cooperation of the Government Printing Office in making the tests, which were an important part of the investigation, is gratefully acknowledged.

The experimental coated papers were substituted for the regular stock being printed by the half-tone process. No changes were made in the printing machine or the inks. The tests showed the coatings to be well bound to the body paper and of very good printing quality. Equally good results were obtained with the American and foreign clays and with the three different kinds of adhesives, although the starch-bound coatings may possibly have absorbed somewhat more ink. Both starch and glue coatings have generally been found to have less water resistance than casein coatings and, therefore, may possibly not be suitable for lithographic processes requiring a high degree of water resistance.[8]

VI. CONCLUSIONS

The tests indicate the following general conclusions relative to the materials studied.

1. Present methods of refining American clay have improved its color, fineness, and suspension quality. American clay that had been washed and chemically treated compared favorably with foreign clays as paper-coating mineral. Diatomaceous earth compounds having a large lime content are not satisfactory when the coating mixtures are prepared by the usual procedure.

2. Graded as to their clay-suspending property, the adhesives used are in the following descending order—starch, casein, and glue. Graded as to the suitability of the coatings for ink writing the apparent order is casein, glue, and starch.

3. Starch coating mixtures are not as free-flowing as mixtures in which casein or glue are used as the adhesive, but the starch mixtures used in the tests spread and brushed out satisfactorily.

4. It is doubtful whether modified starch has quite as strong adhesive quality as casein or glue, but all sheets of the foregoing tests containing 18 parts of starch per 100 parts of clay were entirely satisfactory in this respect, judged by either the sealing wax pick test or the printing experiments. Results reported for subsequent commercial tests were in agreement with those obtained at the bureau.[9]

[8] Reports on a variety of commercial printing tests indicate, however, that "the gum-bound coating does not readily leach off, and this feature seems to explain its adaptability to most lithographic work."

[9] Commercial printing tests on the commercially coated papers (footnote 7, p. 1201) were reported as satisfactory even for the papers for which 15 per cent of gum had been used, "even for multicolor work using tacky inks, including the tackiest solid black."

5. The surface of starch-bound coated papers appears to be more absorbent than that of papers for which glue or casein is used as adhesive for the mineral, and consequently ink may penetrate it to a greater extent. For this reason it might be expected that printings on the starch-bound coatings would tend to be blurred unless special care was used in the operation, but this tendency was not apparent in the printing tests on the experimental papers.

The manufacturer of some coated papers may wish to use casein in order to give his paper good printing quality regardless of whether the paper is dampened. A high degree of water resistance is not required for a large majority of printing papers, such as book, magazine, and catalogue, however, and starch-coated papers could apparently be used for these very satisfactorily.

6. Notwithstanding its lack of water resistance, modified starch has a number of attractive qualities. It is clean, does not have an unpleasant odor, and is cheap. When comparing the price of casein with that for glue or starch, the cost of solvents for the casein must also be taken into consideration, although in the case of starch, the greater percentage required reduces the cost differential somewhat.

WASHINGTON, September 30, 1930.

18296°—30——2

RP255

THE STRUCTURE OF THE SPECTRUM OF SINGLY IONIZED ZIRCONIUM

By C. C. Kiess and Harriet K. Kiess

ABSTRACT

Seventy-five per cent of the lines observed in the spark spectrum of zirconium have been classified as combinations between terms of the quartet and doublet systems of Zr II. The terms which have been found are in all cases those required theoretically for an atom with three outer electrons. All the terms, except one, which can possibly arise from configurations of the electrons when they occupy $4d$, $5s$, and $5p$ orbits have been found. Of the terms possible when one of the electrons removes to a $5d$ or $6s$ orbit only a few have been found, of which some form Rydberg series with the low terms. In all, 10 pairs of series-forming terms have been detected with either ^3F, ^1G, or ^1D of Zr III as limit. The results given by these different series for the distance between $a^4F_{1\frac{1}{2}}$, the lowest term of Zr II, and a^3F_2, the lowest term of Zr III, are very consistent, the mean value being 113,175 cm^{-1}, corresponding to an ionization potential of 13.97 volts for the ion Zr^+. The irregular doublet law shows a close parallelism between the term structures of the neutral Yt atom and the singly ionized Zr atom. The list of Zr II lines appearing in the sun is extended and includes lines which have not been observed in laboratory sources but may be calculated from permissible combinations.

CONTENTS

	Page
I. Introduction	1205
II. Experimental	1206
1. Wave lengths and intensities	1206
2. Zeeman effect	1207
III. Structure of the first spark spectrum	1209
1. The term systems	1209
2. The Zeeman effects	1233
3. Interpretation of the observed terms	1234
4. Series and ionization potential	1237
IV. Ionized zirconium in the sun	1238
V. Conclusion and acknowledgments	1240

I. INTRODUCTION

The analysis of the first spark spectrum of zirconium presented in this paper is a part of a general investigation of the spectra of this element in progress for more than a decade at the National Bureau of Standards. This investigation had as its object not only the accurate description of the spectra as far as the available spectrographic equipment at our disposal would permit, but also the discovery of the series relations which would reveal the structure of the spectra. As a first contribution in the completion of this research a previous paper [1] by one of us, presents lists of wave lengths from 2,100 A in the ultra-violet to 9,300 A in the infra-red which are characteristic of the Zr atom in its neutral and three ionized states.

[1] B. S. Sci. Papers, No. 548, 22, p. 47; 1927.

A second contribution, by Kiess and Lang,[2] presents an analysis of the spectra Zr III and Zr IV. In this paper the extreme ultra-violet portion of the spectrum as observed with a vacuum spectrograph is described, and the classification of the lines, as characteristic of the doubly and trebly ionized Zr atoms, is shown to be in strict accord with recent theories of spectral structure.

With the new wave-length data at our disposal, we soon found many pairs of lines separated by constant wave-number differences, which have since proved to be term separations of Zr I and Zr II. With the clue to the nature of complex spectra which was furnished by the work of Catalán [3] on Mn. and of Frl. Gieseler [4] on Cr, we were able to link together many of the constant difference pairs into more or less fragmentary multiplets. However, progress was slow, for there were no temperature classifications of the lines available at that time, and the interpretation of the anomalous Zeeman effect had not yet been found. So we turned aside from Zr for a while and devoted our attention to the spectrum of Ti for which temperature classifications were available, and in which we expected to find a small-scale pattern of the Zr regularities.

Following our work on Ti,[5] which in the meantime had been advanced as a result of Landé's [6] quantum theoretical interpretation of the anomalous Zeeman effect, we returned again to the Zr spectra. The Zeeman effects observed by Moore [7] were now interpretable, and, through the kindness of Dr. A. S. King, of the Mount Wilson Observatroy, we had an advance copy of the results obtained by him and Miss Carter [8] for the temperature classification of the Zr lines. Little difficulty was now experienced in placing most of the stronger lines into mutiplets of the quintet and triplet systems of Zr I [9] and of the quartet and doublet systems of Zr II.[10]

II. EXPERIMENTAL

1. WAVE LENGTHS AND INTENSITIES

When the analysis of Zr II had progressed far enough to account for nearly all the strong lines in the published tables of wave lengths, it was seen that additional observations in the ultra-violet shorter than 2,100 A were desirable. The Hilger E_1 quartz spectrograph of the Bureau of Standards was, therefore, adjusted to record the region down to 1,900 A, and new observations were obtained with it of both the arc and spark spectra. In addition to these prism spectrograms, a few more were obtained with the spectrograph carrying the concave grating ruled with 20,000 lines per inch. The wave lengths derived from these more recent plates have been averaged with those already published in the lists referred to above, and are presented in the second column of Table 2 of this paper. This list of wave lengths supersedes that published in the earlier paper. Faint lines omitted from Table 2, but present in the earlier list have been found to be

[2] B. S. Jour. Research, **5**, p. 305; 1930.
[3] Phil. Trans. Roy. Soc., **A 223**, p. 127; 1922.
[4] Ann. der Physik (IV) **69**, p. 147; 1922.
[5] J. Opt. Soc. Am. & Rev. Sci. Inst., **8**, p. 607; 1924
[6] Zeit. für Physik, **15**, p. 189; 1923.
[7] Astrophys. J., **28**, p. 15; 1908.
[8] Astrophys. J., **65**, p. 86; 1927.
[9] Popular Astronomy, **31**, p. 647; 1923; **33**, p. 255; 1925.
[10] J. Opt. Soc. Am. & Rev. Sci. Inst., **12**, p. 427; 1926; **14**, p. 140; 1927.

spurious or are due to impurities. The letters *b* and *B* following the intensity estimate indicate that the line is nebulous, and the letter *l* that it is asymmetrically shaded toward the red. Some of these asymmetrical lines closely resemble unresolved band heads, but there is no evidence of band structure on the plates.

Some of the newer spectrograms were given prolonged exposures so that a finer discrimination could be made of the intensities than is to be found in the published lists. On the grating spectrograms all the strong lines show ghosts of the Rowland type. In a study of the ghosts produced by the Bureau of Standards gratings [11] the ratio of the intensities of parent line to first ghost was set equal to 10:1 for the first order spectrum, and 10:3 for the second order spectrum. Lines which were not strong enough to show ghosts were assigned intensities ranging from 0 to 9. Lines with ghosts of intensity 0 to 1 were assigned an intensity 10. The intensities of all stronger lines were obtained by multiplying the estimated intensities of their ghosts by the above ratios. The intensity scale for the prism spectrograms was obtained from the scale set up for the grating plates in the region from 2,200 A to 3,100 A, which was photographed by both spectrographs. The intensities thus derived are entered in Table 2, where they are compared with similar estimates made by King from arc sources.

2. THE ZEEMAN EFFECTS

New observations of the Zeeman effect have also been made for this investigation. In 1924 the late Prof. B. E. Moore, of the University of Nebraska, made for us several exposures with the magnet and spectrograph of the Brace Laboratory. They were made on long strips of Eastman ordinary and panchromatic films and covered the region from 7,000 A in the red to 3,200 A in the ultra-violet. The source employed by Moore was a spark maintained by a 5,000-volt transformer between electrodes of carbon which had been impregnated with zirconium solutions. The field strengths were of the order of 28,000 gausses/cm^2 and were derived from measurements of the sodium D lines and the calcium H and K lines which appeared as impurities on the films. All the films were measured and reduced at the Bureau of Standards.

Quite recently the Bureau of Standards obtained a water-cooled electromagnet of the Weiss type. Preliminary experiments with it in conjunction with the large grating spectrograph have given some very excellent results for several elements, including zirconium. The source was a condensed spark maintained by a 2,500-volt transformer between metallic Zr electrodes mounted in brass holders. With a current of 150 amperes on the magnet a field strength of 32,300 gausses/cm^2 was attained with a 7 mm gap between the poles. Both the parallel and normal components were obtained in juxtaposition on the spectrograms by means of a Wollaston prism. The zinc and copper impurity lines which appeared on the plates proved very useful in calculating the field strength. The region covered by these recent observations extended from 4,100 A to 5,900 A in the second order of the spectrograph. Some ultra-violet lines of the overlapping third order spectrum were thus obtained.

[11] J. Opt. Soc. Am. & Rev. Sci. Inst. **6**, p. 417; 1922.

To secure additional Zeeman effects for lines in the ultra-viole some observations were made with the Hilger E_1 quartz prism spectrograph also. The resolving power of this instrument is only third that of the large grating spectrograph and, therefore, the result obtained with it do not attain very high accuracy. Nevertheless Shenstone and Blair [12] have found such Zeeman effects observed by them with a similar instrument quite serviceable in the interpretatio

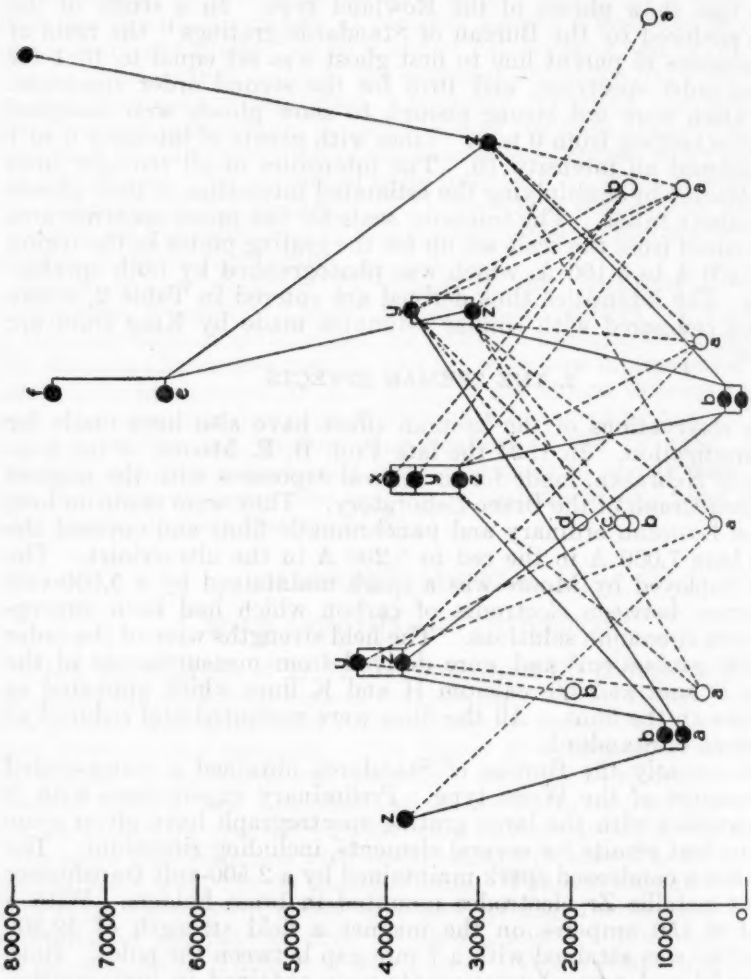

FIGURE 1.—*Term diagram of the quartet system of Zr II*

of Ag II and other spectra. The exposure times are short, ranging from a few seconds for the most intense lines to 5 or 10 minutes for lines listed in Table 2 as of intensity 3. This fact makes it possible to use higher currents on the magnet and narrower gaps between the pole pieces, thereby securing the additional resolution of the magnetic pattern afforded by stronger fields. With a current of 160 amperes

[12] Phil. Mag. (VII), 8, p. 765; 1929.

nd a 5 mm gap between the poles a field strength of 35,500 ausses/cm² was maintained. The Zeeman effects thus obtained this investigation lie between wave lengths 3,061 A and 2,449 A, nd are appropriately marked in Table 2 with the suffix E_1.

III. STRUCTURE OF THE FIRST SPARK SPECTRUM

1. THE TERM SYSTEMS

It was mentioned above that the first regularities detected in the r spectra were pairs of lines separated by constant wave-number ifferences. Of these, $\Delta\nu = 559.5$ and 448.8 were observed to link gether many of the strong lines in the near ultra-violet. Even- ually these $\Delta\nu$'s were found to be characteristic of a low ^4F term in ombination with higher D, F, and G terms of the quartet system. n fact, the four lines at wave lengths 3,572.47, 3,496.18, 3,438.23, nd 3,391.96, which were designated by de Gramont [13] as the *raies ltimes* of Zr in the photographic region, constitute the principal iagonal of the multiplet $^4F - {}^4G°$. The theoretical interpretation f the spectrum, given below, confirms de Gramont's characterization f these lines.

With the basic term of the spectrum established, it was soon ossible to locate the low ^4P terms and the second low ^4F term. The dentity of these terms was verified by the Zeeman effect. The oublet system was more difficult to unravel, but several well-ob- rved Zeeman patterns in Moore's list enabled us to fix with cer- inty the low P, D, F, and G terms, and to connect them with the uartet terms already found. Of the doublet terms a^2D is lowest, ring in the term diagram just above the second of the low ^4F terms. he terms which have been found to account for the spectrum of r^+ are given in Table 1. Figures 1 and 2 show graphically the rela- ons between these terms. The symbols used in defining the terms re those recently proposed as standard by Russell, Shenstone, and urner.[14]

[13] Compt. Rend., **166**, p. 365; 1918.

[14] Phys. Rev., **33**, p. 900; 1929.

TABLE 1.—*The terms of Zr II*

Term	*a*	*b*	*c*	*d*	*z*	*y*	*x*	*w*	*v*	*e*	*f*	*g*
$^4H_{6½}$										79, 280. 30		
										81. 95		
$^4H_{5½}$										79, 198. 35		
										350. 63		
$^4H_{4½}$										78, 847. 67		
										269. 82		
$^4H_{3½}$										78, 577. 85		
$^4G_{5½}$					30, 795. 74							
					955. 87							
$^4G_{4½}$					29, 839. 87							
					930. 83							
$^4G_{3½}$					28, 909. 04							
					955. 21							
$^4G_{2½}$					27, 983. 83							
$^4F_{4½}$	1, 322. 91	3, 757. 66			31, 866. 49	38, 644. 12				64, 901. 71	76, 593. 58	
	558. 47	*458. 02*			*617. 21*	*1, 214. 36*				*553. 43*	*584. 53*	
$^4F_{3½}$	763. 44	3, 299. 64			31, 249. 28	37, 429. 76				64, 368. 28	76, 009. 05	
	448. 77	*404. 59*			*697. 80*	*560. 76*				*499. 85*	*665. 48*	
$^4F_{2½}$	314. 67	2, 895. 05			30, 551. 48	36, 869. 00				63, 868. 45	75, 343. 57	
	314. 67	*322. 84*			*773. 88*	*417. 21*				*265. 81*	*732. 29*	
$^4F_{1½}$	0. 00	2, 572. 21			29, 777. 60	36, 451. 79				63, 602. 64	74, 611. 28	
$^4D_{3½}$					32, 899. 46	38, 041. 49	40, 238. 55					
					284. 75	*870. 27*	*598. 47*					
$^4D_{2½}$					32, 614. 71	37, 171. 22	39, 640. 08					
					358. 00	*532. 72*	*447. 73*					
$^4D_{1½}$					32, 256. 71	36, 638. 50	39, 192. 35					
					275. 46	*401. 46*	*257. 98*					
$^4D_{0½}$					31, 981. 25	36, 237. 04	38, 934. 37					
$^4P_{2½}$	8, 058. 16	9, 968. 65			38, 482. 64	43, 202. 45						
	322. 14	*225. 85*			*349. 14*	*308. 91*						
$^4P_{1½}$	7, 736. 02	9, 742. 80			38, 133. 50	42, 893. 54						
	223. 35	*189. 70*			*70. 10*	*104. 30*						
$^4P_{0½}$	7, 512. 67	9, 553. 10			38, 063. 40	42, 789. 24						
$^4S_{1½}$					37, 681. 75							
$^2I_{5½}$										76, 838. 70		
										443. 20		
$^2I_{6½}$										76, 395. 50		
$^2H_{5½}$	11, 984. 46				41, 738. 21					77, 743. 00	90, 986. 50	
	875. 20				*671. 73*					*537. 80*	*750. 80*	
$^2G_{4½}$	8, 159. 80	14, 109. 45			35, 185. 64	40, 878. 25				69, 983. 28	90, 811. 54	93, 147. 45

$^3H_{4\frac{1}{2}}$	11, 964. 46				41, 738. 21									
$^3G_{4\frac{1}{2}}$	8, 152. 80	14, 190. 45			35, 185. 64	40, 878. 25								83, 447. 45
	817. 08	190. 69			700. 22	973. 61								226. 60
$^3G_{3\frac{1}{2}}$	7, 837. 74	14, 059. 76			34, 485. 42	40, 852. 74								83, 221. 45
$^3F_{3\frac{1}{2}}$	6, 467. 61	19, 433. 24			30, 561. 75	37, 787. 59	42, 504. 11	48, 344. 91	57, 741. 16	66, 192. 68	74, 406. 80			
	714. 69	−81. 60			1, 066. 78	441. 28	356. 61	465. 08	679. 16	390. 27	645. 65			
$^1F_{2\frac{1}{2}}$	5, 752. 92	19, 514. 84			29, 504. 97	37, 346. 31	42, 860. 72	47, 881. 88	57, 062. 00	65, 872. 41	73, 852. 95			
$^1D_{2\frac{1}{2}}$	4, 505. 50	14, 162. 90	14, 733. 37	18, 396. 54	31, 160. 04	33, 419. 45	41, 676. 82	45, 186. 05	56, 569. 44	66, 868. 35				
	267. 20	734. 40	454. 73	782. 64	724. 66	456. 72	209. 10	181. 18	755. 91	182. 10				
$^3D_{1\frac{1}{2}}$	4, 248. 30	13, 428. 50	14, 298. 64	17, 614. 00	30, 435. 38	32, 963. 73	41, 467. 72	45, 004. 87	55, 835. 63	66, 686. 25				
$^1P_{1\frac{1}{2}}$	6, 111. 70	20, 080. 30			35, 914. 81	41, 337. 36	45, 568. 21	52, 876. 80	61, 861. 90					
	387. 32	466. 76			281. 76	610. 10	376. 79	291. 00	1, 047. 40					
$^1P_{0\frac{1}{2}}$	5, 724. 38	19, 613. 54			36, 196. 57	40, 727. 26	45, 944. 00	52, 585. 80	60, 814. 50					
$^3S_{0\frac{1}{2}}$	25, 201. 57				34, 810. 03									

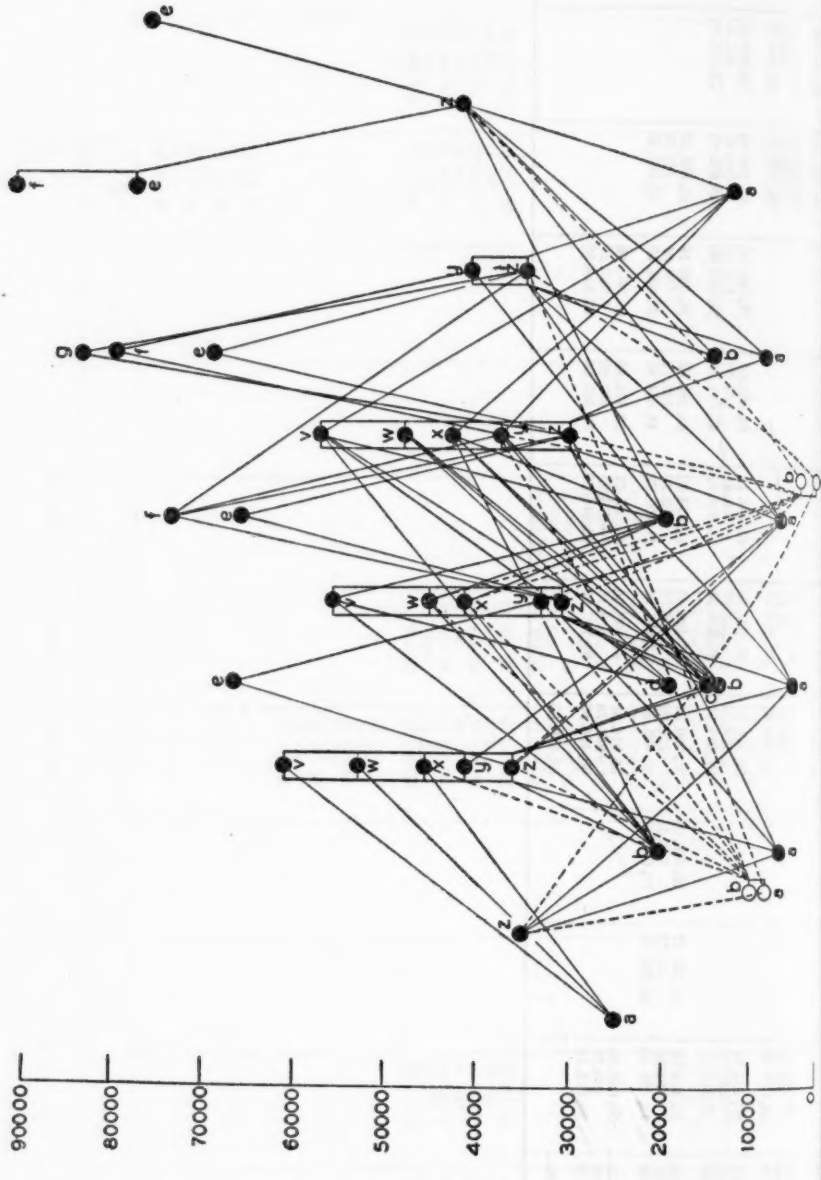
90000
80000
70000
60000
50000
40000
30000
20000
10000
0

The lines belonging to Zr II and their classifications are given in Table 2. In the first column is given the key number of the line, the full significance of which is to be seen in Table 3, which, at a glance shows the term combinations of the different multiplets and also the number and types of terms with which any particular term combines. Thus, for example, it is seen that the term a^2D, the lowest of the doublet system, combines with every odd term of the middle groups except z^2H° with which combination is impossible owing to the restrictions imposed by the selection principle for inner quantum numbers. The wave lengths of all the lines entered in Table 2 were derived from measurements of Bureau of Standards spectrograms, except the last 9, which were measured by Lang on the plates obtained by him with the vacuum grating spectrograph of the University of Alberta.[15] Of more than 900 lines in the table, 75 per cent have been classified on the basis of the terms of Table 1. Of the unclassified lines (210 in number) some may be due to impurities and a few may belong to Zr III and Zr IV; but there is good reason to believe that most of them properly belong to Zr II. Many of them possess the property of being nebulous. In spectra which have been fairly well worked out such lines invariably result from combinations of high terms with those of the middle group. Similar term combinations would satisfactorily account for them in Zr II. Indeed, a few terms of the high group have been found which combine with middle terms, and the lines resulting therefrom are nearly all nebulous. It is not easy to establish the high terms, because satellites are usually missing, and only rarely does a high term combine with more than one of the lower terms. No Zeeman effects are available to interpret such lines, and the best one can do is to estimate their origin from theoretical considerations. The theoretical origin of these unassigned lines is discussed more fully in a subsequent paragraph.

TABLE 2.—*Wave lengths in the spark spectrum of Zr*

Key No.	λ I. A.	Intensities B. S.	Intensities King	ν	Term combinations	Observed Zeeman effects	Theoretical Zeeman effects
1	6,787.15	2		14,729.66	$b^3P_{1\frac{1}{2}}$–$z^3S^0_{1\frac{1}{2}}$	(0.37) 1.09	(0.33) 1.00, 1.67
1a	6,678.03	3		14,970.35	$b^3F_{2\frac{1}{2}}$–$z^3G^0_{3\frac{1}{2}}$		
1a	6,346.54	1	2	15,752.27	$b^3F_{2\frac{1}{2}}$–$z^3G^0_{4\frac{1}{2}}$		
2	6,313.57	1		15,834.53	$b^3P_{1\frac{1}{2}}$–$z^3P^0_{1\frac{1}{2}}$	(0.00) 1.27	(0.00) 1.33
3	6,114.78	2		16,349.30	$b^3D_{1\frac{1}{2}}$–$z^4F^0_{1\frac{1}{2}}$		
4	6,106.47	2		16,371.55	$b^2G_{4\frac{1}{2}}$–$z^3F^0_{3\frac{1}{2}}$		
3	6,100.04	2		16,388.81	$b^3D_{2\frac{1}{2}}$–$z^4F^0_{2\frac{1}{2}}$		
2	6,028.64	2		16,582.91	$b^3P_{0\frac{1}{2}}$–$z^3P^0_{0\frac{1}{2}}$	(0.00) 0.66	(0.00) 0.67
5	5,477.82	2		18,250.38	$c^2D_{2\frac{1}{2}}$–$y^3D^0_{1\frac{1}{2}}$		
6	5,418.01	1		18,451.85	$b^3D_{2\frac{1}{2}}$–$z^4D^0_{2\frac{1}{2}}$		
5	5,350.36	5	6	18,685.15	$c^2D_{1\frac{1}{2}}$–$y^3D^0_{1\frac{1}{2}}$	(0.00) 0.78	(0.00) 0.80
5	5,350.10	5	6	18,686.06	$c^2D_{2\frac{1}{2}}$–$y^3D^0_{2\frac{1}{2}}$	(0.00) 1.21	(0.00) 1.20
7	5,311.78	2	1	18,820.86	$b^3D_{2\frac{1}{2}}$–$y^3D^0_{1\frac{1}{2}}$		
7	5,191.60	7	15	19,256.54	$b^3D_{2\frac{1}{2}}$–$y^3D^0_{2\frac{1}{2}}$	(0.00) 1.17	(0.00) 1.20
8	5,124.98	2		19,506.85	$a^3H_{3\frac{1}{2}}$–$z^4F^0_{3\frac{1}{2}}$		
7	5,112.28	7	5	19,555.32	$b^3D_{1\frac{1}{2}}$–$y^3D^0_{1\frac{1}{2}}$	(0.00) 0.83	(0.00) 0.80
7	5,000.91	3		19,990.80	$b^3D_{1\frac{1}{2}}$–$y^3D^0_{2\frac{1}{2}}$		
9	4,925.90	1		20,295.21	$b^3G_{4\frac{1}{2}}$–$z^3G^0_{4\frac{1}{2}}$		
10	4,908.67	1		20,366.45	$a^3S_{1\frac{1}{2}}$–$z^3P^0_{1\frac{1}{2}}$		
9	4,894.43	0		20,425.70	$b^3G_{3\frac{1}{2}}$–$z^3G^0_{3\frac{1}{2}}$		
11	4,854.65	0		20,593.07	$b^4P_{2\frac{1}{2}}$–$z^3F^0_{3\frac{1}{2}}$		
12	4,841.98	0		20,646.95	$b^3P_{1\frac{1}{2}}$–$y^3P^0_{0\frac{1}{2}}$		
13	4,816.47	1		20,756.36	$a^3G_{4\frac{1}{2}}$–$z^4G^0_{5\frac{1}{2}}$		
9	4,761.67	1		20,995.18	$b^3G_{4\frac{1}{2}}$–$z^3G^0_{4\frac{1}{2}}$		
12	4,734.94	1		21,113.70	$b^3P_{0\frac{1}{2}}$–$y^3P^0_{1\frac{1}{2}}$		

[15] J. Opt. Soc. Am. & Rev. Sci. Inst., **12**, p. 523; 1926.

TABLE 2.—*Wave lengths in the spark spectrum of Zr*—Continued

Key No.	λ I. A.	Intensities B. S.	Intensities King	ν	Term combinations	Observed Zeeman effects	Theoretical Zeeman effects
14	4, 719. 80	1		21, 181. 43	$c^3D_{3\frac{1}{2}}$–$z^3P^0_{3\frac{1}{2}}$		
12	4, 703. 03	5	1	21, 256. 96	$b^2P_{1\frac{1}{2}}$–$y^3P^0_{1\frac{1}{2}}$	(0. 00) 1. 32	(0. 00) 1. 33
15	4, 685. 19	4	1	21, 337. 90	$b^3F_{3\frac{1}{2}}$–$y^1G^0_{3\frac{1}{2}}$	(0. 00) 1. 00	(0. 02, 0. 05, 0. 08) ... 0. 90, 0. 94, 0. 97
16	4, 674. 41	1		21, 387. 11	$b^3P_{1\frac{1}{2}}$–$z^1D^0_{1\frac{1}{2}}$		
15	4, 661. 78	5	1	21, 445. 05	$b^3F_{3\frac{1}{2}}$–$y^3G^0_{3\frac{1}{2}}$	(0. 00) 0. 95	(0. 02, 0. 05, ...) 1. 1. 03, 1. 05, ...
16	4, 629. 07	5	1	21, 596. 58	$b^3P_{1\frac{1}{2}}$–$z^3D^0_{2\frac{1}{2}}$	(0. 00) 1. 07	(0. 07, 0. 20) 1. 1. 13, 1. 27, 1. 40
14	4, 624. 86	1		21, 616. 24	$c^3D_{1\frac{1}{2}}$–$z^3P^0_{1\frac{1}{2}}$		
17	4, 613. 95	5	2	21, 667. 35	$a^3G_{3\frac{1}{2}}$–$z^3F^0_{2\frac{1}{2}}$	(0. 00) 0. 95	(0. 02, 0. 05, 0. 08) ... 0. 90, 0. 94, 0. 97
12	4, 601. 97	2		21, 723. 76	$b^3P_{0\frac{1}{2}}$–$y^3P^0_{1\frac{1}{2}}$		
16	4, 574. 49	6	1	21, 854. 25	$b^3P_{0\frac{1}{2}}$–$z^3D^0_{1\frac{1}{2}}$	(0. 00) 0. 85	(0. 07) 0. 73, 0. 87
14	4, 565. 43	3		21, 897. 62	$c^3D_{1\frac{1}{2}}$–$z^3P^0_{0\frac{1}{2}}$	(0. 00) 0. 85	0. 07) 0. 73, 0. 87
18	4, 553. 96	12	1	21, 952. 78	$b^3F_{3\frac{1}{2}}$–$x^3D^0_{2\frac{1}{2}}$	(0. 00) 0. 99	(0. 03, 0. 09) 0. 77, 0. 0. 89, 0. 94
19	4, 496. 96	15	15	22, 231. 03	$a^3F_{3\frac{1}{2}}$–$z^4G^0_{3\frac{1}{2}}$	(0. 49) 0. 78	(0. 14, 0. 43, 0. 71) ... 0. 43, 0. 71, 1. 00, ...
20	4, 495. 44	3	1	22, 238. 54	$b^4P_{1\frac{1}{2}}$–$z^4D^0_{2\frac{1}{2}}$		
18	4, 494. 41	8	2	22, 243. 64	$b^3F_{3\frac{1}{2}}$–$z^3D^0_{2\frac{1}{2}}$	(0. 00) 1. 08	(0. 03, 0. 09, 0. 14) 1. 1. 06, 1. 11, ...
20	4, 485. 44	2		22, 288. 12	$b^4P_{2\frac{1}{2}}$–$z^4D^0_{1\frac{1}{2}}$	(0. 00) 2. 12	(0. 20, 0. 60) 1. 00, 1. 1. 80, 2. 20
21	4, 482. 04	3		22, 305. 03	$b^3F_{3\frac{1}{2}}$–$z^3H^0_{4\frac{1}{2}}$		
17	4, 461. 22	10	5	22, 409. 12	$a^3G_{4\frac{1}{2}}$–$z^3F^0_{3\frac{1}{2}}$	(0. 00) 1. 06	(0. 02, 0. 05, ...) 1. 1. 03, 1. 06, ...
20	4, 457. 42	8	10	22, 428. 23	$b^4P_{0\frac{1}{2}}$–$z^4D^0_{1\frac{1}{2}}$	(0. 00, **1. 30**) **1. 33**, 2. 17	(1. 33) 1. 33
19	4, 454. 80	10	8	22, 441. 42	$a^3F_{3\frac{1}{2}}$–$z^4G^0_{3\frac{1}{2}}$	(0. 43) 1. 08	(--- 0. 40, 0. 56) ... 0. 91, 1. 06, 1. 22, ...
22	4, 445. 88	1		22, 486. 44	$b^3D_{1\frac{1}{2}}$–$z^3P^0_{1\frac{1}{2}}$		
23	4, 442. 99	25	12	22, 501. 07	$a^3H_{4\frac{1}{2}}$–$z^3G^0_{3\frac{1}{2}}$	(0. 00) 0. 97	(0. 01, 0. 03, ...) ... 0. 94, 0. 96, 0. 98
24	4, 442. 50	2	1	22, 503. 55	$a^4P_{2\frac{1}{2}}$–$z^3F^0_{2\frac{1}{2}}$		
20	4, 440. 45	10	5	22, 514. 17	$b^4P_{1\frac{1}{2}}$–$z^4D^0_{1\frac{1}{2}}$	(0. 80) 0. 91, **1. 42**, 1. 95	(0. 27, **0. 80**) 0. 93, 1. 2. 00
25	4, 429. 34	2		22, 570. 41	$c^3D_{1\frac{1}{2}}$–$y^4F^0_{1\frac{1}{2}}$		
20	4, 414. 54	5	5	22, 646. 08	$b^4P_{2\frac{1}{2}}$–$z^4D^0_{2\frac{1}{2}}$	(0. 57) 1. 42	(--- 0. 34, 0. 57) ... 1. 26, 1. 48, 1. 72, ...
25	4, 404. 81	2		22, 696. 10	$c^3D_{2\frac{1}{2}}$–$y^4F^0_{1\frac{1}{2}}$	(0. 00) 1. 30	(0. 02, 0. 06, 0. 10) ... 1. 22, 1. 26, 1. 29
20	4, 403. 35	6	3	22, 703. 62	$b^4P_{0\frac{1}{2}}$–$z^4D^0_{1\frac{1}{2}}$	(0. 68) **0. 43**, 1. 90	(0. 73) **0. 47**, 1. 93
26	4, 401. 35	2		22, 713. 94	$a^3G_{3\frac{1}{2}}$–$z^4F^0_{2\frac{1}{2}}$		
17	4, 399. 44	2		22, 723. 82	$a^3G_{3\frac{1}{2}}$–$z^3F^0_{3\frac{1}{2}}$		
27	4, 388. 50	2		22, 780. 45	$b^3P_{1\frac{1}{2}}$–$z^3F^0_{2\frac{1}{2}}$		
28	4, 383. 10	1		22, 808. 52	$b^3D_{1\frac{1}{2}}$–$y^4D^0_{0\frac{1}{2}}$		
29	4, 382. 95	1		22, 809. 29	$b^3G_{3\frac{1}{2}}$–$y^4F^0_{2\frac{1}{2}}$		
23	4, 379. 78	9	8	22, 825. 81	$a^3H_{4\frac{1}{2}}$–$z^3G^0_{4\frac{1}{2}}$	(0. 00) 1. 02	(0. 01, 0. 03, ...) 1. 1. 02, ...
20	4, 370. 96	8	6	22, 871. 87	$b^4P_{1\frac{1}{2}}$–$z^4D^0_{2\frac{1}{2}}$	(0. 00) 0. 83	(0. 18, 0. 54) 0. 83, 1. ---
20	4, 359. 74	10	8	22, 930. 72	$b^4P_{2\frac{1}{2}}$–$z^4D^0_{1\frac{1}{2}}$	(0. 00*w*) 1. 07 A[1]	(0. 09, 0. 26, 0. 43) 1. 1. 17, ...
30	4, 342. 23	1	1	23, 023. 19	$b^3D_{1\frac{1}{2}}$–$y^4F^0_{1\frac{1}{2}}$		
31	4, 339. 56	3	1	23, 037. 36	$a^1F_{3\frac{1}{2}}$–$z^3F^0_{2\frac{1}{2}}$		
32	4, 337. 63	5	1	23, 047. 61	$c^3D_{1\frac{1}{2}}$–$y^3F^0_{2\frac{1}{2}}$	(0. 00) 1. 20	(0. 03, 0. 09) ... 0. 0. 94
32	4, 336. 36	2		23, 054. 36	$c^3D_{2\frac{1}{2}}$–$y^3F^0_{1\frac{1}{2}}$		
33	4, 333. 28	15	1	23, 070. 74	$b^3F_{3\frac{1}{2}}$–$z^3F^0_{2\frac{1}{2}}$	(0. 00) 1. 13	(0. 00) 1. 14
34	4, 325. 64	3		23, 111. 49	$b^3G_{3\frac{1}{2}}$–$y^4D^0_{2\frac{1}{2}}$		
35	4, 323. 62	2		23, 122. 29	$b^3P_{1\frac{1}{2}}$–$y^4P^0_{2\frac{1}{2}}$		
19	4, 317. 32	12	3	23, 156. 03	$a^3F_{3\frac{1}{2}}$–$z^4G^0_{3\frac{1}{2}}$	(0. 00) 1. 13	(0. 06, 0. 19, 0. 32) ... 1. 18, 1. 30
36	4, 312. 23	3	1	23, 183. 36	$b^5D_{2\frac{1}{2}}$–$y^5F^0_{3\frac{1}{2}}$		
23	4, 308. 94	4	1	23, 201. 06	$a^3H_{4\frac{1}{2}}$–$z^3G^0_{4\frac{1}{2}}$	(0. 77) 1. 13	(--- 0. 71, 0. 91) ... 0. 81, 1. 01, 1. 21, ...
29	4, 301. 81	5	1	23, 239. 51	$b^3G_{4\frac{1}{2}}$–$y^4F^0_{3\frac{1}{2}}$	(0. 00) 0. 73 A[1]	(0. 06, 0. 19, ...) 0. 0. 80, 0. 92, ...
30	4, 296. 74	8	1	23, 266. 93	$b^3D_{3\frac{1}{2}}$–$y^4F^0_{3\frac{1}{2}}$	(0. 00) 1. 35	(0. 02, 0. 06, 0. 10) ... 1. 26, 1. 29
37	4, 293. 14	7	1	23, 286. 44	$b^3G_{3\frac{1}{2}}$–$y^3F^0_{3\frac{1}{2}}$	(0. 00) 0. 66 A[1]	(0. 02, 0. 05, 0. 08) ... 0. 94, 0. 97

TABLE 2.—*Wave lengths in the spark spectrum of Zr*—Continued

Key No.	λ I. A.	Intensities B. S.	Intensities King	ν	Term combinations	Observed Zeeman effects	Theoretical Zeeman effects
38	4, 289. 18	2		23, 307. 94	$c^3D_{2½}$–$y^4D_{1½}$		
39	4, 286. 51	5	1	23, 322. 46	$a^2G_{3½}$–$z^3D^2_{1½}$	(0. 00*w*) 0. 49 A[1]	(**0. 16,** 0. 47, 0. 78) **0. 11,** 0. 42, 0. 73, ---
33	4, 282. 21	6		23, 345. 88	$b^3F_{3½}$–$z^3F^2_{1½}$	(0. 00) 0. 87	(0. 00) 0. 86
19	4, 277. 37	4	1	23, 372. 30	$a^3F_{3½}$–$z^4G^1_{1½}$	(0. 00) 1. 28	(**0. 02,** 0. 04, ---) ---, 1. 24, **1. 27**
40	4, 273. 52	4	2	23, 393. 35	$a^2P_{1½}$–$z^2F^2_{1½}$	(**0. 21,** 0. 67) 0. 00*w*	(**0. 24,** 0. 71) **0. 14,** 0. 62 ---
41	4, 266. 72	1	5	23, 430. 63	$b^4P_{0½}$–$y^3D^1_{1½}$		
30	4, 264. 91	4	1	23, 440. 58	$b^3D_{1½}$–$y^4F^2_{1½}$	(0. 00*w*) 1. 38	(**0. 11,** 0. 34) ---1. 14, **1. 37**
42	4, 258. 05	12	10	23, 478. 34	$a^3D_{2½}$–$z^4G^2_{1½}$	(0. 70, **1. 27**) 0. 00, 0. 40 **0. 91,** 1. 39, 2. 00	(0. 31, 0. 94, **1. 57**) 0. 26 0. 37, **0. 88,** 1. 51, 2. 14
37	4, 236. 56	5	3	23, 597. 43	$b^3G_{4½}$–$y^3F^3_{1½}$	(0. 00*w*) 0. 76	(**0. 02,** 0. 05, ---) **1. 00,** 1. 03, 1. 06, ---
36	4, 231. 64	8	2	23, 624. 77	$b^3D_{2½}$–$y^3F^2_{1½}$	(0. 00) 1. 21	(**0. 03,** 0. 09, 0. 14) **1. 00** 1. 06, 1. 11, ---
43	4, 224. 27	3	2	23, 666. 09	$a^3P_{1½}$–$z^4F^1_{1½}$		
41	4, 222. 41	3		23, 676. 51	$b^4P_{1½}$–$y^3D^2_{2½}$	(**0. 00**) **0. 63**	(**0. 27,** 0. 80) **0. 40,** 0. 93, ---
26	4, 215. 76	1		23, 713. 86	$a^2G_{4½}$–$z^4F^1_{1½}$		
42	4, 211. 88	12	10	23, 735. 70	$a^3D_{1½}$–$z^4G^2_{1½}$	(0. 00) 0. 61	(**0. 11,** 0. 34) **0. 23,** 0. 46, 0. 69, 0. 91
28	4, 210. 62	5		23, 742. 81	$b^3D_{1½}$–$y^4D^2_{2½}$	(0. 00*w*) 1. 41	(**0. 29,** 0. 86) 0. 51, 1. 08, 1. 66, **2. 23**
31	4, 208. 99	30	20	23, 752. 00	$a^2F_{2½}$–$z^2F^2_{1½}$	(0. 00) 0. 88	(0. 00) 0. 86
44	4, 205. 91	2		23, 769. 40	$b^2F_{3½}$–$y^4P^2_{1½}$		
34	4, 191. 50	6		23, 851. 11	$b^2G_{4½}$–$y^4D^1_{1½}$	(0. 00*w*) 0. 69	(**0. 16,** 0. 48, ---) **0. 00** 0. 32, 0. 63, ---
23	4, 186. 70	12		23, 878. 45	$b^2D_{2½}$–$y^4D^3_{1½}$	(0. 00*w*) 1. 49	(**0. 11,** 0. 34, 0. 57) --- 1. 54, 1. 77, **2. 00**
36	4, 179. 81	15		23, 917. 81	$b^2D_{1½}$–$y^3F^2_{1½}$	(0. 00*w*) 1. 25 A[2]	(**0. 03,** 0. 09) 0. 77, - 0. 83, 0. 89, **0. 94**
45	4, 161. 20	20	15	24, 024. 78	$a^2F_{2½}$–$z^4F^1_{1½}$	(0. 00*w*) 1. 09	(**0. 23,** 0. 69) 0. 17, - 0. 63, 1. 09, **1. 54**
43	4, 156. 24	15	15	24, 053. 45	$a^2P_{0½}$–$z^4F^1_{1½}$	(0. 00) 0. 70	(0. 13) **0. 27,** 0. 53
45	4, 150. 97	10	8	24, 083. 99	$a^2F_{3½}$–$z^4F^2_{2½}$	(0. 00) 1. 26	(**0. 06,** 0. 17, 0. 29) --- 1. 20, 1. 31, **1. 43**
31	4, 149. 22	75	50	24, 094. 14	$a^2F_{3½}$–$z^2F^3_{2½}$	(0. 00) 1. 15	(0. 00) 1. 14
46	4, 131. 31	1		24, 198. 60	$a^4P_{2½}$–$z^4D^1_{1½}$		
46	4, 123. 38	1		24, 245. 13	$a^4P_{1½}$–$z^4D^0_{0½}$		
47	4, 110. 05	3		24, 323. 77	$a^2P_{1½}$–$z^2D^1_{1½}$	(1. 04) 0. 69, **1. 38**	(0. 27, **0. 80**) 0. 53, **1. 07** 1. 60
42	4, 096. 63	4	2	24, 403. 44	$a^2D_{2½}$–$z^4G^2_{2½}$	(0. 00*w*) 0. 81 A[1]	(**0. 11,** 0. 32, 0. 54) **0. 44,** 0. 66, 0. 88, ---
43	4, 090. 52	10	5	24, 439. 89	$a^2P_{1½}$–$z^4F^2_{2½}$	(0. 00*w*) 0. 81 A[1]	(**0. 15,** 0. 46) **0. 57,** 0. 88, 1. 18, 1. 49
46	4, 085. 68	5	5	24, 468. 85	$a^4P_{0½}$–$z^4D^0_{0½}$	(1. 34) 1. 33	(1. 33) 1. 33
46	4, 077. 05	3		24, 520. 64	$a^4P_{1½}$–$z^4D^1_{1½}$		
46	4, 071. 09	4	2	24, 556. 54	$a^4P_{2½}$–$z^4D^1_{2½}$	(0. 52) 1. 45	(0. 11, 0. 34, **0. 57**) --- 1. 26, **1. 48,** 1. 72, ---
48	4, 050. 32	15	15	24, 682. 46	$a^2F_{2½}$–$z^2D^1_{1½}$	(0. 00*w*) 1. 23 A[2]	(**0. 03,** 0. 09) 0. 77, 0. 83, 0. 89, **0. 94**
48	4, 048. 68	25	15	24, 692. 46	$a^2F_{3½}$–$z^2D^2_{2½}$	(0. 00) 1. 20	(**0. 03,** 0. 09, 0. 14) **1. 00,** 1. 06, 1. 11, ---
47	4, 045. 63	15	10	24, 711. 07	$a^2P_{0½}$–$z^2D^1_{1½}$	(0. 00) 0. 58	(0. 07) 0. 73, **0. 87**
46	4, 040. 24	4	2	24, 744. 04	$a^4P_{0½}$–$z^4D^1_{1½}$	(0. 69) **0. 46,** 1. 90	(0. 73) **0. 47,** 1. 93
49	4, 034. 84	0		24, 777. 15	$a^2G_{3½}$–$z^4D^3_{2½}$		
45	4, 034. 10	5	2	24, 781. 70	$a^2F_{3½}$–$z^4F^1_{1½}$	(0. 29) 1. 20	(--- 0. 24, **0. 33**) --- 1. 10, **1. 19,** 1. 29, ---
45	4, 031. 35	2		24, 798. 60	$a^2F_{2½}$–$z^4F^2_{1½}$		
31	4, 029. 68	20	15	24, 808. 88	$a^2F_{3½}$–$z^2F^3_{2½}$	(0. 00) 1. 59 A[2]	(**0. 14,** 0. 43, 0. 71) --- 1. 28, 1. 57, **1. 86**
46	4, 024. 45	12	5	24, 841. 12	$a^4P_{2½}$–$z^4D^0_{2½}$	(0. 00*w*) 1. 25	(**0. 09,** 0. 26, 0. 43) **1. 00,** 1. 17, 1. 34, ---
46	4, 018. 38	10	4	24, 878. 64	$a^4P_{1½}$–$z^4D^0_{2½}$	(0. 00*w*) 0. 89	(**0. 18,** 0. 54) **0. 83,** 1. 19, 1. 55, 1. 92

TABLE 2.—*Wave lengths in the spark spectrum of Zr*—Continued

Key No.	λ I. A.	Intensities B. S.	Intensities King	ν	Term combinations	Observed Zeeman effects	Theoretical Zeeman effects
50	4,002.95	2		24,974.54	$b^3P_{1\frac{1}{2}}-w^3D^1_{1\frac{1}{2}}$		
51	3,998.98	30	20	24,999.33	$a^3D_{2\frac{1}{2}}-z^3F^2_{2\frac{1}{2}}$	(0.75) 1.08	(0.17, 0.51, **0. 86**) ... 0.69, **1. 03**, 1.37, ...
47	3,991.14	40	30	25,048.44	$a^3P_{1\frac{1}{2}}-z^3D^2_{2\frac{1}{2}}$	(0.00) 1.00 A[1]	(**0. 07**, 0.20) **1. 00**, 1.13, 1.27, 1.40
52	3,984.76	4	20	25,088.54	$b^4F_{2\frac{1}{2}}-z^4G^1_{2\frac{1}{2}}$		
50	3,982.01	3		25,105.87	$b^3P_{1\frac{1}{2}}-w^3D^2_{2\frac{1}{2}}$		
51	3,958.24	50	25	25,256.63	$a^3D_{1\frac{1}{2}}-z^3F^2_{2\frac{1}{2}}$	(0.00) 0.91	(**0. 03**, 0.09) 0.77, 0.83, 0.89, **0. 94**
53	3,941.92	3		25,361.20	$a^4P_{2\frac{1}{2}}-y^5D^3_{2\frac{1}{2}}$		
45	3,936.07	7	2	25,398.89	$a^3F_{2\frac{1}{2}}-z^4F^4_{1\frac{1}{2}}$	(0.00*w*) 1.78	(**0. 10**, 0.29, ...) ... 1.62, 1.81, **2. 00**
48	3,934.80	20	10	25,407.08	$a^3F_{2\frac{1}{2}}-z^3D^2_{2\frac{1}{2}}$	(0.56) 1.04	(0.17, 0.51, **0. 86**) 0.34, 0.69, **1. 03**, 1.37, 1.71
52	3,934.14	20	15	25,411.35	$b^4F_{1\frac{1}{2}}-z^4G^2_{2\frac{1}{2}}$	(0.00) 1.10	(**0. 09**, 0.26) 0.31, 0.49, 0.66, **0. 83**
50	3,929.54	8		25,441.09	$b^3P_{0\frac{1}{2}}-w^3D^1_{1\frac{1}{2}}$	(0.00) 1.00	(0.07) 0.73, **0. 87**
54	3,923.92	1		25,477.53	$b^3D_{2\frac{1}{2}}-x^4D^3_{2\frac{1}{2}}$		
55	3,922.36	1		25,487.66	$b^3P_{1\frac{1}{2}}-z^3P^1_{1\frac{1}{2}}$		
56	3,915.94	25	15	25,529.45	$a^3D_{1\frac{1}{2}}-z^4F^1_{1\frac{1}{2}}$	(0.22) 0.74	(0.20, **0. 60**) 0.20, **0. 60**, 1.00
57	3,914.36	7		25,539.75	$b^3F_{2\frac{1}{2}}-w^3D^2_{2\frac{1}{2}}$	(0.00) 0.85	(**0. 03**, 0.09) 0.77, 0.83, 0.89, **0. 94**
52	3,903.77	1		25,609.03	$b^4F_{2\frac{1}{2}}-z^4G^2_{2\frac{1}{2}}$		
57	3,881.97	7		25,752.84	$b^3F_{3\frac{1}{2}}-w^3D^3_{2\frac{1}{2}}$		
58	3,874.37	1		25,803.36	$a^3H_{4\frac{1}{2}}-y^5F^3_{3\frac{1}{2}}$		
59	3,855.43	3		25,930.12	$a^3D_{2\frac{1}{2}}-z^3D^1_{1\frac{1}{2}}$		
60	3,853.07	2		25,946.00	$b^4P_{2\frac{1}{2}}-z^3P^1_{1\frac{1}{2}}$		
52	3,843.03	30		26,013.78	$b^4F_{2\frac{1}{2}}-z^4G^1_{2\frac{1}{2}}$	(0.00) 0.95	(**0. 02**, 0.07, 0.11) **0. 87**, 0.92, 0.96, ...
56	3,838.28	5		26,045.97	$a^3D_{2\frac{1}{2}}-z^4F^2_{2\frac{1}{2}}$		
51	3,836.76	60		26,056.29	$a^3D_{2\frac{1}{2}}-z^3F^2_{3\frac{1}{2}}$	(0.00) 1.12	(**0. 03**, 0.09, 0.14) **1. 00**, 1.06, 1.11, ...
54	3,833.87	2		26,075.93	$b^3D_{2\frac{1}{2}}-x^4D^2_{2\frac{1}{2}}$		
52	3,832.94	1		26,082.26	$b^4F_{4\frac{1}{2}}-z^4G^1_{3\frac{1}{2}}$		
61	3,827.51	1		26,119.26	$c^3D_{2\frac{1}{2}}-y^5G^3_{3\frac{1}{2}}$		
	3,827.27	1		26,120.90			
62	3,823.72	1		26,145.15	$a^3P_{1\frac{1}{2}}-z^4D^1_{1\frac{1}{2}}$		
63	3,823.41	3		26,147.27	$a^3F_{3\frac{1}{2}}-z^4D^2_{3\frac{1}{2}}$		
60	3,819.84	2		26,171.71	$b^4P_{1\frac{1}{2}}-z^3P^1_{1\frac{1}{2}}$		
64	3,818.78	1		26,178.97	$b^3G_{3\frac{1}{2}}-z^4D^1_{2\frac{1}{2}}$		
59	3,817.59	12		26,187.13	$a^3D_{1\frac{1}{2}}-z^3D^1_{1\frac{1}{2}}$	(0.00) 0.72	(0.00) 0.80
65	3,814.97	2		26,205.11	$b^4F_{3\frac{1}{2}}-z^3F^3_{3\frac{1}{2}}$		
54	3,813.98	0		26,211.91	$b^3D_{1\frac{1}{2}}-x^4D^2_{2\frac{1}{2}}$		
62	3,807.41	2		26,257.15	$a^3P_{0\frac{1}{2}}-z^4D^0_{0\frac{1}{2}}$		
56	3,800.73	5		26,303.29	$a^3D_{1\frac{1}{2}}-z^4F^1_{2\frac{1}{2}}$	(0.00) 1.30	(**0. 11**, 0.34) 0.69, 0.91, 1.14, **1. 37**
66	3,796.47	20		26,332.81	$a^3G_{4\frac{1}{2}}-z^3G^3_{3\frac{1}{2}}$	(0.00) 1.62 A[2]	(**0. 11**, 0.33, ...) ... 1.44, 1.67, **1. 89**
60	3,792.32	2		26,361.62	$b^4P_{0\frac{1}{2}}-z^3P^1_{1\frac{1}{2}}$		
67	3,782.72	5		26,428.52	$c^3D_{1\frac{1}{2}}-y^5P^0_{0\frac{1}{2}}$	(0.00) 0.83	(0.07) 0.73, **0. 87**
63	3,782.24	4		26,431.88	$a^3F_{3\frac{1}{2}}-z^4D^3_{2\frac{1}{2}}$		
62	3,772.06	4		26,503.21	$a^3P_{1\frac{1}{2}}-z^4D^2_{2\frac{1}{2}}$	(0.00) 1.40	(**0. 02**, 0.06) 1.31, 1.35, 1.35, 1.39, **1. 43**
63	3,771.98	2		26,503.77	$a^3F_{2\frac{1}{2}}-z^4D^1_{1\frac{1}{2}}$		
62	3,767.89	5		26,532.54	$a^3P_{0\frac{1}{2}}-z^4D^1_{1\frac{1}{2}}$		
52	3,766.83	25	30	26,540.01	$b^4F_{3\frac{1}{2}}-z^4G^1_{4\frac{1}{2}}$	(0.00) 1.04	(**0. 03**, 0.10, ...) **0. 94**, 1.01, 1.07, ...
67	3,757.80	8		26,603.78	$c^3D_{2\frac{1}{2}}-y^5P^1_{1\frac{1}{2}}$	(0.00) 1.18	(**0. 07**, 0.20) (**1. 00**, 1.13, 1.27, 1.40
65	3,756.96	1		26,609.73	$b^4F_{3\frac{1}{2}}-z^3F^2_{2\frac{1}{2}}$		
66	3,751.60	75	30	26,647.74	$a^3G_{3\frac{1}{2}}-z^3G^3_{3\frac{1}{2}}$	(0.00) 0.91	(0.00) 0.89
59	3,750.65	6		26,654.50	$a^3D_{2\frac{1}{2}}-z^3D^2_{2\frac{1}{2}}$	(0.00) 1.15	(0. 00) 1. 20
68	3,745.97	40		26,687.80	$b^5G_{4\frac{1}{2}}-y^5G^4_{3\frac{1}{2}}$	(0.00) 1.07	(0. 00) 1. 11
56	3,738.13	5		26,743.77	$a^3D_{2\frac{1}{2}}-z^4F^3_{3\frac{1}{2}}$	(0. 00) 1. 32	(**0. 02**, 0. 06, 0. 10) ... 1. 22, 1. 26, **1. 29**
68	3,731.26	35	10	26,793.01	$b^5G_{3\frac{1}{2}}-y^5G^5_{3\frac{1}{2}}$	(0. 00) 0. 87	(0. 00) 0. 89
65	3,729.74	5		26,803.92	$b^4F_{4\frac{1}{2}}-z^3F^3_{3\frac{1}{2}}$	(0. 00) 1. 68	(**0. 10**, 0. 29, ...) ... 1. 62, 1. 81, **2. 00**
68	3,727.72	10		26,818.45	$b^5G_{3\frac{1}{2}}-y^5G^3_{3\frac{1}{2}}$	(0. 00*w*) 1. 44	(**0. 11**, 0. 33, ...) ... 1. 44, 1. 67, **1. 89**

TABLE 2.—*Wave lengths in the spark spectrum of Zr*—Continued

Key No.	λ I. A.	Intensities B. S.	Intensities King	ν	Term combinations	Observed Zeeman effects	Theoretical Zeeman effects
63	3, 721. 69	2		26, 861. 90	$a^2F_{2½}$–$z^4D^0_{3½}$		
69	3, 718. 86	6		26, 882. 34	$b^4P_{2½}$–$z^4F^0_{1½}$	(0. 00*w*) 1. 43	(**0. 31,** 0.94) 0.09, 0.71, 1. **34, 1. 97**
70	3, 717. 32	2		26, 895. 65	$b^4P_{1½}$–$y^4D^0_{1½}$		
59	3, 714. 77	15	6	26, 911. 94	$a^2D_{1½}$–$z^2D^0_{2½}$	(0. 00*w*) 1. 31	(**0. 20,** 0.60) 0.60, 1.00, 1. 40, **1. 80**
65	3, 711. 95	1		26, 932. 38	$b^4F_{1½}$–$z^2F^0_{2½}$		
71	3, 710. 47	1		26, 943. 12	$c^2D_{2½}$–$z^2D^0_{2½}$		
72	3, 709. 27	60	30	26, 951. 84	$a^2F_{3½}$–$y^2D^0_{2½}$	(0. 00) 1. 08	(**0. 03,** 0.09, 0.14) **1. 00,** 1. 06, 1. 11, ---
66	3, 698. 17	100	40	27, 032. 74	$a^2G_{4½}$–$z^2G^0_{4½}$	(0. 00) 1. 13	(0. 00) 1. 11
52	3, 697. 49	20	10	27, 037. 71	$b^4F_{4½}$–$z^4G^0_{5½}$	(0. 00) 1. 15	(**0. 03,** 0. 09, 0. 15, ---) **1. 00,** 1. 06, 1. 12, ---
73	3, 692. 60	1		27, 073. 51	$a^4P_{1½}$–$z^2S^0_{½}$		
63	3, 682. 67	2		27, 146. 51	$a^2F_{2½}$–$z^4D^0_{3½}$		
71	3, 679. 64	1		27, 168. 86	$c^2D_{1½}$–$z^2D^0_{1½}$		
74	3, 678. 91	10		27, 174. 25	$b^2D_{2½}$–$y^2P^0_{1½}$	(0. 00) 1. 12	(**0. 07,** 0.20) **1. 00,** 1.13, 1. 27, 1. 40
69	3, 674. 74	40	20	27, 205. 09	$b^4F_{1½}$–$z^4F^0_{1½}$	(0. 39) 0. 58	(0. 00) 0. 40
75	3, 672. 65	2		27, 220. 57	$a^4F_{3½}$–$z^4G^0_{3½}$		
72	3, 671. 28	20	10	27, 230. 73	$a^2F_{2½}$–$y^2D^0_{1½}$	(0. 00) 0. 93	(**0. 03,** 0.09) 0.77, 0.83, 0. 89, **0. 94**
69	3, 668. 46	8	5	27, 251. 66	$b^4F_{3½}$–$z^4F^0_{3½}$	(0. 00*w*) 1. 55	(**0. 10,** 0. 31, 0. 52) --- 1. 34, 1. 55, **1. 76**
76	3, 667. 40	1		27, 259. 54	$a^2P_{0½}$–$y^2D^0_{1½}$		
65	3, 667. 06	3		27, 262. 07	$b^4F_{3½}$–$z^2F^0_{3½}$	(0. 00) 1. 19	(--- 0.24, **0. 33**) --- 1. 10, **1. 19,** 1. 29, ---
74	3, 662. 14	8		27, 298. 69	$b^2D_{1½}$–$y^2P^0_{½}$	(0. 00) 0. 82	(0. 07) 0. 73, **0. 87**
77	3, 661. 33	4		27, 304. 73	$b^2D_{2½}$–$z^2D^0_{1½}$		
76	3, 660. 92	3		27, 307. 79	$a^2P_{1½}$–$y^2D^0_{2½}$		
66	3, 655. 56	7		27, 347. 83	$a^2G_{3½}$–$z^2G^0_{4½}$	(0. 00*w*) 1. 57	(**0. 11,** 0. 33 ---) --- 1. 44, 1. 67, **1. 89**
71	3, 651. 50	2		27, 378. 23	$c^2D_{1½}$–$z^2D^0_{2½}$	(0. 00) 1. 60	(**0. 20,** 0.60) 0.60, 1.00, 1. 40, **1. 80**
78	3, 650. 73	7		27, 384. 01	$a^2S_{0½}$–$w^2P^0_{0½}$	(0. 68) 1. 34	(0. 67) 1. 33
69	3, 636. 46	8	5	27, 491. 46	$b^4F_{4½}$–$z^4F^0_{3½}$	(0. 00) 1. 54	(**0. 05,** 0. 14, ---) --- 1. 48, 1. 57, **1. 67**
77	3, 632. 49	10		27, 513. 93	$b^2D_{2½}$–$z^2D^0_{2½}$	(0. 00) 1. 18	(0. 00) 1. 20
79	3, 630. 03	10	10	27, 540. 16	$b^4F_{2½}$–$z^2D^0_{1½}$	(0. 00*w*) 1. 70	(**0. 11,** 0.34) 0.69, 0.91, 1. **14, 1. 37**
80	3, 629. 12	1		27, 547. 06	$b^2G_{4½}$–$z^2H^0_{4½}$		
69	3, 614. 79	18	40	27, 656. 26	$b^4F_{2½}$–$z^4F^0_{2½}$	(0. 00) 1. 04	(0. 00) 1. 03
72	3, 613. 43	2		27, 666. 65	$a^2F_{2½}$–$y^2D^0_{2½}$		
75	3, 613. 08	12	40	27, 669. 35	$a^4F_{3½}$–$z^4G^0_{3½}$	(0. 86) 0. 94	(0.23, 0.69, **1. 14**) --- 0. 34, **0. 80,** 1. 06 ---
78	3, 612. 34	3		27, 675. 02	$a^2S_{0½}$–$w^2P^0_{1½}$	(0. 37) 0. 53	(0. 33) **1. 00,** 1. 67
80	3, 611. 90	15	8	27, 678. 39	$b^2G_{3½}$–$z^2H^0_{4½}$	(0. 00) 1. 06	(**0. 01,** 0. 03 ---) --- 0. 94, 0. 96, **0. 98**
81	3, 607. 39	7	5	27, 713. 00	$b^4P_{2½}$–$z^4S^0_{1½}$	(0. 00*w*) 1. 33	(**0. 20,** 0.60) **1. 00,** 1. 40, 1. 80, 2. 20
82	3, 599. 91	7		27, 770. 58	$c^2D_{2½}$–$z^2F^0_{3½}$	(0. 00) 1. 02	(**0. 03,** 0.09, 0.14) **1. 00,** 1. 06, 1. 11, ---
83	3, 588. 80	2		27, 856. 55	$a^4P_{2½}$–$z^2P^0_{1½}$	(0. 00) 1. 54	(**0. 13,** 0.40) **1. 20,** 1.47, 1. 73, **2. 00**
79	3, 588. 32	6		27, 860. 27	$b^4F_{2½}$–$z^2D^0_{2½}$	(0. 00) 1. 50	(**0. 02,** 0. 06, 0.10) --- 1. 22, 1. 26, **1. 29**
79	3, 587. 98	7	10	27, 862. 91	$b^4F_{1½}$–$z^2D^0_{1½}$	(0. 26) 0. 52	(0.20, **0. 60**) 0.20, **0. 60,** 1.00
74	3, 582. 08	2		27, 908. 80	$b^2D_{1½}$–$y^2P^0_{1½}$		
81	3, 578. 22	7	4	27, 938. 91	$b^4P_{1½}$–$z^4S^0_{1½}$	**(0. 25) 1. 81**	(0.13, **0. 40**) **1.60. 1. 87,** 2. 13
69	3, 576. 88	20	40	27, 949. 38	$b^4F_{3½}$–$z^4F^0_{3½}$	(0. 00) 1. 25	(0. 00) 1. 24
09	3, 573. 09	8	8	27, 979. 02	$b^4F_{1½}$–$z^4F^0_{2½}$	(**0. 31,** 0.96) ---, 0.67, 1. 35, **2. 01**	(**0. 31,** 0.94) 0.09, 0.71, 1. 34, **1. 97**
75	3, 572. 47	30	100	27, 983. 88	$a^4F_{3½}$–$z^4G^0_{3½}$	(0. 00*w*) 0. 93 A[2]	(**0. 09,** 0.26) 0.31, 0.49, 0. 66, **0. 83**
84	3, 568. 14	4		28, 017. 83	$a^2F_{3½}$–$z^2G^0_{3½}$	(0. 81) 1. 05	(--- 0.64, **0. 89**) --- 0. 76, **1. 02,** 1. 27, ---
77	3, 565. 41	5		28, 039. 29	$b^2D_{1½}$–$z^2D^0_{1½}$	**(0. 00) 0. 84**	(0. 00) 0. 80

TABLE 2.—*Wave lengths in the spark spectrum of Zr*—Continued

Key No.	λ I. A.	Intensities B. S.	Intensities King	ν	Term combinations	Observed Zeeman effects	Theoretical Zeeman effects
70	3, 561. 11	1		28, 073. 17	$b^4P_{2½}-y^4D^0_{3½}$		
85, 69	3, 556. 61	30	60	28, 108. 66	$\{a^2D_{2½}-z^4D^0_{2½}$ $b^4F_{4½}-z^4F^0_{4½}$	(0. 00) 1. 31	(0. 00) 1. 33
81	3, 554. 09	7		28, 128. 59	$b^4P_{0½}-z^4S^0_{1½}$	(0. 37) **1. 55**, 2. 39	(0. 33) **1. 67**, 2. 33
75	3, 551. 94	18	40	28, 145. 62	$a^4F_{3½}-z^4G^0_{3½}$	(0. 69) 1. 14	-- 0. 64, **0. 80**) --- 0. 86, **1. 11**, 1. 37, ---
86	3, 549. 51	10		28, 164. 88	$b^4P_{2½}-z^4P^0_{1½}$	(0. 00) 1. 44	(**0. 07**, 0. 20) **1. 40**, 1. 54, 1. 67, 1. 80
80	3, 542. 65	25	10	28, 219. 42	$b^2G_{4½}-z^2H^0_{5½}$	(0. 00) 1. 11	(**0. 01**, 0. 03, ---) **1. 00**, 1. 02, 1. 04, ---
77	3, 539. 05	4		28, 248. 13	$b^3D_{1½}-z^3D^0_{2½}$	(0. 00) 1. 59	(**0. 20**, 0. 60) 0. 60, 1. 00, 1. 40, **1. 80**
79	3, 536. 94	5		28, 264. 98	$b^4F_{2½}-z^4D^0_{2½}$	(0. 00) 1. 12	(0. 09, 0. 26, **0. 43**) --- 0. 94, **1. 11**, 1. 28, ---
87	3, 530. 85	6		28, 313. 73	$b^2G_{4½}-z^2F^0_{3½}$	(0. 00) 1. 06	(**0. 02**, 0. 05, ---) **1. 00**, 1. 03, 1. 06, ---
86	3, 529. 99	5		28, 320. 63	$b^4P_{1½}-z^4P^0_{0½}$	(0. 41) 1. 09	(0. 47) **1. 27**, 2. 20
93	3, 527. 42	7		28, 341. 26	$b^3D_{2½}-z^3F^0_{3½}$	(0. 00) 1. 06	(**0. 03**, 0. 09, 0. 14) **1. 00**, 1. 06, 1. 11, ---
69	3, 525. 81	8	10	28, 354. 20	$b^4F_{2½}-z^4F^0_{3½}$	(0. 00) 1. 53	(**0. 10**, 0. 31, 0. 52) --- 1. 34, 1. 55, **1. 76**
94, 85	3, 520. 87	5		28, 393. 98	$\{a^2D_{2½}-z^4D^0_{3½}$ $a^4P_{2½}-y^4F^0_{1½}$	(0. 00) 1. 73	
87	3, 514. 64	4		28, 444. 31	$b^2G_{3½}-z^2F^0_{3½}$		
83	3, 512. 67	3		28, 460. 26	$a^4P_{1½}-z^4P^0_{0½}$		
88	3, 511. 55	2		28, 469. 34	$c^2D_{2½}-y^4P^0_{1½}$		
89	3, 510. 46	7	4	28, 478. 18	$a^2D_{2½}-y^2D^0_{1½}$	(0.00*w*) 1. 55	(**0. 20**, 0. 60) 0. 60, 1. 00, 1. 40, **1. 80**
90	3, 507. 66	4		28, 500. 91	$a^4P_{1½}-y^4D^0_{0½}$	(0. 81) 0. 96, **2. 48**	(0. 87) 0. 87, **2. 60**
86	3, 506. 48	2		28, 510. 50	$b^4P_{0½}-z^4P^0_{0½}$		
86	3, 506. 04	4		28, 514. 08	$b^4P_{2½}-z^4P^0_{1½}$	(0. 00) 1. 70	(0. 00) 1. 60
75	3, 505. 67	12	20	28, 517. 09	$a^4F_{4½}-z^4G^0_{4½}$	(0. 80) 1. 27	(--- 0. 57, **0. 73**) --- 1. 09, **1. 25**, 1. 42, ---
91	3, 505. 47	15	10	28, 518. 72	$a^2H_{5½}-y^2G^0_{4½}$	(0. 00) 1. 13	(**0. 01**, 0. 03, ---) **1. 00**, 1. 02, 1. 04, ---
82	3, 500. 15	4		28, 562. 06	$c^2D_{1½}-z^2F^0_{2½}$	(0. 00) 0. 94	(**0. 03**, 0. 09) 0. 77, 0. 83, 0. 89, **0. 94**
69	3, 499. 58	8	6	28, 566. 72	$b^4F_{3½}-z^4F^0_{4½}$	(0. 00) 1. 48	(**0. 05**, 0. 14, ---) --- 1. 48, 1. 57, **1. 67**
90, 86	3, 497. 90	12		28, 580. 43	$\{b^4P_{0½}-z^4P^0_{1½}$ $a^4P^0_{2½}-y^4D^0_{1½}$	(0. 36) **1. 33**, **2. 26**	{(**0. 20**, 0. 60) -1. 00, 1. 40, 1. 80, **2. 20**
79	3, 497. 00	2		28, 587. 76	$b^4F_{1½}-z^3D^0_{2½}$		
75	3, 496. 18	50	200	28, 594. 50	$a^4F_{2½}-z^4G^0_{3½}$	(0. 00) 1. 00	(**0. 02**, 0. 07, 0. 11) **0. 87**, 0. 92, 0. 96, ---
83	3, 485. 31	5		28, 683. 67	$a^4P_{0½}-z^3P^0_{1½}$	(1. 05) 1. 72	(1. 00) 1. 67
93, 92	3, 483. 54	12	30	28, 698. 25	$\{a^2P_{1½}-z^2S^0_{0½}$ $b^2D_{2½}-z^2F^0_{3½}$	(0. 34) **0. 98**, 1. 63	(0. 33) **1. 00**, 1. 67
94	3, 481. 44	2		28, 715. 56	$a^4P_{1½}-y^4F^0_{1½}$		
84	3, 481. 14	35	80	28, 718. 03	$a^2F_{3½}-z^2G^0_{4½}$	((0. 00) 1. 09	(**0. 02**, 0. 05, --- **1. 00**, 1. 03, 1. 06...
90	3, 480. 40	5	5	28, 724. 14	$a^4P_{0½}-y^4D^0_{0½}$	(1. 30) 1. 44	(1. 33) 1. 33
84	3, 479. 39	30	60	28, 732. 47	$a^2F_{2½}-z^2G^0_{3½}$	(0. 00) 0. 90	(**0. 02**, 0. 05, 0. 08) --- 0. 90, 0. 94, **0. 97**
89	3, 479. 02	5	10	28, 735. 53	$a^2D_{1½}-y^2D^0_{1½}$	(0. 00) 0. 90	(0. 00) 0. 80
86	3, 478. 50	3	2	28, 739. 82	$b^4P_{1½}-z^4P^0_{2½}$	(0. 00) 1. 47	(**0. 07**, 0. 20) **1. 40**, 1. 54, 1. 67, 1. 80
95	3, 478. 29	4	5	28, 741. 56	$a^4F_{3½}-z^2F^0_{3½}$	(0. 00) 1. 93	(**0. 19**, 0. 57, 0. 95) --- 1. 43, 1. 81, **2. 19**
87	3, 471. 14	8	100	28, 800. 76	$b^2G_{3½}-z^2F^0_{3½}$	(0. 00) 0. 93	(**0. 02**, 0. 05, 0. 08) --- 0. 90, 0. 94, **0. 97**
94	3, 469. 94	4		28, 810. 72	$a^4P_{2½}-y^4F^0_{2½}$	(1. 20) 1. 43	(0. 29, 0. 86, **1. 43**) --- 0. 74, **1. 31**, 1. 89, ---
91	3, 463. 02	35	30	28, 868. 29	$a^2H_{4½}-y^2G^0_{3½}$	(0. 00) 0. 95	(**0. 01**, 0. 03, ---) --- 0. 94, 0. 96, **0. 98**
91	3, 459. 95	3		28, 893. 91	$a^2H_{4½}-y^2G^0_{4½}$		
90	3, 458. 93	10	10	28, 902. 43	$a^4P_{1½}-y^4D^0_{1½}$	(1.05) 0.63, **1. 37**, 2.02	(0. 27, **0. 80**) 0. 93, **1. 47**, 2. 00

TABLE 2.—*Wave lengths in the spark spectrum of Zr*—Continued

Key No.	λ I. A.	Intensities B. S.	Intensities King	ν	Term combinations	Observed Zeeman effects	Theoretical Zeeman effects
89	3,457.56	12	30	28,913.88	$a^3D_{3\frac{1}{2}}$–$y^3D^0_{3\frac{1}{2}}$	(0.00) 1.20	(0.00) 1.20
94	3,454.57	4	3	28,938.91	$a^4P_{0\frac{1}{2}}$–$y^4F^0_{1\frac{1}{2}}$		
97	3,443.57	7	3	29,031.34	$a^3G_{3\frac{1}{2}}$–$y^4F^0_{2\frac{1}{2}}$	(0.00*w*) 0.64	(**0.07,** 0.21, 0.35) **0.54,** 0.68, 0.82,--
75	3,438.23	100	400	29,076.43	$a^4F_{3\frac{1}{2}}$–$z^4G^0_{3\frac{1}{2}}$	(0.00) 1.11	(**0.03,** 0.10, ---) **0.94,** 1.01, 1.07,--
92	3,437.16	10	20	29,085.73	$a^3P_{0\frac{1}{2}}$–$z^3S^0_{1\frac{1}{2}}$	(0.65) 1.28	(0.67) 1.33
90	3,433.90	8	4	29,113.09	$a^4P_{2\frac{1}{2}}$–$y^4D^0_{2\frac{1}{2}}$	(1.07) 1.42	(0.11, 0.34, **0.57**) --- 1.26, **1.48,** 1.72,---
90	3,432.41	7	5	29,125.73	$a^4P_{0\frac{1}{2}}$–$y^4D^0_{1\frac{1}{2}}$	(0.85) **0.00,** 1.54	(0.73) **0.47,** 1.93
94	3,431.57	6	5	29,132.86	$a^4P_{1\frac{1}{2}}$–$y^4F^0_{1\frac{1}{2}}$	(**0.29,** 0.91) **0.00,** ---	(**0.35,** 1.06) **0.03,** 0.68, 1.38, 2.09
98	3,430.53	30	50	29,141.69	$b^4F_{4\frac{1}{2}}$–$z^4D^0_{3\frac{1}{2}}$	(0.00) 1.19	(**0.05,** 0.14, ---) **1.00,** 1.10, 1.19---
95	3,424.82	7	10	29,190.27	$a^4F_{2\frac{1}{2}}$–$z^2F^0_{1\frac{1}{2}}$	(0.37) 0.84	(0.09, 0.26, **0.43**) --- 0.77, **0.94,** 1.12, --
99	3,424.64	1		29,191.81	$b^4P_{1\frac{1}{2}}$–$x^4D^0_{0\frac{1}{2}}$		
	3,423.82	3*l*		29,198.80			
95	3,419.10	5	6	29,239.11	$a^4F_{4\frac{1}{2}}$–$z^2F^0_{3\frac{1}{2}}$	(0.00) 1.82	(**0.10,** 0.29, ---) --- 1.62, 1.81, **2.00**
97	3,414.65	12	6	29,277.21	$a^3G_{4\frac{1}{2}}$–$y^4F^0_{3\frac{1}{2}}$	(0.00) 0.78	(**0.06,** 0.19, ---) **0.67,** 0.80, 0.92, --
100	3,413.39	5	4	29,288.02	$a^4P_{2\frac{1}{2}}$–$y^2F^0_{2\frac{1}{2}}$	(1.29) 1.40	(0.37, 1.11, **1.86**) --- 0.49, **1.23,** 1.97, --
98	3,410.26	20	60	29,314.90	$b^4F_{3\frac{1}{2}}$–$z^4D^0_{2\frac{1}{2}}$	(0.00) 1.12	(**0.07,** 0.20, 0.33) **0.91,** 1.04, 1.17,---
101	3,408.09	10	8	29,333.56	$a^3G_{3\frac{1}{2}}$–$y^4D^0_{2\frac{1}{2}}$	(0.00) 0.47	(**0.24,** 0.72, 1.21) 0.16, **0.32,** 0.65, --
98	3,404.84	12	50	29,361.56	$b^4F_{2\frac{1}{2}}$–$z^4D^0_{1\frac{1}{2}}$	(0.00) 0.88	(**0.09,** 0.26) **0.77,** 0.94, 1.12, 1.29
94	3,403.69	8	10	29,371.48	$a^4P_{2\frac{1}{2}}$–$y^4F^0_{1\frac{1}{2}}$	(0.00) 0.54	(**0.18,** 0.54, 0.90) **0.35,** 0.70, 1.06, --
102	3,402.87	7	6	29,378.56	$a^3H_{3\frac{1}{2}}$–$z^3H^0_{3\frac{1}{2}}$	(0.00) 1.52	(**0.00,** 0.27, ---) ---1.54, 1.73, **1.91**
99	3,402.52	1		29,381.58	$b^4P_{0\frac{1}{2}}$–$x^4D^0_{0\frac{1}{2}}$		
98	3,399.36	10	40	29,408.90	$b^4F_{1\frac{1}{2}}$–$z^4D^0_{0\frac{1}{2}}$	(0.09) 0.57	(0.20) 0.20, **0.60**
93	3,396.66	6	2	29,432.27	$b^2D_{1\frac{1}{2}}$–$z^2F^0_{2\frac{1}{2}}$	(0.00) 0.95	(**0.03,** 0.09) 0.77, 0.83, 0.89, **0.94**
90	3,396.34	7	8	29,435.04	$a^4P_{1\frac{1}{2}}$–$y^4D^0_{2\frac{1}{2}}$	(**0.30,** 0.90) 0.60	(**0.18,** 0.54) **0.83,** 1.19, 1.55, 1.92
99	3,394.63	3	2	29,449.87	$b^4P_{1\frac{1}{2}}$–$x^4D^0_{1\frac{1}{2}}$	(0.00) 1.58	(0.27, **0.80**) 0.93, **1.47,** 2.00
103	3,393.12	10	25	29,462.97	$a^4F_{2\frac{1}{2}}$–$z^4F^0_{1\frac{1}{2}}$	(0.00) 1.46	(**0.31,** 0.94) 0.09, 0.71, 1.34, **1.97**
75	3,391.96	100	400	29,473.05	$a^4F_{4\frac{1}{2}}$–$z^4G^0_{3\frac{1}{2}}$	(0.00) 1.13	(**0.03,** 0.09, ---) **1.00,** 1.06, 1.12,---
95	3,388.29	15	80	29,504.97	$a^4F_{1\frac{1}{2}}$–$z^2F^0_{2\frac{1}{2}}$	(**0.22,** 0.60) 1.51	(**0.23,** 0.69) 0.17, 0.63, 1.09, **1.54**
104	3,387.87	12	40	29,508.63	$a^3G_{3\frac{1}{2}}$–$y^3F^0_{3\frac{1}{2}}$	(0.00) 0.67	(**0.02,** 0.05, 0.08) --- 0.90, 0.94, **0.97**
97	3,378.30	5	4	29,592.22	$a^3G_{3\frac{1}{2}}$–$y^4F^0_{3\frac{1}{2}}$		
98	3,377.45	6	10	29,599.66	$b^4F_{3\frac{1}{2}}$–$z^4D^0_{3\frac{1}{2}}$	(0.55) 1.30	(--- 0.48, **0.67**) --- 1.14, **1.33,** 1.52, ---
100	3,376.25	7	8	29,610.18	$a^4P_{1\frac{1}{2}}$–$y^2F^0_{2\frac{1}{2}}$	(0.34) **0.00,** 1.00	(**0.44,** 1.31) 0.42, **0.46,** 1.30, 2.17
105	3,374.71	15	30	29,623.70	$a^4P_{2\frac{1}{2}}$–$z^4S^0_{1\frac{1}{2}}$	(0.00*w*) 1.35	(**0.20,** 0.60) **1.00,** 1.40, 1.80, 2.20
104	3,373.42	8	15	29,635.03	$a^3G_{4\frac{1}{2}}$–$y^3F^0_{3\frac{1}{2}}$	(0.00) 0.94	(**0.02,** 0.05, ---) **1.00,** 1.03, 1.06,---
99	3,369.27	3	2	29,671.53	$b^4P_{2\frac{1}{2}}$–$x^4D^0_{2\frac{1}{2}}$	(0.40) 1.48	(0.11, 0.34, **0.57**) --- 1.26, **1.48,** 1.72, ---
98	3,367.81	5	7	29,684.39	$b^4F_{1\frac{1}{2}}$–$z^4D^0_{1\frac{1}{2}}$	(**0.00, 1.13**) **0.79,** 1.53	(0.40, **1.20**) 0.60, **0.80,** 1.60
98	3,363.81	5	8	29,719.69	$b^4F_{2\frac{1}{2}}$–$z^4D^0_{2\frac{1}{2}}$	(0.76) 1.20	(0.17, 0.51, **0.86**) --- 0.86, **1.20,** 1.54,---
100	3,362.70	4	4	29,729.50	a^4P_2–$y^2F^0_{1\frac{1}{2}}$	(0.00) 0.00*w*	(**0.23,** 0.69, 1.14) **0.00,** 0.46, 0.91, ---
102	3,359.96	12	10	29,753.74	$a^3H_{4\frac{1}{2}}$–$z^3H^0_{3\frac{1}{2}}$	(0.00) 0.93	(0.00) 0.91

TABLE 2.—*Wave lengths in the spark spectrum of Zr*—Continued

Key No.	λ I. A.	Intensities B. S.	Intensities King	ν	Term combinations	Observed Zeeman effects	Theoretical Zeeman effects
103	3,357.26	15	50	29,777.67	$a^4F_{1½}$–$z^4F^0_{1½}$	(0.36) 0.53	(**0.00**) 0.40
103	3,356.08	18	60	29,788.14	$a^4F_{3½}$–$z^4F^0_{2½}$	(0.00*w*) 1.56	(**0.10,** 0.31, 0.52) ... 1.34, 1.55, **1.76**
106	3,354.39	7	10	29,803.14	$a^2P_{1½}$–$z^2P^0_{1½}$	(0.00) 1.33	(0.00) 1.33
101	3,344.80	15	15	29,888.59	$a^2G_{4½}$–$y^4D^0_{3½}$	(0.00) 0.57	(**0.16,** 0.48, ...) **0.00** 0.32, 0.63, ...
99	3,343.81	4		29,897.44	$b^4P_{1½}$–$z^4D^0_{2½}$	(0.00) 1.06	(**0.18,** 0.54) **0.83,** 1.19, 1.55, 1.92
103	3,340.55	15	50	29,926.61	$a^4F_{4½}$–$z^4F^0_{3½}$	(0.00) **1.52**	(0.05, 0.14, ...) ... 1.48, 1.57, **1.67**
105	3,338.41	10	12	29,945.80	$a^4P_{1½}$–$z^4S^0_{1½}$	(0.00) **1.82**	(0.13, **0.40**) 1.60, **1.87,** 2.13
104	3,337.93	2	1	29,950.10	$a^3G_{3½}$–$y^2F^0_{3½}$		
107	3,334.62	9	15	29,979.83	$a^2D_{2½}$–$z^2G^0_{3½}$		
90	3,334.25	10	15	29,983.16	$a^4P_{2½}$–$y^4D^0_{3½}$	(0.00) 0.71 A[1]	(**0.09,** 0.26, 0.43) **1.00,** 1.17, 1.34, ...
98	3,331.90	2		30,004.31	$b^4F_{3½}$–$z^4D^0_{3½}$		
98	3,327.67	2		30,042.45	$b^4F_{1½}$–$z^4D^0_{2½}$		
102	3,326.81	15	10	30,050.21	$a^2H_{5½}$–$z^2H^0_{5½}$	(0.00) 1.09	(0.00) 1.09
106	3,322.99	10	20	20,084.75	$a^2P_{1½}$–$z^2P^0_{0½}$	(0.38) 1.00, **1.68**	(0.33) 1.00, **1.67**
108	3,319.03	8	15	30,120.65	$a^4F_{2½}$–$z^2D^0_{1½}$	(0.00) 1.47	(**0.11,** 0.34) 0.60, 0.91, 1.14, **1.37**
109	3,318.52	7	6	30,125.28	$a^3P_{1½}$–$y^4D^0_{0½}$	(0.62) 0.66, **1.34**	(0.67) 0.67, **2.90**
110	3,314.49	10	12	30,161.90	$a^3F_{2½}$–$z^2P^0_{1½}$	(0.00*w*) 0.00*w*	(**0.24,** 0.71) **0.14,** 0.62, 1.09, 1.57
105	3,313.70	8	8	30,169.10	$a^4P_{0½}$–$z^4S^0_{1½}$	(0.36) **1.55,** 2.15	(0.33) **1.67,** 2.33
106	3,311.34	4	4	30,190.60	$a^2P_{0½}$–$z^2P^0_{1½}$	(0.00) 1.56	(0.33) 1.00 **1.67**
101	3,309.90	4	2	30,203.73	$a^2G_{3½}$–$y^4D^0_{3½}$		
103	3,306.27	25	80	30,236.89	$a^4F_{3½}$–$z^4F^0_{3½}$	(0.00) 1.00	(0.00) 1.03
95	3,305.15	15	40	30,247.13	$a^4F_{2½}$–$z^2F^0_{3½}$	(0.00) 1.25	(**0.06,** 0.17, 0.29) ... 1.20, 1.31, **1.43**
99, 96	3,302.66	7*l*	4	30,269.94	$a^2D_{1½}$–$w^1F^0_{3½}$ / $b^4P_{2½}$–$z^4D^0_{1½}$	(0.00) 1.29	(**0.09,** 0.26, 0.43) **1.00,** 1.17, 1.34, ...
111	3,296.41	7	4	30,327.33	$a^4P_{1½}$–$z^4P^0_{0½}$	(0.42) 1.34	(0.47) **1.27,** 2.20
112	3,295.03	1		30,340.03	$a^2P_{1½}$–$y^4F^0_{1½}$		
111, 108	3,288.81	10	8	30,397.41	$a^4P_{1½}$–$z^4P^0_{1½}$ / $a^4F_{2½}$–$z^2D^0_{2½}$	(0.00) 1.73	(0.00) 1.73
113	3,287.31	3	2	30,411.28	$b^4F_{1½}$–$y^2D^0_{1½}$		
111	3,285.89	4	2	30,424.42	$a^4P_{2½}$–$z^4P^0_{1½}$	(0.00) 1.61	(0.00) 1.60
102	3,285.77	3		30,425.53	$a^2H_{4½}$–$z^2H^0_{5½}$	(0.00) 1.60	(**0.09,** 0.27, ...) ... 1.54, 1.73, **1.91**
108	3,284.72	20	80	30,435.26	$a^4F_{1½}$–$z^2D^0_{1½}$	(0.31) 0.58	(0.20, **0.60**) 0.20, **0.60,** 1.00
114	3,282.84	12	4	30,452.68	$c^2D_{2½}$–$w^2D^0_{2½}$	(0.00) 1.19	(0.00) 1.20
106	3,280.75	3		30,472.09	$a^2P_{0½}$–$z^2P^0_{0½}$	(0.00) 0.62	(0.00) 0.67
103	3,279.26	65	125	30,485.93	$a^4F_{3½}$–$z^4F^0_{3½}$	(0.00) 1.28	(0.00) 1.24
115	3,278.89	2		30,489.37	$z^2P^0_{0½}$–$c^2D_{1½}$		
109	3,276.37	1		30,512.82	$a^2P_{0½}$–$y^4D^0_{0½}$		
116	3,275.65	1		30,519.53	$a^2H_{4½}$–$z^2F^0_{3½}$		
113	3,275.15	2	2	30,524.19	$b^4F_{2½}$–$y^2D^0_{2½}$	(0.00) 1.12	(0.09, 0.26, **0.43**) .... 0.94, **1.11,** 1.28, ...
103	3,273.04	75	150	30,543.86	$a^4F_{4½}$–$z^4F^0_{4½}$	(0.00) 1.30	(0.00) 1.33
103	3,272.21	8	40	30,551.61	$a^4F_{3½}$–$z^4F^0_{3½}$	(**0, 33,** 1.00) ---, 1.37, **2.04**	(**0.31,** 0.94) 0.09, 0.71, 1.34, **1.97**
117	3,271.13	7	8	30,561.70	$a^2D_{1½}$–$z^2S^0_{½}$	(0.57) **0.00,** 1.24	(0.60) **0.20,** 1.40
111	3,264.81	6	4	30,620.86	$a^4P_{0½}$–$z^4P^0_{1½}$	(0.46) 1.31	(0.47) **1.27,** 2.20
118	3,256.53	1		30,698.71	$a^2F_{2½}$–$y^4F^0_{1½}$		
114	3,250.44	20	35	30,756.22	$c^2D_{1½}$–$w^2D^0_{1½}$	(0.00) 0.98	(0.00) 0.80
119	3,242.18	3	2	30,834.58	$c^2D_{2½}$–$z^2P^0_{1½}$	(0.00) 1.24	(**0, 07,** 0.20) **1.00,** 1.13, 1.27, 1.40
108	3,241.01	25	40	30,845.71	$a^4F_{2½}$–$z^2D^0_{2½}$	(0.15) 1.09	(0.09, 0.26, **0.43**) ... 0.94, **1.11,** 1.28, ...
120	3,237.54	1		30,878.76	$a^3F_{3½}$–$y^2F^0_{3½}$		
114	3,236.61	4		30,887.64	$c^2D_{1½}$–$w^2D^0_{2½}$	(0.00) 1.51	(**0, 20,** 0, 60) 0.60, 1.00, 1.40, **1.80**
121	3,236.17	1		30,891.85	$b^2D_{2½}$–$w^2D^0_{1½}$		
103	3,231.69	30	70	30,934.66	$a^4F_{2½}$–$z^4F^0_{1½}$	(0.00*w*) 1.55	(**0.10,** 0.31, 0.52) ... 1.34, 1.55, **1.76**
115	3,229.73	1*l*		30,953.43	$z^2P^0_{1½}$–$c^2D_{2½}$		
118	3,228.81	15	15	30,962.25	$a^2F_{3½}$–$y^4F^0_{3½}$	(0.41) 1.22	(... 0.24, **0.33**) ... 1.10, **1.19,** 1.29, ...

TABLE 2.—*Wave lengths in the spark spectrum of Zr*—Continued

Key No.	λ I. A.	Intensities B. S.	Intensities King	ν	Term combinations	Observed Zeeman effects	Theoretical Zeeman effects
121	3, 222. 48	15	5	31, 023. 07	$b^3D_{2\frac{1}{2}}-w^3D^0_{1\frac{1}{2}}$	(0. 00) 1. 15	(0. 00) 1. 20
109	3, 218. 68	1		31, 059. 70	$a^3P_{1\frac{1}{2}}-y^4D^0_{2\frac{1}{2}}$		
103	3, 214. 19	40	60	31, 103. 08	$a^4F_{3\frac{1}{2}}-z^4F^0_{4\frac{1}{2}}$	(0. 00) 1. 53	(**0. 05**, 0. 14, ---) --- 1. 48, 1. 57, **1. 67**
118	3, 212. 85	6	8	31, 116. 06	$a^3F_{2\frac{1}{2}}-y^4F^0_{2\frac{1}{2}}$	(0. 45) 1. 00	(0. 09, 0. 26, **0. 43**) --- 0. 77, **0. 94**, 1. 12, ---
122	3, 210. 98	3		31, 134. 18	$a^4P_{2\frac{1}{2}}-z^4D^0_{1\frac{1}{2}}$		
108	3, 208. 32	4	4	31, 159. 99	$a^4F_{1\frac{1}{2}}-z^2D^0_{2\frac{1}{2}}$		
122	3, 204. 36	4		31, 198. 50	$a^4P_{1\frac{1}{2}}-x^4D^0_{0\frac{1}{2}}$		
123	3, 200. 67	2		31, 234. 46	$a^3P_{1\frac{1}{2}}-y^2F^0_{2\frac{1}{2}}$		
119	3, 197. 08	3		31, 269. 53	$c^3D_{1\frac{1}{2}}-x^3P^0_{1\frac{1}{2}}$		
120	3, 191. 93	12	10	31, 319. 98	$a^3F_{3\frac{1}{2}}-y^3F^0_{3\frac{1}{2}}$	(0. 00) 1. 14	(0. 00) 1. 14
124	3, 182. 86	35	60	31, 409. 23	$a^3D_{2\frac{1}{2}}-z^3P^0_{1\frac{1}{2}}$	(0. 00) 1. 02	(**0. 07**, 0.20) **1. 00**, 1. 13, 1. 27, 1. 40
125	3, 181. 94	7	10	31, 418. 31	$a^3F_{2\frac{1}{2}}-y^4D^0_{2\frac{1}{2}}$	(0. 60) ?	(0. 26, 0. 77, **1. 29**) --- 0. 60, **1. 12**, 1. 63, ---
122	3, 181. 58	8	10	31, 421. 86	$a^4P_{0\frac{1}{2}}-x^4D^0_{0\frac{1}{2}}$	(1. 30) 1. 40	(1. 33) 1. 33
122	3, 178. 10	15	10	31, 456. 27	$a^4P_{1\frac{1}{2}}-x^4D^0_{1\frac{1}{2}}$	(0. 78) 1. 48	(0. 27, **0. 80**) 0. 93, **1. 47**, 2. 00
125	3, 166. 29	8	12	31, 573. 60	$a^3F_{3\frac{1}{2}}-y^4D^0_{3\frac{1}{2}}$	(0. 55) 0. 83	(--- 0.71, **1. 00**) --- 1. **00**, **1. 29**, 1. 57, ---
126	3, 165. 98	10	80	31, 576. 69	$a^4F_{4\frac{1}{2}}-z^4D^0_{3\frac{1}{2}}$		
122	3, 165. 45	7	10	31, 581. 97	$a^4P_{2\frac{1}{2}}-x^4D^0_{2\frac{1}{2}}$	(0. 44) 1. 44	(0. 11, 0.34, **0. 57**) --- 1. 26, **1. 48**, 1. 72, ---
120	3, 164. 32	20	25	31, 593. 25	$a^3F_{2\frac{1}{2}}-y^3F^0_{2\frac{1}{2}}$	(0. 29) 1. 00	(0. 00) 0. 86
121	3, 161. 01	2		31, 626. 33	$b^3D_{1\frac{1}{2}}-w^3D^0_{1\frac{1}{2}}$	(0. 00) 0. 85	(0. 00) 0. 80
119	3, 159. 12	5		31, 645. 25	$c^3D_{1\frac{1}{2}}-x^3P^0_{0\frac{1}{2}}$		
124	3, 157. 00	10	15	31, 666. 50	$a^3D_{1\frac{1}{2}}-z^3P^0_{1\frac{1}{2}}$	(0. 73) 1. 05	(0.27, **0. 80**) 0.53, **1. 07**, 1. 60
118	3, 155. 95	1		31, 677. 04	$a^3F_{2\frac{1}{2}}-y^4F^0_{3\frac{1}{2}}$		
122	3, 155. 68	10	20	31, 679. 75	$a^4P_{0\frac{1}{2}}-x^4D^0_{1\frac{1}{2}}$	(0. 69) **0. 46**, 1. 89	(0. 73) **0. 47**, 1. 93
126	3, 138. 66	25	50	31, 851. 53	$a^4F_{3\frac{1}{2}}-z^4D^0_{2\frac{1}{2}}$	(0. 00) 1. 03	(**0. 07**, 0.20, 0.33) **0. 91**, 1. 04, 1. 17, ---
122	3, 133. 49	25	20	31, 904. 08	$a^4P_{1\frac{1}{2}}-x^4D^0_{2\frac{1}{2}}$	(0. 00) 1. 05	(**0. 18**, 0. 54) **0. 83**, 1. 19, 1. 55, 1. 92
126	3, 129. 76	12	40	31, 942. 10	$a^4F_{2\frac{1}{2}}-z^4D^0_{1\frac{1}{2}}$	(0. 00) 0. 91	(**0. 09**, 0.26) **0. 77**, 0.94, 1.12, 1.29
124	3, 129. 16	10	25	31, 948. 23	$a^3D_{1\frac{1}{2}}-z^3P^0_{0\frac{1}{2}}$	(0. 00) 0. 85	(0.07) 0.73, **0. 87**
127	3, 128. 79	1	1	31, 952. 01	$a^3P_{1\frac{1}{2}}-z^4P^0_{2\frac{1}{2}}$		
126	3, 125. 92	12	40	31, 981. 34	$a^4F_{1\frac{1}{2}}-z^4D^0_{0\frac{1}{2}}$	(0. 00) 0.50	(0. 20) 0. 20, **0. 60**
128	3, 125. 21	4	5	31, 988. 61	$a^3D_{1\frac{1}{2}}-y^4D^0_{0\frac{1}{2}}$	(0. 00) 0. 93	(0. 40) 0. 40, **1. 20**
135	5, 122. 61	1		32, 015. 24	$a^3F_{3\frac{1}{2}}-z^4P^0_{2\frac{1}{2}}$		
	3, 116. 68	4*l*		32, 076. 15			
129	3, 115. 73	2	1	32, 085. 93	$a^3G_{4\frac{1}{2}}-z^4D^0_{3\frac{1}{2}}$		
	3, 113. 92	7b, *l*		32, 104. 58			
128	3, 111. 15	2	3	32, 133. 16	$a^3D_{2\frac{1}{2}}-y^4D^0_{1\frac{1}{2}}$		
126	3, 110. 87	8	20	32, 136. 06	$a^4F_{3\frac{1}{2}}-z^4D^0_{3\frac{1}{2}}$	(0. 50) 1. 31	(--- 0. 48, **0. 67**) --- 1. 14, **1. 33**, 1. 52, --
130	3, 110. 52	1		32, 139. 67	$b^3D_{1\frac{1}{2}}-z^3P^0_{1\frac{1}{2}}$		
122	3, 106. 58	35	40	32, 180. 43	$a^4P_{2\frac{1}{2}}-x^4D^0_{3\frac{1}{2}}$	(0. 00) 1. 19	(**0. 09**, 0.26, 0.43) **1. 00**, 1. 17, 1. 34, ---
126	3, 099. 22	10	25	32, 256. 85	$a^4F_{1\frac{1}{2}}-z^4D^0_{1\frac{1}{2}}$	(1. 18) 0. 00, ?,	(0. 40, **1. 20**) 0. 00, **0. 80**, 1. 60
126	3, 095. 07	12	25	32, 300. 10	$a^4F_{2\frac{1}{2}}-z^4D^0_{2\frac{1}{2}}$	(0. 68) 1. 12	(0. 17, 0. 51, **0. 86**) --- 0. 86, **1. 20**, 1. 54, --
127	3, 091. 30	1		32, 339. 49	$a^3P_{0\frac{1}{2}}-z^4P^0_{0\frac{1}{2}}$		
	3, 089. 34	1b		32, 360. 01			
131	3, 089. 00	1	1	32, 363. 57	$a^3D_{2\frac{1}{2}}-y^4F^0_{3\frac{1}{2}}$		
127	3, 088. 28	1		32, 371. 11	$a^3P_{1\frac{1}{2}}-z^4P^0_{2\frac{1}{2}}$		
128	3, 086. 44	2		32, 390. 41	$a^3D_{1\frac{1}{2}}-y^4D^0_{1\frac{1}{2}}$		
	3, 081. 93	1b		32, 437. 81			
	3, 080. 05	1b		32, 457. 61			
132	3, 075. 55	1		32, 505. 09	$b^3P_{1\frac{1}{2}}-w^3P^0_{0\frac{1}{2}}$		
130	3, 074. 55	1		32, 515. 67	$b^3D_{1\frac{1}{2}}-z^3P^0_{0\frac{1}{2}}$		
	3, 073. 93	1b		32, 522. 23			
	3, 070. 18	0b		32, 561. 95			
	3, 068. 32	2b		32, 581. 69			
126	3, 068. 02	2		32, 584. 87	$a^4F_{3\frac{1}{2}}-z^4D^0_{3\frac{1}{2}}$		

TABLE 2.—*Wave lengths in the spark spectrum of Zr*—Continued

Key No.	λ I. A.	Intensities B. S.	Intensities King	ν	Term combinations	Observed Zeeman effects	Theoretical Zeeman effects
	3, 065. 68	1*b*		32, 609. 75			
126	3, 065. 20	2	3	32, 614. 85	$a^4F_{1½}$–$z^4D^0_{1½}$		
131	3, 064. 64	3	3	32, 620. 81	$a^2D_{1½}$–$y^4F^0_{1½}$		
	3, 063. 63	3*b l*		32, 631. 56			
133	3, 061. 33	3	4	32, 656. 07	$a^4F_{2½}$–$y^2D^0_{2½}$	(0. 00) 1. 31 E_1	(**0, 02,** 0. 06, 0. 10) ... 1. 22, 1. 26, **1, 29**
	3, 060. 56	1*b*		32, 664. 29			
133	3, 060. 11	3	4	32, 669. 09	$a^4F_{2½}$–$y^2D^0_{1½}$	(0. 00) 1. 25 E_1	(**0, 11,** 0. 34) 0. 69, 0. 91, 1. 14, **1, 37**
134	3, 057. 22	5	2	32, 699. 98	$a^2G_{4½}$–$y^2G^0_{3½}$	(0. 00) 1. 59 E_1	(**0, 11,** 0. 33, ...) ... 1. 44, 1. 67, **1, 89**
134	3, 054. 84	30	20	32, 725. 45	$a^2G_{4½}$–$y^2G^0_{3½}$	(0. 00) 1. 22 E_1	(0. 00) 1. 11
135	3, 054. 39	3		32, 730. 27	$a^2F_{3½}$–$z^4P^0_{2½}$		
136	3, 048. 42	2	1	32, 794. 37	$a^4P_{2½}$–$y^2G^0_{3½}$		
132	3, 048. 28	5	1	32, 795. 87	$b^2P_{1½}$–$w^2P^0_{1½}$		
	3, 044. 72	1*b*		32, 834. 22			
137	3, 044. 12	4	1	32, 840. 69	$a^2D_{2½}$–$y^2F^0_{2½}$	(0. 00*w*) 1. 00 E_1	(0. 17, 0. 51, **0. 86**) 0. 34, 0. 69, **1. 03,** 1. 37, 1. 71
	3, 038. 59	2		32, 900. 45			
128	3, 036. 50	7	5	32, 923. 10	$a^2D_{1½}$–$y^4D^0_{1½}$		
131	} 3, 036. 39	15	10	32, 924. 29	{$a^2D_{2½}$–$y^4F^0_{1½}$		
139	}				{$b^4P_{2½}$–$y^4P^0_{1½}$}		
	3, 033. 45	1*b*		32, 956. 20			
132	3, 032. 00	3		32, 971. 96	$b^2P_{0½}$–$w^2P^0_{0½}$	(0. 00) 0. 48 E_1	(0. 00) 0. 67
133	3, 030. 91	10	15	32, 983. 82	$a^4F_{1½}$–$y^2D^0_{1½}$	(0. 59) ?	(0. 20, **0. 60**) 0. 20, **0. 60,** 1. 00
134	3, 028. 05	20	20	33, 014. 97	$a^2G_{3½}$–$y^2G^0_{3½}$	(0. 00) 0. 90	(0. 00) 0. 89
138	3, 026. 18	3*b, l*		33, 035. 37	$z^4F^0_{1½}$–$e^4F_{4½}$		
134	3, 025. 70	2	1	33, 040. 61	$a^2G_{3½}$–$y^2G^0_{3½}$		
139	3, 025. 16	3*b*	1	33, 046. 51	$b^4P_{1½}$–$y^4P^0_{0½}$		
138	3, 024. 72	3*b*		33, 051. 32	$z^4F^0_{2½}$–$e^4F_{1½}$		
140	3, 021. 97	1		33, 081. 39	$a^2P_{1½}$–$z^4D^0_{1½}$		
137	3, 020. 45	5	30	33, 098. 04	$a^2D_{1½}$–$y^2F^0_{2½}$	(0. 00) 1. 16	(**0, 03,** 0. 09) 0. 77, 0. 83, 0. 89, **0. 94**
133	3, 019. 84	3	15	33, 104. 72	$a^4F_{2½}$–$y^2D^0_{2½}$	(0. 00) 1. 07	(0. 09, 0. 26, **0. 43**) ... 0. 94, **1, 11,** 1. 28, ...
	3, 019. 50	1		33, 108. 45			
138	3, 018. 53	3*b*		33, 119. 09	$z^4F^0_{3½}$–$e^4F_{3½}$		
	3, 018. 08	2*b*		33, 124. 02			
141	3, 015. 86	2		33, 148. 40	$c^2D_{2½}$–$w^2F^0_{3½}$		
139	3, 015. 67	1		33, 150. 50	$b^4P_{1½}$–$y^4P^0_{1½}$		
142	3, 013. 66	0		33, 172. 61	$a^2F_{3½}$–$z^4D^0_{3½}$		
143	3, 013. 32	8	8	33, 176. 35	$a^2D_{2½}$–$z^4S^0_{1½}$	(0. 00*w*) 0. 00*w*	(**0, 40,** 1. 20) **0. 00,** 0. 80, 1. 60, 2. 40
140	3, 010. 28	2*b l*		33, 209. 85	$a^2P_{0½}$–$z^4D^0_{0½}$		
144	3, 009. 85	2	2	33, 214. 60	$a^4P_{0½}$–$y^2P^0_{0½}$		
139	3, 008. 13	3		33, 233. 59	$b^4P_{2½}$–$y^4P^0_{2½}$	(0. 00) 1. 71 E_1 90	(0. 00) 1. 60
137	3, 003. 73	15	20	33, 282. 26	$a^2D_{2½}$–$y^2F^0_{3½}$	(0. 00) 1. 23	(**0, 03,** 0. 09, 0. 14) **1, 00,** 1. 06, 1. 11, ...
138	3, 000. 59	3*b*		33, 317. 09	$z^4F^0_{3½}$–$e^4F_{2½}$		
139	2, 998. 49	2	1	33, 340. 43	$b^4P_{0½}$–$y^4P^0_{1½}$	(0. 00) 1. 53 E_1	(0. 47) **1, 27,** 2. 20
145	2, 998. 34	1		33, 342. 10	$b^4F_{1½}$–$z^2P^0_{1½}$		
	2, 994. 05	4*b*		33, 389. 86			
133	2, 991. 40	5	5	33, 419. 44	$a^4F_{1½}$–$y^2D^0_{2½}$	(0. 00*w*) 2. 24 E_2	(**0, 40,** 1. 20) 0. 00, 0. 80, 1. 60, **2, 40**
143	2, 990. 10	3	1	33, 433. 97	$a^2D_{1½}$–$z^4S^0_{1½}$	(1. 44) 0. 00*W* E_1	(0. 60, **1. 80**) 0. 20, **1, 40,** 2. 60
146	2, 988. 74	4*b*		33, 449. 19	$y^2D^0_{2½}$–$e^2D_{2½}$	(0. 00) 1. 14 E_1	(0. 00) 1. 20
139	2, 987. 80	5	40	33, 459. 71	$b^4P_{1½}$–$y^4P^0_{2½}$	(0. 00) 1. 53 E_1	(**0, 07,** 0. 20) **1. 40,** 1. 54, 1. 67, 1. 80
128	2, 981. 02	12	25	33, 535. 81	$a^2D_{2½}$–$y^4D^0_{1½}$	(0. 00) 1. 64 E_1	(**0, 11,** 0. 34, 0. 57) ... 1. 54, 1. 77, **2, 00**
147	2, 979. 18	12	20	33, 556. 52	$b^4F_{2½}$–$y^4F^0_{1½}$	(0. 00) 1. 50 E_1	(**0, 31,** 0. 94) 0. 09, 0. 71, 1. 34, **1. 97**
147	2, 978. 07	12	40	33, 569. 02	$b^4F_{3½}$–$y^4F^0_{2½}$	(0. 00) 1. 45 E_1	(**0, 10,** 0. 31, 0. 52) ... 1. 34, 1. 55, **1. 76**
148	2, 976. 61	10	8	33, 585. 49	$a^2G_{4½}$–$z^2H^0_{3½}$	(0. 58) 1. 18 E_1	(... 0. 50, 0. 71, **0. 91**) 0. 81, **1. 01,** 1. 21, ...

TABLE 2.—*Wave lengths in the spark spectrum of Zr*—Continued

Key No.	λ I. A.	Intensities B. S.	Intensities King	ν	Term combinations	Observed Zeeman effects	Theoretical Zeeman effects
144	2, 975. 16	1		33, 601. 86	$a^4P_{1\frac{1}{2}}$–$y^2P^1_{1\frac{1}{2}}$		
149	2, 973. 69	2		33, 618. 47	$a^4P_{2\frac{1}{2}}$–$z^2D^2_{2\frac{1}{2}}$		
192	2, 972. 79	0		33, 628. 64	$a^2D_{2\frac{1}{2}}$–$z^4P^1_{1\frac{1}{2}}$		
	2, 972. 50	0		33, 631. 92			
150	2, 969. 63	8	20	33, 664. 43	$b^4F_{1\frac{1}{2}}$–$y^4D^1_{0\frac{1}{2}}$	(0. 00) 0. 51	(0. 20) 0. 20, **0. 60**
147	2, 968. 95	12	30	33, 672. 14	$b^4F_{4\frac{1}{2}}$–$y^4F^2_{3\frac{1}{2}}$	(0. 00) 1. 42	(**0. 05**, 0. 14, ---)---- 1. 48, 1. 57, **1. 67**
146	2, 966. 27	2*b*		33, 702. 55	$y^2D^1_{1\frac{1}{2}}$–$e^2D_{1\frac{1}{2}}$		
151	2, 964. 55	4	1	33, 722. 11	$a^4F_{3\frac{1}{2}}$–$z^2G^1_{3\frac{1}{2}}$	(1. 03) 1. 38 E_1	(--- 0. 87, **1. 22**) --- 0. 71, **1. 06**, 1. 41, ---
150	2, 962. 69	12	30	33, 743. 28	$b^4F_{2\frac{1}{2}}$–$y^4D^1_{1\frac{1}{2}}$	(0. 00) 0. 95	(**0. 09**, 0. 26) **0. 77**, 0. 94, 1. 12, 1. 29
	2, 960. 57	1		33, 767. 44			
152	2, 955. 77	20	15	33, 822. 28	$b^2G_{3\frac{1}{2}}$–$w^2F^2_{2\frac{1}{2}}$	(0. 00) 1. 00	(**0. 02**, 0. 05, 0. 08) --- 0. 90, 0. 94, **0. 97**
138, 144	2, 955. 53	2*b*		33, 825. 04	$z^4F^1_{1\frac{1}{2}}$–$e^4F_{1\frac{1}{2}}$ / $a^4P_{0\frac{1}{2}}$–$y^2P^1_{1\frac{1}{2}}$		
151	2, 952. 23	6	8	33, 862. 83	$a^4F_{4\frac{1}{2}}$–$z^2G^1_{4\frac{1}{2}}$	(0. 93) 1. 27 E_1	(--- 0. 78, **1. 00**) --- 1. 00, **1. 22**, 1. 44, ---
150	2, 951. 46	10	25	33, 871. 66	$b^4F_{3\frac{1}{2}}$–$y^4D^2_{2\frac{1}{2}}$	(0. 00) 1. 30 E_1	(**0. 07**, 0. 20, 0. 33) **0. 91**, 1. 04, 1. 17, ---
	2, 949. 81	2*b*		33, 890. 61			
148	2, 948. 94	12	20	33, 900. 60	$a^2G_{3\frac{1}{2}}$–$z^2H^1_{4\frac{1}{2}}$	(0. 00) 1. 00	(**0. 01**, 0. 03, ---) --- 0. 94, 0. 96, **0. 98**
	2, 946. 93	1*b*		33, 923. 73			
242	2, 946. 30	1*b*		33, 930. 98	$z^2G^1_{4\frac{1}{2}}$–$e^2G_{3\frac{1}{2}}$		
149	2, 945. 45	4	3	33, 940. 78	$a^4P_{1\frac{1}{2}}$–$z^2D^2_{2\frac{1}{2}}$	(0. 00*w*) 0. 00*w* E_1	(**0. 27**, 0. 80) **0. 40**, 0. 93, 1. 47, 2. 00
149	2, 944. 19	3		33, 955. 30	$a^4P_{0\frac{1}{2}}$–$z^2D^1_{1\frac{1}{2}}$	(0. 87) 0. 00*w* E_1	(0. 93) **0. 13**, 1. 73
192	2, 942. 26	1		33, 977. 57	$a^2D_{2\frac{1}{2}}$–$z^4P^2_{2\frac{1}{2}}$		
248	2, 941. 55	1		33, 985. 77	$z^2H^1_{5\frac{1}{2}}$–$e^2I_{6\frac{1}{2}}$		
	2, 940. 62	1*b*		33, 996. 52			
	2, 938. 82	1*b*		34, 017. 34			
153	2, 937. 74	4	1	34, 029. 85	$b^4F_{4\frac{1}{2}}$–$y^2F^2_{3\frac{1}{2}}$	(0. 00) 1. 64 E_1	(**0. 10**, 0. 29, ---) --- 1. 62, 1. 81, **2. 00**
153	2, 936. 31	12	20	34, 046. 42	$b^4F_{3\frac{1}{2}}$–$y^2F^2_{2\frac{1}{2}}$	(0. 00) 1. 66 E_1	(**0. 19**, 0. 57, 0. 95) --- 1. 43, 1. 81, **2. 19**
150	2, 934. 62	12	20	34, 066. 02	$b^4F_{1\frac{1}{2}}$–$y^4D^1_{1\frac{1}{2}}$	(0. 96) 0. 77 E_1	(0. 40, **1. 20**) 0. 00, **0. 80**, 1. 60
242	2, 931. 89	3*b*		34, 097. 74	$z^2G^1_{4\frac{1}{2}}$–$e^2G_{4\frac{1}{2}}$		
154	2, 931. 08	8*b*, *l*		34, 107. 17	$z^4G^1_{3\frac{1}{2}}$–$e^4F_{4\frac{1}{2}}$		
147	2, 929. 10	1		34, 130. 22	$b^4F_{3\frac{1}{2}}$–$y^4F^1_{2\frac{1}{2}}$		
152	2, 926. 99	25	20	34, 154. 82	$b^2G_{4\frac{1}{2}}$–$w^2F^2_{3\frac{1}{2}}$	(0. 00) 1. 05	(**0. 02**, 0. 05, ---)**1. 00**, 1. 03, 1. 06, ---
151	2, 925. 62	4	2	34, 170. 82	$a^4F_{2\frac{1}{2}}$–$z^2G^1_{3\frac{1}{2}}$	(0. 00) 0. 62 E_1	(**0. 07**, 0. 21, 0. 35) **0. 54**, 0. 68, 0. 82, ---
155	2, 924. 63	8	2	34, 182. 38	$b^2D_{2\frac{1}{2}}$–$w^2F^1_{3\frac{1}{2}}$	(0. 00) 1. 00 E_1	(**0. 03**, 0. 09, 0. 14) **1. 00**, 1. 06, 1. 11, ---
	2, 922. 93	1*b*		34, 202. 26			
	2, 921. 14	1*b*		34, 223. 22			
	2, 920. 03	3*b*		34, 236. 23			
148	2, 918. 24	18	30	34, 257. 23	$a^2G_{4\frac{1}{2}}$–$z^2H^1_{5\frac{1}{2}}$	(0. 00) 0. 94	(**0. 01**, 0. 03,--) **1. 00**, 1. 02, 1. 04---
150	2, 916. 63	7	8	34, 276. 14	$b^4F_{2\frac{1}{2}}$–$y^4D^2_{2\frac{1}{2}}$	(0. 00*w*) 1. 17 E_1	(0. 17, 0. 51, **0. 86**) 0. 51, 0. 86, **1. 20**, 1. 54, 1. 89
150	2, 915. 98	15	40	34, 283. 77	$b^4F_{4\frac{1}{2}}$–$y^4D^1_{3\frac{1}{2}}$	(0. 00) 1. 41 E_1	(**0. 05**, 0. 14,---) **1. 00**, 1. 10, 1. 19, ---
	2, 914. 71	1*b*		34, 298. 71			
156	2, 910. 26	8	8	34, 351. 16	$a^2G_{4\frac{1}{2}}$–$z^2F^1_{3\frac{1}{2}}$	(0. 00) 1. 00 E_1	(**0. 02**, 0. 05,---) **1. 00**, 1. 03, 1. 06, ---
	2, 907. 99	3*b*		34, 378. 09			
157	2, 907. 37	6	5	34, 385. 30	$a^2F_{3\frac{1}{2}}$–$y^2G^1_{3\frac{1}{2}}$	(0. 68) 1. 02 E_1	(--- 0. 64, **0. 89**) --- 0. 76, **1. 02**, 1. 27, ---
157	2, 905. 22	15	25	34, 410. 87	$a^2F_{3\frac{1}{2}}$–$y^2G^1_{4\frac{1}{2}}$	(0. 00) 1. 07 E_1	(**0. 02**, 0. 05, ---) **1. 00**, 1. 03, 1. 06, ---
151	2, 904. 22	1	1	34, 422. 60	$a^4F_{2\frac{1}{2}}$–$z^2G^1_{4\frac{1}{2}}$		
248	2, 903. 70	15*b*, *l*		34, 428. 76	$z^2H^1_{5\frac{1}{2}}$–$e^2I_{6\frac{1}{2}}$	(0. 00) 1. 05 E_1	(**0. 01**, 0. 02, **0. 03**, ---) **1. 00**, 1. 01, 1. 03, ---

TABLE 2.—*Wave lengths in the spark spectrum of Zr*—Continued

Key No.	λ I. A.	Intensities B. S.	Intensities King	ν	Term combinations	Observed Zeeman effects	Theoretical Zeeman effects
158	2, 902. 24	2	1	34, 446. 07	$a^4P_{3\frac{1}{2}}$–$z^2F^0_{3\frac{1}{2}}$		
153	2, 901. 81	3	6	34, 451. 18	$b^4F_{3\frac{1}{2}}$–$y^2F^0_{3\frac{1}{2}}$		
155	2, 901. 60	5	4	34, 453. 67	$b^2D_{1\frac{1}{2}}$–$w^2F^0_{1\frac{1}{2}}$	(0. 00 0. 72 E_1	(**0. 03,** 0. 09) 0. 77, 0. 83, 0. 89, **0. 94**
153	2, 898. 72	7	12	34, 487. 90	$b^4F_{3\frac{1}{2}}$–$y^2F^0_{3\frac{1}{2}}$	(0. 00*w*) 1. 14 E_1	(--- 0. 24, **0. 33**)---- 1. 10, **1. 19**, 1. 29, ...
	2, 897. 72	1		34, 499. 81			
154	2, 895. 32	6*b*, *l*		34, 528. 40	$z^4G^0_{3\frac{1}{2}}$–$e^4F_{3\frac{1}{2}}$	(0. 00) 1. 12 E_1	(**0. 03,** 0. 10, ---) **0. 94,** 1. 01, 1. 07, ---
147	2, 894. 78	1		34, 534. 84	$b^4F_{3\frac{1}{2}}$–$y^4F^0_{3\frac{1}{2}}$		
	2, 891. 99	3*b*		34, 568. 15			
	2, 891. 75	1		34, 571. 03			
150	2, 889. 41	5	3	34, 599. 02	$b^4F_{1\frac{1}{2}}$–$y^4D^0_{2\frac{1}{2}}$	(0. 00*w*) 2. 03 E_1	(**0. 49,** 1. 46) 0. 09, 0. 88, 1. 86, **2. 83**
159	2, 888. 04	5	6	34, 615. 43	$a^2P_{1\frac{1}{2}}$–$y^2P^0_{1\frac{1}{2}}$	(0. 00) 1. 51 E_1	(0. 33) 1. 00, **1. 67**
242	2, 886. 71	3*b*		34, 631. 38	$z^2G^0_{3\frac{1}{2}}$–$e^2G_{3\frac{1}{2}}$	(0. 00) 0. 00*W* E_1	(0. 00) 0. 89
248	2, 884. 57	7*b*		34, 657. 07	$z^2H^0_{4\frac{1}{2}}$–$e^2I_{4\frac{1}{2}}$	(0. 00) 1. 15 E_1	(**0. 01,** 0. 02, 0. 03, ---) --- 0. 96, 0. 97, **0. 98**
156	2, 883. 79	3	3	34, 666. 45	$a^2G_{3\frac{1}{2}}$–$z^2F^0_{3\frac{1}{2}}$	(0. 57) 1. 21 E_1	(--- 0. 64, **0. 89**) --- 0. 76, **1. 02**, 1. 27, ...
160	2, 882. 08	5	3	34, 687. 02	$\{a^2D_{1\frac{1}{2}}$–$z^4D^0_{0\frac{1}{2}}$ $a^2D_{2\frac{1}{2}}$–$z^4D^0_{1\frac{1}{2}}\}$		
	2, 880. 14	1		34, 710. 38			
150	2, 877. 56	10	10	34, 741. 49	$b^4F_{3\frac{1}{2}}$–$y^4D^0_{3\frac{1}{2}}$	(0. 00*w*) 1. 26 E_1	(--- 0. 48, **0. 67**) ... 1. 14, **1. 33**, 1. 52, ...
	2, 874. 22	3*b*		34, 781. 86			
158	2, 872. 52	6	2	34, 802. 45	$a^4P_{2\frac{1}{2}}$–$z^2F^0_{2\frac{1}{2}}$	(1. 60) 0. 00*W* E_1	(0. 37, 1. 11, **1. 86**) 0. 26 **0. 49**, **1. 23**, 1. 97, 2. 71
161	2, 871. 85	1		34, 810. 57	$a^4F_{1\frac{1}{2}}$–$z^2S^0_{0\frac{1}{2}}$		
162	2, 869. 80	12	40	34, 835. 43	$a^4P_{2\frac{1}{2}}$–$y^4P^0_{1\frac{1}{2}}$	(0. 00) 1. 47 E_1	(**0. 07,** 0. 20) **1. 40**, 1. 54 1. 67, 1. 80
	2, 867. 42	1		34, 864. 35			
	2, 865. 93	1*b*		34, 882. 47			
147	2, 865. 61	5	8	34, 886. 36	$b^4F_{4\frac{1}{2}}$–$y^4F^0_{4\frac{1}{2}}$	(0. 00) 1. 35 E_1	(0. 00) 1. 33
153	2, 865. 09	3	2	34, 892. 70	$b^4F_{3\frac{1}{2}}$–$y^2F^0_{3\frac{1}{2}}$		
	2, 864. 19	1*b*		34, 903. 66			
154	2, 859. 61	4*b*		34, 959. 56	$z^4G^0_{3\frac{1}{2}}$–$e^4F_{2\frac{1}{2}}$	(0. 00) 0. 87 E_1	(**0. 02,** 0. 07, 0. 11) **0. 87**, 0. 92, 0. 96, ...
	2, 858. 33	1*b*		34, 975. 21			
	2, 857. 33	3*b*, *l*		34, 987. 45			
159	2, 856. 05	5	1	35, 003. 14	$a^2P_{0\frac{1}{2}}$–$y^2P^0_{0\frac{1}{2}}$	(0. 00) 0. 44 E_1	(0. 00) 0. 67
156	2, 854. 42	7	3	35, 023. 12	$a^2G_{3\frac{1}{2}}$–$z^2F^0_{3\frac{1}{2}}$	(0. 00) 0. 83 E_1	(**0. 02,** 0. 05, 0. 08) ... 0. 90, 0. 94, **0. 97**
240	2, 853. 66	2*b*		35, 032. 45	$z^2D^0_{2\frac{1}{2}}$–$e^2F_{3\frac{1}{2}}$	(0. 00) 1. 17 E_1	(**0. 03,** 0. 09, 0. 14) **1. 00**, 1. 06, 1. 11, ...
162	2, 851. 98	12	40	35, 053. 08	$a^4P_{1\frac{1}{2}}$–$y^4P^0_{0\frac{1}{2}}$	(0. 00) 1. 47 E_1	(0. 47) **1. 27**, 2. 20
154	2, 851. 28	1*b*		35, 061. 69	$z^4G^0_{4\frac{1}{2}}$–$e^4F_{4\frac{1}{2}}$		
	2, 849. 10	1*b*		35, 088. 52			
157	2, 848. 17	8	15	35, 099. 97	$a^2F_{3\frac{1}{2}}$–$y^2G^0_{3\frac{1}{2}}$	(0. 00) 0. 93 E_1	(**0. 02,** 0. 05, 0. 08) ... 0. 90, 0. 94, **0. 97**
158	2, 846. 16	2		35, 124. 76	$a^4P_{1\frac{1}{2}}$–$z^2F^0_{2\frac{1}{2}}$		
162	2, 844. 57	15	50	35, 144. 39	$a^4P_{2\frac{1}{2}}$–$y^4P^0_{2\frac{1}{2}}$	(0. 00) 1. 58 E_1	(0. 00) 1. 60
162	2, 843. 53	10	10	35, 157. 24	$a^4P_{1\frac{1}{2}}$–$y^4P^0_{1\frac{1}{2}}$	(0. 00) 1. 68 E_1	(0. 00) 1. 73
163	2, 841. 38	1		35, 183. 84	$b^4F_{3\frac{1}{2}}$–$z^4P^0_{2\frac{1}{2}}$		
164	2, 839. 34	10	8	35, 209. 12	$a^2F_{3\frac{1}{2}}$–$z^4D^0_{2\frac{1}{2}}$	(0. 00). 1. 10 E_1	(**0. 03,** 0. 09, 0. 14) **1. 00**, 1. 06, 1. 11, ...
159	2, 838. 00	5	4	35, 225. 75	$a^2P_{1\frac{1}{2}}$–$y^2P^0_{1\frac{1}{2}}$	(0. 00) 0. 90 E_1	(0. 00) 1. 33
165	2, 835. 00	1		35, 263. 02	$d^2D_{1\frac{1}{2}}$–$w^2P^0_{1\frac{1}{2}}$		
166	2, 834. 38	5	3	35, 270. 73	$a^2F_{3\frac{1}{2}}$–$z^2H^0_{4\frac{1}{2}}$		
162	2, 833. 90	8	6	35, 276. 71	$a^4P_{0\frac{1}{2}}$–$y^4P^0_{0\frac{1}{2}}$	(0. 00) 2. 51 E_1	(0. 00) 2. 67
	2, 832. 81	3		35, 290. 28			
	2, 831. 54	2*b*		35, 306. 11			
249	2, 829. 38	0		35, 333. 06	$z^2H^0_{5\frac{1}{2}}$–$e^2H_{4\frac{1}{2}}$		
167	2, 827. 52	3	8	35, 356. 30	$a^2P_{1\frac{1}{2}}$–$z^2D^0_{1\frac{1}{2}}$		
162	2, 825. 54	15	30	35, 381. 08	$a^4P_{0\frac{1}{2}}$–$y^4P^0_{1\frac{1}{2}}$	(0. 00) 1. 52 E_1	(0. 47) **1. 27**, 2. 20
160	2, 824. 56	2*b*		35, 393. 35	$a^2D_{1\frac{1}{2}}$–$z^4D^0_{2\frac{1}{2}}$		
	2, 824. 08	1*b*		35, 399. 37			
240	2, 821. 09	1*b*		35, 436. 88	$z^2D^0_{1\frac{1}{2}}$–$e^2F_{2\frac{1}{2}}$		
154	2, 819. 31	3*l*		35, 459. 25	$z^4G^0_{5\frac{1}{2}}$–$e^4F_{3\frac{1}{2}}$		
162	2, 818. 76	20	20	35, 466. 17	$a^4P_{1\frac{1}{2}}$–$y^4P^0_{2\frac{1}{2}}$	(0. 00) 1. 44 E_1	(**0. 07,** 0. 20) 1. 40, 1. 54, 1. 67, 1. 80

TABLE 2.—*Wave lengths in the spark spectrum of Zr*—Continued

Key No.	λ I. A.	Intensities B. S.	Intensities King	ν	Term combinations	Observed Zeeman effects	Theoretical Zeeman effects
163	2, 816. 77	3b		35, 491. 31	$b^4F_{1\frac{1}{2}}$–$z^4P^0_{0\frac{1}{2}}$		
167	2, 810. 91	15	15	35, 565. 21	$a^2P_{1\frac{1}{2}}$–$z^2D^0_{2\frac{1}{2}}$	(0. 00) 1. 18 E_1	(**0. 07**, 0. 20) **1. 00**, 1. 13, 1. 27, 1. 40
168	2, 809. 40	2		35, 584. 33	$a^2F_{2\frac{1}{2}}$–$y^2P^0_{1\frac{1}{2}}$		
169	2, 808. 15	3	2	35, 600. 17	$a^4F_{2\frac{1}{2}}$–$z^2P^0_{1\frac{1}{2}}$		
	2, 807. 86	3		35, 603. 84			
159, 170	2, 807. 13	3b		35, 613. 10	$a^2S_{0\frac{1}{2}}$–$z^2P^0_{0\frac{1}{2}}$ / $a^2P_{0\frac{1}{2}}$–$y^2P^0_{1\frac{1}{2}}$		
154	2, 806. 68	5		35, 618. 81	$z^4G^0_{2\frac{1}{2}}$–$e^4F_{1\frac{1}{2}}$		
241	2, 805. 71	2b		35, 631. 13	$z^2F^0_{2\frac{1}{2}}$–$e^2F_{2\frac{1}{2}}$		
	2, 804. 78	1b		35, 642. 94			
	2, 800. 10	2		35, 702. 51			
164	2, 799. 16	8	5	35, 715. 50	$a^2F_{2\frac{1}{2}}$–$z^2D^0_{1\frac{1}{2}}$	(0. 00) 1. 05 E.	(**0. 03**, 0. 09) 0. 77 0. 83 0. 89, **0. 94**
	2, 798. 71	1		35, 720. 24			
160	2, 797. 78	3b		35, 732. 11	$a^2D_{2\frac{1}{2}}$–$z^4D^0_{2\frac{1}{2}}$		
167	2, 796. 92	10	12	35, 743. 10	$a^2P_{0\frac{1}{2}}$–$z^2D^0_{1\frac{1}{2}}$	(0. 00) 0. 84 E_1	(0. 07) 0. 73, **0. 87**
173	2, 796. 32	2b		35, 750. 77	$b^2P_{1\frac{1}{2}}$–$y^2D^0_{1\frac{1}{2}}$		
	2, 793. 12	2		35, 791. 73			
249	2, 786. 95	6b, l		35, 870. 96	$z^2H^0_{3\frac{1}{2}}$–$e^2H_{3\frac{1}{2}}$	(0. 00) 1. 11 E_1	(0. 00) 1. 09
154	2, 785. 90	4b		35, 884. 48	$z^4G^0_{3\frac{1}{2}}$–$e^4F_{2\frac{1}{2}}$		
	2, 785. 33	1b		35, 891. 82			
169	2, 783. 56	5	4	35, 914. 64	$a^4F_{1\frac{1}{2}}$–$z^2P^0_{1\frac{1}{2}}$		
164	2, 782. 84	2		35, 923. 93	$a^2F_{2\frac{1}{2}}$–$z^2D^0_{2\frac{1}{2}}$		
	2, 781. 61	2		35, 939. 82			
	2, 777. 05	3b		35, 998. 83			
249	2, 776. 59	3b		36, 004. 79	$z^2H^0_{3\frac{1}{2}}$–$e^2H_{4\frac{1}{2}}$		
171	2, 774. 15	12	15	36, 036. 46	$a^2F_{3\frac{1}{2}}$–$z^2F^0_{3\frac{1}{2}}$	(0. 00) 1. 15 E_1	(0. 00) 1. 14
	2, 772. 56	2b		36, 057. 12			
172	2, 768. 84	15		36, 105. 57	$a^4F_{3\frac{1}{2}}$–$y^4F^0_{3\frac{1}{2}}$		
172	2, 768. 73	15		36, 107. 00	$a^4F_{4\frac{1}{2}}$–$y^4F^0_{3\frac{1}{2}}$		
	2, 767. 45	1b		36, 123. 70			
	2, 766. 82	1b		36, 131. 92			
172	2, 766. 41	1		36, 137. 28	$a^4F_{3\frac{1}{2}}$–$y^4F^0_{1\frac{1}{2}}$		
169	2, 761. 89	6	5	36, 196. 41	$a^4F_{1\frac{1}{2}}$–$z^2P^0_{0\frac{1}{2}}$	(0. 00) 0. 00*w* E_1	(0. 13) **0. 27**, 0. 53
173	2, 760. 10	3b		36, 219. 89	$b^2P_{0\frac{1}{2}}$–$e^2D^0_{1\frac{1}{2}}$		
174	2, 758. 80	20	80	36, 236. 96	$a^4F_{1\frac{1}{2}}$–$y^4D^0_{0\frac{1}{2}}$	(0. 00*w*) 0. 56	(0. 20) 0. 20, **0. 60**
	2, 754. 39	2b		36, 294. 97			
175	2, 754. 23	2	2	36, 297. 08	$b^4F_{2\frac{1}{2}}$–$z^4D^0_{1\frac{1}{2}}$	(0. 00) 0. 99 E_1	(**0. 09**, 0. 26) **0. 77**, 0. 94, 1. 12, 1. 29
	2, 753. 25	3b		36, 310. 00			
184	2, 752. 57	2b		36, 318. 97	$b^2F_{2\frac{1}{2}}$–$y^2D^0_{1\frac{1}{2}}$		
174	2, 752. 21	20	150	36, 323. 72	$a^4F_{3\frac{1}{2}}$–$y^4D^0_{1\frac{1}{2}}$	(0. 00) 1. 00	(**0. 09**, 0. 26) **0. 77**, 0. 94, 1. 12, 1. 29
175	2, 750. 95	4	3	36, 340. 36	$b^4F_{3\frac{1}{2}}$–$z^4D^0_{2\frac{1}{2}}$	(0. 00) 0. 93 E_1	(**0. 07**, 0. 20,0. 33) **0. 91**, 1. 04, 1. 17, ---
176	2, 750. 44	1		36, 347. 09	$a^2D_{2\frac{1}{2}}$–$y^2G^0_{3\frac{1}{2}}$		
	2, 749. 85	2		36, 354. 89			
241	2, 748. 89	2		36, 367. 59	$z^2F^0_{3\frac{1}{2}}$–$e^2F_{3\frac{1}{2}}$		
154	2, 747. 66	1b		36, 383. 86	$z^4G^0_{3\frac{1}{2}}$–$e^4F_{3\frac{1}{2}}$		
174	2, 745. 86	20	100	36, 407. 71	$a^4F_{3\frac{1}{2}}$–$y^4D^0_{3\frac{1}{2}}$	(0. 00) 1. 24	(**0. 07**, 0. 20, 0. 33) **0. 91**, 1. 04, 1. 17,---
	2, 744. 49	3b		36, 425. 89			
172	2, 742. 54	20	125	36, 451. 79	$a^4F_{4\frac{1}{2}}$–$y^4F^0_{3\frac{1}{2}}$		
177	2, 741. 54	8	15	36, 464. 95	$a^4F_{4\frac{1}{2}}$–$y^2F^0_{3\frac{1}{2}}$	(0. 00) 1. 52 E_1	(**0. 10**, 0. 29, ---)----- 1. 62, 1. 81, **2. 00**
178	2, 740. 49	8	8	36, 478. 92	$a^2D_{1\frac{1}{2}}$–$y^2P^0_{2\frac{1}{2}}$	(0. 00) 0. 68 E_1	(0. 07) 0. 73, **0. 87**
175	2, 740. 33	6	4	36, 481. 18	$b^4F_{4\frac{1}{2}}$–$z^4D^0_{3\frac{1}{2}}$		
173	2, 739. 77	1		36, 488. 64	$b^2P_{1\frac{1}{2}}$–$e^2D^0_{2\frac{1}{2}}$		
179	2, 738. 40	1		36, 506. 89	$y^2F^0_{3\frac{1}{2}}$–$f^2F_{3\frac{1}{2}}$		
172	2, 734. 84	20	150	36, 554. 41	$a^4F_{3\frac{1}{2}}$–$y^4F^0_{2\frac{1}{2}}$	(0. 00) 1. 08 E_1	(0. 00) 1. 03
177	2, 732. 72	15	80	36, 582. 77	$a^4F_{3\frac{1}{2}}$–$y^2F^0_{3\frac{1}{2}}$	(0. 00) 1. 50 E_1	(**0. 19**, 0. 57, 0. 95)--- 1. 43, 1. 81, **2. 19**
175	2, 729. 93	3		36, 620. 15	$b^4F_{1\frac{1}{2}}$–$z^4D^0_{1\frac{1}{2}}$		
174	2, 728. 56	2		36, 638. 54	$a^4F_{1\frac{1}{2}}$–$y^4D^0_{1\frac{1}{2}}$		
170	2, 726. 99	3 b		36, 659. 63	$a^2S_{0\frac{1}{2}}$–$z^2P^0_{1\frac{1}{2}}$		
172	2, 726. 48	15	125	36, 666. 49	$a^4F_{3\frac{1}{2}}$–$y^4F^0_{3\frac{1}{2}}$	(0. 00) 1. 20 E_1	(0. 00) 1. 24
174	1, 722. 62	25	150	36, 718. 47	$a^4F_{4\frac{1}{2}}$–$y^4D^0_{3\frac{1}{2}}$	(0. 00) 1. 45 E_1	(**0. 05**, 0. 14, 0. 24, 0. 33) **1. 00**. 1. 10, 1. 19, ---
180	2, 721. 37	2		36, 735. 33	$a^2F_{3\frac{1}{2}}$–$y^4P^0_{2\frac{1}{2}}$		

TABLE 2.—*Wave lengths in the spark spectrum of Zr*—Continued

Key No.	λ I. A.	Intensities B. S.	Intensities King	ν	Term combinations	Observed Zeeman effects	Theoretical Zeeman effects
181	2, 720. 36	5	2	36, 748. 97	$a^3P_{1\frac{1}{2}}$–$x^3F^0_{1\frac{1}{2}}$		
178	2, 714. 22	10	20	36, 832. 10	$a^3D_{2\frac{1}{2}}$–$y^3P^0_{1\frac{1}{2}}$	(0. 00) 1. 08 E_1	(**0. 07,** 0. 20) **1. 00,** 1. 13, 1. 27, 1. 40
174	2, 712. 38	10	25	36, 857. 08	$a^4F_{2\frac{1}{2}}$–$y^4D^0_{1\frac{1}{2}}$	(0. 00*w*) 1. 04 E_1	(0. 17, 0. 51, **0. 86**) 0. 51, 0. 86, **1. 20,** 1. 54, 1. 89
172	2, 711. 48	12	50	36, 869. 32	$a^4F_{1\frac{1}{2}}$–$y^4F^0_{1\frac{1}{2}}$	(0. 00) 1. 89 E_1	(**0. 31,** 0. 94) 0. 09, 0. 71, 1. 34, **1. 97**
175	2, 706. 38	4		36, 938. 79	$b^4F_{2\frac{1}{2}}$–$x^4D^0_{3\frac{1}{2}}$		
182	2, 704. 66	4		36, 962. 28	$a^3D_{2\frac{1}{2}}$–$x^3D^0_{1\frac{1}{2}}$		
183	2, 703. 25	3		36, 981. 56	$b^2P_{1\frac{1}{2}}$–$v^2F^0_{2\frac{1}{2}}$		
	2, 702. 93	1		36, 985. 93			
177	2, 700. 12	18	100	37, 024. 42	$a^4F_{3\frac{1}{2}}$–$y^3F^0_{3\frac{1}{2}}$	(0. 00) 1. 23 E_1	(0. 00) 1. 24
177	2, 699. 59	6	15	37, 031. 69	$a^4F_{3\frac{1}{2}}$–$y^2F^0_{2\frac{1}{2}}$	(0. 00) 1. 20 E_1	(0. 09, 0. 26, **0. 43**) 0. 60, 0. 77, **0. 94,** 1. 12, 1. 29
178	2, 695. 42	8	3	37, 088. 98	$a^3D_{1\frac{1}{2}}$–$y^3P^0_{1\frac{1}{2}}$	(0. 59) 1. 09 E_1	(0. 27, **0. 80**) 0. 53, **1. 07,** 1. 60
171	2, 694. 05	10	20	37, 107. 84	$a^3F_{2\frac{1}{2}}$–$x^3F^0_{2\frac{1}{2}}$	(0. 00) 0. 83 E_1	(0. 00) 0. 86
172	2, 693. 52	9	30	37, 115. 14	$a^4F_{3\frac{1}{2}}$–$y^4F^0_{3\frac{1}{2}}$	(0. 00) 1. 64 E_1	(**0. 10,** 0. 31, 0 52) ... 1. 34, 1. 55, **1. 76**
185	2, 692. 60	6	5	37, 127. 82	$a^4P_{2\frac{1}{2}}$–$w^3D^0_{2\frac{1}{2}}$	(0. 76) 1. 39 E_1	(0. 20, 0. 60, **1. 00**) 0. 60, 1. 00, **1. 40,** 1. 80, 2. 20
184	2, 692. 00	6		37, 136. 10	$b^3F_{3\frac{1}{2}}$–$v^3D^0_{2\frac{1}{2}}$	(0. 00) 1. 23 E_1	(**0. 03,** 0. 09, 0. 14) **1. 00,** 1. 06, 1. 11, ...
182, 174	2, 689. 47	6	5	37, 171. 03	$\{a^3D_{2\frac{1}{2}}$–$x^3D^0_{2\frac{1}{2}}\}$ $\{a^4F_{1\frac{1}{2}}$–$y^4D^0_{2\frac{1}{2}}\}$		
174	2, 681. 75	5	2	37, 278. 03	$a^4F_{3\frac{1}{2}}$–$y^4D^0_{3\frac{1}{2}}$		
	2, 680. 94	1*b*		37, 289. 29			
172	2, 678. 59	25	150	37, 322. 00	$a^4F_{4\frac{1}{2}}$–$y^4F^0_{3\frac{1}{2}}$	(0. 00) 1. 45 E_1	(0. 00) 1. 33
	2, 673. 84	1*b*		37, 388. 30			
	2, 673. 56	1		37, 392. 21			
182	2, 670. 94	10		37, 428. 89	$a^3D_{1\frac{1}{2}}$–$x^3D^0_{2\frac{1}{2}}$	(0. 00) 1. 56 E_1	(**0. 20,** 0. 60) 0. 60, 1. 00, 1. 40, **1. 80**
185, 180	2, 669. 48	8	4	37, 449. 36	$\{a^2F_{2\frac{1}{2}}$–$y^4P^0_{1\frac{1}{2}}\}$ $\{a^4P_{1\frac{1}{2}}$–$w^3D^0_{2\frac{1}{2}}\}$		
177	2, 667. 77	12	20	37, 473. 36	$a^4F_{3\frac{1}{2}}$–$y^3F^0_{3\frac{1}{2}}$	(0. 00) 1. 43 E_1	(**0. 06,** 0. 17, 0. 29) ... 1. 20, 1. 31, **1. 43**
	2, 666. 56	1		37, 490. 36			
186	2, 665. 19	3		37, 509. 64	$a^4P_{2\frac{1}{2}}$–$x^3P^0_{1\frac{1}{2}}$		
187	2, 662. 57	3		37, 546. 54	$b^3F_{3\frac{1}{2}}$–$v^2F^0_{2\frac{1}{2}}$		
	2, 652. 92	1		37, 683. 11			
188	2, 650. 37	12	8	37, 719. 37	$a^4F_{3\frac{1}{2}}$–$z^4P^0_{2\frac{1}{2}}$	(0. 00) 0. 54 E_1	(**0. 18,** 0. 54, 0. 90) **0. 35,** 0. 70, 1. 06, ...
	2, 649. 80	2		37, 763. 96			
	2, 644. 88	1		37, 797. 65			
188	2, 643. 40	6	4	37, 818. 82	$a^4F_{3\frac{1}{2}}$–$z^4P^0_{1\frac{1}{2}}$		
186	2, 642. 51	2		37, 831. 55	$a^4P_{1\frac{1}{2}}$–$x^3P^0_{1\frac{1}{2}}$		
	2, 639. 73	3*b*		37, 871. 39			
172	2, 639. 07	12	30	37, 880. 86	$a^4F_{3\frac{1}{2}}$–$y^4F^0_{4\frac{1}{2}}$	(0. 00) 1. 52 E_1	(**0. 05,** 0. 14, ---) ... 1. 48, 1. 57, **1. 67**
	2, 637. 62	1*b*		37, 901. 68			
189	2, 630. 91	15	40	37, 998. 35	$a^3D_{2\frac{1}{2}}$–$x^3F^0_{3\frac{1}{2}}$	(0. 00) 0. 98 E_1	(**0. 03,** 0. 09, 0. 14) **1. 00,** 1. 06, 1. 11, ...
	2, 629. 52	1*b*		38, 018. 43			
	2, 628. 89	1		38, 027. 54			
186	2, 626. 98	3		38, 055. 19	$a^4P_{0\frac{1}{2}}$–$x^3P^0_{1\frac{1}{2}}$		
188	2, 626. 41	4		38, 063. 45	$a^4F_{1\frac{1}{2}}$–$z^4P^0_{2\frac{1}{2}}$		
188	2, 621. 60	3		38, 132. 88	$a^4F_{1\frac{1}{2}}$–$z^4P^0_{1\frac{1}{2}}$		
188	2, 619. 20	3		38, 168. 22	$a^4F_{2\frac{1}{2}}$–$z^4F^0_{2\frac{1}{2}}$		
252	2, 618. 89	2		38, 172. 73	$d^2D_{2\frac{1}{2}}$–$v^2D^0_{2\frac{1}{2}}$		
252	2, 615. 59	4		38, 220. 89	$d^2D_{1\frac{1}{2}}$–$v^2D^0_{1\frac{1}{2}}$		
187	2, 609. 74	5		38, 306. 56	$b^2F_{3\frac{1}{2}}$–$v^2F^0_{3\frac{1}{2}}$	(0.00) **1.24 E_1**	(0.00) **1.14**
190	2, 604. 99	2		38, 376. 41	$b^4F_{3\frac{1}{2}}$–$x^3D^0_{2\frac{1}{2}}$		
	2, 604. 73	1		38, 380. 24			
191	2, 604. 19	3		38, 388. 20	$a^3D_{2\frac{1}{2}}$–$y^4P^0_{1\frac{1}{2}}$		
	2, 602. 95	1		38, 406. 48			
186	2, 601. 27	3		38, 431. 29	$a^4P_{0\frac{1}{2}}$–$x^3P^0_{0\frac{1}{2}}$		
	2, 598. 16	2		38, 477. 29			
189	2, 589. 02	15		38, 613. 12	$a^3D_{1\frac{1}{2}}$–$x^3F^0_{2\frac{1}{2}}$	(0.00) 1.06 E_1	(**0. 03,** 0. 09) 0. 77, 0. 83, 0. 89, **0. 94**
191	2, 586. 85	4		38, 645. 50	$a^3D_{1\frac{1}{2}}$–$y^4P^0_{1\frac{1}{2}}$		
193	2, 586. 40	1		38, 652. 22	$b^4F_{4\frac{1}{2}}$–$z^3H^0_{3\frac{1}{2}}$		

TABLE 2.—*Wave lengths in the spark spectrum of Zr*—Continued

Key No.	λ I. A.	Intensities B. S.	Intensities King	ν	Term combinations	Observed Zeeman effects	Theoretical Zeeman effects
	2, 583. 99	2		38, 688. 27			
191	2, 583. 38	15		38, 697. 40	$a^2D_{2\frac{1}{2}}$–$y^4P^0_{1\frac{1}{2}}$	(0. 83) 1. 49 E_1	(0. 20, 0.60, **1. 00**) 0.60, 1. 00, **1. 40**, 1. 80, 2. 20
243	2, 581. 71	2		38, 722. 44	$z^2F^0_{3\frac{1}{2}}$–$e^2G_{4\frac{1}{2}}$		
	2, 580. 61	2*b*		38, 738. 94			
	2, 579. 73	1*b*		38, 752. 15			
250	2, 578. 39	3		38, 772. 29	$y^2G^0_{4\frac{1}{2}}$–$f^2G_{3\frac{1}{2}}$		
	2, 573. 64	2		38, 843. 85			
195	2, 571. 42	50		38, 877. 38	$\{a^4F_{3\frac{1}{2}}$–$z^4D^0_{3\frac{1}{2}}\}$ $\{a^4F_{2\frac{1}{2}}$–$z^4D^0_{1\frac{1}{2}}\}$		
195	2, 568. 85	40		38, 916. 27	$a^4F_{4\frac{1}{2}}$–$z^4D^0_{3\frac{1}{2}}$		
195	2, 567. 62	20		38, 934. 91	$a^4F_{1\frac{1}{2}}$–$z^4D^0_{0\frac{1}{2}}$		
247	2, 567. 05	7		38, 943. 56	$a^2P_{1\frac{1}{2}}$–$w^2D^0_{1\frac{1}{2}}$	(0. 75) 1. 15 E_1	(0.27, **0. 80**) 0.53, **1. 07**, 1. 60
247	2, 558. 36	1*b*		39, 075. 83	$a^2P_{1\frac{1}{2}}$–$w^2D^0_{2\frac{1}{2}}$		
	2, 557. 54	1*b*		39, 088. 36			
	2, 554. 18	2*b*		39, 139. 77			
196	2, 553. 06	2		39, 156. 94	$b^2D_{1\frac{1}{2}}$–$w^2P^0_{0\frac{1}{2}}$		
	2, 552. 59	2		39, 164. 15			
195	2, 550. 71	18		39, 193. 02	$a^4F_{1\frac{1}{2}}$–$x^4D^0_{1\frac{1}{2}}$	(1. 26) 1. 22 E_1	(0.40, **1. 20**) 0.00, **0. 80**, 1. 60
194	2, 543. 66	1		39, 301. 63	$a^2F_{2\frac{1}{2}}$–$w^2D^0_{1\frac{1}{2}}$		
197	2, 543. 04	3*b*		39, 311. 22	$z^2G^0_{4\frac{1}{2}}$–$f^2F_{3\frac{1}{2}}$		
195	2, 542. 09	18		39, 325. 90	$a^4F_{3\frac{1}{2}}$–$x^4D^0_{2\frac{1}{2}}$	(0. 82) 1. 29 E_1	(0.17, 0.51, **0. 86**) 0.51, 0.86, **1. 20**, 1.54, 1.89
198	2, 540. 87	3*b*		39, 344. 79	$d^2D_{2\frac{1}{2}}$–$v^2F^0_{3\frac{1}{2}}$		
197	2, 539. 37	2		39, 368. 03	$z^2G^0_{3\frac{1}{2}}$–$f^2F_{2\frac{1}{2}}$		
230, 194	2, 535. 15	5		39, 433. 55	$\{y^2G^0_{4\frac{1}{2}}$–$f^2G_{4\frac{1}{2}}\}$ $\{a^2F_{3\frac{1}{2}}$–$w^2D^0_{2\frac{1}{2}}\}$		
198	2, 534. 16	2*b*		39, 448. 96	$d^2D_{1\frac{1}{2}}$–$v^2F^0_{2\frac{1}{2}}$		
199	2, 533. 65	4		39, 456. 90	$a^2P_{1\frac{1}{2}}$–$x^2P^0_{1\frac{1}{2}}$		
195	2, 532. 47	20		39, 475. 28	$a^4F_{2\frac{1}{2}}$–$x^4D^0_{2\frac{1}{2}}$	(0. 60) 1. 39 E_1	(0.10, 0.29, 0.48, **0. 67**) 1.14, **1. 33**, 1.52, ---
	2, 528. 99	3		39, 528. 60			
	2, 522. 52	2*b*		39, 630. 98			
195	2, 521. 90	5		39, 640. 72	$a^4F_{1\frac{1}{2}}$–$x^4D^0_{1\frac{1}{2}}$		
	2, 520. 01	1*b*		39, 670. 45			
	2, 513. 50	2*b*		39, 773. 19			
	2, 510. 01	2*l*		39, 828. 49			
199	2, 509. 77	3		39, 832. 29	$a^2P_{1\frac{1}{2}}$–$x^2P^0_{0\frac{1}{2}}$		
199	2, 509. 01	2		39, 844. 36	$a^2P_{0\frac{1}{2}}$–$x^2P^0_{1\frac{1}{2}}$		
195	2, 503. 98	4		39, 924. 39	$a^4F_{2\frac{1}{2}}$–$x^4D^0_{3\frac{1}{2}}$		
	2, 503. 59	1		39, 930. 61			
200	2, 501. 38	1*b*		39, 965. 88	$b^4F_{2\frac{1}{2}}$–$z^2F^0_{2\frac{1}{2}}$		
201	2, 496. 48	15		40, 044. 33	$a^2G_{3\frac{1}{2}}$–$w^2F^0_{2\frac{1}{2}}$	(0. 00) 0. 90 E_1	(**0. 02**, 0.05, 0.08) --- 0.90, 0.94, **0. 97**
	2, 489. 83	2*b*		40, 151. 27			
201	2, 487. 28	20		40, 192. 43	$a^2G_{4\frac{1}{2}}$–$w^2F^0_{3\frac{1}{2}}$	(0. 00) 1. 06 E_1	(**0. 02**, 0.05, ---) **1. 00**, 1. 03, 1. 06, ---
199	2, 485. 60	3		40, 219. 59	$a^2P_{0\frac{1}{2}}$–$x^2P^0_{0\frac{1}{2}}$		
	2, 484. 42	2*b*		40, 238. 70			
200	2, 481. 35	5		40, 288. 48	$b^4F_{1\frac{1}{2}}$–$z^2F^0_{2\frac{1}{2}}$		
202	2, 480. 16	2		40, 307. 81	$b^4F_{2\frac{1}{2}}$–$y^4P^0_{2\frac{1}{2}}$		
	2, 471. 42	2		40, 450. 34			
	2, 471. 06	1		40, 456. 23			
	2, 470. 62	1		40, 463. 44			
201	2, 467. 97	2*b*		40, 506. 88	$a^2G_{3\frac{1}{2}}$–$w^2F^0_{3\frac{1}{2}}$		
	2, 467. 24	1*b*		40, 518. 87			
203	2, 465. 37	8		40, 549. 60	$a^2D_{2\frac{1}{2}}$–$w^2D^0_{1\frac{1}{2}}$		
203	2, 457. 43	20		40, 680. 60	$a^2D_{2\frac{1}{2}}$–$w^2D^0_{2\frac{1}{2}}$	(0. 00) 1. 30 E_1	(0. 00) 1. 20
204	2, 454. 61	4		40, 727. 34	$a^4F_{1\frac{1}{2}}$–$y^2P^0_{0\frac{1}{2}}$		
205	2, 454. 21	4		40, 733. 97	$b^2P_{1\frac{1}{2}}$–$v^2P^0_{0\frac{1}{2}}$		
203	2, 449. 83	20		40, 806. 79	$a^2D_{1\frac{1}{2}}$–$w^2D^0_{1\frac{1}{2}}$	(0. 00) 0. 99 E_1	(0. 00) 0. 80
206	2, 443. 41	1		40, 914. 01	$a^4F_{3\frac{1}{2}}$–$z^2D^0_{2\frac{1}{2}}$		
203	2, 441. 97	12		40, 938. 13	$a^2D_{1\frac{1}{2}}$–$w^2D^0_{2\frac{1}{2}}$		
	2, 439. 22	2*b*		40, 984. 28			
	2, 438. 26	1*b*		41, 000. 41			
204	2, 436. 94	1		41, 022. 62	$a^4F_{2\frac{1}{2}}$–$y^2P^0_{1\frac{1}{2}}$		
207	2, 434. 55	8		41, 062. 89	$a^2D_{2\frac{1}{2}}$–$x^2P^0_{1\frac{1}{2}}$		

TABLE 2.—*Wave lengths in the spark spectrum of Zr*—Continued

Key No.	λ I. A.	Intensities B. S.	Intensities King	ν	Term combinations	Observed Zeeman effects	Theoretical Zeeman effects
	2,433.25	3b		41,084.83			
208	2,432.26	3		41,101.72	$c^3D_{3½}$–$v^3D_{3½}$		
	2,431.71	1		41,110.84			
206	2,429.12	1		41,154.67	$a^4F_{3½}$–$x^3D_{3½}$		
205	2,426.38	7		41,201.14	$b^3P_{0½}$–$v^3P_{0½}$		
	2,425.73	1		41,212.18			
	2,423.29	3b		41,253.68			
	2,422.24	3		41,271.56			
207	2,419.37	10		41,320.51	$a^3D_{1½}$–$x^3P_{1½}$		
	2,417.40	2b		41,354.18			
206	2,416.89	2		41,362.91	$a^4F_{2½}$–$x^3D_{2½}$		
	2,414.23	2		41,408.48			
209	2,413.85	3		41,415.00	$a^3F_{3½}$–$w^3F_{3½}$		
	2,412.40	1		41,439.89			
206	2,410.67	1		41,469.62	$a^4F_{1½}$–$x^3D_{1½}$		
208	2,406.83	7		41,535.78	$c^3D_{1½}$–$v^3D_{1½}$		
	2,403.86	1b		41,587.09			
	2,403.28	1b		41,614.44			
	2,402.58	1b		41,626.57			
	2,401.44	1b		41,629.00			
	2,400.62	1		41,643.22			
210	2,398.97	5		41,671.86	$b^3D_{2½}$–$v^3D_{2½}$		
207	2,397.57	5		41,696.19	$a^3D_{1½}$–$x^3P^0_{1½}$		
211	2,393.35	2		41,769.70	$a^3P_{1½}$–$w^3F^0_{2½}$		
205	2,392.66	10		41,781.75	$b^3P_{1½}$–$v^3P_{1½}$		
208	2,389.52	8		41,836.64	$c^3D_{3½}$–$v^3D_{2½}$		
	2,388.21	1		41,859.59			
209	2,387.17	15		41,877.83	$a^3F_{3½}$–$w^3F_{3½}$		
	2,382.32	2		41,963.08			
	2,378.68	1b		42,027.29			
209	2,372.92	12		42,129.29	$a^3F_{3½}$–$w^3F_{2½}$		
	2,371.38	1b		42,156.65			
	2,370.14	5b		42,178.70			
	2,368.99	2b		42,199.18			
	2,367.63	1b		42,223.41			
205	2,366.22	3		42,248.57	$b^3P_{0½}$–$v^3P_{1½}$		
	2,365.61	1b		42,259.46			
208	2,364.95	2		42,271.26	$c^3D_{1½}$–$v^3D^0_{1½}$		
251	2,364.58	2		42,277.87	$y^3F^0_{3½}$–$f^3G_{3½}$		
212	2,363.84	4		42,291.10	$b^4F_{3½}$–$w^3D^0_{2½}$		
	2,362.97	1b		42,306.67			
213	2,361.76	10		42,328.35	$c^3D_{2½}$–$v^3F^0_{3½}$		
	2,359.08	5b		42,376.43			
210	2,357.45	25		42,405.73	$b^3D_{2½}$–$v^3D^0_{2½}$ / $b^3D_{1½}$–$v^3D^0_{1½}$		
	2,354.51	2b		42,458.67			
212	2,353.21	6		42,482.13	$b^4F_{1½}$–$w^3D^0_{1½}$		
214	2,351.69	12		42,509.58	$b^3G_{3½}$–$v^3D^0_{2½}$		
251	2,350.91	3		42,523.69	$y^3F^0_{3½}$–$f^3G_{4½}$		
	2,350.22	3b		42,536.17			
209	2,347.13	4		42,592.16	$a^3F_{2½}$–$w^3F^0_{2½}$		
212	2,345.93	1		42,613.95	$b^4F_{1½}$–$w^3D^0_{2½}$		
	2,342.33	3b		42,679.44			
	2,341.74	1b		42,690.19			
	2,339.39	2b		42,733.07			
	2,338.93	1		42,741.47			
213	2,337.76	1		42,762.86	$c^3D_{1½}$–$v^3F^0_{2½}$		
	2,335.63	2b		42,801.86			
	2,331.57	3b		42,876.38			
215	2,330.38	18		42,898.27	$b^3D_{3½}$–$v^3F^0_{3½}$		
216	2,324.77	15		43,001.78	$b^3G_{3½}$–$v^3F^0_{3½}$		
213	2,324.48	5		43,007.15	$c^3D_{3½}$–$v^3F^0_{3½}$		
	2,321.87	5		43,055.49			
210	2,317.27	15		43,140.95	$b^3D_{1½}$–$v^3D^0_{2½}$		
	2,308.10	6		43,312.33			
	2,307.31	1b		43,327.16			

TABLE 2.—*Wave lengths in the spark spectrum of Zr*—Continued

Key No.	λ I. A.	Intensities B. S.	Intensities King	ν	Term combinations	Observed Zeeman effects	Theoretical Zeeman effects
217	2, 306. 78	2b		43, 337. 11	$z^3D^3_{3½}$–$f^2F_{3½}$		
217	2, 302. 52	2b		43, 417. 28	$z^2D^1_{1½}$–$f^2F_{1½}$		
	2, 301. 61	4b		43, 434. 45			
	2, 300. 42	3b		43, 456. 91			
216	2, 295. 53	10		43, 549. 48	$b^1G_{4½}$–$e^2F^1_{3½}$		
215	2, 294. 08	12		43, 577. 00	$b^3D_{3½}$–$e^2F^1_{3½}$		
218, 215	2, 291. 15	15		43, 632. 73	$b^3D_{1½}$–$e^2F^1_{2½}$; $a^3D_{1½}$–$w^2F^2_{2½}$		
216	2, 288. 63	2		43, 680. 76	$b^3G_{3½}$–$e^2F^1_{3½}$		
253	2, 288. 00	1		43, 692. 74	$z^4D^3_{3½}$–$f^4F_{4½}$		
	2, 283. 18	2		43, 784. 94			
	2, 281. 47	2b		43, 817. 83			
218	2, 280. 36	5		43, 839. 16	$a^3D_{3½}$–$w^2F^1_{3½}$		
	2, 276. 69	5b		43, 909. 91			
219	2, 275. 39	3b		43, 934. 99	$z^2F^1_{3½}$–$f^2F_{3½}$		
	2, 275. 07	1b		43, 941. 17			
	2, 268. 15	2		44, 075. 19			
	2, 265. 02	4		44, 136. 08			
	2, 262. 67	2		44, 181. 87			
	2, 261. 20	4, Ti?		44, 210. 59			
	2, 257. 88	4b		44, 275. 59			
219	2, 254. 20	3b		44, 347. 86	$z^2F^1_{3½}$–$f^2F_{2½}$		
	2, 253. 33	1b		44, 364. 98			
	2, 252. 38	2b		44, 383. 69			
220	2, 250. 44	3		44, 421. 95	$a^4F_{3½}$–$w^2D^2_{3½}$		
	2, 247. 54	1		44, 479. 26			
	2, 245. 38	4, Fe?		44, 522. 04			
	2, 240. 90	1*B*		44, 611. 01			
	2, 239. 67	3*B*		44, 635. 54			
221	2, 235. 10	5		44, 726. 80	$z^4F^1_{4½}$–$f^4F_{4½}$		
220	2, 234. 42	1		44, 740. 40	$a^4F_{1½}$–$w^2D^1_{1½}$		
221	2, 233. 48	5		44, 759. 24	$z^4F^1_{3½}$–$f^4F_{3½}$		
221	2, 231. 86	2		44, 791. 71	$z^4F^2_{2½}$–$f^4F_{2½}$		
	2, 231. 00	4, Ti?		44, 808. 98			
221	2, 229. 74	1b		44, 834. 30	$z^4F^1_{1½}$–$f^4F_{1½}$		
	2, 228. 12	2b		44, 866. 90			
	2, 226. 64	0		44, 896. 71			
	2, 223. 33	2b		44, 963. 55			
219	2, 221. 91	1b		44, 992. 28	$z^2F^2_{2½}$–$f^2F_{2½}$		
	2, 221. 38	1b		45, 003. 01			
	2, 220. 22	4b		45, 026. 53			
	2, 218. 46	1b		45, 062. 24			
222	2, 214. 59	2		45, 140. 98	$a^4P_{1½}$–$w^2P^1_{1½}$		
	2, 212. 92	1b		45, 175. 04			
220	2, 212. 44	0		45, 184. 84	$a^4F_{1½}$–$w^2D^2_{1½}$		
	2, 206. 97	3b		45, 296. 82			
223	2, 206. 31	4b		45, 310. 37	$b^4F_{1½}$–$w^2F^2_{2½}$		
221	2, 199. 17	1b		45, 457. 47	$z^4F^2_{1½}$–$f^4F_{2½}$		
224	2, 193. 84	0b		45, 567. 89	$a^4F_{1½}$–$x^2P^1_{1½}$		
	2, 192. 75	3		45, 590. 54			
	2, 192. 02	1b		45, 605. 72			
	2, 191. 16	3b		45, 623. 62			
	2, 187. 77	1b		45, 694. 30			
225	2, 184. 80	5b		45, 756. 42	$a^2H_{4½}$–$x^2F^1_{3½}$		
226	2, 182. 81	5b		45, 798. 12	$z^4G^1_{4½}$–$f^4F_{4½}$		
	2, 178. 86	2		45, 881. 14			
	2, 176. 69	0		45, 926. 87			
	2, 176. 39	1b		45, 933. 20			
224	2, 175. 81	4b		45, 945. 45	$a^4F_{1½}$–$x^2P^2_{0½}$		
	2, 170. 20	0		46, 064. 20			
	2, 167. 78	3		46, 115. 62			
	2, 166. 54	2b		46, 142. 01			
226	2, 165. 24	4b		46, 169. 71	$z^4G^1_{3½}$–$f^4F_{3½}$		
	2, 162. 16	1b		46, 235. 47			
	2, 159. 96	2b		46, 282. 56			
	2, 159. 67	0		46, 288. 77			

TABLE 2.—*Wave lengths in the spark spectrum of Zr*—Continued

Key No.	λ I. A.	Intensities B. S.	Intensities King	ν	Term combinations	Observed Zeeman effects	Theoretical Zeeman effects
	2, 159. 19	4		46, 299. 06			
	2, 157. 98	2*b*		46, 325. 02			
	2, 154. 07	1*b*		46, 409. 09			
	2, 153. 26	1*b*		46, 426. 55			
226	2, 152. 89	4*b*		46, 434. 53	$z^4G^3_{3½}$–$f^4F_{3½}$		
227	2, 151. 02	6		46, 474. 89	$a^2P_{1½}$–$w^2P^3_{2½}$		
228	2, 145. 24	1		46, 600. 10	$b^4P_{2½}$–$v^2D^2_{2½}$		
	2, 144. 86	0		46, 608. 36			
	2, 144. 33	1		46, 619. 87			
226	2, 144. 01	4*b*		46, 626. 83	$z^4G^2_{3½}$–$f^4F_{1½}$		
	2, 142. 71	1		46, 654. 46			
	2, 141. 43	3		46, 683. 00			
227	2, 137. 67	7		46, 765. 10	$a^2P_{1½}$–$w^2P^1_{1½}$		
	2, 136. 80	1		46, 784. 14			
227	2, 133. 28	7		46, 861. 32	$a^2P_{0½}$–$w^2P^2_{1½}$		
	2, 131. 15	1		46, 908. 16			
	2, 129. 93	2*B*		46, 935. 02			
	2, 126. 56	2		47, 009. 39			
	2, 125. 06	3*b*, *l*		47, 042. 57			
	2, 124. 58	1		47, 053. 19			
226	2, 122. 41	1		47, 101. 30	$z^4G^3_{3½}$–$f^4F_{3½}$		
229	2, 121. 18	1*b*		47, 128. 60	$c^2D_{2½}$–$v^2P^1_{1½}$		
227	2, 120. 12	5		47, 152. 16	$a^2P_{0½}$–$w^2P^1_{1½}$		
	2, 119. 71	2		47, 161. 29			
	2, 113. 10	1		47, 308. 79			
230	2, 109. 66	12		47, 385. 92	$b^2D_{1½}$–$v^2P^2_{0½}$		
	2, 108. 40	2 *b*, *l*		47, 414. 24			
	2, 103. 17	5*b*		47, 532. 13			
	2, 101. 55	1		47, 568. 77			
	2, 099. 30	1		47, 619. 74			
	2, 097. 02	5*b*		47, 671. 51			
230	2, 095. 80	15		47, 699. 26	$b^2D_{2½}$–$v^2P^1_{1½}$		
	2, 091. 75	2		47, 791. 60			
	2, 083. 80	1*b*		47, 973. 91			
	2, 081. 81	1		48, 019. 76			
	2, 080. 99	5*b*		48, 038. 68			
	2, 076. 29	2		48, 147. 41			
	2, 074. 90	3		48, 179. 66			
	2, 074. 03	6*b*		48, 199. 86			
231	2, 068. 09	3		48, 338. 29	$a^2D_{1½}$–$w^2P^1_{1½}$		
232	2, 067. 08	4		48, 361. 90	$z^2G^2_{4½}$–$g^2G_{4½}$		
244	2, 065. 35	3		48, 402. 41	$z^4G^3_{4½}$–$e^4H_{5½}$		
	2, 064. 37	0		48, 425. 38			
230	2, 063. 89	6		48, 436. 64	$b^2D_{1½}$–$v^2P^1_{1½}$		
244	2, 061. 85	6		48, 484. 56	$z^4G^2_{4½}$–$e^4H_{4½}$		
	2, 061. 35	5*b*		48, 496. 32			
245	2, 057. 96	1*b*		48, 576. 19	$g^2H^2_{4½}$–$f^2H_{4½}$		
	2, 055. 42	3		48, 636. 21			
	2, 054. 30	2		48, 662. 73			
	2, 051. 83	1*b*		48, 721. 30			
232	2, 051. 21	4		48, 736. 02	$z^2G^2_{4½}$–$g^2G_{3½}$		
	2, 050. 85	0		48, 744. 57			
	2, 048. 19	0		48, 807. 87			
	2, 046. 94	0		48, 837. 67			
	2, 044. 43	0		48, 897. 62			
	2, 041. 98	0*b*		48, 956. 28			
	2, 040. 52	0		48, 991. 31			
	2, 040. 11	0*b*		49, 001. 15			
244	2, 039. 84	1		49, 007. 64	$z^4G^1_{4½}$–$e^4H_{4½}$		
232	2, 037. 58	1		49, 061. 98	$z^2G^3_{4½}$–$g^2G_{4½}$		
233	2, 030. 73	6		49, 227. 46	$a^2G_{3½}$–$v^2F^2_{3½}$		
245	2, 029. 81	3*b*		49, 248. 31	$z^2H^3_{4½}$–$f^2H_{4½}$		
	2, 028. 03	1		49, 292. 99			
245	2, 026. 61	5*b*		49, 327. 52	$z^2H^3_{4½}$–$f^2H_{5½}$		
244	2, 025. 33	4		49, 358. 69	$z^4G^3_{4½}$–$e^4H_{5½}$		

TABLE 2.—*Wave lengths in the spark spectrum of Zr*—Continued

Key No.	λ I. A.	Intensities		ν	Term combinations	Observed Zeeman effects	Theoretical Zeeman effects
		B. S.	King				
	2,021.36	0*b*		49,455.62			
	2,019.65	0		49,497.49			
	2,016.52	0		49,574.30			
233	2,015.86	5		49,590.53	$a^3G_{4\frac{1}{2}}$–$e^3F^1_{3\frac{1}{2}}$		
	2,013.21	0		49,655.80			
244	2,012.66	0		49,669.36	$z^4G^1_{3\frac{1}{2}}$–$e^4H_{3\frac{1}{2}}$		
	2,012.03	0		49,684.92			
233	2,003.18	0		49,904.39	$a^3G_{3\frac{1}{2}}$–$e^3F^1_{3\frac{1}{2}}$		
244	2,001.90	4		49,938.79	$z^4G^1_{3\frac{1}{2}}$–$e^4H_{4\frac{1}{2}}$		
245	1,999.43	1*b*		49,998.25	$z^2H^1_{4\frac{1}{2}}$–$f^2H_{3\frac{1}{2}}$		
234	1,996.05	6		50,082.89	$a^3F_{3\frac{1}{2}}$–$e^3D^1_{3\frac{1}{2}}$		
234	1,995.24	7		50,103.21	$a^3F_{3\frac{1}{2}}$–$e^3D^2_{2\frac{1}{2}}$		
235	1,994.91	1		50,111.50	$a^3P_{0\frac{1}{2}}$–$e^3D^1_{1\frac{1}{2}}$		
	1,990.70	0		50,217.44			
235	1,981.21	2		50,457.91	$a^3P_{1\frac{1}{2}}$–$e^3D^2_{2\frac{1}{2}}$		
244	1,975.90	3		50,593.46	$z^4G^2_{4\frac{1}{2}}$–$e^4H_{3\frac{1}{2}}$		
	1,961.37	2		50,968.14			
236	1,949.65	2		51,274.43	$a^3F_{3\frac{1}{2}}$–$e^3F^1_{3\frac{1}{2}}$		
236	1,948.23	1		51,311.79	$a^3F_{3\frac{1}{2}}$–$e^3F^2_{2\frac{1}{2}}$		
237	1,947.46	1		51,332.07	$a^3D_{2\frac{1}{2}}$–$e^3D^1_{1\frac{1}{2}}$		
237	1,937.64	3		51,592.40	$a^3D_{1\frac{1}{2}}$–$e^3D^1_{1\frac{1}{2}}$		
237	1,920.76	5		52,062	$a^3D_{2\frac{1}{2}}$–$e^3D^2_{2\frac{1}{2}}$		
237	1,911.32	4		52,319	$a^3D_{1\frac{1}{2}}$–$e^3D^2_{2\frac{1}{2}}$		
238	1,902.78	3		52,554	$a^3D_{2\frac{1}{2}}$–$e^3F^2_{2\frac{1}{2}}$		
238	1,893.52	1		52,811	$a^3D_{1\frac{1}{2}}$–$e^3F^2_{2\frac{1}{2}}$		
246	1,887.07	1		52,992	$z^2F^2_{3\frac{1}{2}}$–$g^2G_{4\frac{1}{2}}$		
238	1,878.53	4		53,233	$a^3D_{3\frac{1}{2}}$–$e^3F^2_{3\frac{1}{2}}$		
246	1,861.71	0		53,714	$z^2F^2_{3\frac{1}{2}}$–$g^2G_{3\frac{1}{2}}$		
239	1,767.85	0		56,565	$a^3D_{1\frac{1}{2}}$–$e^3P^0_{0\frac{1}{2}}$		
239	1,743.53	0		57,354	$a^3D_{2\frac{1}{2}}$–$e^3P^1_{1\frac{1}{2}}$		

TABLE 3.—*Key to the term combinations of Zr II*

Even terms \ Odd terms	$z^4G°$	$z^4F°$	$y^4F°$	$z^2D°$	$y^4D°$	$z^4D°$	$z^2P°$	$y^4P°$	$z^4S°$	$z^2H°$	$z^4G°$	$y^4G°$	$z^2F°$	$y^2F°$	$z^2F°$	$w^2F°$	$v^2F°$	$z^2D°$	$y^2D°$	$z^2D°$	$w^2D°$	$e^2D°$	$z^2P°$	$y^2P°$	$x^2P°$	$w^2P°$	$v^2P°$	$z^2S°$
e^4H	244																											
a^4F	75	103									151		95					108					169					
b^4F	82	69	172	126	174	195	188			193			65	177	200	223		79	133	206	220		145	204	224			161
c^4F	154	138	147	98	160	175	163	202						153					113	190	212							
f^4F	226	221																										
a^4P			94	46	90	122	111	162	105			136	24	100	158				53	149	185		83	144	186	222		73
b^4P				20	70	99	86	139	81				11						41			228	60					
e^2I		8								248	23	91		58	116		225										
a^2H										102																		
e^2H										249																		
f^2H										245																		
a^2G	13	26	97	49	101	129				148	66	134	17	104	156	201	233	39			214							
b^2G			29		34	64				80	9	68	4	37	87	152	216											
e^2G											242		243															
f^2G												250		251														
g^2G	19	45	118	63	125	142	135	180			232	157	246	120	171	209	236	48	72	164	194	234	110	168				
a^2F								44			84	15	31		33		187			18	57	184						
b^2F											1a							240										
e^2F													241					217										
f^2F											197		219	179														
a^2D	42	56	131	85	128	160	192	191	143		107	176	51	137	189	218	238	59	89	182	203	237	124	178	207	231	239	117
b^2D		3	30	6	28	54								36	93	155	215		7	77	121	210	22	74	130	196	230	
c^2D			25		38			88				61		32	82	141	213		5	71	114	208	14	67	119		229	
d^2D																96	198					252				165		
e^2D																			146				115	159	199	227	205	92
a^2P		43	112	62	109	140	127	35					40	123	181	211	183	47	76	167	247	235	106	12	55	132	170	1
b^2P															27					16	50	173	2		10	78		
a^2S																												

2. THE ZEEMAN EFFECTS

Following the term designations of the lines in Table 2 are the observed Zeeman effects. For the most part these have been taken from the lists published by Moore and have proved of inestimable worth in unraveling not only Zr II, but also Zr I. Some of his published patterns, however, are in error because of overlapping of close lines. In such instances the observed patterns given in the table are those derived from the more recent observations made in the Brace Laboratory and at the Bureau of Standards, as stated above. In some instances, too, the new measurements have given improved values for patterns marked uncertain by Moore, and these also have been included in Table 2. For comparison with the observed Zeeman effects, the final column of Table 2 contains the theoretical pattern for weak fields as calculated according to Landé. These theoretical patterns have been taken from the Tables of Theoretical Zeeman Effects, published recently by Kiess and Meggers.[16]

Except for lines observed with the E_1 spectrograph, inspection of the table shows that there is good agreement between the observed and theoretical Zeeman effects for all lines which are simple triplets and for complex patterns whose components are separated by ½ a or more, a being the normal triplet separation. For complex lines whose components are separated by less than ½ a the agreement between the observed and calculated patterns is only qualitative. For some lines with components close to the undisturbed position a definite widening was noticed, and this is indicated in the table by a letter w following the pattern. Many of the apparent triplets are unresolved patterns with the strongest theoretical components either on the inside or on the outside, of the types designated as A^1 and A^2 by Back.[17] Such designations in Table 2 were derived from the recent observations described above. For lines of such types the rule noted by Russell[18] for Ti and by Meggers[19] for Yt was found to hold, namely, that the observed Zeeman effect is increased or decreased by one-fourth the separation between the strongest and weakest components of the theoretical pattern.

For the Zeeman effects observed with the prism spectrograph there is only qualitative agreement between the observed and theoretical patterns. No complex patterns were resolved and the only ones measured were either triplets or quartets. However, a few complex patterns on the verge of resolution were noted and these are indicated in Table 2 by the letter W. These observations were made after the lines had been classified and have served the purpose of checking the term combinations which have been assigned. They are published here to illustrate the possibilities and limitations of the E_1 spectrograph, or similar instrument, in Zeeman effect work. One is led to the conclusion that, of themselves, these observations are not sufficiently accurate to establish the identity spectral terms.

In general the g values of the terms appear to be normal, being those required by Landé's theory for weak fields. For two terms, however, $z^4F_{1\frac{1}{2}}$ and $y^2F_{2\frac{1}{2}}$, abnormal g values were noted. Combinations involving these terms and having observed Zeeman effects are given in Table 4. The calculated patterns in the last column are based on the observed and not on the theoretical g values of the two terms.

[16] B. S. Jour. Research, **1**, p. 641; 1928.
[17] Zeit. für Physik, **15**, p. 206; 1923.
[18] Astrophys. J., **66**, p. 308; 1927.
[19] B. S. Jour. Research, **2**, p. 745; 1929.

TABLE 4.—*Zeeman effects from anomalous g values*

Term combination	λ	Observed Zeeman effect	Calculated Zeeman effect
$a^4F_{1½}$–$z^4F^1_{1½}$	3,357.26	(0.36) 0.53	(0.15, **0.40**) 0.25, **0.55**, 0.85
$b^4F_{1½}$–$z^4F^1_{1½}$	3,674.74	(0.39) 0.58	
$a^4F_{2½}$–$z^4F^1_{1½}$	3,393.12	(0.00) 1.46	(**0.16**, 0.49) 0.54, 0.86, 1.19, **1.52**
$b^4F_{2½}$–$z^4F^1_{1½}$	3,718.86	(0.00) 1.43	
$a^2F_{2½}$–$z^4F^1_{1½}$	4,161.20	(0.00) 1.09 A[2]	(**0.07**, 0.23) 0.62, 0.78, 0.93, **1.09**
$a^2D_{1½}$–$z^4F^1_{1½}$	3,915.94	(0.22) 0.74	(0.05, **0.15**) 0.65, **0.75**, 0.85
$a^2P_{0½}$–$z^4F^1_{1½}$	4,156.24	(0.00) 0.70	(0.02) 0.68, **0.72**
$b^4F_{2½}$–$y^2F^2_{2½}$	2,936.31	(0.00) 1.66	(**0.13**, 0.39, 0.65) 0.58, 0.84, 1.11, 1.37, 1.63, **1.89**
$a^4F_{2½}$–$y^2F^2_{2½}$	2,732.72	(0.00) 1.50	
$a^4F_{2½}$–$y^2F^2_{2½}$	2,699.59	(0.00) 1.20	(0.03, 0.08, **0.13**) 0.90, 0.95, **1.00**, 1.05, 1.11
$a^2G_{3½}$–$y^2F^2_{2½}$	3,387.87	(0.00) 0.67	(**0.04**, 0.13, 0.22) **0.67**, 0.76, 0.84, 0.93, 1.02, 1.10
$b^2G_{3½}$–$y^2F^2_{2½}$	4,293.14	(0.00) 0.66 A[1]	
$a^2F_{3½}$–$y^2F^2_{2½}$	3,164.32	(0.29) 1.00	(0.06, 0.18, **0.30**) 0.68, 0.80, **0.92**, 1.03, 1.15
$a^2D_{2½}$–$y^2F^2_{2½}$	3,044.12	(0.00*w*) 1.00	(0.11, 0.34, **0.56**) 0.64, 0.86, **1.09**, 1.31, 1.54
$a^2D_{1½}$–$y^2F^2_{2½}$	3,020.45	(0.00) 1.16	(**0.03**, 0.26) 0.71, 0.89, 1.06, **1.24**
$b^2D_{1½}$–$y^2F^2_{2½}$	4,179.81	(0.00) 1.25 A[2]	
$c^2D_{1½}$–$y^2F^2_{2½}$	4,337.63	(0.00) 1.20	

	g values	
	Observed	Theoretical
$z^4F^1_{1½}$	0.700	0.400
$y^2F^2_{2½}$	.975	.857

Among the Zr Zeeman effects are two complex patterns which beautifully illustrate the power of a magnetic field to resolve two very close or coincident lines which have not been resolved with the most powerful gratings used in observing them. The lines in question are at wave lengths 4,457.42 and 4,282.21 A. Each belongs to both Zr I and Zr II, and represents the term combinations given in Table 5.

TABLE 5.—*Zeeman effects of coincident lines of Zr I and Zr II*

λ	Terms	Theoretical Zeeman effect	Observed Zeeman effect
4,457.42	$^5P_2$–$^5D_1$	(**0.00**, 0.33) 1.50, 1.83, **2.17**	(0.00, **1.30**) **1.33**, 2.17
	$^4P_{2½}$–$^4D_{0½}$	(1.33) 1.33	
[1] 4,282.21	$^5F_2$–$^5F_3$	(**0.00**, 0.25, 0.50) 0.75, 1.00, 1.25, 1.50, **1.75**	(0.00) **0.87**, 1.54, **1.77**
	$^5F_{2½}$–$^5F_{2½}$	(0.00) 0.86	

[1] From the apparent wave lengths of the *n* components the wave length of the Zr I line comes out 4,282.18 A.

3. INTERPRETATION OF THE OBSERVED TERMS

The present accepted explanation of the terms of a spectrum is that they are the resultants of the interaction of the valence electrons of an atom in the various configurations they can assume. The neutral Zr atom in its unexcited state has two 4_3 and two 5_1 electrons external to the krypton shell, the configuration of these electrons being designated by the symbol $4d^2\ 5s^2$. The singly ionized atom has lost one of the *s* electrons, whence the configuration of the unexcited state, corresponding to its minimum energy stage, is designated as $4d^2 \cdot 5s$. But the difference in energy between the binding of an electron in a 5_1 orbit and a 4_3 orbit is small, so that stages of low energy may also result from the configurations $4d^3$ and $4d\ 5s^2$. The terms which result from these three configurations are shown in Table 6. As the present analysis shows all have been found for Zr II.

When the ion Zr^+ absorbs energy an electron is removed from one of the configurations just described to a higher orbit of the *ns*, *np*, *nd*, *nf*, etc., types, and new electron configurations ensue. The terms resulting from these excited configurations are also shown in Table 6. The most conspicuous of these terms are those which arise when the dislodged electron enters a 5_2 orbit. All the terms coming from the configurations $4d^2\ 5p$ and $4d\ 5s\ 5p$ have been found, as Table 6 shows. It is the combinations of these odd terms of the middle group with the terms of the low configurations that account for nearly all the strong lines of the spectrum.

TABLE 6.—*Theoretical and observed terms of Zr II*

Electron configuration	Theoretical terms	Observed terms	Limit in Zr III
$4d^2 \cdot 5s$	$^4F, {}^2F$ $^4P, {}^2P$ ^2G ^2D ^2S	a^4F, a^2F a^4P, a^2P b^2G a^2D a^2S	$4d^3F$ $4d^3P$ $4d^1G$ $4d^1D$ $4d^1S$
$4d^3$ $4d \cdot 5s^2$	$^4F, {}^4P, {}^2H, {}^2G, {}^2F, {}^2D, {}^2P, {}^2D$ ^2D	$b^4F, b^4P, a^2H, a^2G, b^2F, b^2D, b^2P, c^2D$ d^2D	$5s^2D, 5s^1D$
$4d^2 \cdot 5p$	$^4G^0, {}^4F^0, {}^4D^0, {}^2G^0, {}^2F^0, {}^2D^0$ $^4D^0\ {}^4P^0, {}^4S^0, {}^2D^0, {}^2P^0, {}^2S^0$ $^2H^0, {}^2G^0, {}^2F^0$ $^2F^0, {}^2D^0, {}^2P^0$ $^2P^0$	$z^4G^0, z^4F^0, z^4D^0, z^4G^0, z^2F^0, z^2D^0$ $y^4D^0, y^4P^0, z^4S^0, y^2D^0, y^2P^0, z^2S^0$ z^2H^0, y^2G^0, y^2F^0 z^2F^0, x^2D^0, z^2P^0 x^2P^0	$4d^3F$ $4d^3P$ $4d^1G$ $4d^1D$ $4d^1S$
$4d \cdot 5s \cdot 5p$	$^4F^0, {}^4D^0, {}^4P^0, {}^2F^0, {}^2D^0, {}^2P^0$ $^2F^0, {}^2D^0, {}^2P^0$	$y^4F^0, x^4D^0, z^4P^0, v^2F^0, v^2D^0, v^2P^0$ w^4F^0, w^2D^0, w^2P^0	$5s^2D$ $5s^1D$
$4d^2 \cdot 6s$	$^4F, {}^2F$ $^4P, {}^2P$ ^2G ^2D ^2S	e^4F, e^2F e^2G e^2D	$4d^3F$ $4d^3P$ $4d^1G$ $4d^1D$ $4d^1S$
$4d^2 \cdot 5d$	$^4H, {}^4G, {}^4F, {}^4D, {}^4P, {}^2H, {}^2G, {}^2F, {}^2D, {}^2P$ $^4F, {}^4D, {}^4P\ {}^2F, {}^2D, {}^2P$ $^2I, {}^2H, {}^2G, {}^2F, {}^2D$ $^2G, {}^2F, {}^2D, {}^2P, {}^2S$ ^2D	$e^4H,\quad f^4F,\quad f^2H, g^2G, f^2F$ e^2I, e^2H, f^2G	$4d^3F$ $4d^3P$ $4d^1G$ $4d^1D$ $4d^1S$

With increase in energy of the ion the dislodged electron may enter the 5_3 and 6_1 orbits. The configurations $4d^2\ 6s$ and $4d^2\ 5d$ give high groups of terms of the same type and parity as those of the low configurations. In the case of the $4d^2\ 5d$ configuration all the terms will appear which have been excluded from the $4d^3$ group because of Pauli's restriction. These high terms will combine with those of the middle group, and, because of their electronic origin, will be in Rydberg sequence with corresponding terms of the low groups. The combinations between the high and middle terms will, in general yield faint lines which appear nebulous. The high terms are not easy to identify and as Table 6 shows, only a few of those theoretically possible have actually been found.

As the current electron recedes from the core of the Zr^+ ion, there comes a stage when it is completely removed and the atom is doubly ionized with its two remaining outer electrons forming the configurations $4d^2$ or $4d\ 5s$. From these arise the lowest and metastable terms of Zr III. These terms, which belong to the triplet and singlet systems, have all been found, as is shown in a previous paper by Kiess and Lang.[20] They are the limiting terms of Zr III from which

[20] B. S. Jour. Research, 5, p. 305; 1930.

the terms of Zr II may be found by adding to them the $4d$, $5s$, $5p$, $5d$, etc., electrons.

The minimum energy that the singly ionized Zr atom can absorb is represented by the transition $4d^2\,5s \longrightarrow 4d^2\,5p$. The lowest term belonging to the group arising from the $4d^2\,5p$ configuration is $z^4G°$, although the components of both $z^4F°$ and $z^2D°$ overlap it. The chief lines of the term combination a^4F–$z^4G°$, therefore, constitute not only the resonance lines of Zr II, but also the *raies ultimes*, according to the rules enunciated by Meggers, Kiess, and Walters,[21] and subsequently elaborated by Laporte and Meggers,[22] and by Russell.[23] These are the lines which were selected empirically as the *raies ultimes* by de Gramont as stated above.

In spectra resulting from systems of one or two outer electrons the coordination of term groups with electron configurations is fairly simple. The spectra of systems with three or more electrons are generally complex and the assignment of terms to their proper configurations is attended with some uncertainty. There are, however, certain guiding principles which may be of service in making the assignments. In general, a complex term will exhibit $\Delta\nu$'s of the same order of magnitude as its parent term. All the quartet terms of Zr II will arise from triplet terms of Zr III; but of the doublet terms some will arise from singlet terms and some from triplet terms of Zr III. Inspection of Table 1 shows that the $\Delta\nu$'s of the doublet terms fall into two groups, those under 467 cm^{-1}, and those over 610 cm^{-1}.

Another guide in the assignment of terms to their proper electron configurations is to be found in the multiplet intensities. Here the lack of quantitative intensity measurements for spectrum lines is felt, but for limited regions of the spectrum in which there is no very great change in the sensitivity of the photographic plate qualitative estimates prove satisfactory. The intensities of multiplets resulting from combinations between a triad of high terms and a common lower term will differ, that being strongest for which the change in the term quantum numbers, ΔL, is the same as the change Δk in the azimuthal quantum number of the current electron. For example, the triad of odd terms $z^4G°$, $z^4F°_2$ and $z^4D°$ of the $4d^2\,5p$ configuration combines with the term a^4F ($4d^2\,5s$), and also with the term b^4F ($4d^3$). In the first case the electron change is $5p \rightarrow 5s$, $\Delta k = -1$, and the multiplet $a^4F \leftarrow z^4G°$ for which $\Delta L = -1$, is strongest. In the second case the electron change is $5p \rightarrow 4d$, $\Delta k = +1$, and the multiplet $b^4F \leftarrow z^4D°$ for which $\Delta L = +1$, is strongest. This principle, due to Kronig,[24] represents an extension of Sommerfeld's qualitative intensity rule, and was first actually tested by Laporte,[25] several years ago, on the Zr II multiplets here discussed.

A check on the correctness of the term assignments is furnished by the irregular doublet law according to which the values of $\sqrt{\nu/R}$ for corresponding terms of isoelectronic systems should differ by a constant. Here ν is the distance separating a term from its limit and R is the Rydberg number. The only system isoelectronic with Zr^+ whose spectrum has been almost completely worked out is the neutral Yt atom. The analysis of Yt I is due to Meggers and Rus-

[21] J. Opt. Soc. Am. & Rev. Sci. Inst., **9**, p. 372; 1924.
[22] J. Opt. Soc. Am. & Rev. Sci. Inst., **11**, p. 460; 1925.
[23] Astrophys. J., **66** p. 212; 1927.
[24] Zeit. für Physik, **33**, p. 261; 1925.
[25] J. Opt. Soc. Am., **13**, p. 18; 1926.

sell [26] who established for it nearly all the terms required theoretically for the low and middle groups. From their work were derived the data entered in Table 7 for comparison with Zr II. The differences in the fifth column of Table 7 run as smoothly as can be expected and indicate a close parallelism between the term structures of Yt I and Zr II, although the relative importance of the corresponding terms in their respective spectra differs considerably. Thus, the lowest term of Yt I is ^{2}D coming from $4d\ 5s^2$, the configurations $4d^2\ 5s$ and $4d^3$ yielding metastable terms of less prominence. In Zr II, however, the lowest term, ^{4}F, and the more prominent metastable terms come from the configurations $4d^2\ 5s$ and $4d^3$, respectively, the term d^2D coming from $4d\ 5s^2$ being doubtful and relatively inconspicuous. And in like manner similar comparisons may be made between the odd terms of the middle groups arising from the configurations $4d\ 5s\ 5p$ and $4d^2\ 5s$, the former yielding the more prominent terms in Yt I, the latter in Zr II.

TABLE 7.—*Values of* $\sqrt{\nu/R}$ *for Yt I and Zr II*

Electron configuration	Term	Limit	Yt I	Δ	Zr II
$4d^3 \cdot 5s$	$^4F_{0\frac{1}{2}}$	$4d^3, {}^3F_4$	0.684	*0.333*	1.017
	$^4P_{2\frac{1}{2}}$	$4d^3, {}^3F_3$	.694	*.326*	1.020
	$^2G_{4\frac{1}{2}}$	$4d^3, {}^1G_4$	.684	*.278*	.962
	$^2F_{3\frac{1}{2}}$	$4d^3, {}^3F_4$	.655	*.338*	.993
	$^2D_{2\frac{1}{2}}$	$4d^3, {}^1D_2$	.694	*.317*	1.011
	$^2P_{1\frac{1}{2}}$	$4d^3, {}^3P_2$	.667	*.361*	1.028
$4d^3 \cdot 5p$	$^4G_{5\frac{1}{2}}$	$4d^3, {}^3F_4$	.549	*.325*	.874
	$^4F_{4\frac{1}{2}}$	$4d^3, {}^3F_4$	.529	*.340*	.869
	$^4D_{3\frac{1}{2}}$	$4d^3, {}^3F_4$	.516	*.347*	.863
	$^2G_{4\frac{1}{2}}$	$4d^3, {}^3F_4$	.515	*.336*	.851
	$^2F_{3\frac{1}{2}}$	$4d^3, {}^3F_4$	.513	*.363*	.876
	$^2D_{2\frac{1}{2}}$	$4d^3, {}^3F_4$	.511	*.362*	.873
	$^4D_{3\frac{1}{2}}$	$4d^3, {}^3P_2$	.539	*.336*	.875
	$^4P_{2\frac{1}{2}}$	$4d^3, {}^3P_2$	.529	*.344*	.873
	$^4S_{1\frac{1}{2}}$	$4d^3, {}^3P_2$	.536	*.341*	.877
	$^2D_{2\frac{1}{2}}$	$4d^3, {}^3P_2$	.501	*.398*	.899
	$^2P_{1\frac{1}{2}}$	$4d^3, {}^3P_2$			.886
	$^2S_{0\frac{1}{2}}$	$4d^3, {}^3P_2$	.555	*.337*	.892
	$^2H_{5\frac{1}{2}}$	$4d^3, {}^1G_4$	.539	*.279*	.818
	$^2G_{4\frac{1}{2}}$	$4d^3, {}^1G_4$	.533	*.293*	.826
	$^2F_{3\frac{1}{2}}$	$4d^3, {}^1G_4$	.495	*.348*	.843
	$^2F_{3\frac{1}{2}}$	$4d^3, {}^1D_2$	.535	*.287*	.822
	$^2D_{2\frac{1}{2}}$	$4d^3, {}^1D_2$	.543	*.283*	.826
	$^2P_{1\frac{1}{2}}$	$4d^3, {}^1D_2$	.538	*.319*	.857
$4d \cdot 5s \cdot 5p$	$^4F_{4\frac{1}{2}}$	$4d\ 5s, {}^3D_3$	.599	*.327*	.926
	$^4D_{3\frac{1}{2}}$	$4d\ 5s, {}^3D_3$	.592	*.326*	.918
	$^4P_{2\frac{1}{2}}$	$4d\ 5s, {}^3D_3$	.576	*.351*	.927
	$^2F_{3\frac{1}{2}}$	$4d\ 5s, {}^3D_3$	.554	*.273*	.827
	$^2D_{2\frac{1}{2}}$	$4d\ 5s, {}^3D_3$	.600	*.233*	.833
	$^2P_{1\frac{1}{2}}$	$4d\ 5s, {}^3D_3$	.532	*.272*	.804
	$^2F_{3\frac{1}{2}}$	$4d\ 5s, {}^1D_2$	.545	*.314*	.859
	$^2D_{2\frac{1}{2}}$	$4d\ 5s, {}^1D_2$	.546	*.330*	.876
	$^2P_{1\frac{1}{2}}$	$4d\ 5s, {}^1D_2$	.517	*.318*	.835

4. SERIES AND IONIZATION POTENTIAL

Among the terms of Table 1, there are eight sequences of two members each available for calculating series limits. Four of the term sequences arise from the migration of the *s* electron, and four from the *d* electron. Experience with other spectra shows, however, that term sequences coming from the *d* electron, when represented by a simple Rydberg formula, give results out of harmony with those for

[26] B. S. Jour. Research, **2**, p. 733; 1929.

series resulting from the *s* electron. This is accounted for theoretically by the firm binding of the lowest *d* electron in its orbit. The value derived for the series limits of Zr II, and also the value of the ionization potential of Zr^+, are based, therefore, on the series, coming from the *s* electron. The component series, however, have different limits in the low and metastable terms of Zr III. The manner in which the individual series approach their limits has been given by Hund.[27] In Table 8 results are given for 10 series which converge to the different components of ^3F, ^1G, and ^1D, respectively, of Zr III, the relative positions of which are known from the analysis of Zr III referred to above. The individual values for the separation of the lowest terms of Zr II and Zr III agree as well as can be expected from the limited data available and their mean, 113,175 cm^{-1}, is adopted as the value of $a^3F_2 - a^4F_{1½}$. From this an ionization potential of 13.97 volts is derived for the ion Zr^+.

TABLE 8.—*Series limits of Zr II*

Term	$a^2D_{1½}$	$a^2D_{2½}$	$a^2F_{2½}$	$a^2F_{3½}$	$b^2G_{3½}$	$b^2G_{4½}$	$a^4F_{1½}$	$a^4F_{2½}$	$a^4F_{3½}$	$a^4F_{4½}$
Distance from limit, cm^{-1}	111, 820	111, 696	108, 528	107, 944	101, 284	101, 308	113, 460	113, 392	113, 460	113, 4
Reduction to $^3F_2$, Zr III	−3, 392	−3, 392	−682	−1, 487	−2, 534	−2, 534	0	0	−682	−1, 4
Reduction to $^4F_{1½}$, Zr II	+4, 288	+4, 505	+5, 753	+6, 468	+14,060	+14, 190	0	+315	+763	+1, 3
$a^3F_2 - a^4F_{1½}$	112, 676	112, 809	113, 599	112, 925	112, 810	112, 964	113, 460	113, 707	113, 541	113, 2

Mean $(a^3F_2 - a^4F_{1½}) = 113,175$
Ionization potential $= 113,175 \times 1.2345 \times 10^{-4} = 13.97v$

IV. IONIZED ZIRCONIUM IN THE SUN

Zirconium is present in the sun in both its neutral and ionized states. In the recent Revision of Rowland's Preliminary Table of Solar Spectrum Wave-Lengths [28] by St. John and his collaborators 238 dark lines are assigned to Zr^+. These include nearly all the strong lines and many of the fainter ones listed in Table 2 down to wave length 2,975 A, which marks the limit of transparency of the earth's atmosphere to solar radiation. The method used in identifying Fraunhofer lines with those of terrestrial elements was that of coincidences; that is, the direct comparison of solar wave lengths with those of emission lines observed in the laboratory. That this method of identification has its limitations is shown by the fact that of the 20,000 lines recorded by Rowland only 57 per cent have had their chemical origins assigned in the Revision of Rowland.

Perhaps the chief reason why the method of coincidences has not been more fruitful in establishing the identity of the solar lines is that most of the elements of astrophysical importance have not had their spectra measured with the same order of precision as that applied to the sun's spectrum. In the case of the fainter lines, therefore, which constitute a great majority of the 43 per cent remaining unidentified, direct comparisons of wave lengths are often uncertain and must await improved laboratory wave lengths. As stated above, however, the wave lengths entered in Table 2 are the results of new measure-

[27] Linienspektren und periodisches System der Elemente, p. 184, Julius Springer, Berlin; 1927.
[28] Carnegie Institution of Washington, Publ. No. 396; 1928.

ments made at the National Bureau of Standards in the second order of the large concave grating, and are regarded as sufficiently accurate to warrant the assignment of additional lines to the spectrum of singly ionized zirconium. The new identifications which have thus been made, by the method of coincidences, are presented in Table 9.

TABLE 9.—*Identification of Fraunhofer lines with* Zr^+

Observed		Solar			Observed		Solar		
λ	Intensity	λ	Intensity	Identification	λ	Intensity	λ	Intensity	Identification
4,841.98	0	1.975	−2		3,565.41	5	5.397	12	Fe
4,565.43	3	.427	−1		3,561.11	1	.137	−3	
4,445.88	1	.858	−2 N		3,554.09	7	.123	5	Fe
4,040.24	4	.265	−1		3,539.05	4	.077	−1	Ce^+
4,031.35	2	.345	0	Ce^+	3,514.64	4	.636	2	Fe ?
3,855.43	3	.414	1		3,512.67	3	.647	6	Co
3,800.73	5	.741	−1		3,431.57	6	.587	4	Co
3,782.24	4	.220	0	CN−	3,402.87	7	.901	0	NH
3,767.89	5	.899	−1		3,394.63	3	.612	3	Fe
3,757.80	8	.812	−1 N		3,340.55	15	.571	2	Fe
3,710.47	1	.449	−1 N		3,337.93	2	.924	0	
3,709.27	60	.257	8	Fe	3,313.70	8	.726	0	Fe
3,692.60	1	.571	−3		3,287.31	3	.335	−2	
3,667.40	1	.425	−3 N		3,157.00	10	.032	2	Fe
3,667.06	3	.098	−3d?		3,155.68	10	.659	3	Ti^+
3,660.92	3	.922	−3 N		3,060.11	3	.087	−1	
3,655.56	7	.581	−3		3,057.22	5	.277	−1	
3,633.49	10	.513	−1d?		3,030.91	10	.943	1	
3,612.34	3	.383	−3 N		2,998.49	2	.505	−1	
3,572.47	30	.479	4		2,991.40	3	.436	−2	
					2,990.10	3	.071	−1	

Another limitation to the method of coincidences, however, is the fact that not all the lines theoretically possible appear in emission spectra obtained by the ordinary methods of excitation. This is true of Zr II, as revealed by the foregoing analysis. Only a few of the multiplets have their full complement of lines; in many only those lines which represent the stronger transition probabilities are present; and in yet others no lines appear at all in the spectrum. But with a well-established set of terms based on accurate wave lengths it is possible to calculate wave lengths for lines which are missing from a spectrum though not forbidden by the selection principles. We have done this for all the multiplets of Zr II which lie in the Rowland region of the solar spectrum. The calculated wave lengths which agree with solar lines and the terms used in deriving them are presented in Table 10. It is of interest to note that the multiplets $b^4P - z^4G°$, $b^4P - z^4F°$, and $b^4F - z^2G°$ which do not appear at all in emission are represented in the solar spectrum by two or more lines.

TABLE 10.—*Identification of Fraunhofer lines with calculated lines of* Zr^+

Calculated λ	Solar			Term combination
	λ	Intensity	Identification	
6,085.98	5.921	−3		$c^1D_{2\frac{1}{2}}$–$z^3D^0_{3\frac{1}{2}}$
5,881.72	.728	−2	Fe	$b^3D_{2\frac{1}{2}}$–$z^3D^0_{3\frac{1}{2}}$
5,549.34	.332	−3		$b^4P_{2\frac{1}{2}}$–$z^4G^0_{3\frac{1}{2}}$
5,278.26	.252	−1N	Cr	$b^4P_{2\frac{1}{2}}$–$z^4G^0_{2\frac{1}{2}}$
4,989.93	.973	−2		$b^4P_{1\frac{1}{2}}$–$z^4F^0_{1\frac{1}{2}}$
4,857.07	.101	−2		$b^4P_{2\frac{1}{2}}$–$z^4F^0_{2\frac{1}{2}}$
4,794.63	.666	−3		$a^4P_{2\frac{1}{2}}$–$z^4G^0_{3\frac{1}{2}}$
4,697.80	.810	−2		$b^4P_{2\frac{1}{2}}$–$z^4F^0_{3\frac{1}{2}}$
4,050.04	.028	−1	Cr ?	$b^4F_{3\frac{1}{2}}$–$z^4G^0_{3\frac{1}{2}}$
3,748.49	.508	1	Fe	$b^4P_{2\frac{1}{2}}$–$y^4D^0_{1\frac{1}{2}}$
3,716.37	.379	−1	Ce^+	$b^4P_{2\frac{1}{2}}$–$y^4F^0_{2\frac{1}{2}}$
3,690.98	.974	−3N		$b^4P_{0\frac{1}{2}}$–$y^4D^0_{1\frac{1}{2}}$
3,675.08	.120	−3N		$b^4P_{2\frac{1}{2}}$–$y^4D^0_{2\frac{1}{2}}$
3,554.25	.278	−2		$c^2D_{2\frac{1}{2}}$–$z^2F^0_{3\frac{1}{2}}$
3,496.99	7.010	1	Zr, CN	$b^4F_{1\frac{1}{2}}$–$z^2D^0_{2\frac{1}{2}}$
3,457.79	.775	−3N		$b^2F_{3\frac{1}{2}}$–$w^1F^0_{3\frac{1}{2}}$
3,354.93	.891	−1N		$a^4F_{3\frac{1}{2}}$–$z^2F^0_{3\frac{1}{2}}$
3,287.28	.335	−2		$b^4F_{2\frac{1}{2}}$–$y^2D^0_{1\frac{1}{2}}$
3,240.85	.874	−3		$b^4F_{1\frac{1}{2}}$–$y^2D^0_{2\frac{1}{2}}$
3,205.67	.654	−2		$b^4F_{3\frac{1}{2}}$–$z^2G^0_{3\frac{1}{2}}$
3,180.96	.992	−2		$b^4F_{4\frac{1}{2}}$–$z^2G^0_{4\frac{1}{2}}$
3,120.72	.733	0	Zr	$a^2F_{2\frac{1}{2}}$–$y^2F^0_{3\frac{1}{2}}$

V. CONCLUSION AND ACKNOWLEDGMENTS

The foregoing analysis of Zr II has shown that it is possible to account for 75 per cent of the lines of this spectrum as combinations of terms which can be predicted as to number and type from modern theoretical concepts of the atom. All the terms theoretically possible for the low, metastable group have been found. All the middle group terms arising from configurations containing *p* electrons have also been found except the term $^2P^\circ$ coming from $5s^2\ 5p$. This term, which is prominent in Yt I through its combinations with the lowest term a^2D and higher terms, would reveal its existence in Zr II only through combination with d^2D, itself uncertain. No terms of the middle group arising from the configuration $4d^2\ 4f$ have been found, although in Zr III and Zr IV there are prominent terms arising from the binding of the current electron in a $4f$ orbit. If such terms exist for Zr II they would combine with the low terms coming from $4d^3$. But search through the available wave length data has failed to reveal $\Delta\nu$'s characteristic of these low terms from which the $4f$ terms must be established.

Of the high terms, which combine with those of the middle group, only a few have been established with certainty. As stated above many of the lines originating in these high terms are nebulous. It is reasonable to attribute, therefore, the remaining unclassified lines, many of which are nebulous, to combinations with unidentified high terms which are predictable. All these unclassified lines are relatively faint, and if they are the strongest members of multiplets originating in the unknown high terms, it will be almost impossible to classify them since the still fainter satellites, necessary to reveal the characteristic $\Delta\nu$'s, are missing.

As stated in the introduction the analysis of the first spark spectrum of Zr presented in this paper has been carried forward at various times during the past eight years. A similar analysis of Zr I, which we shall describe in a forthcoming paper in this journal, has been carried on at the same time. In the laborious task of making the necessary observations and calculations we have received assistance from Mrs. F. J. Stimson, and E. Z. Stowell, D. D. Laun, and Bourdon F. Scribner, former and present members of the bureau's staff. For the help they have given us we here wish to record our appreciation. We are also indebted to the late Prof. B. E. Moore, of the Brace Laboratory, University of Nebraska, for placing at our disposal not only his recent observations of the Zeeman effect of Zr, but also a set of plates obtained by him in 1907 in Göttingen; to Dr. A. S. King and Miss Edna Carter, of the Mount Wilson Observatory, who sent us copies of their furnace spectra of Zr and lists of temperature classifications in advance of publication; to Dr. K. Burns, of the Allegheny Observatory, for preliminary values of ultra-violet standard wave lengths of Fe; and finally to Prof. R. J. Lang, of the University of Alberta, who has furnished us with lists of Zr wave lengths observed by him with the vacuum spectrograph.

WASHINGTON, June 6, 1930.

A REDETERMINATION OF THE CONSTANT OF GRAVITATION

By Paul R. Heyl

ABSTRACT

A redetermination of the constant of gravitation has been made, using the torsion balance in vacuo. The large masses were steel cylinders weighing about 66 kg, and the small masses spheres of gold, platinum, and optical glass. The final result obtained is 6.670×10^{-8} cm^3 g^{-1} sec.$^{-2}$.

While the results obtained appeared to differ slightly with small balls of gold, platinum, or glass, it was shown by a special experiment with the form of torsion balance used by Eötvös that this is not to be attributed to difference in material.

CONTENTS

	Page
I. Introduction	1244
1. The nature of the constant of gravitation	1244
2. Summary of earlier measurements	1245
3. Work of Boys	1245
4. Work of Braun	1246
5. Organization of the present work	1247
II. Plan of method	1247
III. Description of apparatus	1248
1. Observation room	1248
2. The large masses	1249
3. The supporting system	1250
4. The small masses	1251
5. The moving system	1252
6. The container	1254
7. The optical system	1255
8. Measurements of time	1256
9. Measurements of length	1256
IV. Mathematical theory	1257
1. The attraction of a finite cylinder at any external point	1257
2. Formula for time of swing	1269
V. Method of observing	1275
1. Centering adjustments	1275
2. Length measurements	1277
(*a*) Horizontal	1277
(*b*) Vertical	1279
3. Time measurements	1279
VI. Computations	1282
VII. Results	1284
1. Gold balls	1284
2. Platinum balls	1284
3. Glass balls	1285
4. Mean value	1286
5. Discussion of results	1286
VIII. The specific attraction of platinum and glass	1287
IX. Summary and general conclusions	1290

I. INTRODUCTION

1. THE NATURE OF THE CONSTANT OF GRAVITATION

The constant of gravitation is the multiplying factor G in the formula

$$F = G\frac{Mm}{d^2} \tag{1}$$

giving the force F of gravitational attraction between two masses M and m, with a distance d between their centers of attraction.

This constant of nature is one of the few that best deserve the name. It is known to be independent of the nature of the attracting materials to a precision of 6 parts in 10.[1] It is known to be independent of the temperature to a precision of about 1 part in 10,000.[2] It appears also to be unaffected by the presence of different materials in the space between the attracting bodies.[3]

In theoretical importance the constant of gravitation ranks with the velocity of light and Planck's constant of action. In Einstein's theory of gravitation it appears in a formula for the curvature of space due to the density of distribution of matter.[4] It undoubtedly has some intimate connection not yet understood with the ultimate structure of the universe.

Practically this constant is of importance as it enables us to determine the mean density of the sun and of the other planets of the solar system.

In thus applying the constant of gravitation it should be pointed out that we are making an assumption—that this constant is the same between the earth and the sun as between two bodies on the earth's surface. The arbitrary nature of this assumption becomes clear when, following Einstein, we regard gravitation as due to space curvature arising from the presence of matter. We are, in fact, assuming space to be everywhere equally resistant to deformation. We do know that the constant of gravitation is approximately the same at several points on the earth's surface, and there is no reason to suspect the contrary; but we do not know that the same will hold true for different radii, as between the earth and the moon, or even between the center and the surface of the earth.

But if we are wrong in this assumption it is of little practical importance. Our estimates of the masses of the heavenly bodies might be in error, yet their mutual attractions and relative motions would still be the same. However, in the case of a body moving in a very long elliptical orbit, such as a periodic comet, there might be a small differential perturbation from this cause.

And we are not entirely without evidence that our estimate of the mass of the sun, at least, is not grossly erroneous. The Einstein shift of the lines in the solar spectrum depends on the solar mass. While experimental evidence on this point is not of the highest precision, it is perhaps safe to say that our estimate of the mass of the sun is not in error by as much as 20 per cent.

---

[1] Eötvös, Pekar, and Fekete, Annalen der Physik, **68**, 1, pp. 11–66; 1922.
[2] P. E. Shaw and N. Davy, Proc. Roy. Soc., **102**, pp. 46–47; 1922.
[3] Russell, Astrophys. J., **54**, p. 334; 1921; Eichelberger and Morgan, Astronom. J., No. 795; January, 1922; Heyl (summary of evidence), Sci., Mar. 31, 1922.
[4] Einstein, Sitzungsberichte der Preuss. Akad. d. Wiss.; Feb. 8, 1917.

2. SUMMARY OF EARLIER MEASUREMENTS

An excellent summary of experimental work on the constant of gravitation may be found in Poynting's article "Gravitation" in the Encyclopædia Britannica (11th ed.). To this is to be added a reference to the work of Crémieu (Comptes rendus, vol. 141, pp. 653, 713; 1905, and vol. 149, p. 700; 1909).

The value accepted for this constant for the last 30 years has rested upon the independent work of Boys and of Braun.[5] These two experimenters obtained results agreeing to 4 significant figures, 6.658×10^{-8} cm^3 g^{-1} sec.$^{-2}$, but because their individual values varied in the third figure (by as much as 4 units in Braun's work and by 2 units in that of Boys) Poynting, in his discussion of the subject, adopts the value 6.66×10^{-8}, subject to an uncertainty of 1 unit in the third figure.

3. WORK OF BOYS

Because of the importance of the work of Boys and of Braun it will be well to consider their experiments in more detail. Both used the torsion balance, which has been employed in one form or another by half a dozen different experimenters since the days of Cavendish, but each employed a different arrangement.

Boys, guided by theoretical considerations which show that a short beam may, under certain conditions, give increased sensitivity, constructed his apparatus so that the horizontal distance between centers of the small masses was 1 inch and that between centers of the large masses 6 inches. Since with centers of all masses at the same level the proximity of a large mass to both small ones would largely wipe out the increased sensitivity arising from the short beam, Boys arranged the masses in pairs, one large and one small mass in each pair, the two pairs being at different levels.

The large masses used by Boys weighed about 7.4 kg each and the small masses each about 2.65 g.

Boys did not use a vacuum in his apparatus; in fact, he stated in his published paper (p. 70) that he was sure the use of a high vacuum was out of the question. He did, however, carry out one experiment with a hydrogen-filled apparatus, but the results were not encouraging. In fact, no experimenter previous to Braun had made any attempt to work at reduced pressure, and all had experienced trouble from convection currents. Boys was forced to go to great lengths in the way of screens and heat insulation in the attempt to eliminate this difficulty.

Of the two methods of using the torsion balance, direct deflection and time of swing, Boys used the first only. In this method the large masses are set in a position of maximum attraction on the moving system. (*a*, *a*, fig. 1.) After determining the resting point the moving system then takes up, the large masses are moved to a similar position with opposite turning effect (*b*, *b*), and the resting point again noted. Half the angle between the two positions of the moving system measures the deflection produced by the mutual attraction of the masses.

Boys aimed at a precision of 1 part in 10,000, and so designed his apparatus as to afford the accuracy theoretically necessary to attain

[5] C. V. Boys, Phil. Trans. Roy. Soc., A, Pt. 1, p. 1; 1895. Carl Braun, Denkschriften der k. Akad. d. Wiss. (Wien), math. u. naturwiss. Classe, **64**, p. 187; 1897.

this end. His final results, however, fell considerably short of this precision. Omitting the experiment with the hydrogen-filled apparatus, he obtained the following nine results (omitting a fifth figure given by Boys):

6.665×10^{-8}	6.658×10^{-8}
6.670×10^{-8}	6.653×10^{-8}
6.671×10^{-8}	6.658×10^{-8}
6.668×10^{-8}	6.670×10^{-8}
6.655×10^{-8}	

The mean of these values, assumed of equal weight, is 6.663, with an extreme variation of 0.018 and an average departure from the mean of 0.006. Boys remarks, however, that conditions of disturbance varied greatly in the different experiments, and he selected the fifth, sixth, seventh, and eighth of the above series as being most likely to give a true value. Moreover, he seems to have assigned nearly all the weight to the sixth and eighth, adopting as his final figure 6.658×10^{-8}.

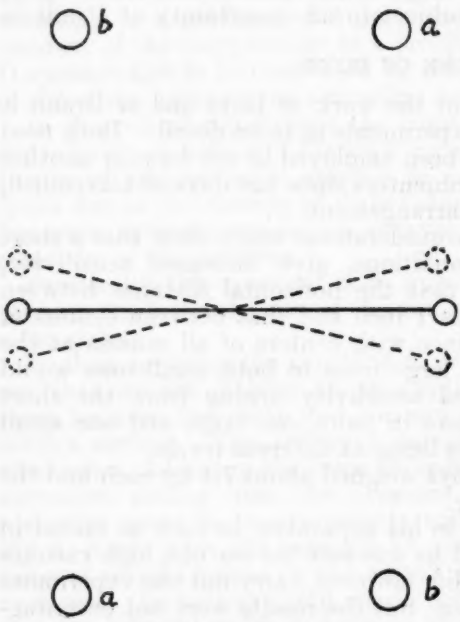

FIGURE 1.—*Direct deflection method*

4. WORK OF BRAUN

Braun used a torsion balance of larger dimensions than that constructed by Boys, the distance between centers of the small masses being about 25 cm and that between centers of the large masses about 42 cm. The large masses weighed about 9 kg each and the small masses each about 54 g. His apparatus was arranged in the usual way, with the centers of all four masses at the same level. For a long beam there is little objection to this plan.

Braun was the first to perform this experiment at reduced pressure, part of his results being obtained at 16 mm Hg and part at 4 mm Hg.

Braun used both the direct deflection and the time-of-swing methods. In the latter method the time of swing is measured with the large masses in two positions which may be called "near" and "far." (Fig. 2.) A little study of this figure will show that in the near position the attraction of the large masses upon the moving system is such as to accelerate the swing, while in the far position it retards it. With the masses and dimensions used by Braun the difference between the two times of swing was about 46 seconds.

Braun stated his results in terms of the mean density of the earth rather than of the constant of gravitation. He published results

of 46 separate experiments, 26 by the time-of-swing method and 20 by the method of direct deflection, the individual results being weighted from 1 to 4. The individual results vary by as much as 4 units of the third significant figure.

5. ORGANIZATION OF THE PRESENT WORK

So well done was the work of Boys and Braun that the difficulty of improving upon it was clearly recognized. Such a task requires the resources of an institution rather than of an individual. Practically every division in the Bureau of Standards has contributed tangibly or intangibly to the successful completion of this experiment. The work would probably not have been undertaken had it not been for the encouragement of the director, Dr. George K. Burgess, whose interest in the subject dates back to his student days, and for the like encouragement of Dr. L. J. Briggs, chief of the division of mechanics and sound, whose interest in gravity measurements at sea is well known.

The completion of the undertaking in a reasonable time has been made possible by the cooperation of E. R. Frisby, who has done about 90 per cent of the very laborious computations and, in addition, worked out the formulas for the time of swing.

Drs. H. L. Dryden, of the Bureau of Standards, and E. W. Woolard, of George Washington University, have rendered valuable services in checking the mathematical work at different stages.

The apparatus was constructed almost entirely in the Bureau of Standards instrument shops by J. F. Draper. The task required nearly a year for completion. Acknowledgment is made of the helpful suggestions offered by Mr. Draper in the course of the work.

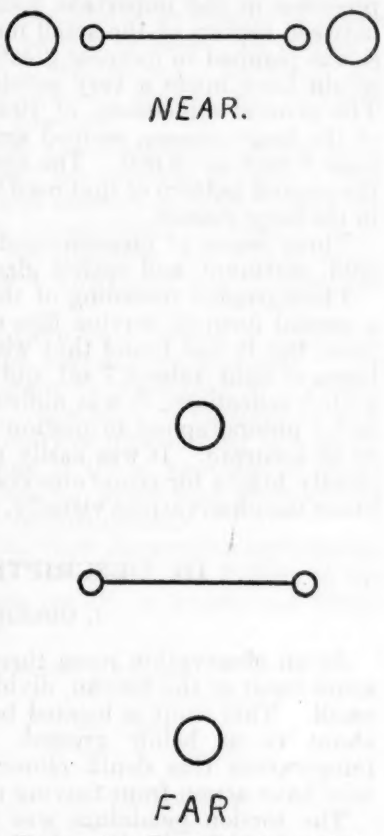

FIGURE 2.—*Time of swing method*

II. PLAN OF METHOD

A study of the work of Boys and Braun led to the conclusion that little was to be hoped for in the way of increased precision by a repetition of the direct-deflection method. As this was carried out by Boys, the only serious objection is the presence of air about the moving system. Yet Boys's work seems to have been very well

done, for in Braun's experiments this objection does not hold, yet his result by the direct-deflection method confirms that of Boys.

With the time-of-swing method the case is different. Braun says in his published paper that the possibilities of this method much exceed those of the other, and expresses his regret that he was unable to make full use of them. It was therefore decided to use this method only in the repetition of the experiment.

Of the two arrangements of the torsion balance Braun's form seemed preferable to that of Boys for two reasons—it is easier to obtain precision in the important measurement of the horizontal distance between centers of the small masses when this distance is large; and it was planned to increase greatly the size of the large masses, which would have made a very considerable difference of level necessary. The general dimensions of Braun's apparatus, apart from the size of the large masses, seemed ample for obtaining a precision of perhaps 1 part in 10,000. The apparatus was, therefore, designed after the general pattern of that used by Braun, with a considerable increase in the large masses.

Three series of measurements were made, using small masses of gold, platinum, and optical glass.

Photographic recording of the time of swing was considered, and a special form of moving film camera was constructed for this purpose; but it was found that with the distance to be traveled by the beam of light (about 7 m) and the passage through 8 pieces of glass with 2 reflections, it was difficult to obtain an image bright enough to be photographed in motion and at the same time sharp enough to be accurate. It was easily possible to obtain a sharp image sufficiently bright for visual observation, and it was therefore decided to make the observations visually, and to record them by a chronograph.

III. DESCRIPTION OF APPARATUS

1. OBSERVATION ROOM

As an observation room there was available the constant-temperature vault of the bureau, divided into two rooms, one large and one small. This vault is located below the East Building at a depth of about 12 m below ground. In addition to furnishing uniform temperature this depth eliminated any trouble that might otherwise have arisen from moving masses near by.

The torsion pendulum was set up in the small room, the floor space of which was about 2×2.7 m and the height about 4 m. The observing apparatus was placed in the large room, the intervening brick wall being pierced by a window about 30 cm square. A pier was built in each room, in the small room at its center, and in the large room close to the far wall, the distance between centers of piers being about 3.5 m. At this distance calculation shows that the effect of the observer's mass upon the moving system is less than one ten-thousandth that of the two large masses. It was deemed advisable, however, that the observer remain in the same place during the whole period of observations, rising from his chair when necessary to attend to the chronograph at his side, but not moving horizontally from his location.

The observation room proved ideal for the purpose. No vibration was observable, and it was possible to work by day with results equally as good as those obtained by night. Practically all the work was therefore done by day.

2. THE LARGE MASSES

When it is a question of dealing with large masses in an experiment of this kind the nature of the material becomes important. Cavendish (and later Baily) used spheres of lead weighing nearly 160 kg. Such large masses of lead or lead alloy can hardly be trusted to maintain their shape accurately over long periods of time. In addition, there is always the possibility of holes in the casting. To avoid this latter difficulty several experimenters (Braun among the number) have used hollow spheres filled with mercury.

For the present work it seemed most practicable to employ steel, because of ease of accurate shaping and permanence of form. Tool steel of about 0.90 per cent carbon was selected as being most uniform in structure and least liable to segregation. To avoid blowholes and pipes a large ingot of 30 cm diameter was forged down to 20 cm and annealed for machining. This work was done at the Washington Navy Yard.

Nearly all previous experimenters have used masses of spherical form because of the simplicity of the calculations involved. The practical difficulties incident to the accurate machining of a sphere of the weight planned (over 60 kg), especially in cutting off and rounding the ends, as well as the difficulty of determining accurately the center of the sphere when mounted in place, appeared so great that it was decided to adopt a cylindrical form, thus shifting the burden to the broad shoulders of the mathematician.

After machining the cylinders to size, their dimensions and masses were determined, respectively, by Mr. Miller and Mr. Peffer, of the weights and measures division. These results, in grams and centimeters at 20° C., are given in Table 1.

TABLE 1.—*Dimensions and masses of cylinders*

	Cylinder mark	
	0	—
Diameter (extreme variation)	19.4514	19.4727
	19.4552	19.4758
Average diameter	19.4534	19.4743
Length (extreme variation)	28.4974	28.4804
	28.5042	28.4852
Average length	28.5007	28.4827
Mass (in vacuum)	66,302.6	66,404.6

When in place in the apparatus the cylinders are surrounded by air, and the attraction of a cylinder at any point will be that due to the mass of the cylinder in vacuum minus the mass of the displaced air. We may consider a cylinder of this slightly reduced mass superposed upon a continuous and uniform distribution of air. The air being infinite and continuous exerts no resultant attraction at any point within it, and the total resultant attraction is therefore that due to

the superposed cylinder. Thus the effective values of the mass and density of the cylinder will be found by correcting for displaced air at the temperature, pressure, and humidity existing at the time of the experiment.

Calculation shows that for a variation in relative humidity from 57 to 86 and for the usual pressure variation the mass of air displaced by a cylinder is constant to the first decimal place, namely, 9.9 g; and this is also the precision to which the masses of the cylinders are known. Applying this correction to the values given in Table 1 we obtain the effective values given in Table 2:

TABLE 2.—*Effective masses and densities of cylinders*

	Cylinder mark	
	0	−
Mass	66,292.7	66,394.7
Density	7.82583	7.82608

Uniformity of density is an important consideration. There can hardly be any question of appreciable pipes or blowholes after the preliminary reduction by forging, but we must consider the possibility that by this forging the outer layers of the cylinder may have been made slightly denser than the center. Segregation also might cause a change in density of like distribution. As a check upon this, samples were taken from the bosses cut off from an end of each cylinder in the final stages of machining, and the density of these samples determined. Each sample had a diameter of about one-fifth that of the cylinder, and may thus be taken as representing approximately the density of the cylinder near its axis. Table 3 shows the comparison of these densities with the calculated values for the whole cylinders.

TABLE 3.—*Variation in density of cylinders (in vacuum)*

	Cylinder mark	
	0	−
Density near axis	7.8255	7.8250
Calculated mean density	7.8270	7.8273

In no case is there a difference in density greater than about 1 part in 4,000. An approximate calculation shows that the error introduced in the value of the attraction by the assumption (for instance) of a uniform density of 7.8273 instead of one varying uniformly from 7.8250 at the center to 7.8285 at the outer surface (with a mean of 7.8273) amounts to less than 1 part in 50,000, negligible for present purposes.

3. SUPPORTING SYSTEM

The large masses were supported so as to be free to turn in azimuth about a vertical axis midway between them. The general arrangement is shown in Figure 3.

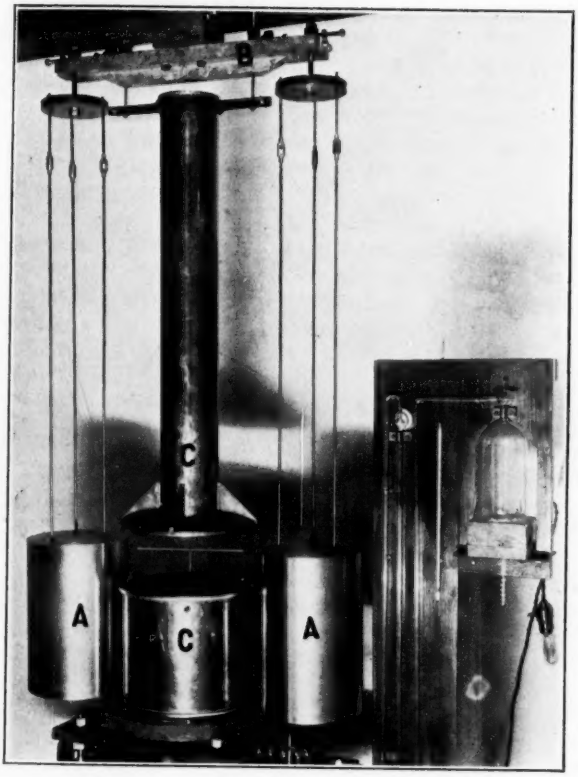

FIGURE 3.—*General arrangement of apparatus*

Two 15 cm I beams were set into the brick walls of the room with a space of about 20 cm between them. Across these beams was fastened by screw clamps a steel plate 2.5 cm thick and 15 cm wide. This crosspiece was pierced at the center by a hole 3.7 cm in diameter, through which passed by a snug fit the vertical axis of the supporting system.

This vertical axis was capped at the upper end by a disk resting upon a ring of steel balls rolling in a channel cut in the crosspiece. Fastened to the upper surface of the desk was a graduated circle 35 cm in diameter provided with a vernier reading to 0.1°.

The vertical axis carried at its lower end an arrangement of dovetailed blocks allowing two sliding adjustments at right angles, for the purpose of centering the cylinders with respect to the point of support of the pendulum.

Fastened to the lowest of these sliding blocks was the crossbeam *B* (fig. 3), from the ends of which hung the cylinders *A*, *A*. Each cylinder was supported by three steel rods, 0.5 cm in diameter, screwed into the cylinder by tapped holes, each hole threaded all the way down to a flat bottom against which the flat end of the rod fitted. Each rod was provided with a lock nut where it entered the cylinder and, near its upper end, with a turnbuckle by which the cylinder could be leveled. The vertical adjustment of the cylinder as a whole could be secured by raising or lowering a disk from which the three rods hung. Each disk was supported by a bolt and nut passing through a slot in the crossbeam *B*, thus permitting separate horizontal adjustments of the cylinders.

4. THE SMALL MASSES

Small masses, spherical in shape, were used of three different materials, gold, platinum, and optical glass. In each case the mass was about 50 g.

This use of different materials was not prompted by any suspicion that a specific difference in attraction might be found. Rather was it the result of circumstances. The use of gold balls was suggested by the employment of this metal by Boys and by the fact that Braun used gilded balls of brass. There was no objection to this in the case of the work of Boys, who did not employ a vacuum, and Braun mentions no trouble with his gilded balls; but in the present work it was found on opening the container, after a period of several months required for the observations, that the gold balls had absorbed quite appreciable quantities of mercury, probably derived in vapor form from the manometer connected to the container.

A second set of measurements was made with platinum balls, coated thinly with lacquer by dipping. No appreciable change of weight was observed in this case.

A third set was made with balls of optical glass, the idea being that holes in the interior could be detected visually.

The metallic balls were constructed from ingots which (in the case of gold) had been fused in a vacuum furnace to avoid gas bubbles. The platinum ingots were fused in the oxyhydrogen flame in the usual manner. The ingots were first roughly hammered into shape between hemispherical steel dies, as described by Boys, and finally

shaped to size by a scraping process suggested by J. F. Draper, of the bureau's instrument shops.

In a piece of thin sheet steel was cut a circular hole of the diameter desired for the finished sphere. The ball, after having been hammered to a diameter but little in excess of the final size, was laid in this hole and turned this way and that between the thumb and finger until it had scraped its way through the hole. In the case of the platinum balls this operation was conducted under water. The resulting balls were so nearly spherical that micrometer measurements (to about 2.5 μ) could detect no variation in diameter.

In each metallic ball there was drilled a hole 1 mm in diameter and 3 mm deep, which was threaded. A piece of copper wire 6 mm long, threaded for half its length, was screwed into the hole. The projecting portion of the wire was shaped into a hook.

The glass balls were drilled with holes 1 mm in diameter and 4 mm deep, the lower part of the whole being enlarged to a diameter of 2 mm by a dental burr. In this hole was inserted a doubled piece of copper wire, loop downward. The space between wire and glass was packed with small scraps of tin foil after the manner of filling a tooth, using a blunted needle and light taps from a small hammer. The tinfoil packing was stopped about half a millimeter from the top of the hole and the rest of the space filled with wax. The protruding ends of the wire were joined by a trace of solder and bent into a hook.

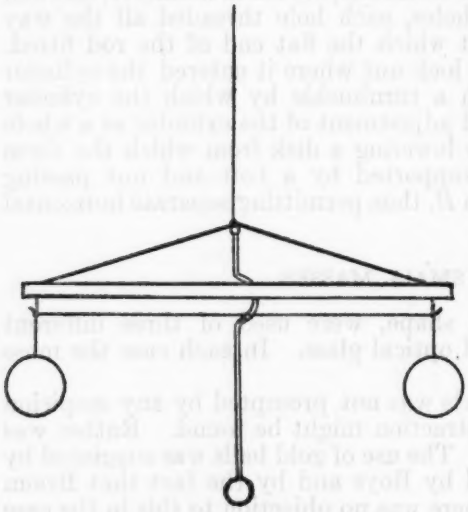

FIGURE 4.—*The moving system*

In each case the mass of a ball was determined before drilling it. At the conclusion of a set of measurements the ball was cut from the suspending filament close to the hook, and reweighed with hook, knot of filament, and trace of wax used to keep the knot from slipping. The slight excess of mass over that of the solid ball was regarded for purposes of calculation as a massive point added at the north pole of the ball.

5. THE MOVING SYSTEM

The moving system, or torsion pendulum, consisted of the two small masses, a light separating rod and the necessary supporting filaments. (Fig. 4.) In the design of this system the object was to throw as much as possible of the moment of inertia into the balls so that the system should approximate a simple pendulum. Actually over 99 per cent of the moment of inertia was thus concentrated.

The horizontal separating rod was of aluminum, 0.24 cm in diameter, 20.59 cm long, and weighted in vacuum 2.4401 g. Close to each end

was drilled a small hole through which passed the ends of a copper wire constituting a truss. These ends, after passing through the rod, were bent into hooks. The cooper truss wire was 0.36 mm in diameter, 22.1 cm long and weighed in vacuum 0.2385 g.

The balls were hung from a piece of tungsten lamp filament, 0.025 mm in diameter, tied to their hooks, and laid across the hooks at the ends of the copper truss wire. In tying the filament to the hooks of the balls the filament was wrapped four or five times around the hook and the end twisted around the main portion of the filament. This twist was held from slipping by a trace of wax. In cutting off the balls for the final weighing the twisted portion of the filament was included.

The supporting filament for the moving system as a whole was also of tungsten, 0.025 mm in diameter, commercial lamp filament annealed in hydrogen at the factory. Tungsten is preferable to silica in that it may be confidently relied on for a long program of observations. Filaments of silica, as Boys found, occasionally break for no apparent reason, often with loss of previous observations. Moreover, tungsten may be tied firmly to the object which it supports.

Our experience indicates that tungsten is quite reliable, returning well to its resting point after large deflections. One such filament was in use three years, during which the apparatus experienced a slight earthquake.

The supporting filament was about 1 m long, provided with copper wire hooks at its ends. By the lower hook the copper truss wire hung at its apex and was fastened by a trace of wax. The upper hook was fastened to a movable torsion head contained in the chimney of the bell jar. This device (patterned after one used by Braun) consisted of a train of wheel work, to the slow motion end of which the upper hook of the supporting filament was attached. By turning the other end of the train a very small twist could be given to the filament to correct, if necessary, for drift of the resting point. In order to operate this device from outside without breaking the vacuum a bar magnet was attached to the upper end of the train. By the use of a large horseshoe magnet outside the chimney the requisite twist could be given.

The train of wheel work was geared to a ratio of 3,600:1, so that one complete turn of the upper end produced a twist of one-tenth of a degree in the filament.

The moving system was provided with a silvered glass mirror, about 2 cm in diameter, 1 mm thick, weighing about 0.6 g, ground and polished optically flat. This mirror was attached at its upper edge by a little wax to a brass rod 1 mm in diameter. At its upper end this brass rod was provided with a small wire loop by which it was hung from the lower hook of the main suspension filament. The brass rod, where it passed the horizontal aluminum rod, was bent into a detour to avoid contact. (Fig. 4.)

The total mass of the swinging system was about 102 g. The breaking strength of the suspending filament was about 165 g.

To start the moving system gravitational attraction was employed. Two bottles, each holding about 2 kg of mercury, were placed close to the container in positions of maximum attraction for the pendulum. When the latter had been twisted to its greatest extent (which required about 15 minutes) the bottles were placed so as to reverse the attrac-

tion. By repeatedly reversing the positions of the mercury bottles in time with the swing of the pendulum the latter could be given any amplitude desired. In two hours time an amplitude of about 4° could be obtained, which (at the reduced pressure employed) was sufficient to keep the pendulum swinging for 20 hours.

6. THE CONTAINER

The container was of metal resting on a plate-glass base. The general shape is shown in Figure 3. The tall chimney was of brass, open at the upper end, which was closed by a piece of plate glass. This permitted observation of the magnet connected with the wheel work. The wide lower portion of the container and the lid fitting it were, in the series of measurements with the gold balls, of brass wrapped with thin sheets of silicon steel for magnetic shielding. This arrangement proved cumbersome, and in the measurements with platinum and glass balls this part of the container was made of a piece of wrought-iron tubing with a lid of the same material. A circular piece of iron was laid inside the container upon the plate-glass base, thus completing the magnetic shielding.

This precuation was necessary because of the steel cylinders, which when moved from the near to the far position altered the earth's magnetic field in the vicinity of the pendulum. Since all materials are either paramagnetic or diamagnetic to an appreciable degree, and since the gravitational attraction of a cylinder upon the nearest ball was only about 0.001 dyne, it is quite possible that the effect of the change in magnetic field upon the time of swing of the moving system might be comparable with that of gravitational attraction.

This suspicion was experimentally confirmed in the case of the brass container used with the gold balls. Before applying the silicon steel wrapping a bar electromagnet was mounted outside the container with one pole in the maximum attraction position with respect to one of the balls. On energizing the magnet the ball was repelled with an acceleration approximately equal to that produced by one of the mercury bottles. By raising the magnet to the level of the aluminum rod an attraction was produced. The magnetic susceptibility of gold is -0.15 and that of aluminum $+0.65$.

By wrapping the lower part of the container with several layers of thin silicon steel sheet these disturbances were completely prevented. In the later form of the apparatus, used with platinum and glass balls, the wrought-iron wall of the container was similarly protective.

To test the shielding more closely, measurements of time of swing were made with the outside magnet alternately magnetized and demagnetized. The magnetic field at the outer surface of the container with the electromagnet excited was about twelve times as strong as the earth's horizontal field, as determined by the rate of vibration of a small compass needle. The strength of field close to one of the large steel cylinders was about three times that of the earth's field, or one-fourth that used for testing the shielding, and the presence or absence of the testing field produced no effect upon the time of swing as great as 1 part in 10,000. Any effect to be expected by moving the cylinders must therefore be less than 1 part in 40,000.

A pressure of about 2 mm of mercury was maintained in the container, the joints of which were sealed by soft universal wax. A mercury barometric seal was used instead of a stopcock.

It may be of interest to record here the effect of pressure upon the damping exhibited by the moving system. Table 4 gives the damping factor (ratio of successive amplitudes in the same direction) at various pressures.

TABLE 4.

Damping factor	Pressure, mm mercury
0.70	150
.84	50
.85	20
.85	10
.85	7
.85	5
.86	3
.87	1.5

Windows were provided at strategical points in the container for the purpose of obtaining such measurements as the level of the centers of the balls and the position of the filament supporting the moving system.

When it was desired to raise the chimney and lid of the container a yoke was clamped about the upper end of the chimney. From the ends of this yoke two threaded rods passed up through holes in the beam *B* (fig. 3) and were supported above by nuts. By turning these nuts the upper portion of the container and the whole moving system could be raised or lowered slowly and steadily enough to avoid breaking the suspension.

The temperature of the container was read by means of a thermometer fastened closely in parallel contact with the chimney, the bulb touching the metal. On its outer side the bulb was shielded by a layer of cotton, the whole being bound to the chimney by strips of adhesive tape. The temperature inside the container was assumed to be that of the metal case as shown by the thermometer.

7. THE OPTICAL SYSTEM

The basis of reference for observing the time of swing was a scale of millimeters in the form of a photographic negative on glass, bright lines on a dark background. (Fig. 5.) Parallel to the scale and close to it was a broad bright band against which could be seen the vertical cross wire of the observing telescope. The scale was mounted in a metal box and illuminated from behind by several small electric lamps, and was set on a pier in the observing room, 3.5 m from the torsion apparatus.

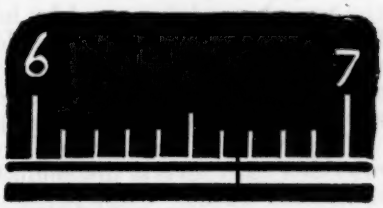

FIGURE 5.—*Scale and cross wire*

The light from the scale passed to a reflecting prism below the glass base of the container, which reflected it vertically upward, passing through the iron floor of the container by a hole. The light then encountered a second prism which reflected it horizontally to the mirror attached to the moving system. The reflected beam retraced

approximately its entering path and was finally received by a telescope on the observing pier, 3.5 m distant from the center of the moving system. A motion of one minute of arc of the moving system produced a shift of about 2 mm of the scale in the field of the telescope.

8. MEASUREMENT OF TIME

The working standard of time was a Riefler clock set up in a constant-temperature vault in another building of the bureau, and rated daily against the Naval Observatory signals. Its usual daily rate was but a few hundredths of a second. Second signals from this clock are electrically transmitted to all parts of the bureau laboratories.

The transits of the pendulum were recorded on a 2-pen chronograph. One pen recorded the clock signals and the other the transits of the scale divisions as observed by the operator.

In making the observations it was customary to adjust the resting point of the pendulum by means of the torsion head to somewhere between the twelfth and thirteenth centimeter marks on the scale, and to record the transit of every millimeter from the eleventh to the fourteenth centimeter. The calculation of the time of swing will be described in a later section.

9. MEASUREMENTS OF LENGTH

The length measurements fall into two classes—those in which approximate values are sufficient and those requiring higher precision. As an example of the first class may be mentioned the vertical difference of level between centers of balls and cylinders. In the second class are found the distance between centers of balls and the distance between cylinders.

Measurements of the first class were made to 0.1 mm, mostly with a kathetometer. Measurements of the second class were made with an optical compass similar to that used by Boys; it consisted essentially of two micrometer microscopes mounted approximately parallel to each other on a rigid bar. The distance between microscopes could be adjusted as desired.

A supporting framework of iron was clamped to the pier carrying the torsion pendulum, and by leveling the optical compass upon this framework the microscopes could be directed to view any two points whose horizontal distance apart might be desired. When the setting of the microscopes had been made the optical compass was placed in another stand so as to view a scale below it.

This scale was made from a steel bar 2.5 cm square in cross section, provided with several platinum-faced plugs, upon which fine graduations were traced. Sufficient plugs were provided to give the various lengths required. The scale was calibrated in terms of the standard meter by Doctor Judson, of the weights and measures division of the bureau.

Steel was used as a basis for the scale rather than invar, as the experience of the bureau has been that invar, while low in expansion, shows much hysteresis, and is on the whole less satisfactory for such a purpose than steel. The coefficient of steel may be higher, but it is more safely to be counted upon than that of invar.

The steel chosen for this purpose was machined to size and allowed to age for several months to eliminate the warping that usually follows removal of the surface layers. This process of aging was accelerated by rattling the bar in a shaking apparatus for several periods of a day each. The finished scale was mounted in a wooden case provided with leveling screws.

IV. MATHEMATICAL THEORY

1. THE ATTRACTION OF A FINITE CYLINDER AT ANY EXTERNAL POINT

The use in the Cavendish experiment of attracting bodies of other than a spherical shape has been rare. Boys in one of his experiments

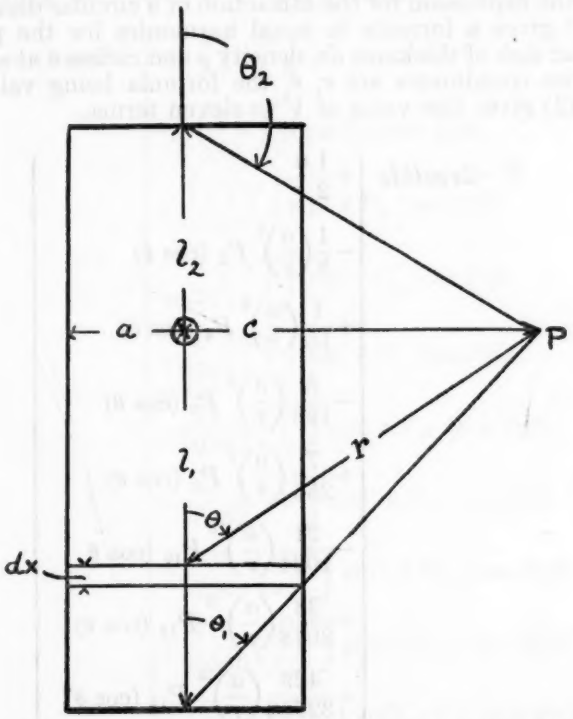

FIGURE 6.—*Attraction of finite cylinder at outside point*

used cylinders of gold one-fourth inch long and the same in diameter. He states that calculation showed that the attraction of such a cylinder at a point at the center of one of the large balls was less than that which would have been exerted had the cylinder been a sphere of equal mass by 3 parts in 10,000. Small masses of cylindrical and also of chain form were used by P. E. Shaw [6] in his work on a supposed temperature coefficient of gravitation, but as his work was concerned with relative rather than absolute values it was not necessary to calculate the actual force. Crémieu used large cylindrical masses, but does not mention the computations.

[6] P. E. Shaw, Phil. Trans. Roy. Soc., A, 216, 1916.

Calculations for nonspherical masses are not simple; in fact, the labor involved in making a nonspherical calculation to anything but a rough approximation has rather been looked upon as prohibitive. For practical reasons earlier mentioned it was desirable to use large masses of cylindrical form. It was an agreeable surprise to find that in the case of the dimensions used it was possible to obtain a formula in zonal harmonics which converged fairly rapidly. Working to 1 part in 100,000 there were necessary only seven terms in the near position and six in the far position.

A formula for the attraction of a finite cylinder at any external point has never, as far as we know, been published. It may therefore be a convenience to future workers if the development of this formula is given somewhat in detail. The best method of procedure is to integrate the expression for the attraction of a circular disk. (Fig. 6.)

Byerly [7] gives a formula in zonal harmonics for the potential V of a circular disk of thickness dx, density ρ and radius a at any external point whose coordinates are r, θ, the formula being valid if $r>a$. Formula (2) gives this value of V to eleven terms.

$$V=2\pi\rho aGdx\left\{\begin{aligned}&+\frac{1}{2}\frac{a}{r}\\&-\frac{1}{8}\left(\frac{a}{r}\right)^3 P_2(\cos\theta)\\&+\frac{1}{16}\left(\frac{a}{r}\right)^5 P_4(\cos\theta)\\&-\frac{5}{128}\left(\frac{a}{r}\right)^7 P_6(\cos\theta)\\&+\frac{7}{256}\left(\frac{a}{r}\right)^9 P_8(\cos\theta)\\&-\frac{21}{1024}\left(\frac{a}{r}\right)^{11} P_{10}(\cos\theta\\&+\frac{33}{2048}\left(\frac{a}{r}\right)^{13} P_{12}(\cos\theta)\\&-\frac{429}{32768}\left(\frac{a}{r}\right)^{15} P_{14}(\cos\theta)\\&+\frac{715}{65536}\left(\frac{a}{r}\right)^{17} P_{16}(\cos\theta)\\&-\frac{2431}{262144}\left(\frac{a}{r}\right)^{19} P_{18}(\cos\theta)\\&+\frac{4199}{524288}\left(\frac{a}{r}\right)^{21} P_{20}(\cos\theta)\end{aligned}\right.$$

[7] Byerly, Fourier's Series, p. 155, art. 80.

Following the notation of Figure 6 in which x is measured positively downward from O, and expressing all variables in (2) in terms of θ,

$$\left.\begin{aligned} \text{n}\ \theta &= \frac{c}{r} \\ \frac{a}{r} &= \frac{a}{c}\sin\theta \\ x &= c\cot\theta \\ dx &= -\frac{cd\theta}{\sin^2\theta} \end{aligned}\right\} \tag{3}$$

and integrating for θ from θ_1 to θ_2 we obtain:

$$V = -2\pi\rho acG\left\{\begin{aligned} &+\frac{1}{2}\frac{a}{c}\int\frac{d\theta}{\sin\theta} \\ &-\frac{1}{8}\left(\frac{a}{c}\right)^3\int\sin\theta.P_2\ (\cos\theta)d\theta \\ &+\frac{1}{16}\left(\frac{a}{c}\right)^5\int\sin^3\theta.P_4\ (\cos\theta)d\theta \\ &-\frac{5}{128}\left(\frac{a}{c}\right)^7\int\sin^5\theta.P_6\ (\cos\theta)d\theta \\ &+\frac{7}{256}\left(\frac{a}{c}\right)^9\int\sin^7\theta.P_8\ (\cos\theta)d\theta \\ &-\frac{21}{1024}\left(\frac{a}{c}\right)^{11}\int\sin^9\theta.P_{10}\ (\cos\theta)d\theta \\ &+\frac{33}{2048}\left(\frac{a}{c}\right)^{13}\int\sin^{11}\theta.P_{12}\ (\cos\theta)d\theta \\ &-\frac{429}{32768}\left(\frac{a}{c}\right)^{15}\int\sin^{13}\theta.P_{14}\ (\cos\theta)d\theta \\ &+\frac{715}{65536}\left(\frac{a}{c}\right)^{17}\int\sin^{15}\theta.P_{16}\ (\cos\theta)d\theta \\ &-\frac{2431}{262144}\left(\frac{a}{c}\right)^{19}\int\sin^{17}\theta.P_{18}\ (\cos\theta)d\theta \\ &+\frac{4199}{524288}\left(\frac{a}{c}\right)^{21}\int\sin^{19}\theta.P_{20}\ (\cos\theta)d\theta \end{aligned}\right. \tag{4}$$

Byerly (p. 151) gives expansions of $P_m(x)$ up to $m=8$. Additional values follow:

$$
\begin{aligned}
P_{10}(x) &= \frac{1}{256}\Big(46189x^{10}-109395x^{8}+90090x^{6}\\
&\quad -30030x^{4}+3465x^{2}-63\Big)\\
P_{12}(x) &= \frac{1}{1024}\Big(676039x^{12}-1939938x^{10}+2078505x^{8}\\
&\quad -1021020x^{6}+225225x^{4}-18018x^{2}\times 231\Big)\\
P_{14}(x) &= \frac{1}{2048}\Big(5014575x^{14}-16900975x^{12}+22309287x^{10}\\
&\quad -14549535x^{8}+4849845x^{6}-765765x^{4}\\
&\quad +45045x^{2}-429\Big)\\
P_{16}(x) &= \frac{1}{32768}\Big(300540195x^{16}-1163381400x^{14}\\
&\quad +1825305300x^{12}-1487285800x^{10}\\
&\quad +669278610x^{8}-162954792x^{6}\\
&\quad +19399380x^{4}-875160x^{2}+6435\Big)\\
P_{18}(x) &= \frac{1}{65536}\Big(2268783825x^{18}-9917826435x^{16}\\
&\quad +18032411700x^{14}-17644617900x^{12}\\
&\quad +10039179150x^{10}-3346393050x^{8}\\
&\quad +624660036x^{6}-58198140x^{4}\\
&\quad +2078505x^{2}-12155\Big)\\
P_{20}(x) &= \frac{1}{262144}\Big(34461632205x^{20}-167890003050x^{18}\\
&\quad +347123925225x^{16}-396713057400x^{14}\\
&\quad +273491577450x^{12}-116454478140x^{10}\\
&\quad +30117537450x^{8}-4461857400x^{6}\\
&\quad +334639305x^{4}-9699690x^{2}+46189\Big)
\end{aligned}
\tag{5}
$$

Making the necessary substitutions in formula (4) we obtain:

$$
\begin{aligned}
V = -2\pi\rho acG\Big[&+\frac{1}{2}\frac{a}{c}\int\frac{d\theta}{\sin\theta}\\
&-\frac{1}{16}\left(\frac{a}{c}\right)^{3}\int\sin\theta\,(3\cos^{2}\theta-1)\,d\theta\\
&+\frac{1}{128}\left(\frac{a}{c}\right)^{5}\int\sin^{3}\theta\,(35\cos^{4}\theta-30\cos^{2}\theta+3)\,d\theta\\
&-\frac{5}{2048}\left(\frac{a}{c}\right)^{7}\int\sin^{5}\theta\,(231\cos^{6}\theta-315\cos^{4}\theta\\
&\qquad +105\cos^{2}\theta-5)\,d\theta\Big]
\end{aligned}
\tag{6}
$$

$$
\begin{aligned}
V = -2\pi\rho acG \Bigg\{ & +\frac{7}{32768}\left(\frac{a}{c}\right)^{9}\int \sin^{7}\theta\,(6435\cos^{8}\theta - 12012\cos^{6}\theta \\
& \qquad + 6930\cos^{4}\theta - 1260\cos^{2}\theta \\
& \qquad + 35)\,d\theta \\
& -\frac{21}{262144}\left(\frac{a}{c}\right)^{11}\int \sin^{9}\theta\,(46189\cos^{10}\theta \\
& \qquad - 109395\cos^{8}\theta \\
& \qquad + 90090\cos^{6}\theta - 30030\cos^{4}\theta \\
& \qquad + 3465\cos^{2}\theta - 63)\,d\theta \\
& +\frac{33}{2097152}\left(\frac{a}{c}\right)^{13}\int \sin^{11}\theta\,(676039\cos^{12}\theta \\
& \qquad - 1939938\cos^{10}\theta \\
& \qquad + 2078505\cos^{8}\theta \\
& \qquad - 1021020\cos^{6}\theta \\
& \qquad + 225225\cos^{4}\theta \\
& \qquad - 18018\cos^{2}\theta + 231)\,d\theta \\
& -\frac{429}{67108864}\left(\frac{a}{c}\right)^{15}\int \sin^{13}\theta\,(5014575\cos^{14}\theta \\
& \qquad - 16900975\cos^{12}\theta \\
& \qquad + 22309287\cos^{10}\theta \\
& \qquad - 14549535\cos^{8}\theta \\
& \qquad + 4849845\cos^{6}\theta \\
& \qquad - 765765\cos^{4}\theta \\
& \qquad + 45045\cos^{2}\theta - 429)\,d\theta \\
& +\frac{715}{2147483648}\left(\frac{a}{c}\right)^{17}\int \sin^{15}\theta\,(300540195\cos^{16}\theta \\
& \qquad - 1163381400\cos^{14}\theta \\
& \qquad + 1825305300\cos^{12}\theta \\
& \qquad - 1487285800\cos^{10}\theta \\
& \qquad + 669278610\cos^{8}\theta \\
& \qquad - 162954792\cos^{6}\theta \\
& \qquad + 19399380\cos^{4}\theta \\
& \qquad - 875160\cos^{2}\theta \\
& \qquad + 6435)\,d\theta \\
& -\frac{2431}{17179869184}\left(\frac{a}{c}\right)^{19}\int \sin^{17}\theta\,(2268783825\cos^{18}\theta \\
& \qquad - 9917826435\cos^{16}\theta \\
& \qquad + 18032411700\cos^{14}\theta \\
& \qquad - 17644617900\cos^{12}\theta \\
& \qquad + 10039179150\cos^{10}\theta \\
& \qquad - 3346393050\cos^{8}\theta \\
& \qquad + 624660036\cos^{6}\theta \\
& \qquad - 58198140\cos^{4}\theta \\
& \qquad + 2078505\cos^{2}\theta \\
& \qquad - 12155)\,d\theta
\end{aligned}
\qquad (6)
$$

$$V=-2\pi\rho acG\left\{+\frac{4199}{137438953472}\left(\frac{a}{c}\right)^{21}\int \sin^{19}\theta\,(34461632205\cos^{20}\theta - 167890003050\cos^{18}\theta + 347123925225\cos^{16}\theta - 396713057400\cos^{14}\theta + 273491577450\cos^{12}\theta - 116454478140\cos^{10}\theta + 30017537450\cos^{8}\theta - 4461857400\cos^{6}\theta + 334639305\cos^{4}\theta - 9699690\cos^{2}\theta + 46189)\,d\theta\right\} \tag{6}$$

Integrating and applying the limits θ_1 and θ_2

$$\begin{aligned}V=-2\pi\rho acG\Bigg\{&+\frac{1}{2}\frac{a}{c}\left[\log\tan\frac{\theta_2}{2}-\log\tan\frac{\theta_1}{2}\right]\\&-\frac{1}{16}\left(\frac{a}{c}\right)^3\left[\cos\theta_2\sin^2\theta_2-\cos\theta_1\sin^2\theta_1\right]\\&+\frac{1}{128}\left(\frac{a}{c}\right)^5\left[5\cos^3\theta_2\sin^4\theta_2-3\cos\theta_2\sin^4\theta_2\right.\\&\left.\quad+\text{similar terms of opposite sign in }\theta_1\right]\\&-\frac{5}{2048}\left(\frac{a}{c}\right)^7\left[21\cos^5\theta_2\sin^6\theta_2-\frac{70}{3}\cos^3\theta_2\sin^6\theta_2\right.\\&\left.\quad+5\cos\theta_2\sin^6\theta_2+\text{etc.}\right]\\&+\frac{7}{32768}\left(\frac{a}{c}\right)^9\left[429\cos^7\theta_2\sin^8\theta_2-693\cos^5\theta_2\sin^8\theta_2\right.\\&\left.\quad+315\cos^3\theta_2\sin^8\theta_2-35\cos\theta_2\sin^8\theta_2+\text{etc.}\right]\\&-\frac{21}{262144}\left(\frac{a}{c}\right)^{11}\left[2431\cos^9\theta_2\sin^{10}\theta_2\right.\\&\left.\quad-5148\cos^7\theta_2\sin^{10}\theta_2+\frac{18018}{5}\cos^5\theta_2\sin^{10}\theta_2\right.\\&\left.\quad-924\cos^3\theta_2\sin^{10}\theta_2+63\cos\theta_2\sin^{10}\theta_2+\text{etc.}\right]\\&+\frac{33}{2097152}\left(\frac{a}{c}\right)^{13}\left[29393\cos^{11}\theta_2\sin^{12}\theta_2\right.\\&\left.\quad-\frac{230945}{3}\cos^9\theta_2\sin^{12}\theta_2+72930\cos^7\theta_2\sin^{12}\theta_2\right.\\&\left.\quad-30030\cos^5\theta_2\sin^{12}\theta_2+5005\cos^3\theta_2\sin^{12}\theta_2\right.\\&\left.\quad-231\cos\theta_2\sin^{12}\theta_2+\text{etc.}\right]\Bigg\}\end{aligned} \tag{7}$$

$$
\begin{aligned}
V = -2\pi\rho acG\Bigg(& -\frac{429}{67108864}\left(\frac{a}{c}\right)^{15}\Big[185725\cos^{13}\theta_2\sin^{14}\theta_2 \\
& -579462\cos^{11}\theta_2\sin^{14}\theta_2+692835\cos^{9}\theta_2\sin^{14}\theta_2 \\
& -\frac{2771340}{7}\cos^{7}\theta_2\sin^{14}\theta_2+109395\cos^{5}\theta_2\sin^{14}\theta_2 \\
& -12870\cos^{3}\theta_2\sin^{14}\theta_2+429\cos\theta_2\sin^{14}\theta_2 \\
& +\text{etc.}\Big] \\
& +\frac{715}{2147483648}\left(\frac{a}{c}\right)^{17}\Big[9694845\cos^{15}\theta_2\sin^{16}\theta_2 \\
& -35102025\cos^{13}\theta_2\sin^{16}\theta_2 \\
& +50702925\cos^{11}\theta_2\sin^{16}\theta_2 \\
& -37182145\cos^{9}\theta_2\sin^{16}\theta_2 \\
& +13718133\cos^{7}\theta_2\sin^{16}\theta_2 \\
& -2909907\cos^{5}\theta_2\sin^{16}\theta_2+255255\cos^{3}\theta_2\sin^{16}\theta_2 \\
& -6435\cos\theta_2\sin^{16}\theta_2+\text{etc.}\Big] \\
& -\frac{2431}{17179869184}\left(\frac{a}{c}\right)^{19}\Big[64822395\cos^{17}\theta_2\sin^{18}\theta_2 \\
& -267146840\cos^{15}\theta_2\sin^{18}\theta_2 \\
& +452426100\cos^{13}\theta_2\sin^{18}\theta_2 \\
& -405623400\cos^{11}\theta_2\sin^{18}\theta_2 \\
& +\frac{1859107250}{9}\cos^{9}\theta_2\sin^{18}\theta_2 \\
& -59491432\cos^{7}\theta_2\sin^{18}\theta_2 \\
& +9053044\cos^{5}\theta_2\sin^{18}\theta_2 \\
& -\frac{1847560}{3}\cos^{3}\theta_2\sin^{18}\theta_2 \\
& +12155\cos\theta_2\sin^{18}\theta_2+\text{etc.}\Big] \\
& +\frac{4199}{137438953472}\left(\frac{a}{c}\right)^{21}\Big[883631595\cos^{19}\theta_2\sin^{20}\theta_2 \\
& -4083810885\cos^{17}\theta_2\sin^{20}\theta_2 \\
& +7934261148\cos^{15}\theta_2\sin^{20}\theta_2 \\
& -8415125460\cos^{13}\theta_2\sin^{20}\theta_2 \\
& +5293385370\cos^{11}\theta_2\sin^{20}\theta_2 \\
& -2007835830\cos^{9}\theta_2\sin^{20}\theta_2 \\
& +446185740\cos^{7}\theta_2\sin^{20}\theta_2 \\
& -\frac{267711444}{5}\cos^{5}\theta_2\sin^{20}\theta_2 \\
& +2909907\cos^{3}\theta_2\sin^{20}\theta_2 \\
& -46189\cos\theta_2\sin^{20}\theta_2+\text{etc.}\Big]
\end{aligned}
\qquad (7)
$$

We must now express all quantities in terms of c and of the constants of the cylinder.

$$\left.\begin{aligned}
&\tan\frac{\theta}{2}=\left[\frac{1-\cos\theta}{1+\cos\theta}\right]^{\frac{1}{2}}\\
&\cos\theta_2=-\frac{l_2}{(c^2+l_2^2)^{\frac{1}{2}}}\ \text{(always negative)}\\
&\sin\theta_2=\frac{c}{(c^2+l_2^2)^{\frac{1}{2}}}\ \text{(always positive)}\\
&\cos\theta_1=\frac{l^1}{(c^2+l_1^2)^{\frac{1}{2}}}\ \text{(always positive)}\\
&\sin\theta_1=\frac{c}{(c^2+l_1^2)^{\frac{1}{2}}}\ \text{(always positive)}\\
&c^2+l_1^2=r_1^2 \qquad\qquad c^2+l_2^2=r_2^2
\end{aligned}\right\}\tag{8}$$

Substituting these values in formula (7):

$$\left.\begin{aligned}
V=-2\pi\rho aG\Bigg\{&+\frac{1}{2}a\log\left[\frac{1-\cos\theta_2}{1+\cos\theta_2}\cdot\frac{1+\cos\theta_1}{1-\cos\theta_1}\right]^{\frac{1}{2}}\\
&=\frac{a}{4}\log\left[\frac{(c^2+l_2^2)^{\frac{1}{2}}+l_2}{(c^2+l_2^2)^{\frac{1}{2}}-l_2}\cdot\frac{(c^2+l_1^2)^{\frac{1}{2}}+l_1}{(c^2+l_1^2)^{\frac{1}{2}}-l_1}\right]\\
&=\frac{a}{4}\Big[\log(r_2+l_2)-\log(r_2-l_2)\\
&\qquad+\log(r_1+l_1)-\log(r_1-l_1)\Big]\\
&+\frac{1}{16}a^3\left[\frac{l_2}{r_2^3}+\frac{l_1}{r_1^3}\right]\\
&+\frac{1}{128}a^5\left[-\frac{5l_2^3}{r_2^7}+\frac{3l_2}{r_2^5}-\frac{5l_1^3}{r_1^7}+\frac{3l_1}{r_1^5}\right]\\
&+\frac{5}{2048}a^7\left[\frac{21l_2^5}{r_2^{11}}-\frac{70l_2^3}{3r_2^9}+\frac{5l_2}{r_2^7}\right.\\
&\qquad\left.+\text{ similar terms in } l_1 \text{ and } r_1\right]\\
&+\frac{7}{32768}a^9\left[-\frac{429l_2^7}{r_2^{15}}+\frac{693l_2^5}{r_2^{13}}-\frac{315l_2^3}{r_2^{11}}\right.\\
&\qquad\left.+\frac{35l_2}{r_2^9}-\text{etc.}\right]\\
&+\frac{21}{262144}a^{11}\left[\frac{2431l_2^9}{r_2^{19}}-\frac{5148l_2^7}{r_2^{17}}+\frac{18018l_2^5}{5r_2^{15}}-\frac{924l_2^3}{r_2^{13}}\right.\\
&\qquad\left.+\frac{63l_2}{r_2^{11}}+\text{etc.}\right]
\end{aligned}\right\}\tag{9}$$

$$
\begin{aligned}
V = -2\pi\rho aG \Bigg\{ & + \frac{33}{2097152}a^{13}\left[-\frac{29393 l_2^{11}}{r_2^{23}} + \frac{230945 l_2^{9}}{3 r_2^{21}} - \frac{72930 l_2^{7}}{r_2^{19}} \right. \\
& \left. + \frac{30030 l_2^{5}}{r_2^{17}} - \frac{5005 l_2^{3}}{r_2^{15}} + \frac{231 l_2}{r_2^{13}} - \text{etc.} \right] \\
& + \frac{429}{67108864}a^{15}\left[\frac{185725 l_2^{13}}{r_2^{27}} - \frac{579462 l_2^{11}}{r_2^{25}} \right. \\
& \qquad + \frac{692835 l_2^{9}}{r_2^{23}} - \frac{2771340 l_2^{7}}{7 r_2^{21}} \\
& \qquad + \frac{109395 l_2^{5}}{r_2^{19}} - \frac{12870 l_2^{3}}{r_2^{17}} \\
& \qquad \left. + \frac{429 l_2}{r_2^{15}} + \text{etc.} \right] \\
& + \frac{715}{2147483648}a^{17}\left[-\frac{9694845 l_2^{15}}{r_2^{31}} + \frac{35102025 l_2^{13}}{r_2^{29}} \right. \\
& \qquad - \frac{50702925 l_2^{11}}{r_2^{27}} + \frac{37182145 l_2^{9}}{r_2^{25}} \\
& \qquad - \frac{14549535 l_2^{7}}{r_2^{23}} + \frac{2909907 l_2^{5}}{r_2^{21}} \\
& \qquad \left. - \frac{255255 l_2^{3}}{r_2^{19}} + \frac{6435 l_2^{2}}{r_2^{17}} - \text{etc.} \right] \\
& + \frac{2431}{17179869184}a^{19}\left[\frac{64822395 l_2^{17}}{r_2^{35}} - \frac{267146840 l_2^{15}}{r_2^{33}} \right. \\
& \qquad + \frac{452426100 l_2^{13}}{r_2^{31}} \\
& \qquad - \frac{405623400 l_2^{11}}{r_2^{29}} \\
& \qquad + \frac{1859107250 l_2^{9}}{9 r_2^{27}} \\
& \qquad - \frac{59491432 l_2^{7}}{r_2^{25}} \\
& \qquad + \frac{9053044 l_2^{5}}{r_2^{23}} - \frac{1847560 l_2^{3}}{3 r_2^{21}} \\
& \qquad \left. + \frac{12155 l_2}{r_2^{19}} + \text{etc.} \right]
\end{aligned}
\qquad (9)
$$

$$V=-\pi\rho aG\left\{+\frac{4199}{137438953472}a^{21}\left[-\frac{883631595l_2^{19}}{r_2^{39}}\right.\right.$$
$$+\frac{4083810885l_2^{17}}{r_2^{37}}$$
$$-\frac{7934261148l_2^{15}}{r_2^{35}}$$
$$+\frac{8415125460l_2^{13}}{r_2^{33}}$$
$$-\frac{5293385370l_2^{11}}{r_2^{31}}$$
$$+\frac{2007835830l_2^{9}}{r_2^{29}}$$
$$-\frac{446185740l_2^{7}}{r_2^{27}}$$
$$+\frac{267711444l_2^{5}}{5r_2^{25}}$$
$$\left.\left.-\frac{2909907l_2^{3}}{r_2^{23}}+\frac{46189l_2}{r_2^{21}}-\text{etc.}\right]\right\} \tag{9}$$

Differentiate with respect to c, noting the following relations:

$$\left.\begin{aligned} r_2&=(c^2+l_2^2)^{\frac{1}{2}}\\ \frac{dr_2}{dc}&=\frac{c}{r_2}\\ \frac{dr_1}{dc}&=\frac{c}{r_1}\end{aligned}\right\} \tag{10}$$

and similarly:

We obtain the following formula for the component of the force of attraction in the direction of c, that is, perpendicular to the axis of the cylinder:

$$F=\frac{dV}{dc}=\pi\rho a^2cG\left\{\frac{l_2}{r_2(r_2^2-l_2^2)}+\frac{l_1}{r_1(r_1^2-l_1^2)}+\frac{3a^2}{8}\left[\frac{l_2}{r_2^5}+\frac{l_1}{r_1^5}\right]\right.$$
$$-\frac{5a^4}{64}\left[\frac{7l_2^3}{r_2^9}-\frac{3l_2}{r_2^7}+\text{similar terms in } l_1 \text{ and } r_1\right]$$
$$+\frac{35a^6}{1024}\left[\frac{33l_2^5}{r_2^{13}}-\frac{30l_2^3}{r_2^{11}}+\frac{5l_2}{r_2^9}+\text{etc.}\right]$$
$$-\frac{63a^8}{16384}\left[\frac{715l_2^7}{r_2^{17}}-\frac{1001l_2^5}{r_2^{15}}+\frac{385l_2^3}{r_2^{13}}-\frac{35l_2}{r_2^{11}}+\text{etc.}\right]$$
$$\left.+\frac{231a^{10}}{131072}\left[\frac{4199l_2^9}{r_2^{21}}-\frac{7956l_2^7}{r_2^{19}}+\frac{4914l_2^5}{r_2^{17}}-\frac{1092l_2^3}{r_2^{15}}\right.\right. \tag{11}$$

$$F=\frac{dV}{dc}=\pi\rho a^2cG\left\{\begin{array}{l}
+\dfrac{63l_2}{r_2^{13}}+\text{etc.}\Big]-\dfrac{429a^{12}}{1048576}\Big[\dfrac{52003l_2^{11}}{r_2^{25}}\\
-\dfrac{124355l_2^{9}}{r_2^{23}}+\dfrac{106590l_2^{7}}{r_2^{21}}-\dfrac{39270l_2^{5}}{r_2^{19}}+\dfrac{5775l_2^{3}}{r_2^{17}}\\
-\dfrac{231l_2}{r_2^{15}}+\text{etc.}\Big]+\dfrac{6435a^{14}}{33554432}\Big[\dfrac{334305l_2^{13}}{r_2^{29}}\\
-\dfrac{965770l_2^{11}}{r_2^{27}}+\dfrac{1062347l_2^{9}}{r_2^{25}}-\dfrac{554268l_2^{7}}{r_2^{23}}\\
+\dfrac{138567l_2^{5}}{r_2^{21}}-\dfrac{14586l_2^{3}}{r_2^{19}}+\dfrac{429l_2}{r_2^{17}}+\text{etc.}\Big]\\
-\dfrac{12155a^{16}}{1073741824}\Big[\dfrac{17678835l_2^{15}}{r_2^{33}}-\dfrac{59879925l_2^{13}}{r_2^{31}}\\
+\dfrac{80528175l_2^{11}}{r_2^{29}}-\dfrac{54679625l_2^{9}}{r_2^{27}}+\dfrac{19684665l_2^{7}}{r_2^{25}}\\
-\dfrac{3594591l_2^{5}}{r_2^{23}}+\dfrac{285285l_2^{3}}{r_2^{21}}-\dfrac{6435l_2}{r_2^{19}}+\text{etc.}\Big]\\
+\dfrac{46189a^{18}}{8589934592}\Big[\dfrac{119409675l_2^{17}}{r_2^{37}}-\dfrac{463991880l_2^{15}}{r_2^{35}}\\
+\dfrac{738168900l_2^{13}}{r_2^{33}}-\dfrac{619109400l_2^{11}}{r_2^{31}}+\dfrac{293543250l_2^{9}}{r_2^{29}}\\
-\dfrac{78278200l_2^{7}}{r_2^{27}}+\dfrac{10958948l_2^{5}}{r_2^{25}}-\dfrac{680680l_2^{3}}{r_2^{23}}\\
+\dfrac{12155l_2}{r_2^{21}}+\text{etc.}\Big]\\
-\dfrac{88179a^{20}}{68719476736}\Big[\dfrac{1641030105l_2^{19}}{r_2^{41}}\\
-\dfrac{7195285845l_2^{17}}{r_2^{39}}+\dfrac{13223768580l_2^{15}}{r_2^{37}}\\
-\dfrac{13223768580l_2^{13}}{r_2^{35}}+\dfrac{7814045070l_2^{11}}{r_2^{33}}\\
-\dfrac{2772725670l_2^{9}}{r_2^{31}}+\dfrac{573667380l_2^{7}}{r_2^{29}}-\dfrac{63740820l_2^{5}}{r_2^{27}}\\
+\dfrac{3187041l_2^{3}}{r_2^{25}}-\dfrac{46189l_2}{r_2^{23}}+\text{etc.}\Big]
\end{array}\right\} \qquad (11)$$

As an illustration of the rapidity with which the series (11) converges, take the following simple case of the attraction of a cylinder upon a point at the middle of its lateral surface:

$$a=c=l_1=l_2=10$$
$$r_2=r_1=10\sqrt{2}$$

Omitting the factor $\pi\rho cG$, the successive terms and their sums are shown in Table 5.

TABLE 5.—*Convergency of series*

Term	Value of term	Sum of series
1	+1.4142136	1.4142136
2	+.1325825	1.5467961
3	−.0069053	1.5398908
4	−.0052869	1.5346039
5	+.0005735	1.5351774
6	+.0005233	1.5357007
7	−.0000708	1.5356299
8	−.0000698	1.5355601
9	+.0000105	1.5355706
10	+.0000108	1.5355814
11	−.0000017	1.5355797

For points farther distant from the axis of the cylinder the convergence is more rapid.

Equation (11) may seem formidable, but it is comparatively simple in practical application. Inspection of the formula shows that, as often happens in series, the first term is apparently anomalous, but that beginning with the second term certain laws are discoverable.

Disregarding for the moment the numerical factors, it will be seen that within the parentheses we have a series of literal terms containing l_2 and r_2 followed by an exactly similar series containing l_1 and r_1. Moreover, as we pass down the terms of the whole equation, we find (still disregarding the numerical factors) that there are certain moduli or multiplying factors by which any term can be converted into the next following. An example will make this clear. Take the second, third, and fourth terms of (11), bringing in the factor a^2 from the general factor $\pi\rho a^2cG$:

$$\left.\begin{array}{ll} +\dfrac{a^4l_2}{r_2^5}; & +\dfrac{a^4l_1}{r_2^5} \\ -\dfrac{a^6l_2^3}{r_2^9}+\dfrac{a^6l_2}{r_2^7}; & -\dfrac{a^6l_1^3}{r_1^9}+\dfrac{a^6l_1}{r_1^7} \\ +\dfrac{a^8l_2^5}{r_2^{13}}-\dfrac{a^8l_2^3}{r_2^{11}}+\dfrac{a^8l_2}{r_2^9}; & +\dfrac{a^8l_1^5}{r_1^{13}}-\dfrac{a^8l_1^3}{r_1^{11}}+\dfrac{a^8l_1}{r_1^9} \end{array}\right\} \quad (12)$$

It will be noticed first that the term heading every column is positive, and that the signs alternate as we go down the column. Moreover, the terms in each column have a common ratio, $\dfrac{a^2l_2^2}{r_2^4}$ or $\dfrac{a^2l_1^2}{r_1^4}$ as the case may be. This ratio may be called the vertical modulus.

There is also a common ratio running diagonally downward and to the right, $\dfrac{a^2}{r_2^2}$ or $\dfrac{a^2}{r_1^2}$, which we may call the diagonal modulus. And there will be consequently a similar horizontal modulus, $\dfrac{r_2^2}{l_2^2}$ or $\dfrac{r_1^2}{l_1^2}$. Hence, given the second literal term, each succeeding literal

term may be constructed by means of the vertical and diagonal moduli and checked by the horizontal modulus; and since each modulus is concerned only with a, r, and l (constants of the cylinder and of the position of the balls), these moduli may be calculated once for all the beginning of the computation.

In addition to these moduli we have the numerical coefficients, unity in the first term, three-eighths in the second, and so on. In the third and later terms we have more than one coefficient. Table 5 gives these coefficients for the first seven terms to a sufficient number of decimal places to secure an accuracy of 1 part in 100,000 in the value of the attraction when $a=10$ cm, $l_1+l_2=28$ cm, and $c=13$ cm, which correspond closely to the actual working conditions.

TABLE 6.—*Working coefficients*

Term	Coefficients					
1						
2	+0.375000					
3	−.546875	+0.234375				
4	+1.12793	−1.02539	+0.17090			
5	−2.7493	+3.8491	−1.4804	+0.13458		
6	+7.400	−14.022	+8.6604	−1.9245	+0.1110	
7	−21.28	+50.88	−43.609	+16.066	−2.363	+0.0945

The steps in the computation of the force of attraction of a finite cylinder at any external point may now be summarized as follows:

1. From a, r_1, r_2, l_1, l_2, and c, calculate the vertical, diagonal, and horizontal moduli.
2. Calculate the first literal term of (11).
3. Calculate the second literal term of (11).
4. By means of the moduli calculate the succeeding literal terms (exclusive of the numerical factors).
5. Complete the calculation by applying to the literal terms the proper numerical factors from Table 6.

2. FORMULA FOR TIME OF SWING

We have to deal with a torsion pendulum swinging in a nonuniform but symmetrical gravitational field, the axis of symmetry, in the near position of the masses, coinciding with the axis of the moving system, and in the far position being at right angles to this axis. Were the field uniform and parallel the formula for the time of swing would be

$$T=2\pi\sqrt{\frac{I}{\tau+\Sigma(FR)}} \tag{13}$$

in which I is the moment of inertia of the moving system and $\tau+\Sigma(FR)$ the restoring moment per unit angular displacement. In this latter expression τ is the part contributed by the modulus of torsion of the filament and $\Sigma(FR)$ the part arising from the gravitational field.

It might be thought that the effect of the nonuniformity of the gravitational field would disappear in the reduction of the time of

swing to zero amplitude. As a matter of fact, such a procedure gives a value of the constant of gravitation about 60 per cent too great. As will shortly be shown we must substitute for R in (13) the quantity $R(1+R/c)$ in the near position, where R/c is approximately 10/13, and in the far position a much more complicated factor is necessary. We, therefore, have instead of $\Sigma(FR)$ in (13) a quantity $\Sigma(FK)$, where K is a more or less complicated function of R, and the working formula for the time of swing becomes:

$$T=2\pi\sqrt{\frac{I}{\tau+\Sigma(FK)}} \quad (14)$$

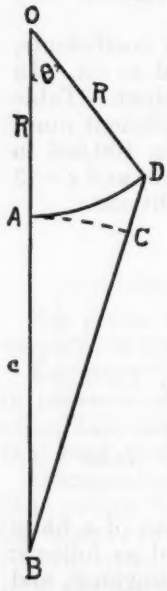

FIGURE 7.—*Close ball plan, near position*

This equation, together with the factors K for the near and the far position, may be derived as follows. We assume the cylinder axes parallel and vertical. Figures 7 and 8 show sections perpendicular to the axis of the cylinder. In these figures let

B = axis of cylinder.
O = center of rotation of ball.
A = neutral position of ball when $\theta=0$.
D = displaced position of ball.
c = distance between centers of ball and cylinder in neutral position of ball = AB.

For the near position and for the ball close to the cylinder (fig. 7):

$$BD=[(OA+AB)^2+\overline{OD}^2$$
$$-2(OA+AB)OD\cos\theta]^{\frac{1}{2}}$$
$$=[(R+c)^2+R^2-2(R+c)R\cos\theta]^{\frac{1}{2}}$$
$$=c\left[1+\frac{2R}{c}\left(1+\frac{R}{c}\right)(1-\cos\theta)\right]^{\frac{1}{2}}$$

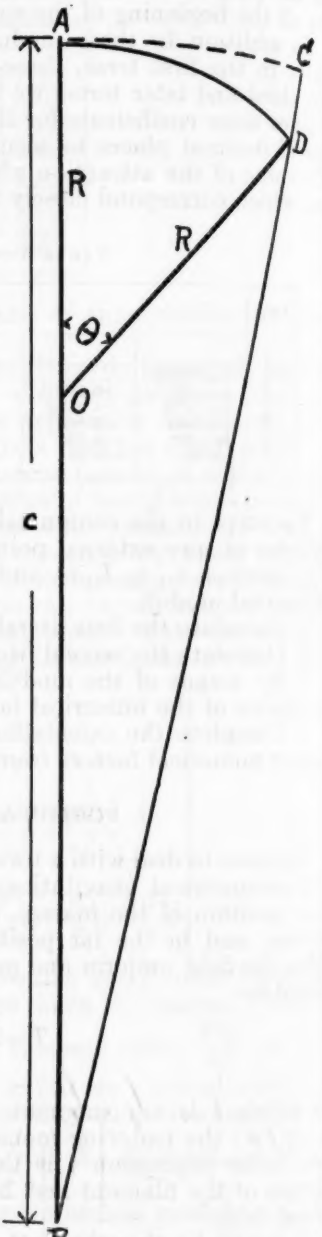

FIGURE 8.—*Distant ball plan, near position*

Expanding by the binomial theorem:

$$BD = c\left[1+\frac{R}{c}\left(1+\frac{R}{c}\right)(1-\cos\theta) - \frac{1}{2}\frac{R^2}{c^2}\left(1+\frac{R}{c}\right)^2(1-\cos\theta)^2+\cdots\cdots\right]$$

$$DC = BD - BC = BD - c$$

$$= c\left[\frac{R}{c}\left(1+\frac{R}{c}\right)(1-\cos\theta) - \frac{1}{2}\frac{R^2}{c^2}\left(1+\frac{R}{c}\right)^2(1-\cos\theta)^2+\cdots\right]$$

When θ is small

$$1-\cos\theta = \frac{\theta^2}{2};\quad (1-\cos\theta)^2 = \frac{\theta^4}{4}$$

Neglecting small terms involving the fourth and higher powers of θ:

$$L = \text{Lift} = DC = c\left[\frac{1}{2}\frac{R}{c}\left(1+\frac{R}{c}\right)\theta^2\right] \tag{15}$$

Let F_0 denote the force of attraction upon the ball at A, and F_θ that upon the ball when at D. The force F will be a function of the distance BD between centers of cylinder and ball, though not exactly proportional to $1/BD^2$, since the cylinder is not barycentric. This variable distance BD will differ slightly from the small quantity $DC = L$ by the constant c; hence $d(BD) = dL$.

Expand F_θ as a function of BD by Taylor's theorem:

$$F_\theta = F_0 + L\frac{dF}{dL} + \frac{L^2}{2}\frac{d^2F}{dL^2} + \text{-------}$$

$$= F_0[1 + VL + V_1L^2 + \text{-----}]$$

in which

$$V = \frac{1}{F_0}\frac{dF}{dL} \text{ and } V_1 = \frac{1}{2F_0}\frac{d^2F}{dL^2}$$

Since F decreases with increase of BD, $\frac{dF}{dL}$ is negative; and since the rate of decrease of F diminishes with increase of BD (the F curve being concave upward) $\frac{d^2F}{dL^2}$ is positive. The usual values for these quantities were about -0.07 for V and $+0.0015$ for V_1. We shall find it convenient to write:

$$\text{Force at } D = F_\theta = F_0[1 - VL + V_1L^2 + \text{----}]$$

considering both V and V_1 as positive. For the case of the close ball which we are considering L is also positive.

As the ball passes from A to D its differential increase in potential energy will be:

$$F_\theta dL = F_0[dL - VLdL + V_1L^2dL + \text{----}]$$

For the small angle θ and the small change in BD contemplated V and V_1 will vary but little. Integrating the last equation we obtain:

$$\text{Potential energy} = F_0\left[L - \frac{1}{2}VL^2 + \frac{1}{3}V_1L^3\right]$$

Applying (15):

$$\text{Potential energy} = F_0\left[\frac{c}{2}\left\{\frac{R}{c}\left(1+\frac{R}{c}\right)\right\}\theta^2\right] + \text{------}$$

$$= \frac{1}{2}F_0R\left(1+\frac{R}{c}\right)\theta^2 \tag{16}$$

For the distant ball (fig. 8) proceeding similarly:

$$BD = c\left[1 - \frac{2R}{c}\left(1-\frac{R}{c}\right)\left(1-\cos\theta\right)\right]^{\frac{1}{2}}$$

Expanding and neglecting small terms:

$$BD = c\left[1 - \frac{R}{c}\left(1-\frac{R}{c}\right)(1-\cos\theta)\right]$$

$$DC = BD - c$$

$$= c\left[-\frac{R}{c}\left(1-\frac{R}{c}\right)(1-\cos\theta)\right]$$

$$L = \text{Lift} = DC = -c\left[\frac{1}{2}\frac{R}{c}\left(1-\frac{R}{c}\right)\theta^2\right]$$

$$\text{Force at } D = F_\theta = F_0[1 - VLdL + V_1L^2dL]$$

in which V and V_1 are considered positive and, for the distant ball, L is negative.

$$d\ (\text{potential energy}) = F_\theta dL = F_0[dL - VLdL + V_1L^2dL]$$

$$\text{Potential energy} = F_0\left[L - \frac{1}{2}VL^2 + \frac{1}{3}V_1L^3\right]$$

$$= F_0\left[-\frac{1}{2}c\,\frac{R}{c}\left(1-\frac{R}{c}\right)\theta^2\right]$$

$$= -\frac{1}{2}F_0R\left(1-\frac{R}{c}\right)\theta^2 \tag{17}$$

Since (16) and (17) are identical except for sign of R, we may regard R as positive for the close ball and negative for the distant ball, and

with this understanding write for the potential energy of a cylinder-ball system in the near position:

$$+\frac{1}{2}F_0R\left(1+\frac{R}{c}\right)\theta^2 \tag{18}$$

A typical case of the values which (18) may give may be cited from the platinum ball set. Denoting the two cylinders by E and W, the ball close to cylinder E by A and the ball close to cylinder W by B, we have:

$$EA = +228179G\theta^2$$
$$EB = -19417G\theta^2$$
$$WA = -19562G\theta^2$$
$$WB = +233141G\theta^2$$

The far position is illustrated in Figures 9 and 10, in which the letters have the same meaning as in Figures 7 and 8. By the close ball

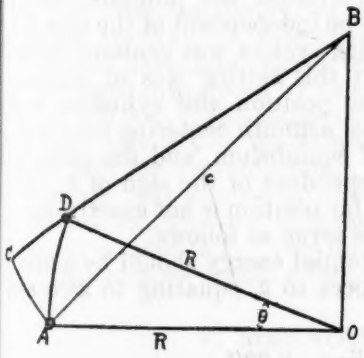

FIGURE 9.—*Close ball plan, far position*

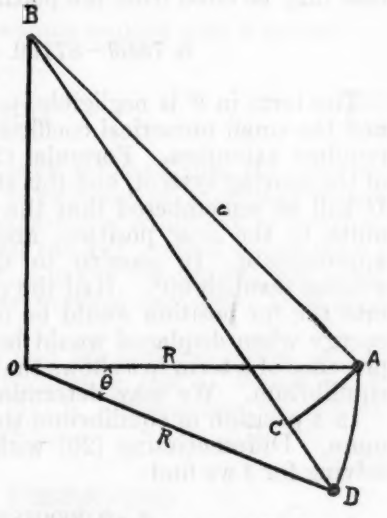

FIGURE 10.—*Distant ball plan, far position*

in this case is meant that ball which is swinging from A to D toward the cylinder at B. Proceeding as in the near position, but keeping terms including θ^3, we find for the potential energy of the system including both cylinders and both balls:

$$\text{Potential energy} = -\Sigma\left[F_0R\left(1-\frac{R^2}{c^2}\right)^{\frac{1}{2}}\right]\theta$$
$$-\frac{1}{2}\Sigma\left[F_0\left(\frac{1+Vc}{c}\right)R^2\left(1-\frac{R^2}{c^2}\right)\right]\theta^2 \tag{19}$$
$$-\frac{1}{2}\Sigma\left[F_0\left(\frac{1+Vc+\frac{2}{3}V_1c^2}{c^2}\right)R^3\left(1-\frac{R^2}{c^2}\right)^{\frac{3}{2}}\right]\theta^3$$

Each sum consists of four terms, of signs determined as follows. θ is always assumed positive, the two cylinders are designated as N and S (having now been turned 90° from the near position), the ball close to the N cylinder is called A and the ball close to the S cylinder B, the term close being used in the sense defined above. The signs of the different terms within the summation are given in Table 7.

TABLE 7.—*Signs of terms in formula (19)*

Term	Coefficient of θ	Coefficient of θ^2	Coefficient of θ^3
NA	+	+	+
NB	−	+	−
SA	−	+	−
SB	+	+	+

In formula (19) the most important term is that in θ^2. A typical case may be cited from the platinum ball set.

$$6.78G\theta - 87199.42G\theta^2 + 64.63G\theta^3 \tag{20}$$

The term in θ^3 is negligible, jointly because of the small value of θ and the small numerical coefficient, but the presence of the term in θ requires attention. Formula (20) represents the potential energy of the moving system, and this should be independent of the sign of θ. It will be remembered that the moving system was centered in azimuth in the near position, and that this setting was of necessity approximate. In passing to the far position the cylinders were rotated through 90°. Had the original azimuth centering been accurate the far position would be one of equilibrium, and the potential energy when displaced would be independent of the sign of θ. The presence of a term in θ shows that the far position is not exactly one of equilibrium. We may determine this error as follows.

In a position of equilibrium the potential energy should be a maximum. Differentiating (20) with respect to θ, equating to zero and solving for θ we find:

$$\theta = 0.00003888 \text{ radian} = 8.02''$$

This correction is so small that we might feel justified in dropping the term in θ at once; but to confirm this impression we substitute in (20) for θ the corrected value $\theta + 0.00003888$, and we find that the coefficient of θ now becomes zero as it should, while the coefficient of θ^2 is 87199.40, very near the value in (20). In consequence we have to consider in the far position as well as in the near only the term in θ^2.

The formula for the time of swing (14) may now be derived. For any displacement θ from the equilibrium point:

Kinetic energy of pendulum + potential energy due to filament + potential energy of attraction = constant. (21)

Let I = moment of inertia of pendulum.

τ = modulus of torsion of filament (moment required to give the beam an angular displacement of one radian)

and (21) becomes:

$$\frac{I}{2}\left(\frac{d\theta}{dt}\right)^2+\frac{1}{2}\tau\,\theta^2+\frac{1}{2}\,\Sigma\,(FK)\,\theta^2=\text{constant}$$

By reference to (16) and (17) we see that the values of K for the close and the distant balls in the near position are respectively

$$R\left(1+\frac{R}{c}\right) \text{ and } -R\left(1-\frac{R}{c}\right)$$

In the far position we find the values of K by reference to (19) and Table 7.

Differentiating and reducing:

$$\frac{d^2\theta}{dt^2}+\frac{\tau+\Sigma\,(FK)}{I}\,\theta=0 \qquad (22)$$

an equation of the usual form for harmonic motion with a period:

$$T=2\pi\sqrt{\frac{I}{\tau+\Sigma\,(FK)}} \qquad (14)$$

In the foregoing derivation it has been assumed that the cylinder axes are vertical. A more general calculation of a similar nature for inclined axes shows that if the inclination of either axis is less than 15′ the error introduced by considering the axis vertical is less than 1 part in 100,000. The actual inclination in any experiment was much less than this, hence the formulas for vertical axes have been used throughout the computations.

Formula (14) applied to the near and far positions gives us two equations for the two unknown quantities τ and G, which latter quantity appears in F. (See formula (11).) Eliminating τ from these two equations we obtain a formula for G.

V. METHOD OF OBSERVING

1. CENTERING ADJUSTMENTS

In the foregoing discussion it is assumed that the center of rotation of the moving system is at the middle point of a straight line joining the axes of the cylinders. The fulfilling of this condition requires three centering adjustments, azimuth, longitudinal and transverse, as indicated in Figure 11. These adjustments are best made in the near position of the cylinders.

The azimuth adjustment was made by observing the time of swing at various angular settings of the cylinders. If the moving system is centered transversely, the curve of time of swing against azimuth will have a single minimum. If the transverse adjustment is sufficiently off two minima will be present.

A typical azimuth centering curve is shown in Figure 12. Such curves were usually characterized by a rather broad and flat minimum; a well-marked double minimum was rare. The minimum

point is best determined by means of pairs of points on the steep slopes, and could usually be fixed to one or two tenths of a degree. So flat is the minimum that such an accuracy is quite sufficient.

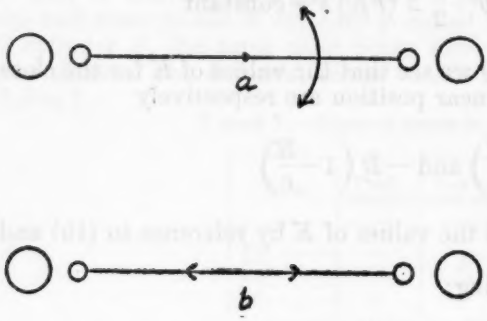

FIGURE 11.—*Centering adjustments*
a, Azimuth; *b*, longitudinal; *c*, transverse.

Having made a first adjustment for azimuth, the next step was to adjust transversely. This adjustment might have been made by direct observation of the filament, but it was more convenient to work by time of swing. The desired point is marked here, as in azimuth, by a minimum or, in case the azimuth centering is out, by a double minimum.

The longitudinal setting was made by observing the filament through windows in the chimney. The curve for time of swing in this case would be characterized by a maximum. Such a curve was actually obtained as a check, but the maximum was so very flat that it was impossible to locate the desired point in this way within several millimeters.

After a first adjustment of all three kinds, the azimuth and transverse settings were repeated, sometimes twice. The longitudinal adjustment, having a very flat maximum, required little precision.

Theoretically, no further adjustment would be required in the far position. The new azimuth could be set by the scale and vernier to 0.1°, a precision equal to that obtainable by centering. As to the other adjustments, a little consideration will show that the maximum or minimum must be much flatter than in the near position, and that these adjustments consequently require less precision in the far than in the near position.

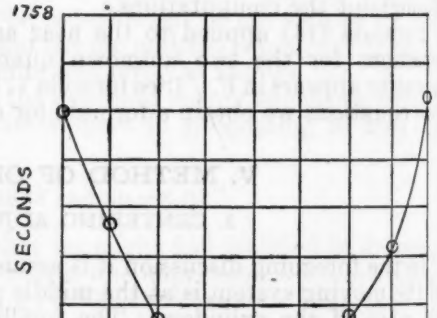

FIGURE 12.—*Azimuth centering curve*

In practice the transverse and longitudinal adjustments were made by moving the sliding dovetailed blocks which held up the beam *B*.

(Fig. 3.) Such shifts of course necessitated further shifts for correction of the transverse and longitudinal adjustments after turning the cylinders into the far position. To provide for this the dovetailed blocks carried millimeter scales by means of which it was possible to recover the center promptly.

2. LENGTH MEASUREMENTS

(a) HORIZONTAL

The horizontal measurements necessary were: (1) Distance between centers of balls, and (2) distance between axes of cylinders. From these may be calculated the distances from centers of balls to axes of the two cylinders, the quantity c entering into the formula for the force of attraction. In practice the second of these measurements was replaced by the distance between the nearest elements of the surfaces of the cylinders. This, in conjunction with the radii of the cylinders, gave the desired quantity.

The distance between centers of balls had to be measured with the lid of the container lifted. This measurement was therefore made twice, before the container was closed and again, some months later, at the conclusion of the campaign, when the container was reopened. In measuring this distance the microscopes of the optical compass were sighted on the tungsten filaments by which the balls were suspended, and at a point as far above the balls as possible (about 3 cm). Settings were made on both sides of the filament (diameter 0.025 mm) and the mean value assumed to represent the point of suspension, vertically above the center of gravity of the ball.

The distance between cylinders was the most troublesome and time consuming of all the length measurements. The first thing was to set the cylinders with their axes approximately vertical. To prevent swaying of the cylinders a small block of aluminum weighing about 1 g was placed between container and cylinders at the bottom of the latter and fastened in place by a little wax. Similar blocks were attached to the container at points 90° from the first blocks, to be used in the far position of the cylinders. In changing the position of the cylinders the blocks were left in place, and consequently played no part in the computation.

The cylinders thus fixed at the bottom were adjusted by the turnbuckles guided by a small plumb bob with a fine thread. Calculation showed that a variation of 15′ from the vertical was allowable with a precision of 1 part in 100,000, and the actual error was always much less than this.

Direct sighting of the microscopes tangentially upon the surface of the cylinders being impracticable, the following device was found to give satisfactory results.

In a piece of straight brass rod about 1.5 mm in diameter there was inserted the point of a fine steel needle. (Fig. 13.) This rod was let down into the space between the container and one of the cylinders, and supported by a screw passing through a heavy piece of brass which, in its turn, was supported by a block of wood fastened temporarily with wax to the lid of the container. A similar arrangement was provided for the other cylinder. Brass rods of two different lengths were provided in order that the distance between the cylinders might be measured near the upper and lower ends.

In order to record and reproduce the position of the brass rod each wooden block was provided on the top with a short piece of paper scale across which lay the piece of metal supporting the brass rod.

It was not difficult to adjust the needle perpendicular to the line of sight with sufficient accuracy. The magnifying power of the microscope was such that any serious departure in this respect showed itself at once by an impairment of focus at the ends of the needle, and the apparent change of length being a cosine function the adjustment was one which did not require the highest precision.

The needle was first hung a little distance from the cylinder so that its point was visible, and a sighting mark sought on the needle some little distance back of the point. If there was no slight irregularity available on the needle one was made by a slight touch of a file. The distance from this sighting mark to the point of the needle (in terms of turns of the micrometer) was recorded for each needle immediately before use.

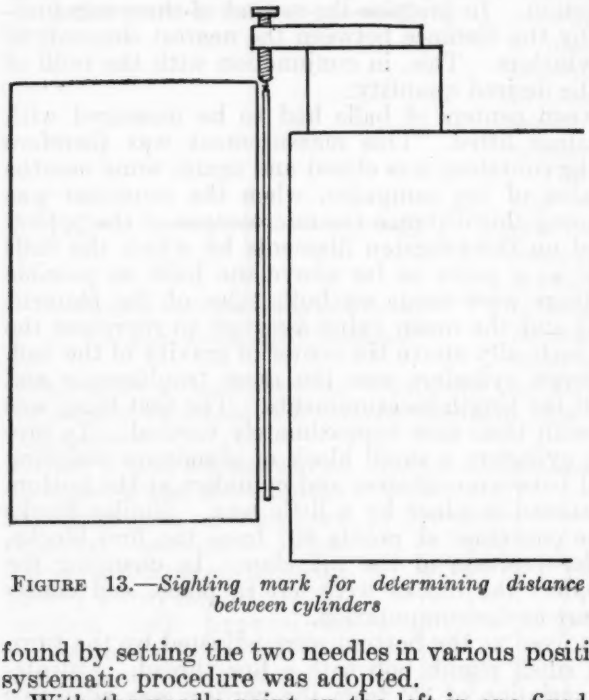

FIGURE 13.—*Sighting mark for determining distance between cylinders*

The needle points were now placed in contact with the cylinders at a determined level and settings made upon the sighting marks.

The distance required is evidently the minimum distance that can be found by setting the two needles in various positions. The following systematic procedure was adopted.

With the needle point on the left in one fixed position the one on the right was moved step by step along the paper scale until a minimum reading was obtained. It was not difficult to obtain a symmetrical set of readings in this way. An example is given in Table 8.

TABLE 8.—*Determination of minimum distance*

Left needle	Right needle	Distance
		cm
18.3	15.5	27.8527
18.3	15.6	27.8484
18.3	15.7	27.8476
18.3	15.8	27.8485
18.3	15.9	27.8530

Such a series of measurements could usually be repeated with an accuracy better than 0.001 cm.

Having located a minimum on one side in this way the needle was set at this place and a minimum sought with the other needle. After having found this, a second setting for minimum was again made on each side, resulting usually in a very small correction.

As a check of this method the diameter of one of the cylinders was measured at several places. The mean agreed with that obtained by the weights and measures division of the bureau to 5 μ.

(b) VERTICAL

The vertical measurements necessary were those involved in the relative positions of centers of balls and tops of cylinders, the inclination of the aluminum rod to the horizontal and the altitude of the triangular truss. (Fig. 4.) These measurements were made with a kathetometer to a precision of about 0.1 mm. For the relative level of balls and cylinder tops measurements were taken through the windows in the container at the conclusion of each determination of time of swing. For the other two measurements, observations were made with the lid of the container lifted.

3. TIME MEASUREMENTS

In making measurements of the time of swing the general plan used by Braun was followed.

On the day before a series of time observations was intended the resting point of the moving system was adjusted so as to lie as near as possible to the 12.5 cm mark. On the observing day the initial resting point was noted and the pendulum started swinging by means of the mercury bottles. Since the swings always passed off the scale, the successive amplitudes were watched and controlled by observing the speed with which the centimeter containing the resting point passed the cross wire of the telescope. The amplitudes of any two successive swings are proportional to the central speeds preceding (or following) the peak of the swing.

The multiplying factor in this case was determined by observations made on swings small enough to allow direct measurements of the amplitude. The results are given in Table 9. In this table the central speed is the speed at which the image of the scale passed the cross wire of the observing telescope, and the amplitude is that of the deflection of the image of the scale.

TABLE 9.—*Relation between amplitude and central speed*

Scale reading in centimeters	Resting point	Central speed	Amplitude	Amplitude / Speed
		cm/min.	*cm*	
4.68		1.11	6.32	5.7
16.93	11.00	1.02	5.93	5.8
5.44	11.04	.97	5.60	5.8
16.22	11.01	.92	5.21	5.7
6.15	11.01	.86	4.86	5.7
15.51				Mean.. 5.7

It was found possible to bring up the central speed to about 9 cm/min. in about two hours by repeated changing of the positions of the mercury bottles. This speed corresponds to an amplitude of about 51 cm. Since the radius of the reflected ray was about 350 cm this amplitude corresponded to an angular deflection of about 4°. The actual amplitudes employed in the measurements ranged from something near this figure at starting to perhaps 1½° at the end of a day's observing.

Having obtained the desired initial amplitude the mercury bottles were removed, the temperature and pressure within the container noted, and the apparatus room darkened. The observer then took his seat at the telescope in the observing room and observed 24 successive transits, recording on the chronograph the time of transit of each millimeter mark from 11.0 to 14.0 cm. This required six hours in the near position and seven in the far position, during which time the observer remained in the same place.

By the time the observations were finished the central speed had diminished to about one-third of its initial value. If the final speed was slow, it was difficult to time the transits accurately; if, on the other hand, the initial speed was too high a large reduction to zero amplitude had to be made in the subsequent computation. Such a reduction involves an extrapolation which it is desirable to keep as small as possible. These two modes of procedure, high and low initial speeds, were both used, the initial speeds with the glass ball set being about 10 per cent higher than those with the platinum balls.

The form of the amplitude-time curve for the pendulum was not strictly that of the form $y=Ae^{-bt}\sin ct$, and because the pendulum moved in a nonuniform gravitational field and because of the damping factor, was not exactly isochronous. This difference amounted at most to about 1 part in 3,000. Strictly speaking, the method of reduction employed by Braun and in the present work is not applicable to a nonisochronous curve of this description, but the departure from isochronism was so small and the damping factor so nearly unity that it was found that results sufficiently accurate could be obtained in the manner about to be described.

The first step was the determination of the damping factor. By inspection of the chronograph records the middle point of a swing could be approximately located as the point where the intervals between consecutive transits were equal. At this point of the scale the ratio of the central speeds for any two successive swings in the same direction gave the damping factor. This proved to be about 0.9, and was very nearly constant throughout any given day's run. The absolute value of this factor varied from day to day with variations of pressure in the container, being in fact a far more sensitive indicator of change of pressure than the manometer. The constancy of the damping factor for any given run showed that the successive amplitudes of the curve followed a geometrical progression.

The second step was a more accurate location of the middle point of the swings. This can be done with considerable precision by the procedure indicated in Table 10. In this table the column headed II contains the difference of the numbers in columns 2.5 and 1.5. Where the numbers in Column II change sign is the middle point, and from this column four values of the middle point are obtainable, interpolating between scale readings 12.2 and 12.3; 12.1 and 12.4;

12.0 and 12.5; 11.9 and 12.6. These four values are set down below Column II, and their mean, 12.265, is taken as representing the middle point during swings 1 and 2. Similarly, swings 2 and 3 yield the almost identical value 12.269.

Any large departure from isochronism would bring about a considerable difference in the two middle points just calculated. Middle points later in the series, where the departure from isochronism is less, would show less and less difference.

It was customary to calculate the middle point only at the beginning and end of a run, as indicated in Table 10. It will be seen that in this case there has been a drift of the middle point amounting to 0.13 cm during the day's observations. Where the drift was as small as this it was customary to interpolate linearly between the initial and final values to obtain the middle points throughout the run; but if there was any suspicion of irregularity or sudden change this calculation was repeated all through the series.

TABLE 10.—*Calculation of middle point*

Scale	1.5 (2–1)	2.5 (3–2)	3.5 (4–3)	21.5 (22–21)	22.5 (23–22)	23.5 (24–23)
11.9	17 25.7	17 15.7	17 26.5	17 40.0	16 59.6	17 42.7
12.0	24.5	17.0	25.0	35.8	17 04.2	38.2
.1	23.1	18.4	23.5	32.0	08.4	34.0
.2	21.8	19.8	21.9	28.4	12.5	29.2
.3	20.3	21.4	20.4	24.4	16.7	24.8
.4	19.0	22.8	18.8	20.2	20.7	20.9
.5	17.6	24.2	17.4	16.2	25.0	16.5
.6	16.3	25.6	15.9	12.4	29.0	12.3
.7	14.9	27.0	14.3	08.7	32.9	08.2
.8	13.6	28.4	12.9	04.8	36.9	03.9
12.9	12.3	29.7	11.4	00.7	41.1	16 59.1

II (2.5–1.5)	III (3.5–2.5)	Scale	XXII (22.5–21.5)	XXIII (23.5–22.5)
−10.0	+10.8	11.9	−40.4	+43.1
−7.5	+8.0	12.0	−31.6	+34.0
−4.7	+5.1	.1	−23.6	+25.6
−2.0	+2.1	.2	−15.9	+16.7
+1.1	−1.0	.3	−7.7	+8.1
+3.8	−4.0	.4	+0.5	+0.2
+6.6	−6.8	.5	+8.8	−8.5
+9.3	−9.7	.6	+16.6	−16.7
+12.1	−12.7	.7	+24.2	−24.7
+14.8	−15.5	.8	+32.1	−33.0
+17.4	−18.3	12.9	+40.4	−42.0
12.265	12.268		12.394	12.402
.266	.268		.393	.398
.266	.270		.394	.402
.263	.269		.396	.406
			.401	.403
12.265	12.269		12.396	12.402

Mean.....12.27 12.40

The third step was the application of sinusoidal corrections. In a curve of the form $y = Ae^{-bt} \sin ct$, to which the actual curve closely approximates (fig. 14), the period can be found by the interval between intersections with the axis Ot, for which the amplitude $y = 0$, but not from intersections with any other line parallel to Ot, such as a_1 a_2. The point a_2 must be brought down to its proportionate level a_3 by the application of the damping factor, after which the period may be

found by the difference between the values of t for a_1 and a_3. In this way values of the period may be obtained for every recorded transit of a mark on the scale, whether at the middle point or not, and a mean value of considerable precision obtained.

From 24 transits we may thus obtain 22 values of the period, corresponding to steadily decreasing amplitudes of the curve. Of these periods, 11 are obtained from transits occuring on up slopes of the curve and 11 on down slopes. Theoretically, in a sinusoid these two slopes differ slightly in form, and, consequently, the periods derived from the two slopes will differ slightly. For this reason the 22 periods were reduced to 11 by taking means of consecutive pairs of up and down values of the period.

After correction of these 11 values for damping they were reduced to zero amplitude. For this purpose an equation was used which involved the second power of the amplitude. From the 11 values of the period normal equations were set up, and solved for the reduced time of swing.

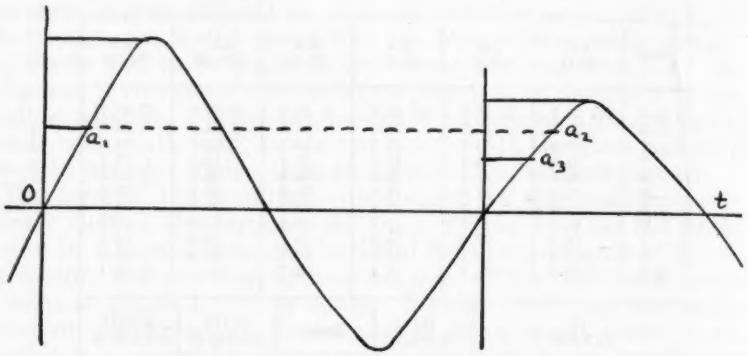

FIGURE 14.—*Sinusoidal correction*

The time of swing in the near position was usually about 1,754 seconds and in the far position about 2,081 seconds, and each could be measured with a precision of about 0.1 second. The difference, 327 seconds, formed the critical quantity of the whole measurement, and may be presumed accurate to about 1 part in 3,300. It was gratifying to find that the average departure from the mean in each of the two best sets of observations (with the platinum and the glass balls) proved to be of this magnitude.

VI. COMPUTATIONS

No useful purpose would be served in reproducing here the computations involved in obtaining the results, as these details would be of interest only to some one planning to repeat the work. The complete computations, covering about 1,000 folio sheets, and the original notebooks are preserved at the library of the Bureau of Standards.

It may, however, be of general interest to see the relative importance of the attraction due to the different moving parts of the apparatus. Table 11 summarizes these attractions for a typical case in the near

position, and Table 12 does the same for the far position. The figures quoted are for one of the experiments with platinum balls. The numbers given represent the contributions of the different moving parts to the quantity $\Sigma (FK)$ in formula (14). The force due to the balls is, of course, the preponderating factor, being about 99 per cent of the whole. The next largest figure is that due to the aluminum rod, less than 1 per cent of the total.

TABLE 11.—*Partial values of* $\Sigma (FK)$ *in the near position*

Attraction of both cylinders on moving parts named		
Parts	Attraction	
Balls	419, 215G	
Aluminum rod	2, 714G	
Copper truss	245G	
Copper in bar	14G	
Copper hooks	10G	
Tungsten in moving system	6G	
Mirror	2G	
		422, 206G
Attraction of other fixed parts on balls		
Supporting rods	87G	
Lower nuts	8G	
Turnbuckles	0	
Disks	6G	
Upper nuts	0	
Beam	5G	
		106G
Total		422, 312G

TABLE 12.—*Partial values of* $\Sigma (FK)$ *in the far position*

Attraction of both cylinders on moving parts named		
Parts	Attraction	
Balls	−174, 399G	
Aluminum rod	−1, 608G	
Copper truss	−146G	
Copper in bar	−6G	
Copper hooks	−4G	
Tungsten in moving system	−4G	
Mirror	−2G	
		−176, 169G
Attraction of other fixed parts on balls		
Supporting rods	−44G	
Lower nuts	−8G	
Turnbuckles	0	
Disks	−4G	
Upper nuts	0	
Beam	−4G	
		−60G
Total		−176, 229G

VII. RESULTS

1. GOLD BALLS

It has already been stated in the description of the small masses that trouble was encountered by reason of the gold balls absorbing mercury vapor during the seven months' period occupied by the observations. The total increase in mass of the balls is shown in Table 13.

TABLE 13.—*Mass of gold balls in vacuo*

Date	Ball A	Ball B
Nov. 15, 1924	48.9688	48.9847
June 15, 1925	49.1067	49.1164
Increase	.1379	.1317

The actual observations for time of swing were all grouped rather closely together during the last half of this period. The balls were weighed initially on November 15, 1924, and placed in position in the apparatus, which was then closed and exhausted of air. The centering operations required some time and other delays ensued. As a consequence, the first actual measurement of time of swing was made on March 12, 1925. Seven swings were made in all, alternately in the near and the far positions, the final swing occurring on June 8, 1925. The apparatus was opened and the balls reweighed on June 15, 1925.

The average time that elapsed between swings was two weeks. If we assume the absorption of mercury to have proceeded regularly during the whole seven months, the increase in two weeks would be about 0.01 g. for each ball, or about one-twentieth of 1 per cent. If we assume also that the mercury penetrated the gold balls with spherical symmetry (which from the final appearance of the balls seems reasonable) we may interpolate for the mass of the balls at any period of observation without introducing an error of more than perhaps 1 part in 10,000.

Calculation shows that an error of this magnitude in the mass of the balls will give rise to an error of about 4 parts in 10,000 in the value of G. It was, therefore, thought worth while to compute the results for the gold ball set on the basis of the assumptions that have been mentioned. The results are shown in Table 14.

TABLE 14.—*Constant of gravitation derived from experiments with gold balls*

	6.683×10^{-8}
	6.681×10^{-8}
	6.676×10^{-8}
	6.678×10^{-8}
	6.679×10^{-8}
	6.672×10^{-8}
Mean	6.678×10^{-8}
Average departure from mean	.003

2. PLATINUM BALLS

To avoid the difficulty of mercury absorption a second set of measurements was made with platinum balls coated thinly with

lacquer. The balls were weighed initially on October 10, 1925, and finally on November 17, 1926. The initial weight was that of ball and hook; the final weight included such portion of the tungsten filament as was wrapped around the hook, together with the trace of wax that held it in place. The final weight was used in the computations. The results obtained are shown in Table 15.

TABLE 15.—*Masses in vacuo of platinum balls*

Date	Ball A	Ball B
Oct. 10, 1925	50.7146	50.7271
Nov. 7, 1926	50.7162	50.7297

Five values of the constant of gravitation were obtained from this set-up, shown in Table 16.

TABLE 16.—*Constant of gravitation derived from experiments with platinum balls*

	6.661×10^{-8}
	6.661×10^{-8}
	6.667×10^{-8}
	6.667×10^{-8}
	6.664×10^{-8}
Mean	6.664×10^{-8}
Average departure from mean	.002

3. GLASS BALLS

A third set of experiments was made with balls of optical glass, of density 3.6. These balls, like those of metal, had a mass of approximately 50 g, and, consequently, a diameter of about 3 cm. The balls were made with a finely ground finish and were truly spherical to 0.001 cm.

The masses of the balls are given in Table 17.

TABLE 17.—*Masses of glass balls in vacuo*

	Ball A	Ball B
Ball with hole empty	51.1578	51.1531
Ball with hook, filament and wax	51.2270	51.2324

The glass removed in making the hole was in each case about 0.02 g. The final weight, with hook, adhering filament, and wax, was used in the computations.

Five results were obtained with the glass balls, shown in Table 18.

TABLE 18.—*Constant of gravitation derived from experiments with glass balls*

	6.678×10^{-8}
	6.671×10^{-8}
	6.675×10^{-8}
	6.672×10^{-8}
	6.674×10^{-8}
Mean	6.674×10^{-8}
Average departure from mean	.002

It is interesting to compare these mean results and their measures of precision. This is done in Table 19.

TABLE 19.—*Comparison of results*

Material	Extreme values	Mean value	Average departure from mean
Gold	6.683 6.672	6.678	0.003
Platinum	6.667 6.661	6.664	.002
Galss	6.678 6.671	6.674	.002

4. MEAN VALUE

It will be seen that the spread of the gold ball results is about twice as great as those with either platinum or glass, and that there is an overlapping of the spreads with gold and glass. It is evident that the gold ball results are much less reliable than either of the other sets.

The results with platinum and glass may be rated as of equal excellence, the average departure being the same and the spreads small and approximately equal. Discarding the gold results and giving equal weights to platinum and glass we obtain

$$6.669 \times 10^{-8}$$

with an average departure from the mean of 0.005. It seems advisable to us, however, to retain the gold results at one-third the weight of either platinum or glass. This gives as a final result

$$6.670 \times 10^{-8}$$

with an average departure from the mean of 0.005.

5. DISCUSSION OF RESULTS

The first thing that attracts attention in the results given in Table 19 is the apparent difference with the nature of the material. The mean values of the platinum and glass sets, for instance, differ by an amount five times as great as the average departure of either set. Moreover, there is no overlap in their spreads.

However, an explanation of this variation on the basis of difference of material is not admissible. As already stated (footnote (1)) Eötvös, by his very ingenious torsion balance method, has demonstrated the constancy of the gravitation constant for a number of materials (including platinum) to a precision of 6 parts in 10^9. He did not, however, test optical glass. While there is no doubt that the result obtained by Eötvös is universally valid, it seemed best to repeat his torsion balance experiment with the balls of platinum and glass. This work was carried out by Dr. G. S. Cook, of the Bureau of Standards, and is described in Section VIII. The high precision of the negative results obtained rules out any attempt to explain the variation of results on a basis of difference of material. Some other explanation is necessary.

To account for the observed differences it is necessary to find some factor which varies in the several series of experiments and does not eliminate in the near and far positions. Perhaps the first explanation that suggests itself is that of incomplete magnetic shielding. The evidence on this point (III, 6) appears conclusive, but is strengthened by the following considerations.

Gold is diamagnetic and platinum paramagnetic. Any residual magnetic effect would, therefore, weaken the attraction on the gold balls and strengthen it on platinum; but the values of G actually obtained are less for platinum than for gold.

It was recognized that the gravitational field in the room was not uniform, due partly to the upright stand carrying the pump attachments, and partly to the walls of the room. Two of these were backed with earth and two were merely partitions.

Such a field, however, being stationary, should produce no effect that would not be eliminated in the near and far positions.

It was recognized also that the resting position of the moving system was slightly different with respect to the field of the room in the several series of experiments, but it is not apparent that this would produce any effect that would not be eliminated.

Probably the solution of this difficulty can best be attained by working with an apparatus sufficiently sensitive to give the next decimal place. Should the variation found fail to appear in its present place, but be shifted farther on, the difficulty, while not explained, would obviously be ascribable to some experimental error.

Such an apparatus has been constructed, in which the difference of the two times of swing is about 100 minutes. This apparatus awaits the construction of the next new building at the Bureau of Standards, when opportunity may offer to provide a basement room large enough to contain it comfortably.

VIII. THE SPECIFIC ATTRACTION OF PLATINUM AND GLASS [8]

The experimental values of the constant of gravitation as given in the preceding section vary for small masses of different materials by an amount greater than the averag edeparture of the single values for any particular material. It seems reasonable to attribute this to experimental error of some nature, but it is possible to interpret it as a departure from Newton's law of the proportionality of mass and weight.

The Cavendish apparatus is not suited for the detection of very small departures from this law, since the forces involved are so small, but it is possible to test this point in other ways to a very high degree of precision. Such experiments have invariably shown, to the degree of precision of which the apparatus was capable, that the ratio of mass to weight is independent of the material. Pendulum experiments conducted by Newton [9] established this to 1 part in 1,000, and similar experiments by Bessel [10] of a more refined character car-

[8] This section and the experimental work it describes are due to Dr. G. S. Cook, of the Bureau of Standards.

[9] Principia, Book III, Prop. 6, Theorem 6.

[10] Pogg. Annalen, 25, p. 401; 1832.

ried the precision to one part in 60,000. It is worthy of note that Bessel included among the substances tested by him meteoric iron and meteoric stone.

The most precise experiments are those of Eötvös,[11] who by an ingenious application of the torsion balance succeeded in pushing the precision to 6 parts in 10^9. The substances examined by him were water, copper, platinum, magnalium, copper sulphate (solid and solution), asbestos and talc. As he did not test glass, it was thought worth while to repeat the Eötvös experiment with one of the glass balls actually employed in the determination of the constant of gravitation balanced against a ball of platinum.

In the Eötvös experiment two masses of different materials are suspended from the ends of the beam of a torsion balance. These masses may be thought of as acted upon by the gravitational attraction of the earth (a force which may not be proportional to the masses of the two bodies), and by a centrifugal force due to the rotation of the earth, which will be proportional to the masses. If then the gravitational force is not proportional to the masses the resultant forces on the two bodies will be in different directions, and in consequence a torque must be supplied by the suspending filament in order to hold the beam in equilibrium in an east and west position. This torque must be reversed if the beam (together with the torsion head) is turned through 180°.

In practice, the whole apparatus, including observing telescope and scale, was rotated. In this way the effect sought would show itself as a change in the equilibrium position.

H. A. Wilson [12] has given the theory of this experiment in a somewhat simpler form than that employed by Eötvös. The apparatus used in the present work was in dimensions and arrangement similar to that described by Wilson.

The torsion balance consisted of a light aluminum beam about 5 cm long carrying a glass ball at one end and a platinum ball at the other. The beam was supported at its center by a tungsten filament 0.025 mm in diameter and about 43 cm long. The beam was inclosed in a case of cast iron with walls 1 cm thick to avoid magnetic disturbances, and the case was exhausted of air to a pressure of about 2 mm of mercury.

To the case was attached a reading telescope and scale such as are used with wall galvanometers. The whole apparatus was placed on a level plate and pivoted so that it might be readily turned about its vertical axis. Deflections were read through a window in the case by means of the telescope and scale. Table 20 shows the readings obtained.

---

[11] Annalen der Physik, **68**, 1, pp. 11–66; 1922. [12] Phys. Rev., **20**, pp. 75–77; July, 1922.

TABLE 20.—*Resting points in centimeters observed with Eötvös apparatus*

Platinum ball east	Platinum ball west
1.40	1.40
1.38	1.37
1.36	1.34
1.32	1.31
1.27	1.27
1.26	1.26
1.24	
Mean..... 1.319	1.325
Difference, 0.006 cm clockwise Scale distance from mirror on beam, 50 cm	

The formula given by Wilson is as follows:

$$\frac{g-g'}{g'}=\left(2\Delta\right)\frac{2dt^2}{rT^2\sin 2\theta} \tag{23}$$

in which

g = acceleration of gravitation.
2Δ = change in azimuth angle when beam is turned 180°.
$2d$ = distance between centers of balls suspended from beam.
t = period of the earth's rotation.
θ = latitude of place of the experiment.
T = period of vibration of the torsion balance.
r = radious of earth.

At Washington $\theta = 38°\ 54'$, and the following values were observed:

$$T = 315 \text{ sec.}$$
$$2d = 4.9 \text{ cm}$$

Taking $g = 980$, we get:

$$\frac{g-g'}{g'}=2\Delta\times 6\times 10^{-4} \tag{24}$$

In the experiment, $2\Delta = 6\times 10^{-3}$ consequently

$$\frac{g-g'}{g'}=3.6\times 10^{-8} \tag{25}$$

While this result, from its minuteness, is of no importance in the present instance, it may be stated for the sake of completeness that the difference, regarded as real, is in the direction which would correspond to the different values of G obtained for glass and platinum. Its only value in the present work is to prove that the difference apparently found with glass and platinum is not to be explained on a basis of difference of material.

The value of 2Δ obtained from Table 20 is just about at the readable limit, being read from a scale of millimeters. The gradual change

in resting point shown in Table 20 is the typical behavior of a sus pension immediately after a load has been placed upon it. It quite marked here because of the fact that several hours alway elapsed between successive readings. This lapse of time was neces sary because of the small damping.

IX. SUMMARY AND GENERAL CONCLUSIONS

The value adopted for the constant of gravitation as a result o experiments with small masses of gold, platinum, and glass, weighted respectively, as 1, 3, and 3, is, in c. g. s. units

$$6{,}670 \times 10^{-8}\ \text{cm}^3\ \text{g}^{-1}\ \text{sec.}^{-2}$$

with a precision, as measured by the average departure from th mean, of 0.005.

This result agrees well with that obtained by Boys and Braun namely 6.66 ± 0.01.

The different results obtained with the various materials used fo the small masses are yet to be explained, but evidence is given tha this difference is not to be ascribed to the nature of the material.

Washington, April 10, 1930.

RP257

THE PROPERTIES OF PURE NICKEL

By Louis Jordan and William H. Swanger [1]

ABSTRACT

Rather pure electrolytic nickel was further purified by annealing in hydrogen. A study was made of suitable refractory crucibles and of melting conditions to produce extremely pure compact metal. The ingots finally prepared were of a purity of 99.94 per cent. New determinations of many of the physical properties of nickel have been made on the very pure metal thus made available. Data are given on density, crystal-lattice constant, melting point, electrical resistivity, magnetic properties, thermal e. m. f., thermal expansion, hardness, tensile strength, and reflectivity.

CONTENTS

	Page
I. Introduction	1291
II. Material	1292
III. Preliminary melting experiments	1293
IV. Melts of pure electrolytic nickel	1296
V. Mechanical working and preparation of test specimens	1298
VI. Physical properties	1299
1. Density	1299
2. Crystal structure and lattice dimensions	1300
3. Melting point	1300
4. Electrical resistivity	1301
5. Magnetic properties	1302
6. Thermal transformation	1304
7. Thermoelectromotive force	1304
8. Thermal expansion	1305
9. Hardness	1306
10. Tensile properties	1306
11. Reflectivity	1306
VII. Summary	1307

I. INTRODUCTION

In October, 1925, the International Nickel Co., through the courtesy of Dr. Paul D. Merica, assistant to the president, made available to the National Bureau of Standards small amounts of two lots of rather pure electrolytic nickel for use in such determinations of the physical properties of the pure metal as it might prove possible for the Bureau of Standards to undertake.

Preliminary melting experiments were carried out with the less pure of these two lots of materials. Some further purification of the better of the two lots was undertaken, and vacuum fused ingots of this nickel were made. Suitable specimens were prepared for a variety of determinations of physical properties, namely, density, lattice constants, hardness, thermal transformation, melting point, magnetic properties, electrical resistivity, temperature coefficient of electrical resistance, thermal electromotive force, thermal expansion, and reflectivity.

[1] With the collaboration of members of the bureau staff, as indicated in the various sections of the report.

A detailed discussion of the preparation and purity of the materials used in the above determinations is given in the present paper as well as a fairly detailed summary of all of the above work on physical properties. The methods and results involved in certain of the determinations of the properties of nickel are, or will be, described in still greater detail in separate papers.

A great many members of the bureau staff have cooperated in the securing of these data on pure nickel. In addition to those to whom credit is given in the various sections of this report, thanks are especially due to H. C. Vacher, of the division of metallurgy, for the determination of the gases, and to J. A. Scherrer and C. P. Larabee, of the chemistry division, for the determinations of the other impurities of the nickel specimens.

II. MATERIALS

The two lots of cathode nickel, which were in the form of thin flakes of metal, were designated as lot Ni–1–A and lot Ni–2–B. As received they were of the following purity:

	Ni–1–A	Ni–2–B
	Per cent	*Per cent*
C	0.03	0.05
S	.005	(1)
Si	.007	.003
Fe	.005	.007
Cu	.004	.07
Co	.013	.01

[1] Uncertain (possibly 0.005 to 0.012).

Some difficulty was experienced in making satisfactory determinations of sulphur in the original cathode nickel, particularly in the metal of lot Ni–2–B. Some analyses indicated no sulphur in Ni–2–B, others gave about 0.005 per cent, while still others showed as high as 0.012. As is shown later, the sulphur found in fused samples of both Ni–1–A and Ni–2–B melted under conditions which should not introduce sulphur, indicated that the actual sulphur content of both lots of nickel was of the order of 0.010 per cent.

TABLE 1.—*Effect of vacuum fusion in various types of crucibles on the composition of electrolytic nickel of lot Ni–2–B*

Melt No.	Type of crucible	Type of furnace	Purity of resulting ingot					
			C	P	S	Si	Fe	Cu
			Per cent	*Per cent*	*Per cent*	*Per cent*	*Per cent*	*Per cent*
N–1 [1]	Zirconium silicate	Arsem	<0.01	0.59	0.015	0.003		
N–2 [2]	do	do	<.01	.59	.015	.008		
N–3	RR alundum and No. 518 alundum cement.	do		.009	.016	.31		
N–4	Ziroconium silicate [3]	do		.24	.011	.079		
N–5	Sillimanite porcelain (aluminum silicate).	do	.015	.005	.008	.01	0.017	
N–6	C. P. MgO+shellac	do	.04	<.003	.014	.03	.027	0.028
N–7	Same as N–6; second melt	do			.009	.02		
N–8	Same as N–6; third melt	do	.015		.009	.01	.004	
N–9	New C. P. MgO+shellac	High-frequency.	.03	<.001	.010	.009		
N–10	Reground C. P. MgO+Shellac	Arsem			.008	.006		
N–11	Commercial sintered MgO; inside of crucible fused and glazed under electric arc.	do			.031			

[1] The cathode nickel of the crucible charge was a mixture of coarse flakes and the finer as received.
[2] The nickel of the charge was sifted free of the finer flakes.
[3] A different lot of $ZrSiO_4$ from that used in N–1 and N–2 melts.

III. PRELIMINARY MELTING EXPERIMENTS

The details of the preliminary melting experiments, carried out in order to select the most satisfactory type of crucible and furnace for preparing the final specimens, are given in Table 1. The material used for the crucible charge in all melts from N–1 to N–11, inclusive (Table 1), was the less pure nickel, Ni–2–B. The first eight melts were made in an Arsem vacuum furnace (pressures of 5 to 10 mm of mercury) as were also melts N–10 and N–11. Ingot N–9 was fused in vacuum (pressure of less than 1 mm of mercury) in the high-furnace induction furnace.

The three melts made in zirconium silicate crucibles were all contaminated by phosphorus (N–1, N–2, and N–4), although the zirconium silicate used was the commercial refined grade. The carbon content of all melts was slightly lower than that of the original cathode nickel. This decarburization was noticeable with all types of crucibles, although it was very slight in the first melt in a magnesia-shellac crucible.[2]

The silicon in the nickel increased very noticeably when the metal was melted in aluminum oxide (N–3) or in zirconium silicate (N–4). The alumina crucible, however, contained some commercial alundum cement (No. 518), which was probably considerably higher in silica than the RR alundum. Increase of silicon in the melt took place after some melts in C. P. MgO crucibles (N–6 and N–7) but appeared to be not necessarily characteristic of all melts in this refractory (N–8, N–9, and N–10). Melts N–7 and N–8 were, respectively, the second and third melts of fresh charges of cathode nickel in the same magnesia crucible. In these cases the solidified ingot did not wet or stick to the magnesia crucible and could be removed after cooling to room temperature by gentle tapping and without injury to the crucible. The remelts were made to determine if appreciable purification of the refractory occurred on continued use, particularly as indicated by an increase in the sulphur content of the nickel ingot.

The most serious contamination in any of these trial melts was that due to sulphur. It has been shown by Merica and Waltenberg [3] that remelted electrolytic nickel is rendered almost completely non-malleable by as little as 0.01 per cent sulphur and malleability was, of course, essential in the preparation of the specimens necessary for the present work.

In all of the preliminary melts, N–1 to N–10, regardless of the nature of the crucible, the sulphur content of the resulting ingot was practically 0.01 to 0.02 per cent, whereas the analysis of the original cathode nickel of lot Ni–2–B had shown generally not over 0.005 per cent sulphur. As has been noted before there may be reason to doubt the accuracy of the analytical values for sulphur obtained, even with great pains in the analytical procedure, in the case of this cathode nickel.

A final melt of this lot of nickel (N–11) was made in a crucible of commercial electrically sintered magnesia. The inside surface of this crucible was fused and glazed by spinning the crucible while an arc

[2] The magnesia-shellac crucibles were made as described by R. F. Mehl, J. L. Whitten, and D. P. Smith, Laboratory Production of Pure Magnesia Ware. Ind. Eng. Chem., **17**, p. 1171, 1925.

[3] P. D. Merica and R. G. Waltenberg, Malleability and Metallography of Nickel, B. S. Tech. Papers No. 281; 1925.

was burning between two graphite electrodes inside the crucible. It was known that the commercial sintered magnesia crucibles which had not been glazed inside were prone to contaminate melts with sulphur, but it was thought that possibly a dense glaze on the surface might reduce this contamination and that the glazed surface might be purified in the course of the fusion process. However, the resulting ingot (N–11) contained the most sulphur of any of the ingots of this first series.

TABLE 2.—*Effect of hydrogen treatment and of melting in various types of crucibles on the composition of electrolytic nickel of lot Ni–1–A*

Melt No.	Type of crucible	Type of furnace	C	Mn	P	Purity of resulting ingot						
						S	Si	Fe	Cu	Co	Mg	Ni direct determination
			Per cent	*Per cent*	*Per cent*	*Per cent*	*Per cent*	*Per cent*	*Per cent*	*Per cent*	*Per cent*	*Per cent*
N–12	Mullite (aluminum silicate)	Arsem				0.01	0.07					
N–13	Fused Al_2O_3	do				.010	.12					
N–14	C. P. MgO–shellac	do				.011	.03					
NH–1	Alundum	Pt –resistance furnace at 1,450° C. in H_2				<.002	.14					
NH–2	Fused silica	Nichrome resistance furnace at 1,050° C. in H_2	<0.005			.003	.006					
N–15	C. P. MgO – shellac	Arsem	.05			<.002	.02					
N–16	C. P. MgO + $MgCl_2$	do										
N–17	do	do										
N–18	do	do										
N–19	do	High-frequency	(1)	(1)	(1)	.004	(1)	0.024	0.016	0.016	0.003	
N–20	do	Arsem										
N–21	do	do										
N–22	do	do										
N–23	do	High-frequency	.005	(1)	(1)	.004	.006	.03	.006	.016	(1)	99.94

[1] Not detected.

IV. MELTS OF THE PURE ELECTROLYTIC NICKEL

Attention was next turned to the purer electrolytic nickel of lot Ni–1–A in the hope that this material would prove lower in sulphur after fusion than had the Ni–2–B nickel. The first three ingots prepared from this material, however, all showed 0.01 per cent sulphur (N–12, N–13, and N–14, Table 2). They were melted, respectively, in crucibles of mullite (aluminum silicate), in fused alumina (RR alundum), and in C. P. magnesia bonded with shellac. The contamination of the melt with silicon from both the aluminum silicate and the fused alumina was excessive and was very considerable even from the C. P. magnesia.

It appeared from the foregoing melts (N–1 to N–14, inclusive), that the electrolytic nickel contained at least 0.01 per cent sulphur in some form in spite of the lower values indicated by analyses of the original cathode metal, for all melts of both lots of nickel contained at least that proportion of suphur, regardless of the refractory crucible material used. There were also indications that new crucibles of magnesia bonded with shellac tended either to introduce carbon into the melt (N–6 and N–9) or at least to prevent the small, but appreciable, decarburization caused by melting in other oxide crucibles (N–1, N–2, N–5, and N–8). Furthermore, when the carbon in the resulting ingot was of the order of 0.04 per cent (N–6), or from the type of crucible used might be expected to contain carbon to about that amount (N–14), the increase of silicon in the melt even from the C. P. magnesia crucible was very considerable.

It was, therefore, decided to treat the cathode nickel in hydrogen at an elevated temperature (for the removal of both carbon and sulphur from the metal) and to use C. P. magnesia crucibles bonded with a solution containing 2 g of magnesium chloride ($MgCl_2$, $6H_2O$) in 100 ml of water.[4]

The first hydrogen treatment of nickel was carried out by placing a small charge of metal from lot Ni–1–A in an alundum boat within a porcelain tube and heating to approximately 1,450° C. in a platinum resistance furnace. A stream of dry purified hydrogen was passed through the tube during the heating. The temperature actually reached was somewhat higher than had been intended and the nickel sample fused. As might be expected, the silicon content of this fused nickel button was high, namely, 0.14 per cent (NH–1, Table 2), but the sulphur was gratifyingly low. It was less than 0.002 per cent.

The next hydrogen treatment of nickel was carried out by packing rather tightly a 3 or 4 inch length of the middle section of a 1-inch diameter fused silica combustion tube with the cathode nickel and heating this in a stream of hydrogen to 1,050° C. in a nichrome resistance furnace. The heating was continued for about one and one-half hours. The metal resulting from this treatment (NH–2) was of quite satisfactory purity; it contained less than 0.005 per cent of carbon, together with 0.003 sulphur and 0.006 silicon. There had thus been a very appreciable improvement as regards carbon and sulphur. A small trial melt of this hydrogen-treated nickel was made in a magnesia-shellac crucible (N–15) in the Arsem furnace

[4] L. Jordan, A. A. Peterson, and L. H. Phelps, Refractories for Melting Pure Metals; Iron, Nickel, Platinum, Trans. Am. Electrochem. Soc., **50**, p. 155; 1926.

and produced an ingot entirely satisfactory as regards its sulphur content (less than 0.002 per cent sulphur), but had very clearly been carburized (to 0.05 per cent carbon) by the crucible and had consequently picked up silicon to the extent of 0.02 per cent.

Two small ingots of about 90 g each were next made by melting the hydrogen-treated nickel in the Arsem furnace in magnesia crucibles bonded with magnesium chloride (N–16 and N–17). One of the troubles encountered in melting these crucible charges of rather thin flakes of nickel, which could not be compressed to a very compact charge, was that the nickel charge in the crucible appeared to lag rather far behind the magnesia crucible in attaining the melting temperature. As a consequence, the reaction quite frequently encountered in Arsem furnace work in which the graphite of the supporting shell surrounding the magnesia crucible reacts with the magnesia at elevated temperatures to form magnesium vapors and carbon monoxide gas, got well under way while the nickel in the crucible was still considerably below its melting point. On all colder surfaces close to the heated zones in the Arsem furnace this reaction reverses and a deposit of magnesium oxide and carbon is produced.

There were thus formed thin films of magnesia on the surfaces of many of the nickel flakes and when the nickel melted complete coalescence was prevented by the thin films of magnesia. When the charge was held molten for some time these magnesia films tended to be rejected to the metal-crucible wall interface and to the top surface of the ingot.

In order to eliminate these magnesia films, the two small ingots N–16 and N–17 were etched in HCl, washed, and then melted together in the same type of crucible in the Arsem furnace so as to give a single 180 g ingot, N–18. As a final step, ingot N–18 was remelted in a vacuum, high-frequency induction furnace under a pressure of less than 1 mm of mercury. The magnetic stirring of the liquid metal in this furnace very effectively cleaned out all remaining visible traces of magnesia films.

The complete analysis of the resulting ingot (N–19) showed that carbon, manganese, phosphorus, and silicon were not detectable. The sulphur content was 0.004 per cent, which was believed to be sufficiently low to give a malleable nickel. Copper appeared to have increased over that present in the original cathode nickel, namely, from 0.004 to 0.016 per cent. Cobalt was also 0.016 per cent, about the same as in the original material. Iron had increased noticeably, to 0.024 per cent, and a small amount of magnesium, 0.003 per cent, was present.

A larger ingot of nickel was prepared by this same procedure. Ingots N–20 and N–21, each weighing about 150 g, were cleaned, remelted in the Arsem to give ingot N–22, and a final remelt in the high-frequency furnace was designated as N–23. This ingot was of approximately the same purity as N–19, containing 0.005 per cent carbon, 0.004 sulphur, 0.006 silicon, 0.03 iron, 0.006 copper, and 0.016 cobalt. Manganese, phosphorus, and magnesium were not detected and a direct determination of nickel gave 99.94 per cent. Later analyses for oxygen, hydrogen, and nitrogen in this ingot showed the presence of only 0.001 per cent oxygen and hydrogen, and nitrogen not detected. The complete analysis thus totaled 100.008 per cent.

V. MECHANICAL WORKING AND PREPARATION OF TEST SPECIMENS

Ingot N–23 had an over-all length of 9.5 cm and a central primary pipe opening at the top surface and extending for a little less than 5.5 cm down into the ingot. (Fig. 1.) The upper portion (1.5 to 2.0 cm) of the ingot was removed by a milling machine for samples for chemical analysis. The remainder of the ingot was then cut in two portions such that all the pipe came in the top portion and the bottom (3.5 cm in length) was entirely sound. The portion containing the pipe was then divided longitudinally in two approximately equal parts, designated as B and C. The sound portion at the bottom was designated as D.

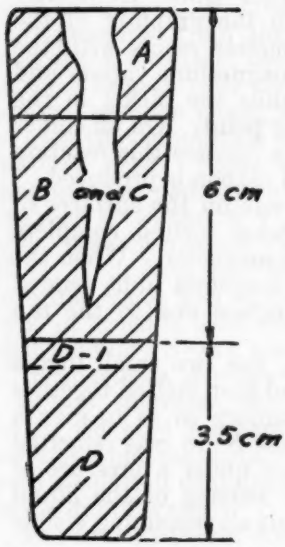

FIGURE 1.—*Sections of the split ingot No. 23*

The longitudinal sections B and C were mechanically worked to specimens for physical tests. Preliminary to working, the sharp projecting edges in the portion of the pipe in each piece were carefully cut off with a small cold chisel. Section B (or C) was then carefully hammered cold, with frequent annealing, the specimen being manipulated in a grooved anvil block so that the pipe was worked completely to the outer surface of the hammered bar and no seams or laps were formed at the edges of the pipe.

In the early stages of the cold hammering of specimen B sufficiently high annealing temperatures were not employed and a few minute cracks appeared in the metal surface in the pipe cavity. The sections of metal about these cracks were very carefully fused with a small, sharp oxy-hydrogen flame. This specimen was then heated for one-half hour at each of the following temperatures, and scleroscope and Rockwell B hardness numbers were determined. The results indicated that the pure nickel must be annealed at a temperature certainly above 850° C., probably at 950° C., in order to eliminate work hardening.

TABLE 3.—*Hardness of nickel*

Temperature of heating for one-half hour after cold working (° C.)	Hardness	
	Rockwell B	Scleroscope
As cold worked	63–68	12–19
650	52–59	8–13
750	51–59	8–13
850	35–52	7–11
950	[1] (15–18)	4–6

[1] Too soft for satisfactory Rockwell B measurements.

Subsequent annealings of specimens B and C were carried out by heating the bar in an oxy-hydrogen flame to about 950° to 1,000° C.

(as judged by eye) for two or three minutes. The nickel was supported on fragments of C. P. magnesia crucibles during such heatings.

The specimen was hand forged to a rod which would enter the 0.330-inch swaging dies. It was then cold swaged, with annealing after each pass, through the 0.330, 0.300, 0.275, and 0.250 inch swaging dies. The bar was not annealed after the 0.250-inch pass. The finished bar weighed 59 g and was 19.5 cm (7.7 inches) long, and 0.65 cm (0.257 inch) in diameter.

The other portion of ingot N–23 (C, fig. 1) was worked in the same manner as B to a bar of very nearly the same size. If differed only in being 0.5 cm (0.2 inch) longer.

Each of the swaged bars (B and C) was then cut into five specimens as shown in Figure 2.

Section D of ingot N–23 was at first held in reserve in case any specimens from the B or C sections proved unsatisfactory, but finally was used as follows: A small disk (marked D–1 in fig. 1) was cut from the top of the original D piece for reflectivity measurements; the remainder was cut in halves longitudinally; one-half was used for melting-point determinations and the other for analyses for oxygen, hydrogen, and nitrogen.

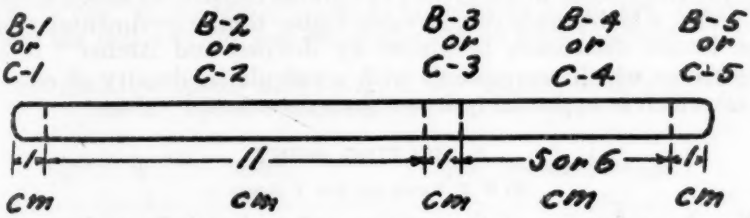

FIGURE 2.—*Designation, position, and length of specimens cut from swaged nickel rods*

VI. PHYSICAL PROPERTIES

1. DENSITY

(By E. L. Peffer [1])

The density of the pure nickel of ingot N–23 was determined (*a*) in the "as-cast" condition, or rather as quite slowly cooled from the liquid and frozen in very large crystals (secs. B or C and D, fig. 1); (*b*) as cold-worked after cold swaging from 0.257 to 0.225 inch diameter without annealing; and (*c*) as annealed by heating at 950° C. for one hour in vacuum. The results are given in Table 4.

TABLE 4.—*Density of nickel*

Specimen No.	Form of specimen	Condition	Density
			g/cm³
B or C	Part of ingot N–23	"As cast"	8.907 (23° C.)
D	do	do	8.907 (23° C.)
B–4	Rod 0.225 inch diameter	Cold swaged	8.901 (25° C.)
C–4	do	do	8.900 (25° C.)
B–4	do	Annealed at 950° C	8.903 (25° C.)
C–4	do	do	8.901 (25° C.)

[1] Chief, section of capacity and density.

The maximum density 8.907 g/cm³ was obtained in the very coarsely crystalline ingot metal which had received no mechanical working. The density of the worked metal was slightly less, about 8.901 g/cm³ either as annealed or after a 30 per cent reduction in area by cold working.

The International Critical Tables [6] give the density of nickel as 8.90 g/cm³ at 20° C. The average density of commercial nickel, of purity of about 99.2 per cent, has been given as 8.85 ± 0.03 g/cm³.[7]

2. CRYSTAL STUCTURE AND LATTICE DIMENSIONS

(By R. G. Kennedy, jr.[8])

Preliminary measurements of the lattice constant of the unit cube (face centered) of nickel were made on a portion of specimen B-2 after this bar had been used for thermal expansion measurements. The dimension of the side of the unit cube was found to be 3.525 Ångstroms. The calculated density of nickel, based upon this value for the lattice dimension, is 8.917 g/cm³ as compared with the determined values of 8.907 "as cast" (large crystals) and 8.901 for the worked specimens.

The length of the side of the unit cube of nickel as given by Clark [9] is 3.499 Ångstroms which gives a calculated density for nickel of about 9.1 g/cm³, which is very considerably higher than experimental values. The lattice dimension tabulated by Jeffries and Archer [10] is 3.54 Ångstroms which corresponds with a calculated density of only 8.8 g/cm³ which is appreciably lower than determined values.

3. MELTING POINT

(By H. T. Wensel and Wm. F. Roeser [11])

For determination of the melting point of nickel, specimens C-3, B-5, C-5, and one-half of D, all of N-23, were combined to give a single sample of sufficient size for determinations by the crucible method. All of ingot N-19 remaining after the chemical analysis was used for a second or check determination.[12] The specimens were alternately melted and allowed to freeze. Heating and cooling curves were obtained with a precision optical pyrometer sighted into a magnesia tube surrounded by the pure nickel held in a pure magnesia crucible. The crucible and metal were heated or cooled very gradually and uniformly, in vacuum, in a platinum resistance furnace. Very excellent agreement was shown by the data taken by three different observers on the two specimens which represented two ingots of pure nickel. The best value rounded off to the nearest degree for the freezing point of nickel, as shown by this work, is 1,455° C. This is 3° higher than the generally accepted value of 1,452° C. It is assumed that the temperature of the melting point is the same as that of the freezing point thus obtained.

---

[6] I. C. T., 1, p. 104.
[7] P. D. Merica, Physical and Mechanical Properties of Nickel, Trans. Am. Soc. Steel Treating, 15, p. 1054; 1929.
[8] Assistant metallurgist, section of optical metallurgy.
[9] Geo. L. Clark, X-Ray Metallography in 1929, Metals and Alloys, 1, p. 98; 1929.
[10] Jeffries and Archer, The Science of Metals, pp. 4 and 5, McGraw-Hill Book Co.; 1924.
[11] Chief and associate physicist, respectively, pyrometry section.
[12] H. T. Wensel and Wm. F. Roeser, The Freezing Point of Nickel as a Fixed Point on the International Temperature Scale, B. S. Jour. Research, 5 (RP 258), p. 1309; December, 1930.

TABLE 5.—*Melting or freezing point of nickel*

Specimen No.	Number of determinations	Average temperature
	Freezes	*° C.*
N–19	9	1,455
N–23	11	1,455

As evidence of the absence of any significant contamination of these nickel samples during the many remeltings in the melting point work there is offered the fact that the temperature coefficient of resistance of wires prepared from nickel samples N–19 and N–23 after their use for the melting point determinations was not lower than it had been before the many remeltings in vacuum in the course of the melting point determinations. (See Table 7.)

Analyses for the oxygen, hydrogen and nitrogen content of these two lots of nickel were also made by vacuum fusion before and after the melting-point determinations. A slight increase in oxygen during the remelting was indicated (Table 6), but this increase was without any detectable effect on the melting point as evidenced by the fact that no "drift" in the temperature of the melting point was observed between the first and the last determination on either sample.

TABLE 6.—*Gases in samples of nickel before and after repeated fusions in determinations of the melting point*

Sample No.	Condition	Oxygen	Hydrogen	Nitrogen
		Per cent	*Per cent*	*Per cent*
N–19	Before M. P. determinations	0.001	0.0002	(1)
N–19	After M. P. determinations	.008	(1)	(1)
N–23	Before M. P. determinations	.001	(1)	(1)
N–23	After M. P. determinations	.015	0.0002	0.004

[1] Not detected.

4. ELECTRICAL RESISTIVITY

(By F. Wenner and F. R. Caldwell [12])

Specimens B–4 and C–4 of N–23, after being used for density determinations and magnetic measurements, were cold-rolled until long enough to handle with ease in the swaging machines and were then cold swaged to wire 0.079 inch in diameter. This wire was cold drawn to 0.0385-inch diameter through a steel draw plate, except for the last three passes which were through sapphire dies. During this working the metal was annealed in an oxy-hydrogen flame between successive passes through the grooved rolls or through the swaging dies and annealed after every two passes through the drawing dies. Lengths of 120 cm of approximately 1 mm (0.0385-inch) diameter wire of specimens B–4 and C–4 were used for the resistivity measurements, first as cold-drawn through the last two sapphire dies from 0.0435 to 0.0385 inch diameter, and then after having been annealed. The single strand wire, suspended in still air, was annealed at about 800° C. by means of an electric current passed through the wire.

[12] Respectively, chief, section of electrical resistance and assistant physicist, pyrometry section.

Following the determinations of the resistivity, sections of the 0.0385-inch wire from both B–4 and C–4 were drawn to 0.0078-inch diameter for the determination of the temperature coefficient of resistance. In addition to these specimens, there had also been prepared wire specimens of N–19 before and after it was used for determination of the melting point and of N–23 after use for the same determination.

The temperature coefficient of resistance was determined on these additional samples. These values, agreeing within experimental error with those found for the other specimens, showed that no significant contamination occurred while the melting point was being determined.

TABLE 7.—*Electrical resistivity of nickel*

Specimen No.	Condition of metal	Resistivity at 20° C.	Temperature coefficient of resistance 0° to 100° C.
		Microhm-cm	*Ohms per° C. per ohm at 0° C.*
B–4	Cold-drawn	7. 289	
C–4	do	7. 292	
B–4	Annealed	7. 235	0. 00667
C–4	do	7. 237	. 00667
N–19	Before M. P. determination		. 00658
N–19	After M. P. determination		. 00674
N–23	do		. 00672

The resistivity of nickel has been given as low as 6.5 microhm-cm[14] and 6.9 microhm-cm[15] at 0° C. This latter value is from Fleming's work[16] and was obtained on a metal whose temperature coefficient between 0° and 100° C. was 0.0061. Copaux[17] gave 0.0066 as the temperature coefficient, more nearly the value found in the present work, but gave the resistivity at 0° C. as 6.4 microhm-cm. Giess and v. Liempt[18] found the temperature coefficient of an "annealed" specimen of very pure nickel to be 0.00667. After further heating of the specimen for 30 minutes at 1,000° C. in vacuum, this value rose to 0.00706.

5. MAGNETIC PROPERTIES

(By R. L. Sanford[19])

Specimen C–2 both as cold worked and after annealing was used for determinations of normal induction, residual induction, and coercive force. The effect of annealing on the normal induction is shown in Figure 3.

The maximum permeability of the cold-worked sample was about 70, while in the annealed specimen the value increased to nearly 1,000. Values for maximum permeability as high as 1,200 were obtained in other specimens of nickel from this same ingot N–23.

For a maximum magnetizing force of 1,000 gilberts per centimeter the residual induction in the cold-worked rod C–2 was 3,280 gausses

[14] P. D. Merica, Physical and Mechanical Properties of Nickel, Trans. Am. Soc. Steel Treat., **15**, p. 1054; 1929.
[15] Int. Crit. Tables, **6**, p. 136.
[16] J. A. Fleming, Electrical Resistivity of Electrolytic Nickel, Proc. Roy. Soc. (London), **66**, p. 50; 1900.
[17] M. H. Copaux, Experimental Researches on Cobalt and Nickel, Ann. Chem. Phys., **6** (8), p. 508; 1906.
[18] W. Giess and J. A. M. v. Liempt, Electric Measurements on Metals of High Purity, Zeit. fur Metallkunde, **17**, p. 194; 1925.
[19] Chief of magnetic section.

with a coercive force of 26.0 gilberts per centimeter. After annealing these values were 5,040 and 6.0, respectively.

Measurements with magnetizing forces up to 300 gilberts per centimeter were made with the magnetic comparator as described by Fischer.[20] For magnetizing forces from 100 to 3,000 gilberts per centimeter the modified isthmus method as described by Cheney[21] was used. There was good agreement between the two methods in the range 100 to 300 gilberts per centimeter common to both.

The saturation value of intrinsic induction $(B-H)_\infty$, of a ferromagnetic material is a function of the constitution and is not otherwise dependent upon its condition. The value found for sample C–2, both in the cold-worked condition and after annealing, was 6,150, which agrees with the value given by Droz[22] and Hegg.[23] This is also given as the best value by McKeehan[24] in his article on "Ferromagnetism."

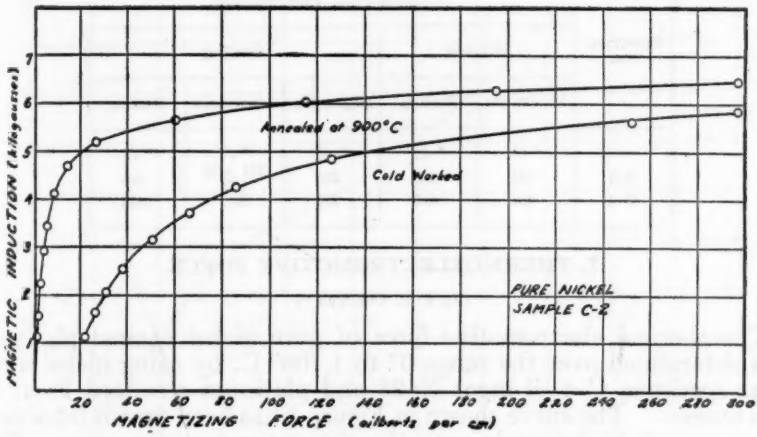

FIGURE 3.—*Normal induction of pure nickel*

The temperature of the magnetic transformation of nickel from the ferromagnetic to the paramagnetic state is rather indefinite and depends somewhat upon previous history. Various authors give values ranging from 340° to 380° C. The temperature appears to be higher the purer the material.

Several determinations made by the magnetometric method using an astatic magnetometer[25] gave on sample C–2 an average value of 380° C. on heating and 371° C. on cooling from approximately 500° C. The individual values ranged from 372° to 387° C. on heating and 367° to 377° C. on cooling. The uncertainty seems to be characteristic of the material and does not depend upon the conditions of test, as no such variation was found for pure iron with the same apparatus under similar conditions.

[20] M. F. Fischer, Apparatus for the Determination of the Magnetic Properties of Short Bars, B. S. Sci. Paper No. 458; 1922.
[21] W. L. Cheney, Magnetic Testing of Straight Rods in Intense Fields, B. S. Sci. Paper No. 361; 1920.
[22] Droz, Abram, Determination of Absolute Value of Intensity of Magnetization at Saturation, Arch. des Sci. Phys. et Nat. (4), **29**, p. 204; 1910.
[23] Hegg, Felix, A Thermomagnetic Study of Nickel Steel, Arch. des Sci. Phys. et Nat. (4), **29**, p. 592; 1910.
[24] McKeehan, L. W., Ferromagnetism, J. Frank. Inst., **197**, Nos. 5 and 6; 1924.
[25] Sanford, R. L., Apparatus for Thermomagnetic Analysis, B. S. Jour. Research, **2** (RP 50); 1929.

6. THERMAL TRANSFORMATION

(By H. C. Cross [26])

The temperature of the thermal transformation of solid nickel was determined by thermal analysis on specimens B–3 and C–3. These specimens, mounted on a platinum/platinum-rhodium thermocouple inclosed in a quartz tube were heated and cooled at a definite rate in a modified Rosenhain furnace.[27] A vacuum equivalent to 0.01 to 0.001 mm of mercury was maintained in the tube. Readings every 0.02 mv (approximately 2° C.) were automatically plotted as an inverse-rate curve on a recording chronograph.[28] From these the transformation temperatures given in Table 8 were obtained.

TABLE 8.—*Temperature of thermal transformation in nickel. Determined by thermal analysis*

Specimen No.	Temperature of transformation				
	Heating		Cooling		
	Maximum	Ending	Beginning	Maximum	Ending
	° C.	° C.	° C.	° C.	° C.
B–3	353	359	355	351 and 332	316
C–3	351	357	357	351	342

7. THERMOELECTROMOTIVE FORCE

(By F. R. Caldwell [29])

The thermal electromotive force of pure nickel against platinum was determined over the range 0° to 1,100° C. by using nickel wires from specimen C–4 of ingot N–23 and platinum standard Pt 27 of this bureau. The curve shown in Figure 4 has been drawn from data taken at 25° C. intervals over the entire temperature range. The change in the curve in the region of the magnetic transformation of nickel is readily noticeable. The values of the electromotive force at 100° C. intervals with the cold junctions at 0° C. are given in Table 9.

TABLE 9.—*Thermal electromotive force of nickel against platinum*

Temperature of hot junction	E. m. f.* Pt-Ni	Temperature of hot junction	E. m. f.* Pt-Ni
° C.	*Millivolts*	° C.	*Millivolts*
100	1. 485	700	8. 105
200	3. 105	800	9. 359
300	4. 590	900	10. 695
400	5. 450	1, 000	12. 130
500	6. 165	1, 100	13. 625
600	7. 040		

*Nickel is thermoelectrically negative to platinum; that is, in a simple thermoelectric circuit formed by these two metals, the current flows from the platinum to the nickel at the cold junction.

[26] Formerly assistant metallurgist section of thermal metallurgy.
[27] Scott, H., and Freeman, J. R., jr., Use of a Modified Rosenhain Furnace for Thermal Analysis, B. S. Sci. Paper No. 348; 1919.
[28] French, H. J., A Recording Chronograph for the Inverse Rate Method of Thermal Analyses, B. S. Tech. Paper No. 230; 1923.
[29] Assistant physicist, pyrometry section.

8. THERMAL EXPANSION

(By P. Hidnert [20])

The thermal expansion of nickel was determined on specimen B–2 of ingot N–23. This specimen, originally 10 cm (4 inches) long by 0.6 cm (0.24 inch) in diameter as used in the magnetic tests, was annealed and then cold swaged to a diameter of 0.35 cm (0.14 inch) and 31.1 cm (12 inches) long. During the swaging the specimen was annealed after each pass.

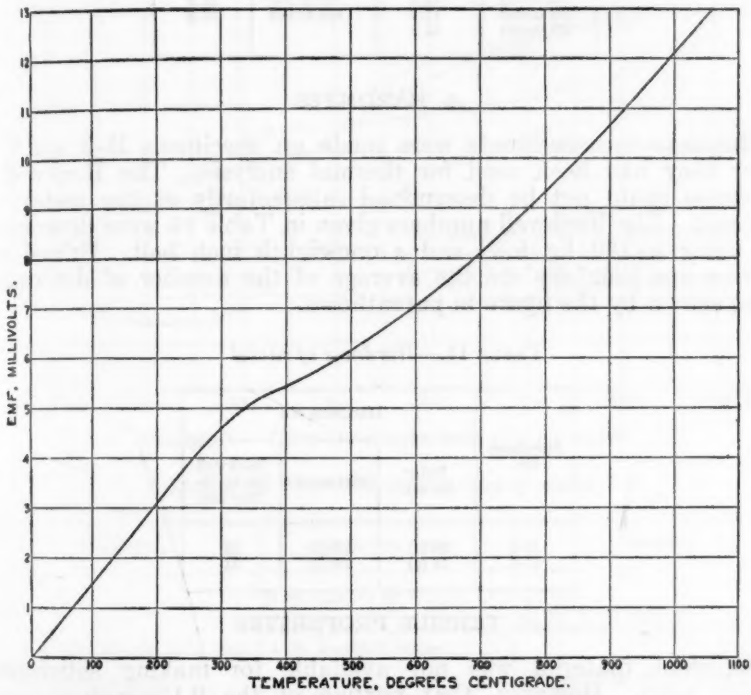

FIGURE 4.—*Thermal electromotive force of pure nickel*

Ordinates are the thermal e. m. f. of the couple Pt-Ni; at the cold junction, the current flows from Pt to Ni.

Expansion measurements were taken from 25° to 900° C. A large number of observations were taken between 300° and 400° C. in an attempt to locate a transformation region.

An irregularity in the rate of expansion was shown in the region near 350° C.

[20] Associate physicist, section of thermal expansivity.

TABLE 10.—*Thermal expansion of nickel*

Temperature range (in ° C.)	Average coefficient per ° C. $\times 10^6$	Temperature range (in ° C.)	Average coefficient per ° C. $\times 10^6$
25 to 100	13.3	400 to 500	15.9
25 to 300	14.4	500 to 600	16.9
25 to 600	15.5	600 to 700	17.1
25 to 900	16.3	700 to 800	17.7
100 to 200	14.4	800 to 900	18.6
200 to 300	15.4	300 to 600	16.5
300 to 350	17.2	600 to 900	17.8
350 to 400	16.4		

9. HARDNESS

Hardness measurements were made on specimens B–3 and C–3 after they had been used for thermal analysis. The Rockwell B hardness could not be determined satisfactorily as the metal was too soft. The Rockwell numbers given in Table 11 were determined by using a 100 kg load and a one-eighth inch ball. Brinell and Scleroscope numbers are the average of the number of determinations shown by the figure in parentheses.

TABLE 11.—*Hardness of nickel*

Specimen No.	Hardness No.		
	Baby Brinell	Scleroscope	Rockwell 100 kg 1/8-inch ball
B–3	68 (4)	5.0 (3)	42
C–3	78 (4)	5.0 (3)	44

10. TENSILE PROPERTIES

Sufficient material was not available for making satisfactory tensile tests. However, that portion of the 0.139-inch diameter rod remaining after thermal expansion measurements and after cutting a portion for spectrographic tests was broken in tension. The annealed bar broke under a load equivalent to 46,400 lbs./in.^{2} The surface of the bar became so roughened during the flow resulting from the tension loading that the gage marks were entirely obliterated. The elongation was certainly 25 per cent in 2 inches, probably considerably more.

11. REFLECTIVITY

Measurements of the ultra-violet reflectivity of a specimen of this pure nickel (D–1 fig. 1) have been made and already reported by Coblentz and Stair [31] and compared with the reflectivity of electroplated nickel and of commercial refined nickel. Their results are fully recorded in Figure 5, the curve designated as "C & S vacuum

[31] Coblentz, W. W., and Stair, R., Reflecting Power of Beryllium, Chromium, and Several Other Metals, B. S. Jour. Research, **2** (RP39); 1929.

fused" representing the results obtained with the pure nickel described in this paper.

VII. SUMMARY

The physical properties of nickel of a purity of 99.94 per cent are summarized in Table 12. This metal was electrolytic nickel fused in vacuum and contained not over 0.001 per cent oxygen.

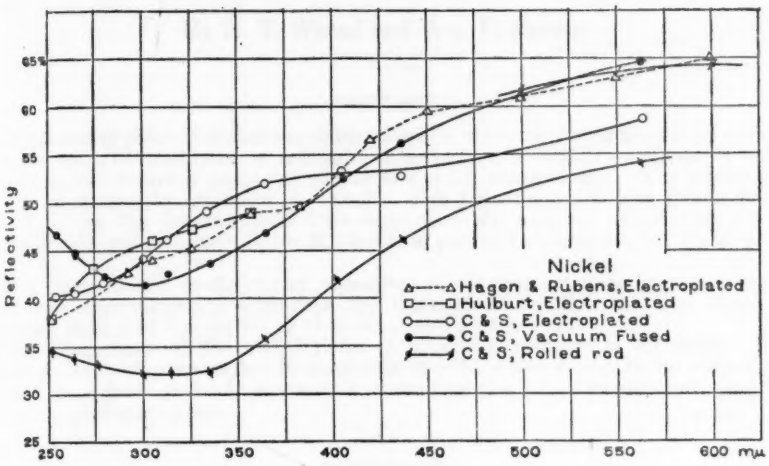

FIGURE 5.—*Ultra-violet reflectivity of pure nickel*

TABLE 12.—*Summary of properties of nickel*

Property	Numerical value	Remarks
Density	8.907 g/cm³ at 23° C	As cast.
	8.901	Worked and annealed.
	8.917	Calculated from lattice dimensions.
Length of side of unit cube (face centered).	3.525 Ångstrom units	
Melting or freezing point	1,455° C	International Temperature Scale.
Electrical resistivity	7.236 microhm-cm at 20° C	Annealed.
Temperature coefficient of electrical resistance.	0.0067 ohms per ° C. per ohm at 0° C.	From 0° to 100° C.
Saturation value of intrinsic induction.	6,150 gausses	
Magnetic transformation	370° to 380° C	By magnetometer measurements.
Thermal transformation	350° C	By thermal analysis.
Thermal e. m. f. vs. Pt	1.485 mv at 100° C	Nickel is thermoelectrically negative to platinum.
	6.165 mv at 500° C	
	12.130 mv at 1,000° C	
Average coefficient of thermal expansion	13.3×10^{-6}	25° to 100° C
	14.4×10^{-6}	25° to 300° C.
	16.5×10^{-6}	300° to 600° C.
	17.8×10^{-6}	600° to 900° C.
Hardness:		
Baby Brinell	68 to 78	
Scleroscope	5.0	
Rockwell	42 to 44	100 kg load; ⅛-inch ball.
Tensile strength	46,400 lbs./in.²	1 specimen only.
Reflectivity	See Figure 5	

WASHINGTON, October 3, 1930.

THE FREEZING POINT OF NICKEL AS A FIXED POINT ON THE INTERNATIONAL TEMPERATURE SCALE

By H. T. Wensel and Wm. F. Roeser

ABSTRACT

The freezing point of nickel was determined by measuring with an optical pyrometer the ratio of brightness of red light of wave length 0.6533 μ emitted by black bodies at the freezing points of nickel and gold, respectively. The nickel was frozen in magnesia crucibles in vacuo. The freezing point was found to be 1,455° C. on the International Temperature Scale with an uncertainty of 1°, based on the value 1,063° C. for the freezing point of gold and 1,432 cm deg. for C_2.

The temperature coefficient af resistance of the two separate ingots of nickel used was approximately 0.0067 in the interval 0° to 100° C. The chemical analyses indicated the purity of the nickel as 99.94 per cent.

The importance of the nickel point in optical pyrometry is discussed. The freezing point of pure nickel in magnesia crucibles was found to be very satisfactory as a fixed point in accurately extending the high-temperature scale beyond the platinum point.

CONTENTS

		Page
I.	Introduction	1309
II.	Previous work	1313
III.	Purity of nickel	1314
IV.	Experimental work and results	1315
V.	Discussion	1317

I. INTRODUCTION

From the standpoint of optical pyrometry, the freezing point of nickel occupies a unique place on the temperature scale. The location of this point is such that it may be very usefully employed as a starting point in fundamental work in optical pyrometry at very high temperatures. The manner in which the nickel point can be used and the reason for its importance will appear from a brief description of the procedure followed in measuring such temperatures.

On the International Temperature Scale,[1] adopted in 1927, the temperature t of a black body above 1,063° C. or 1,336° K. (the freezing point of pure gold) is defined by the formula

$$\log_e R = \log_e \frac{J}{J_1} = \frac{1.432}{\lambda}\left(\frac{1}{1{,}336} - \frac{1}{t+273}\right) \tag{1}$$

whence

$$\frac{1}{t+273} = \frac{1}{1{,}336} - \frac{\lambda \log_e R}{1.432} \tag{2}$$

[1] G. K. Burgess, B. S. Jour. Research, 1 (RP22), p. 635; 1928.

In this formula J_1 is the intensity of monochromatic visible radiation of wave length λ cm emitted by a black body at the gold point and J is the intensity of radiation of the same wave length emitted by a black body at temperature $t°$ C.

In principle, the procedure followed in determining the temperature of a black body is as follows: An optical pyrometer is sighted into a black body at the melting or freezing point of gold. This black body may be either a furnace in which is mounted a thermocouple with a bit of gold welded between the hot junction ends (wire method) or preferably a hollow inclosure or sight tube immersed in a crucible of melting or freezing gold (crucible method). The current which must be sent through the pyrometer lamp to secure a brightness match in the field of view is determined. When operating at this current, the lamp is said to be operating "at the gold point" although the actual temperature of the filament may not be 1,063° C. The optical pyrometer is next sighted into the black body at temperature t and, still operating the lamp at the gold point, an absorption device of known transmission is introduced which will reduce the light from the black body to the proper intensity to again produce a photometric match. The reciprocal of the transmission of the absorption device may then be substituted for R in equation (2). If a spectral pyrometer is used the value of λ may be obtained from the monochrometer setting. If a Morse pyrometer is used the value of λ for the red screen may be computed by methods described elsewhere[2] from the spectral transmission of the screen and the observer's visibility curve. The transmission and the value of λ are sufficient to determine t.

For precise work in optical pyrometry, the only absorption devices whose transmission can be determined with sufficient accuracy are either rotating sector disks or absorption glasses whose effective transmission has been accurately compared with that of sector disks. In either case the determination of the ratio of brightness in the formula (2) rests upon a geometrical measurement of the angular opening of a sector disk. For small angular openings of the order of 1° or less, the percentage error in determining the transmission is significant.

While the definition of the temperature scale requires a measurement of the ratio of brightness R in a primary temperature measurement, it is not necessary that this ratio be determined in one step. Suppose the intensity of a black body whose temperature t is to be determined is J, that of a black body at the gold point is J_1, and that of a black body at an intermediate temperature t_m is J_m. We may determine separately the ratios $\frac{J}{J_m}$ and $\frac{J_m}{J_1}$, without resorting to sectors of very small angular openings. Two sector disks are used whose transmissions are approximately equal to these ratios or one will serve if these ratios themselves are not very different.

After the values of current for the pyrometer lamp have been determined for the gold point and for the temperature t_m through the appropriate sector, the current value is then determined for the temperature t_m with the sector removed. The pyrometer is then sighted upon the black body at temperature t through the other

[2] Fairchild, Hoover, and Peters, B. S. Jour. Research, 2 (RP65), p. 930, 1929.

sector which will produce a brightness match with the lamp operating at the intermediate temperature t_m.

Then

$$\frac{1}{1{,}336}-\frac{1}{t_m+273}=\frac{\lambda \log_e \frac{J_m}{J_1}}{1.432}=A_1 \tag{3}$$

$$\frac{1}{t_m+273}-\frac{1}{t+273}=\frac{\lambda' \log_e \frac{J}{J_m}}{1.432}=A_2 \tag{4}$$

Adding

$$\frac{1}{1{,}336}-\frac{1}{t+273}=A_1+A_2 \tag{5}$$

The values of λ and λ' will differ slightly but can easily be computed as previously stated.

In sighting into a black body through a sector disk, it is necessary for accurate work to use a disk of fixed opening, which can be accurately measured on a circular dividing engine because sector disks of adjustable opening can not be made accurately enough. Therefore, since a sector must be made before the proper opening is known exactly, it can not be expected to produce a match when the lamp is operating exactly at the gold point, and the pyrometer lamp, in actual practice, must be operated at some neighboring temperature, say t_0, to secure a match. The working equation then becomes

$$\frac{1}{t+273}=\frac{1}{t_0+273}+\frac{\lambda \log_e T}{1.432} \tag{6}$$

where T is $\frac{1}{360}$ of the angular opening of the sector in degrees. The value of t_0 may be obtained from the current-temperature relation [3] for the lamp and, if it does not differ very much from 1,063° C., can usually be determined to 0.1° or 0.2° C.

Since the light of wave length 0.65μ given out by a black body in the neighborhood of the gold point varies approximately as the seventeenth power of the absolute temperature, the angular openings of the sector disks used in optical pyrometry are small, usually a few degrees or less. As an illustration, Table 1 shows the angular opening and corresponding per cent transmission of sector disks that will permit measurement of various temperatures first, when the lamp is operated at the gold point and second, when the lamp is operated at some higher temperature, such as the nickel point. The nickel point has been taken as 1,455° C. and λ as 0.65μ, approximately the effective wave length of the types of red screen usually used.

[3] The methods for determining this relation are fairly obvious and will not be discussed further.

TABLE 1.—*Temperatures measurable with various sector disk openings using two fixed points*

Sector disk opening		Temperature to be measured	
Transmission	Angle	Lamp at 1,063° C.	Lamp at 1,455° C.
Per cent	°	°C.	°C.
50	180.0	1,119	1,550
20	72.0	1,208	1,705
10	36.0	1,280	1,836
5	18.0	1,360	1,986
2	7.2	1,476	2,215
1	3.6	1,581	2,432
½	1.8	1,686	2,684
¼	0.9	1,825	2,987

A glance at the table will show that if a primary measurement is to be made of a temperature above 1,800° C., a sector of opening less than 1° must be used or the pyrometer lamp must be operated above the gold point. It is not practicable to use openings of this size, since the uncertainty in their measurement can not easily be reduced below 20 seconds of arc or about one-half of 1 per cent for a 1° sector.

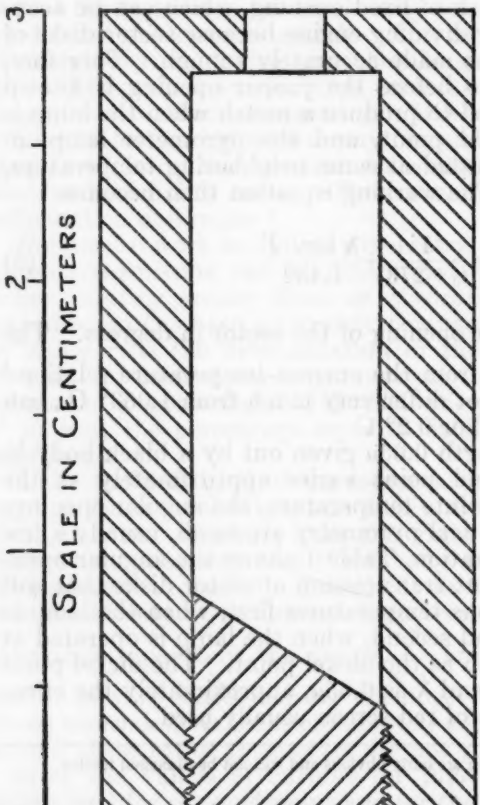

FIGURE 1.—*Cylindrical platinum black body for use in electrically heated furnace*

For some years the practice at the National Bureau of Standards has been to use, for securing the intermediate temperature, a platinum cylinder of the form shown in Figure 1, heated in a platinum-wound furnace. The thermal conductivity of platinum is great enough to insure a fairly high degree of temperature uniformity in the cylinder and by the use of storage batteries for supplying power to the furnace, the temperature may be kept constant except for a slight drift. It would be far better, however, to use a fixed point and make observations on a black body immersed in a freezing metal. A fixed point would insure that the observations, both with and without the sector, are being made upon a source of the same brightness. Another advantage lies in the fact that

the ratio of brightness from the fixed point used to the gold point can be determined once for all if a really satisfactory point can be found.

The upper limit above which a pyrometer lamp should not be operated is determined largely by the changes which take place in the current-temperature relation with continued use at high temperatures. It is, of course, possible to determine and take account of these changes, but when the drift is not very slow, this work becomes both laborious and doubtful.

An inventory of the metals whose freezing points lie within the usual range of operation of pyrometer lamps shows a scarcity of metals which are readily available in a state of purity satisfactory for use as fixed points. The palladium point, which has been recently determined [4] as 1,554° within 2° and probably within 1° on the International Temperature Scale, is unfortunately somewhat above this range. The copper point is too near the gold point to offer any advantages. Nickel is unique in being the only promising metal with a freezing point in the usable temperature range and also provides a fixed point near the upper limit of this range so that its use extends the range of temperatures measurable in this manner as far as practicable.

The present work was undertaken not only to obtain a more accurate value of the freezing point of nickel, but also to investigate the suitability of this point as a base from which to determine temperatures beyond the reach of the optical pyrometer when using only sector disks and a lamp operated near the gold point.

II. PREVIOUS WORK

Between 1895 and 1905 a number of values for the melting point of nickel were reported as shown in Table 2. These values were all determined by the use of thermocouples which had been calibrated at a number of points and for which an equation was deduced for the e. m. f. temperature relation. The values in Table 2 are of historical interest only. Curiously enough the mean of the four values given, 1,450° C. is not very different from the values obtained in later work.

TABLE 2.—*Early observations on the melting point of nickel*

Observers	Year	Purity of nickel	Melting point
			°C.
Holborn and Wien [1]	1895		1,484
Harker [2]	1905	0.996	1,427
Guertler and Tamman [3]	1905	.977	1,419
Copaux [4]	1905		1,470

[1] Holborn and Wien Wied., Ann., **56**, p. 360; 1895.
[2] J. A. Harker, Roy. Soc. Proc. Ser., **A 76**, p. 235; 1905.
[3] W. Guertler and G. Tamman, Zeits. f. Anorg. Chem., **45**, p. 205; 1905.
[4] H. Copaux, C. R., **140** p. 657; 1905.

In 1907 Burgess,[5] using an optical micropyrometer, determined the melting point of small bits of nickel in contact with an electrically heated platinum strip. He obtained 1,435° C. on an optical scale of

[4] See footnote 2, p. 1310.

[5] G. K. Burgess, Bull. B. of S., **3**, p. 345; 1907.

gold = 1,064° and platinum = 1,753°. From the work of Hoffmann [6] and from unpublished work done at the National Bureau of Standards it is known that the scale used by Burgess is about 20° lower at the platinum point than the present International Scale and would probably be some 10° lower at the nickel point.

In 1911 Day and Sosman [7] obtained the value, 1,452.3° C. with a nitrogen constant-volume gas thermometer. This value, rounded to 1,452 has been, with very good reason, the generally accepted value. However, since this value is based almost entirely upon one investigation in which the scale employed was not defined in the same manner as the present scale, it seemed highly desirable that this important fixed point be accurately determined on the present International Scale. As is indicated in Table 5, the values obtained by Day and Sosman for the gold, palladium, and platinum points are all somewhat lower than these fixed points on the present scale.

III. PURITY OF NICKEL

The nickel used in the present work was from a special preparation of electrolytic nickel made by the International Nickel Co. This material was further purified at the National Bureau of Standards by removal of carbon and sulphur as described by Jordan and Swanger elsewhere in this journal.[8] In our work two separate ingots were used having the chemical analyses shown in Table 3.

TABLE 3.—*Chemical analyses* [1] *of nickel previous to use in freezing-point determinations*

	Ingot N-19	Ingot N-23
	Per cent	*Per cent*
C	(2)	0.005
Mn	(2)	(2)
P	(2)	(2)
S	0.004	.004
Si	(2)	.006
Fe	.024	.03
Cu	.016	.006
Co	.016	.016
Mg	.003	(2)
Ni	[3] 99.94	[4] 99.94
Total	100.003	100.007

[1] Analyses by J. A. Scherrer and C. P. Larabee, of the chemistry division.
[2] Not detected.
[3] Difference.
[4] Direct determination.

The two ingots were also analyzed for gases before and after the freezing point determinations, the quantities found being listed in Table 4.

[6] Fr. Hoffmann, Zs. f. Phys., **27**, p. 285; 1924.
[7] A. L. Day and R. B. Sosman, Carnegie Inst. of Wash. Pub. No. 157, p. 107; 1911.
[8] L. Jordan and W. H. Swanger, B. S. Jour. Research, **5** (RP257), p. 1291; 1930.

TABLE 4.—*Analyses*[1] *of nickel for gases before and after use in freezing-point determinations*

Gas	Ingot N–19		Ingot N–23	
	Before	After	Before	After
	Per cent	*Per cent*	*Per cent*	*Per cent*
O_2	0.001	0.008	0.001	0.015
N_2	(2)	(2)	(2)	.004
H_2	< .0002	<.0002	<.0002	<.0002

[1] Analyses by H. C. Vacher of the metallurgy division.
[2] Not detected.

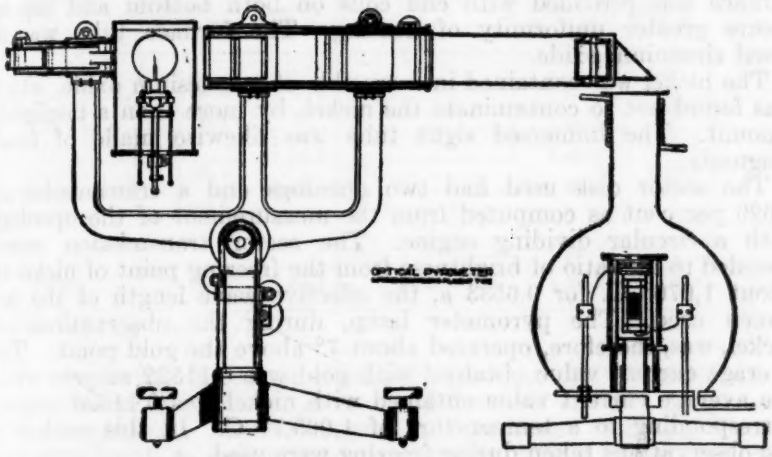

FIGURE 2.—*Arrangement of optical pyrometer, furnace, and crucible of metal.*

Since ingot N–23 apparently picked up over twice as much gas as did ingot N–19 without any resulting difference in the freezing point, it is concluded that the dissolved gases present had no appreciable effect.

The average temperature coefficient of resistance, for the interval 0° to 100° C. was found to be 0.00667 for the material before and 0.00672 for samples taken from the ingots after use in the freezing-point work. The samples giving the value 0.00667 were from the same lots, but not the actual material used, while the value 0.00672 was obtained on material taken from the ingots. The difference is considered not significant.

The unusually high temperature coefficient and the chemical analyses indicate that the nickel of the two ingots N–19 and N–23 was of purity as high as any nickel that has ever been produced.

IV. EXPERIMENTAL WORK AND RESULTS

The arrangement of optical pyrometer and melting furnace is shown in Figure 2, except that a pyrometer lamp with optically flat windows was used. The gold point was determined by sighting into a graphite tube immersed in a crucible of gold. The furnace was

contained in a 6-liter pyrex flask which was evacuated with a mercury diffusion pump to a pressure of about 0.001 mm of mercury. The pyrometer telescope was equipped with a 45° total reflecting prism for convenience in making observations.

The same arrangement was used in the observations on the crucibles of nickel, except that a sector disk was rotated in the space between the prism and furnace window. The same prism and furnace window were used in the observations on gold and nickel, so that the light absorbed by these optical parts need not be determined.

The furnace used for melting the gold was wound with platinum ribbon and the one used for melting the nickel was wound with an alloy wire of 20 per cent rhodium-80 per cent platinum. The nickel furnace was provided with end coils on both bottom and top to secure greater uniformity of heating. The furnace tube was of fused zirconium oxide.

The nickel was contained in a crucible of magnesium oxide, which was found not to contaminate the nickel, by more than a negligible amount. The immersed sight tube was likewise made of fused magnesia.

The sector disk used had two openings and a transmission of 2.629 per cent as computed from the measurement of the openings with a circular dividing engine. The sector transmission corresponded to the ratio of brightness from the freezing point of nickel to about 1,070° C. for 0.6533 μ, the effective wave length of the red screen used. The pyrometer lamp, during the observations on nickel, was, therefore, operated about 7° above the gold point. The average current value obtained with gold was 0.11522 ampere while the average current value obtained with nickel was 0.11625 ampere corresponding to a temperature of 1,069.7° C. In this work only the observations taken during freezing were used.

The calculation for the freezing point, t, is made from equation (6). If logarithms to the base 10 are used and the effective wave length is expressed in microns, this equation becomes

$$\frac{1}{t+273}=\frac{1}{t_0+273}+\frac{\lambda \log_{10} T}{6{,}219}$$

$$t=1{,}069.7^\circ \text{ C.}$$
$$\lambda=0.6533\mu$$
$$T=0.02629.$$

whence

$$t=1{,}454.8^\circ \text{ C.}$$

The ratio of brightness, nickel to gold, for the above wave length, may be calculated from equation (2) to be 41.28, the reciprocal of which is 0.02422.

The order of observation was as follows:

1. Five freezes on gold.
2. Nine freezes on nickel, ingot N–19.
3. Four freezes on gold.
4. Six freezes on nickel, ingot N–23.
5. Four freezes on gold.
6. Five freezes on nickel, ingot N–23.
7. Five freezes on gold.

The observations at the freezing point of gold indicated that no detectable drift occurred in the pyrometer lamp during the period covered by the above work. The average current through the lamp for the first nine gold freezes differed from that for the last nine freezes by only 1 part in 11,000, corresponding to a difference in temperature of less than 0.1° C.

The results obtained on the individual freezes are listed in Table 5.

TABLE 5.—*Determinations of the freezing point of nickel*

Freeze No.	Ingot N-19		Freeze No.	Ingot N-23		
	Observer H. T. W.	Observer W. F. R.		Observer H. T. W.	Observer W. F. R.	Observer F. R. C.
	° C.	° C.		° C.	° C.	° C.
1	1,454.6		10	1,455.0		
2	1,454.8		11		1,454.8	
3	1,455.1		12	1,454.2		
4		1,454.3	13		1,455.0	
5		1,454.6	14	1,454.8		
6	1,455.3		15		1,454.6	
7		1,454.9	16	1,454.6		
8	1,454.6		17			1,454.4
9		1,455.0	18		1,455.1	
			19			1,454.7
			20	1,454.7		
Mean	1,454.9	1,454.7	Mean	1,454.7	1,454.9	1,454.6

Mean of 20 freezes, 1,454.8° C.

In comparing the result obtained with that of Day and Sosman, consideration should be given to differences in the temperature scales employed. The values given in Table 6 and plotted in Figure 3 are significant as indicating a systematic difference between their scale and the International Scale adopted in 1927.

TABLE 6.—*Differences between International Temperature Scale and the scale of Day and Sosman*

Fixed point	Day and Sosman (gas thermometer)	Present values (International Scale	Difference
	° C.	° C.	° C.
Gold	1,062.4	1,063.0	0.6
Nickel	1,452.3	1,454.8	2.5
Palladium	1,549.2	1,553.6	4.4
Platinum	[1] 1,752	1,772	20

[1] By extrapolation of the thermocouple calibrated at lower points against gas thermometer.

V. DISCUSSION

The behavior of the nickel used in the present work and the agreement between the values obtained with two separate ingots indicate that the freezing point of nickel of high purity is very satisfactory for use as a fixed point from which to start in measuring temperatures above the platinum point where the brightness relative to that of a black body at the gold point can not well be measured in one step with a sector disk. It is advisable to determine the freezing point of

the particular lot of nickel so used, this freezing point serving merely to provide a steady, uniform, and reproducible temperature. The freezing should be done in an evacuated space at pressures of not more than 0.01 mm of mercury.

There was no evidence of appreciable contamination of the metal by the crucibles of magnesium oxide. No decrease in the temperature coefficient of resistance took place nor did the freezing point show any drift with successive melts and freezes.

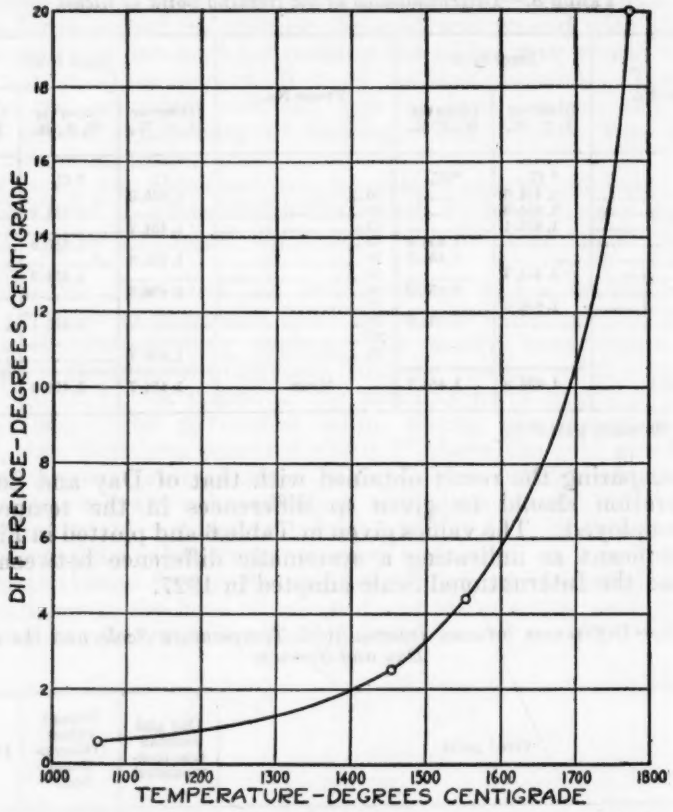

FIGURE 3.—*Differences between International Temperature Scale and the scale of Day and Sosman as obtained from data on fixed points*

The freezing point of the nickel used is probably slightly lower than that for the absolutely pure metal, but calculation indicates the maximum difference to be less than 1°. Very likely this difference is not over 0.5° C. For this reason we have considered it advisable to round our result from 1,454.8° to 1,455° C. On the International Scale, which is based on the value 1,063° C. for the freezing point of gold and the value 1.432 cm deg. for C_2. The value 1,455° C. here obtained is believed to be within 1° on the present scale of the true value either for pure nickel or the nickel actually used.

WASHINGTON, July 16, 1930.

(Cut here)

SUPERINTENDENT OF DOCUMENTS,
Government Printing Office,
Washington, D. C.

DEAR SIR: Send me the Bureau of Standards publications marked X below. I inclose remittance* to cover the cost.

Mark X	Title of publication	Price		Amount inclosed
		United States, Canada, Cuba, Newfoundland, Republic of Panama	Foreign countries	
----	Commercial Standards Monthly (one year)	$1.00	$1.25	----
----	Bureau of Standards Journal of Research (one year)	2.75	3.50	----
----	Technical News Bulletin (one year)	.25	.40	----
----	Standards Yearbook, 1930	.75	1.00	----
	Total remittance	----	----	----

Send to ----

Number and Street ----

City and State (or County) ----

* Remittances should be either in the form of a post-office money order, coupons (issued for the specific purpose of purchasing Government publications), express money order, New York draft, or cash, at the sender's risk.

BUREAU OF STANDARDS JOURNAL OF RESEARCH

CONTENTS OF RECENT NUMBERS—Continued

September, 1930 (Vol. 5, No. 3)

RP225. The chloroplatinate-chloroplatinite electrode. Edgar R. Smith.

RP226. A new crystalline calcium chloride compound of *a-d* gulose and its rotation and mutarotation in aqueous solution. Horace S. Isbell.

RP227. Note on the electrical resistance of contacts between nuts and bolts. Frank Wenner, G. W. Nusbaum, and B. C. Cruickshanks.

RP228. Addition agents in copper electrotyping solutions. R. O. Hull and W. Blum.

RP229. Terms of the arc and spark spectra of chromium. C. C. Kiess.

October, 1930 (Vol. 5, No. 4)

RP230. Strength of welded shelf-angle connections. James H. Edwards, H. L. Whittemore, and A. H. Stang.

RP231. Measurement of surface temperatures. Wm. F. Roeser and E. F. Mueller.

RP232. Stress distribution in welded steel pedestals. James H. Edwards, H. L. Whittemore, and A. H. Stang.

RP233. The X-ray method applied to a study of the constitution of Portland cement. L. T. Brownmiller and R. H. Bogue.

RP234. Photo-ionization of cæsium vapor by absorption between the series lines. C. Boeckner and F. L. Mohler.

RP235. Efficiency of production of X rays. Warren W. Nicholas.

RP236. On the determination of the empirical formula of a hydrocarbon. Edward W. Washburn.

RP237. The importance of particle size in samples of certain metallurgical materials. J. A. Scherrer and G. E. F. Lundell.

RP238. A radiobeacon and receiving system for blind landing of aircraft. H. Diamond and F. W. Dunmore.

RP239. The isolation of the isomers of hexane from petroleum. Johannes H. Bruun and Mildred M. Hicks-Bruun.

RP240. Determination of carbon in high sulphur steels by direct combustion. H. A. Bright and G. E. F. Lundell.

RP241. Surface tension of soap solutions and its relation to the thickness of adsorbed films. Ronald Bulkley and F. G. Bitner.

RP242. The measurement of sound absorption. V. L. Christer and W. F. Synder.

November, 1930 (Vol. 5, No. 5)

RP243. Mechanism of heat flow in fibrous materials. J. L. Finck.

RP244. Compressibility and thermal expansion of petroleum oils in the range 0° to 300° C. R. S. Jessup.

RP245. Interference measurements in the first spectra of Krypton. C. J. Humphreys.

RP246. Kennelly-Heaviside layer height observations for 4,045 and 8,650 kc. T. R. Gilliland.

RP247. A study of the method for titrating aldose sugars with standard iodine and alkali. G. M. Kline and S. F. Acree.

RP248. Properties of lead-bismuth, lead-tin, type metal, and fusible alloys. J. G. Thompson.

RP249. A study of the adsorption of sulphuric acid by leather. John Beck, jr.

RP250. A study of the so-called "over-reduced" condition in molten steel. J. V. McCrae, R. L. Dowdell, and Louis Jordan.

RP251. The constant occurrence of nonreducing disaccharides in hydrolzyed inulin.

RP252. Precision of color temperature measurements under various observing conditions; a new color comparator for incandescent lamps. Deane B. Judd.

RP253. The ring structure of mannose. The optical rotation of 4-glucosido-α-mannose. Horance S. Isabell.

Research papers are available as separates for purchase from the Superintendent of Documents United States Government Printing Office, Washington, D. C.

A monthly periodical of pure and applied science published by our National Government

BUREAU OF STANDARDS JOURNAL OF RESEARCH

PUBLISHED AT WASHINGTON, D. C.

¶With the July issue, the JOURNAL began its third year and fifth volume. The JOURNAL contains the bureau's research papers and critical reviews in the fields of science and technology. These will be comparable in interest and importance with the bureau papers already issued.

¶Several hundred researches are always in progress at the Bureau of Standards and the outlet for the results is the "BUREAU OF STANDARDS JOURNAL OF RESEARCH."

¶If you are interested in following the latest developments in science and technology you need the BUREAU OF STANDARDS JOURNAL OF RESEARCH. If you are a subscriber, renew your subscription promptly; if not, your subscription will be appreciated. Copies are limited and it is not always possible to supply back numbers.

PRICES

New subscription (or renewal)[1] to Journal of Research for United States, Canada, Cuba, Mexico, Newfoundland, and the Republic of Panama $2.75*

Blue buckram bound { Volume 1, July to December, 1928 . . . . $2.75* / Volume 2, January to June, 1929 . . . . $2.75* / Volume 3, July to December, 1929 . . . . $2.75* }

[1] Yearly subscription, 12 issues. *For other countries, add 75 cents.

Research papers (printed separately with durable paper cover and priced according to cost) see list of research papers on cover pages 2 and 3 of this issue.

Address orders only to
Superintendent of Documents
Government Printing Office
Washington, D. C.
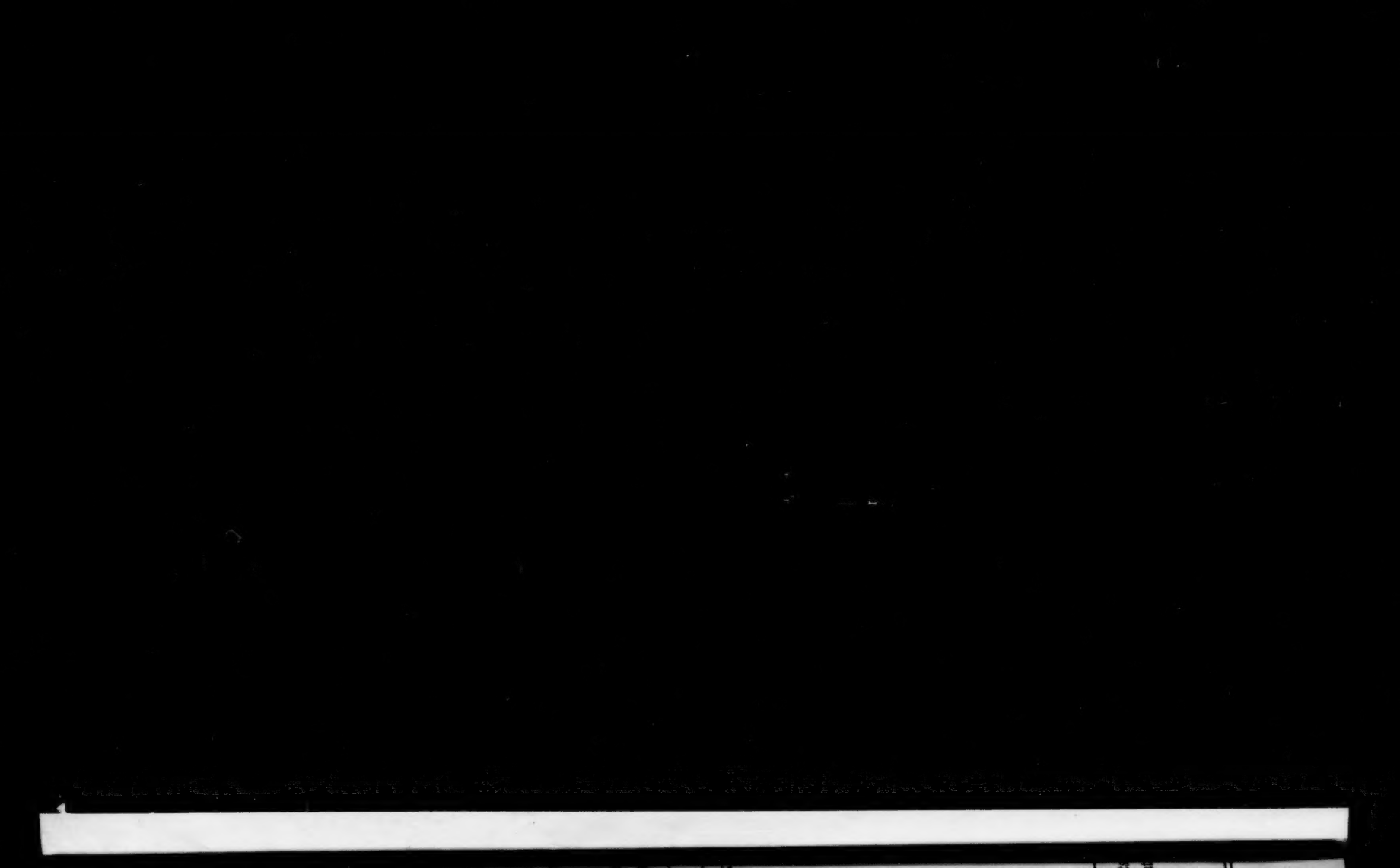
The value of prompt and adequate news of the latest research results can not be measured by ordinary standards. They are permanent gainful assets for the expert. He can hardly afford to be without such basic sources